6-3/14

Journal of Polymer Science: Part C, Polymer Symposia, No. 6

Thermal Analysis of High Polymers

American Chemical Society Symposium

Held at New York, New York, September 11–12, 1963

edited by *Bacon Ke*

Charles F. Kettering Research Laboratory, Yellow Springs, Ohio

published 1964 by INTERSCIENCE PUBLISHERS a division of John Wiley & Sons, Inc.

No. 6

Journal of Polymer Science, Part C, POLYMER SYMPOSIA

Thermal Analysis of High Polymers

edited by BACON KE

Charles F. Kettering Research Laboratory,
Yellow Springs, Ohio

American Chemical Society Symposium
Held at New York, New York, September 11–12, 1963

published by INTERSCIENCE PUBLISHERS,
a division of John Wiley & Sons, Inc.

JOURNAL ON POLYMER SCIENCE, PART C, *Polymer Symposia*

Editors: H. MARK C. G. OVERBERGER R. S. STEIN

Editorial Board: R. M. FUOSS J. J. HERMANS

H. W. MELVILLE G. SMETS

Published at irregular intervals by Interscience Publishers, a Division of John Wiley & Sons, Inc. Publication Office at 20th and Northampton Streets, Easton, Pennsylvania. Executive, Editorial, and Circulation Offices at 605 Third Avenue, New York, New York 10016. Subscription price, $225.00 per volume (including Part A: General Papers; and Part B: Polymer Letters). Foreign postage, $5.00 per volume (including Parts A and B).

Copyright © 1964, by John Wiley & Sons, Inc., Printed in U.S.A.

PREFACE

A symposium on "Thermal Analysis of High Polymers," sponsored by the Polymer Chemistry Division, was held during the 145th national meeting of the American Chemical Society in New York City in September 1963. This volume contains almost all the papers presented at the symposium.

Serious efforts to apply thermal analytical methods to polymer studies began only a few years ago. The growth of interest in this field is shown by the increasing number of publications concerning polymer applications and development of new and more sophisticated instruments. To assure a more complete coverage of thermal analytical techniques and applications concerning high polymers, this symposium was planned to include reports of work done in many laboratories. Thus, this volume represents a cross-sectional view of current developments, which may, perhaps, point to some trends for the immediate future.

The editor thanks the many investigators both from this country and from abroad for their active participation in the symposium. It is hoped that this volume will serve not only as a written record of the symposium but also as a valuable aid to all investigators interested in this expanding field.

Bacon Ke

Charles F. Kettering Research Laboratory
Yellow Springs, Ohio

Contents

ROBERT F. SCHWENKER, JR., and ROBERT K. ZUCCARELLO: Differential Thermal Analysis of Synthetic Fibers 1

R. M. SCHULKEN, JR., R. E. BOY, JR., and R. H. COX: Differential Thermal Analysis of Linear Polyesters 17

PHILIP E. SLADE, JR., and LLOYD T. JENKINS: Thermal Analysis of Polyurethane Elastomers 27

H. WILSKI and T. GREWER: The Specific Heat of Poly-1-butene 33

BERT H. CLAMPITT and RICHARD H. HUGHES: Differential Thermal Analysis of Polybutene-1 43

H. W. HOLDEN: A Differential Thermal Analysis Study of the Effects of Thermal History on Polyethylene 53

WALTER K. TANG and WAYNE K. NEILL: Effect of Flame Retardants on Pyrolysis and Combustion of α-Cellulose 65

F. H. MÜLLER und H. MARTIN: Kalorimetrische Messungen der Kristallisations- und Schmelzvorgänge an Polymeren 83

H. J. DONALD, E. S. HUMES, and L. W. WHITE: Crystallization of Polypropylene Measured by Differential Thermal Analysis 93

E. HELLMUTH, H. G. KILIAN, und F. H. MÜLLER: Differentialkalorimetrische Messungen an verschieden verzweigten und verschieden chlorierten Polyäthylenen in Verbindung mit Röntgenmessungen 101

JAMES M. O'REILLY, FRANK E. KARASZ, and HARVEY E. BAIR: Thermodynamic Properties of Lexan Polycarbonate from 110–560° K 109

F. H. MÜLLER und N. WEIMANN: Kalorimetrische Messungen von Wärmeeffekten bei Verstreckung 117

JOHN K. GILLHAM and ARMAND F. LEWIS: Studies of the Thermal Behavior of Polymers by Torsional Braid Analysis 125

BERNARD WUNDERLICH and DAVID M. BODILY: Dynamic Differential Thermal Analysis of the Glass Transition Interval 137

ISMAT ABU-ISA, V. A. CRAWFORD, A. R. HALY, and MALCOLM DOLE: Specific Heat of Synthetic High Polymers. XI. The Glass Transition in Isotactic Polypropylene 149

K. EIERMANN: Thermal Conductivity of High Polymers 157

J. HENNIG and W. KNAPPE: Anisotropy of Thermal Conductivity in Stretched Amorphous Linear Polymers and in Strained Elastomers 167

HUGH C. ANDERSON: Thermogravimetry of Polymer Pyrolysis Kinetics 175

HENRY L. FRIEDMAN: Kinetics of Thermal Degradation of Char-Forming Plastics from Thermogravimetry. Application to a Phenolic Plastic 183

C. GEACINTOV, R. S. SCHOTLAND, and R. B. MILES: Form III to Form II Phase Transition of Polybutene-1 197

H. W. HOLDEN: The Low-Melting Crystalline Modifications of Isotactic Polybutene-1 209

Author Index 213

Subject Index 214

JOURNAL OF POLYMER SCIENCE: PART C NO. 6, PP. 1–16 (1964)

Differential Thermal Analysis of Synthetic Fibers

ROBERT F. SCHWENKER, JR., and ROBERT K. ZUCCARELLO,
Textile Research Institute, Princeton, New Jersey

Synopsis

The application of differential thermal analysis (DTA) for the characterization and the investigation of the thermal degradation of synthetic textile fibers, to include polyester, nylon 6, propropylene, and polytetrafluoroethylene fibers, has been studied. The temperature range was from 50 to 650°C. using laboratory-built DTA apparatus. Experimental considerations and techniques are discussed and such variables as sample preparation, size, cell packing, atmosphere control, and heating rate have been investigated. The conventional technique of grinding or milling DTA samples is shown to cause significant changes in certain samples, particularly in undrawn fibers. The control of sample atmosphere by dynamic gas flow through the sample cell gave peaks that were generally sharper and larger than those found when control was by gas diffusion. Data are given on the various low temperature transitions found in such fibers. Significant differences in low temperature transitions were observed between polypropylene fiber and the bulk polymer as well as between drawn and undrawn nylon 6 fibers. The interpretation of the DTA curves for the decomposition and other reactions at elevated temperatures is discussed. Nylon 6 and polypropylene showed only endothermic reactions indicative of depolymerization processes whereas other fibers showed both endothermic and exothermic reactions in the decomposition range.

Differential thermal analysis (DTA) is a dynamic method whereby the phase transitions and chemical transformations that occur during the heating of a polymeric or other material may be detected. Earlier work[1–4] in these laboratories demonstrated the potential applications of DTA for the identification, characterization, and thermal degradation studies of textile fibers. In the case of synthetic textile materials the detectable thermal changes include the glass transition, crystallization, fusion, moisture desorption, and irreversible reactions and thermal degradation processes.[2,5–9] The application of DTA in studying textile materials is of such recent date that standards for experimental techniques and instrumentation have not yet been established. Therefore, in this paper consideration is given to (*1*) instrumentation, (*2*) experimental techniques, (*3*) changes caused by certain fiber processing steps, and (*4*) high temperature reactions involving polymer decomposition.

Experimental

Apparatus

Two different DTA units, built in the laboratory, were used in the work. One apparatus featured atmosphere control by diffusion into and out of the

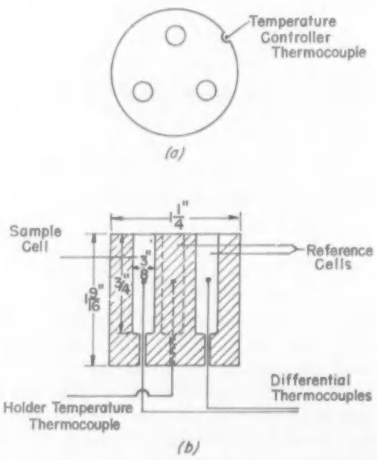

Fig. 1. DTA sample holder: (*a*) top view; (*b*) cross section view.

sample holder cells and its design was based on instrumentation described by Gordon and Campbell.[10] A metal sample holder fitted with thermocouples, is suspended in the ceramic core of a standard combustion furnace from a rod attached to a metal plate. With the holder in position the metal plate rests on the top of the vertically positioned furnace completely covering the opening but the furnace tube remains open at the bottom. The sample holder, made of a nickel-chrome alloy (Inconel X), is shown in Figure 1. Chromel-alumel thermocouples of 28 gage wire are introduced through the base of the holder and cemented in a fixed position. The emf representing the temperature difference is amplified by a L & N dc amplifier No. 9835-B. Temperature was measured in the reference substance, calcined alumina (α-Al_2O_3), in a separate well and the rate control thermocouple was located in the outer wall of the sample holder. The signals for the differential temperature and the reference temperature were recorded on time-base chart recorders using either two 10 in. single pen recorders or a double pen, X_1X_2, recorder (Leeds and Northrup instruments). The rate of heating was controlled by a cam-operated temperature programmer (West Instrument Co.) or by a solid state temperature programmer (F & M Model 240 Programmer).

The atmosphere is controlled by discharging the desired gas or gases under pressure into the open end of the furnace at flow rates of 3,000 to 6,000 cc./min. via a metal coil gas spreader. Thus, the sample holder is blanketed with the gas and the atmosphere within the sample well is achieved by diffusion of gas into the well. The removal of volatile products arising from the thermal degradation of the sample during a run is apparently accomplished by the driving force accompanying volatilization and is also dependent on diffusion.

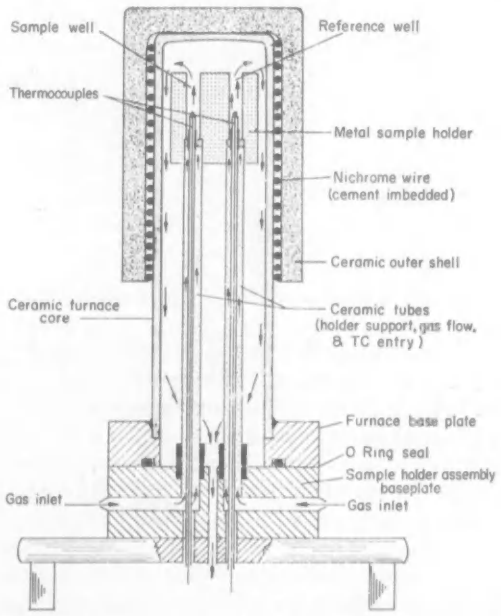

Fig. 2. Dynamic gas flow apparatus: sample holder and furnace assembly.

The other apparatus used, based on instrumentation described by Whitehead and Breger[11] and Lodding and Hammel,[12] differed primarily in atmosphere control, featuring the "dynamic gas flow" technique as described by Stone,[13] and is shown in Figure 2. In a dynamic gas flow apparatus the atmosphere is provided by passing the desired gas through the sample holder cells. Thus, the sample is continuously swept with fresh atmosphere gas insuring the removal of any degradation products from the sample cavity. Gas flow rates into the sample holder were of the order of 30 cc./min. The auxiliary instrumentation for signal amplification, recording, and heating rate control was the same as that described for the gas diffusion apparatus.

Under optimum conditions with either apparatus a temperature difference ΔT of 0.05°C., which is equivalent to 2 μv, could be detected. As previously indicated the reference temperature and not sample temperature was measured so that the temperatures shown on the DTA curves are reference temperatures. Sample temperature is simply determined from the following relationship.

$$T_{\text{sample}} = T_{\text{ref}} + \Delta T$$

Procedures

Fiber, fabric, and some bulk polymer samples of 5 to 50 mg. were run at heating rates of 1° to 10°C./min. from about 50 to 650°C. Samples were

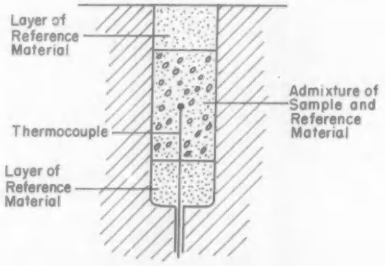

Fig. 3. Packing arrangement in sample cell.

usually prepared by cutting into small squares of $^1/_{16}$ in. or $^1/_{16}$ in. lengths. Samples were run in an atmosphere of either purified nitrogen or compressed air to provide both oxidizing and non-oxidizing conditions. At elevated temperatures the reactions of organic substances are so complex that some separation of oxidative and nonoxidative reactions must be achieved. In general the DTA curves obtained in the inert atmosphere were found to be less ambiguous and the most consistently informative.

The sample packing technique involved the dilution of all samples with the alumina used as the reference material. In the case of organic materials samples are admixed with reference material so that the packing and thermal properties will be determined principally by the reference material regardless of sample shrinkage, melting, decomposition etc.[14–16] A modified "sandwich" packing, developed in previous studies,[1,2] was used in the present work as shown diagrammatically in Figure 3. About one-third of the reference material to be used is deposited in the sample well as a base layer. The cut pieces of sample are then placed around the thermocouple junction together with reference material and the balance of the reference material constitutes a covering layer.

Results and Discussion

The effects of sample preparation, sample size, cell packing, atmosphere control, and other experimental variables have been studied. The usual method for DTA sample preparation involves grinding or milling to 40–200 mesh.[14] The effects of sample preparation and packing are shown in Figure 4 by representative curves obtained on the samples of undrawn Dacron* polyester fiber and, using the top curve, the main curve features are identified as (*1*) the second-order or glass transition T_g at 84°C., which is manifested as a well-defined downward shift in the base line reflecting an increase in the heat capacity of the polymer, (*2*) polymer crystallization shown by the exotherm with a peak at 148°C., (*3*) polymer fusion shown by the endotherm with a peak at 266°C., and (*4*) polymer decomposition represented by the endothermic process with a peak temperature of 450°C.

* Du Pont trademark.

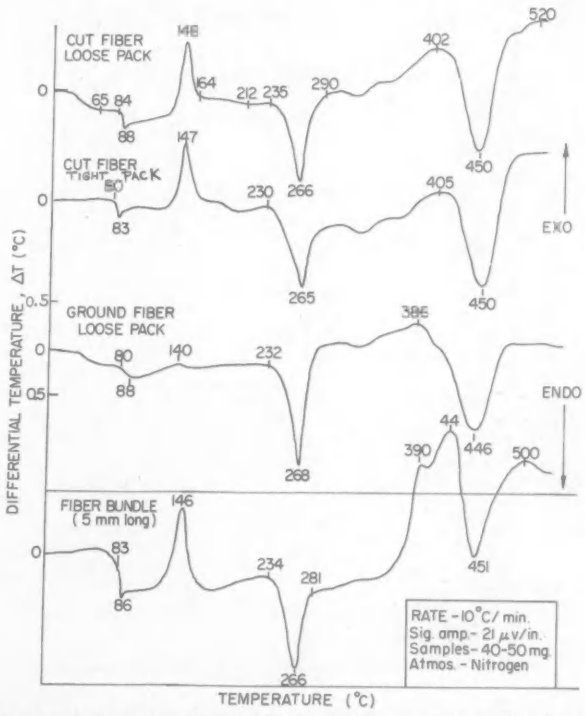

Fig. 4. DTA curves of undrawn Dacron (GD-gas diffusion apparatus): effect of sample preparation and packing.

Following polymer fusion there are also indications of one or more exothermic reactions beginning around 350°C. By means of dynamic mechanical measurements T_g for polyethylene terephthalate fibers has been estimated to be 80°C.[17] and available DTA data from the literature indicates values of 78°C.[9] It should be noted that due to the relatively fast heating rate of 10°C./min. the actual peak temperatures shown can be expected to differ from those from DTA curves obtained at lower heating rates. Some of the effects of heating rate are discussed subsequently.

Tightly packing the fiber sample by tamping the sample mixture in the well does not significantly alter peak temperatures although the base line appears to shift slightly. However, in the cases where the fiber was ground to 40 mesh by a Wiley mill the curve indicates some reduction in the glass transition shift, the crystallization peak has virtually disappeared, and the curve has changed shape somewhat in the region just prior to the decomposition endotherm. In the grinding or milling operation there is apparently sufficient heat generated such that, unless adequate cooling is provided, samples of largely amorphous bulk polymers or undrawn fibers will undergo the low temperature transitions and crystallization process.

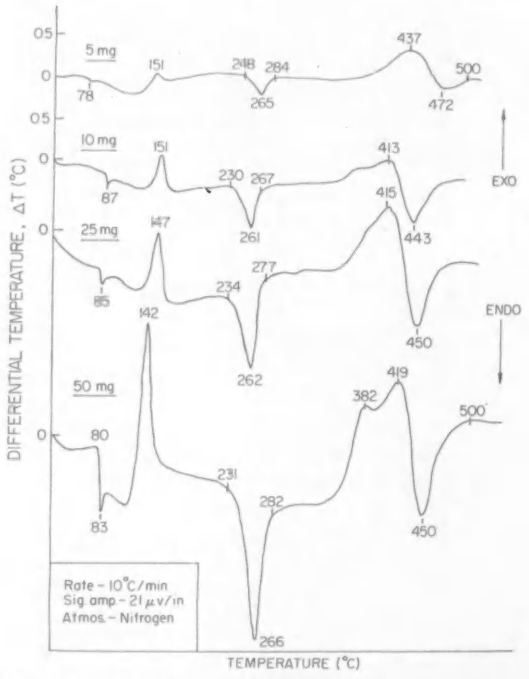

Fig. 5. DTA curves of undrawn Dacron (DGF-dynamic gas flow apparatus): effect of sample size.

It has been shown that milling can cause polymer degradation[18,19] and severe mechanical damage may cause other significant changes in certain fibers[20] that may be reflected in the DTA curve. The curve obtained with the sample in the form of a fiber bundle shows very well defined features with the appearance of two distinct exothermic reactions prior to decomposition. In this case a fiber bundle was slid down over the thermocouple so that the bead was positioned halfway up in the bundle. Samples of fibers cut to a length of about $^1/_{16}$ in. and fabric cut into $^1/_{16}$ in. squares have been found to give highly reproducible results.

Sample size is another extremely important variable to be considered. Intuitively, the smaller the sample the more realistic the results should be. Thus, in the case of a small sample the effect of a thermal gradient will be minimized. The effects of heat capacity differences vis a vis the reference material would also be minimized. Since a finite time is required for a transformation to occur sample size may unduly affect the observed temperature of a given reaction.[15] In Figure 5 the effect of sample concentration is shown for undrawn Dacron fiber in nitrogen atmosphere using the dynamic gas flow apparatus. The DTA curves show that 5 mg. samples give weak reactions with some curve distortion.

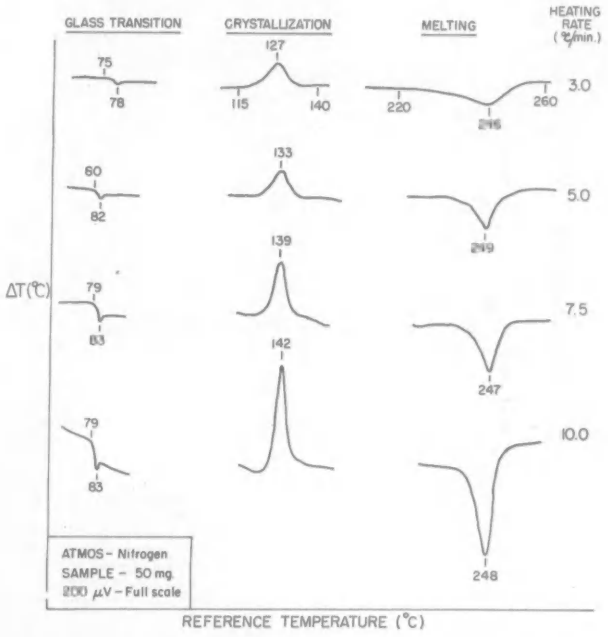

Fig. 6. DTA (GD) curves of undrawn Dacron: effect of heating rate.

Heating rate has long been recognized as a potent variable in DTA[14] that can cause shifts in peak temperature. Dacron, nylon 6, and polypropylene samples were run in the gas diffusion DTA apparatus at heating rates of 1, 3, 5, 7.5, and 10°C./min. The results obtained on Dacron are shown in Figure 6. All of the results are summarized in Figure 7. The data show that (*1*) T_g tends to increase slightly as heating rate increases, (*2*) crystallization temperature is definitely affected by heating rate, increasing as heating rate increases, (*3*) melting is not much affected but tends to increase slightly as high rates of heating are reached, and (*4*) decomposition temperature increases markedly as heating rate increases.

Results have been obtained on some fiber and bulk polymer samples, described in Table I, in air and in purified nitrogen on 50 mg samples of cut fiber.

In Figure 8 the DTA curves of drawn and undrawn Caprolan* nylon 6 in nitrogen on the gas diffusion apparatus are presented. There is a well-defined endothermic peak for polymer fusion indicating a melting point of 231°C. for drawn fiber versus 231°C. for the undrawn fiber. The fusion peak for the drawn fiber is much larger and sharper than the undrawn indicating a higher degree of crystallinity and/or orientation,

* Allied Chemical Corporation trademark.

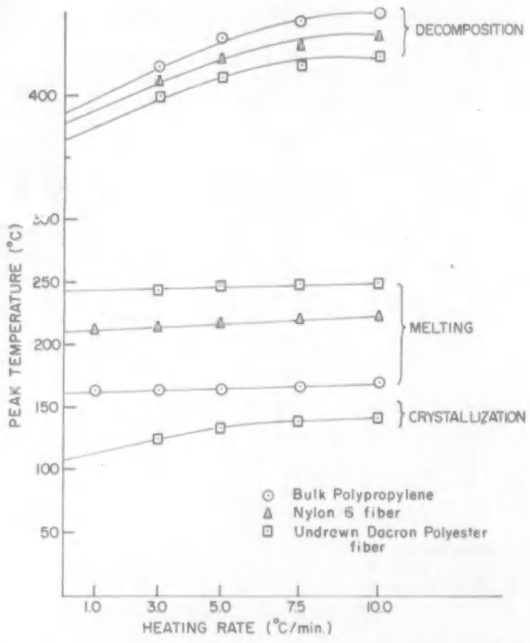

Fig. 7. Variation of DTA peak temperatures with heating rate.

as might be expected. Both melts are observed to start depolymerization, around 370°C. and two reactions are indicated, one much smaller than the other. Strauss and Wall[21] in a study of the pyrolysis of nylon 6 in vacuum concluded that the decomposition involved two competing mechanisms: (*1*) random hydrolytic scission and (*2*) free radical depolymerization. The DTA curves for nylon 6 appear to fit this hypothesis leading to the interpretation of the small endotherm around 400°C. as due to random hydrolytic scission followed by the major reaction of depolymerization by a

TABLE I
Special DTA Samples

Sample	Description
Pure nylon 6	High tenacity, bright, drawn yarn
	High tenacity, bright, undrawn yarn
Polypropylene	Experimental samples of drawn fiber from pure polymer
	pure, bulk polymer

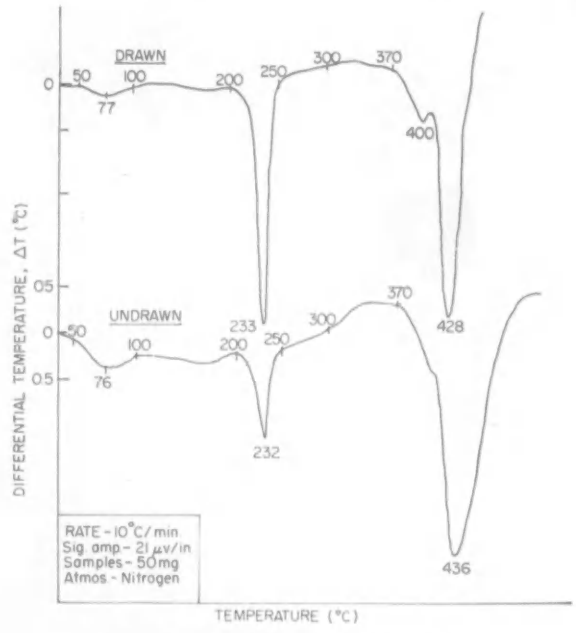

Fig. 8. DTA (GD) curves of nylon 6 fiber.

free radical mechanism. The resolution of the decomposition reactions is better in the case of the drawn fiber.

The air curves for both the drawn and undrawn fibers on the two DTA apparatuses have also been obtained. The gas diffusion DTA curves show a weak endotherm around 90°C. followed by an exothermic rise which is interrupted by the fusion reaction (reference peaks 232–233°C.) with the peak for the drawn fiber being the sharper of the two. The fusion peaks are followed by strong exothermic processes showing a peak at 387°C. for the drawn fiber and 408°C. for the undrawn. These represent oxidative reactions since they are not found in the nitrogen curves. Both samples exhibit strong endotherms with peak temperatures comparable to the main decomposition endotherms found in the nitrogen curves. However, no indication of two reactions is evident probably due to the interference of oxidative reactions. The air curves for dynamic gas flow DTA are generally similar except that the major reactions appear larger as was the case for the nitrogen curves.

Samples of bulk polypropylene and fiber made therefrom have been run in nitrogen on both DTA apparatuses. The gas diffusion curves in Figure 9 show a possible phase change around 95–100°C which may represent a transition associated with one crystalline modification changing to another followed by the main fusion peak. The reaction at 98°C. in the bulk

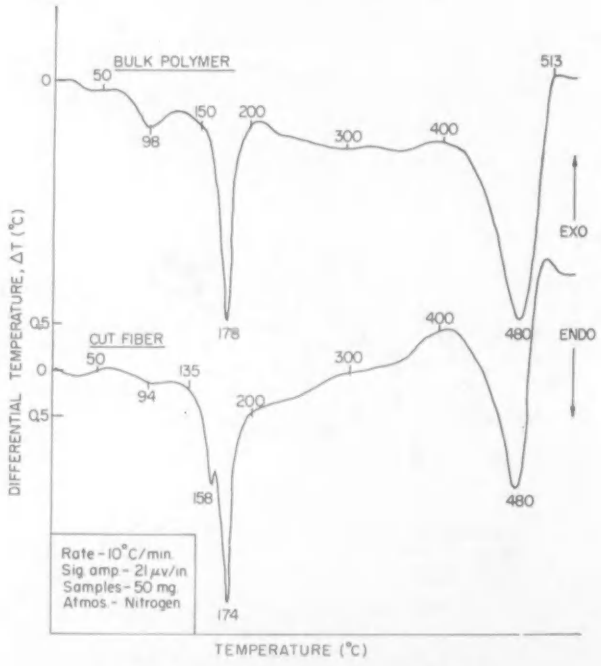

Fig. 9. DTA (GD) curves of polypropylene.

polymer is much reduced in the fiber and the main fusion process in the fiber now shows two peaks. The polymer melt begins to show a decomposition endotherm beginning about 425°C. with a peak at 480°C. The dynamic gas flow DTA curves, shown in Figure 10 follow a similar pattern except that the melting endotherms and decomposition endotherms appear to be larger. The double peaks at 158 and 174°C. observed in the melting region are found only for the drawn fiber and a similar phenomenon has been observed in the case of nylon 66.[2,5] This appearance of two peaks was first reported by White[5] in the DTA curves of nylon 66 yarn and, based on x-ray and birefringence data, he concluded that the first peak involved disorientation prior to crystallite melting. The DTA curve of undrawn polypropylene does not show the early peak at 158°C. and if the melt from the drawn fiber is cooled and rerun the first peak disappears so that this peak at 158°C. is tentatively ascribed to disorientation. The relatively small size of the polypropylene decomposition endotherms has been interpreted as indicating partial degradation to chain fragments rather than to monomer. Madorsky et al.[22] found that vacuum pyrolysis of polyethylene gave products with an average molecular weight of about 700 and Grassie[19] reports the thermal degradation products of polypropylene to be primarily large chain fragments.

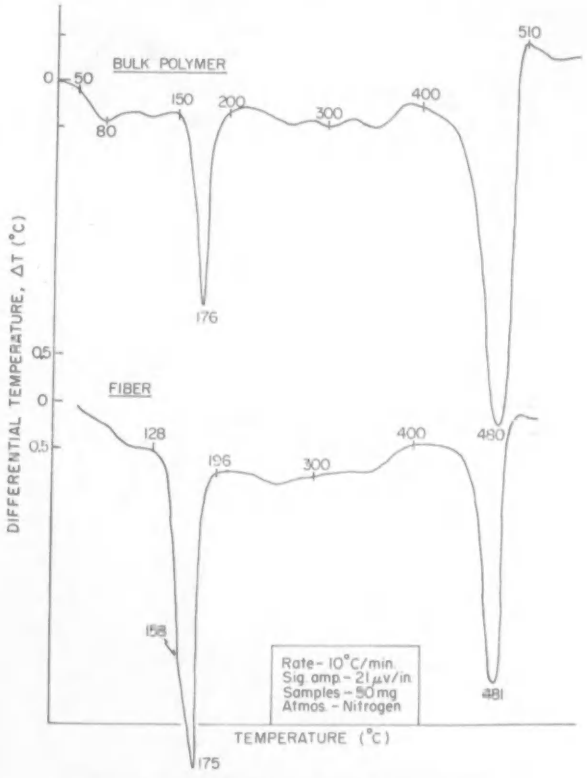

Fig. 10. DTA (DGF) curves of polypropylene.

TABLE II
Comparison of DTA Peak Data

Sample	Gas diffusion		Dynamic gas flow	
	T(°C.)	Hgt. (in.)	T(°C.)	Hgt. (in.)
	Fusion Peak Data			
Dacron	266	1.7	266	3.0
Nylon 6	233	4.9	236	7.0
Polypropylene-fiber	174	4.4	175	6.2
Polypropylene-bulk	178	4.1	176	4.0
	Decomposition Peak Data			
Dacron	450	2.1	450	3.0
Nylon 6	428	5.2	434	7.0
Polypropylene-fiber	480	3.3	481	5.0
Polypropylene-bulk	480	3.5	480	6.7

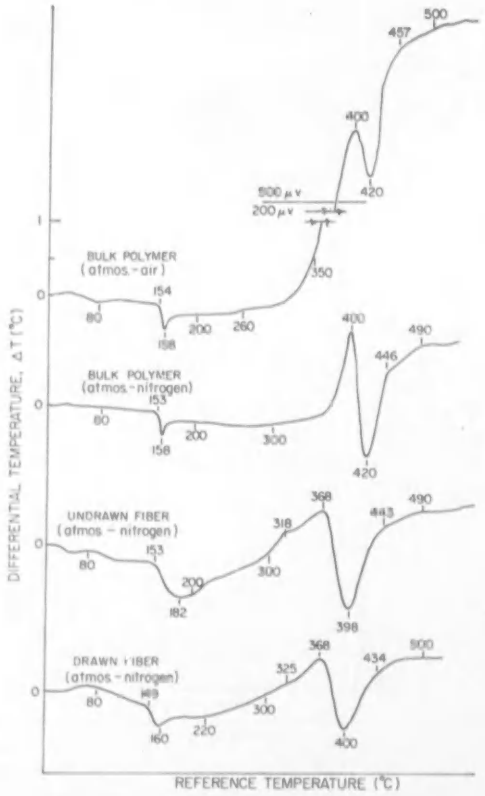

Fig. 11. DTA curves of polycarbonate bulk polymer and fiber.

In order to facilitate the comparison of gas diffusion DTA with dynamic gas flow DTA, data on the temperatures and heights of fusion peaks and decomposition peaks are presented in Table IV. The results show that in every instance save one the peak heights obtained under dynamic gas flow conditions are increased about 45% over the gas diffusion peak heights. However, peak temperatures are quite comparable. It is also apparent by inspection of the various DTA curves shown herein that in the case of dynamic gas flow generally sharper major peaks are obtained but that the resolution of small peaks is not very different from those obtained under gas diffusion conditions.

The curves for polycarbonate bulk polymer (Lexan-General Electric Corp.[23]) and experimental fibers made therefrom are shown in Figure 11. The glass transition T_g is reported to be 145 to 150° C. and it is difficult to induce crystallization in the polymer.[24,25] In the case of partially crystalline samples the melting point has been reported as 267°C.[24] DTA

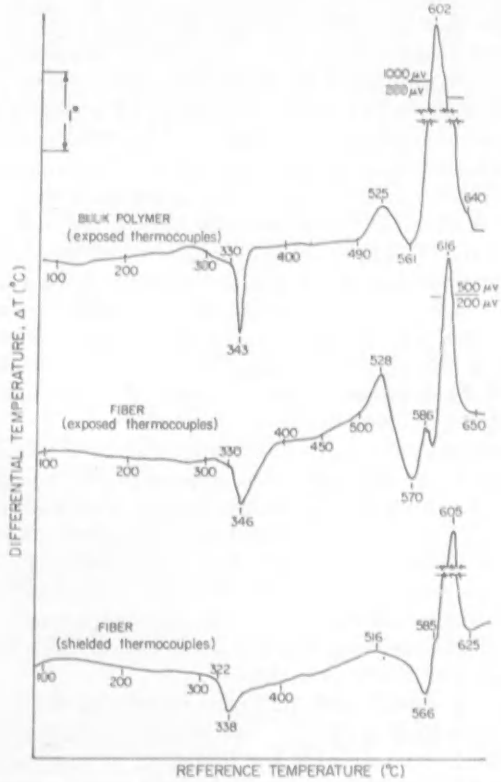

Fig. 12. DTA curves of Teflon bulk polymer and fiber (10°C./min.-nitrogen atmospheres).

curves of the bulk polymer in air and nitrogen show a T_g of about 153°C. but there is no evidence of subsequent crystallization or melting. The effect of oxidation can be seen in the air curve with a strong exothermic process beginning around 300°C. which is interrupted by an endothermic decomposition process with a peak at 420°C. followed by further oxidation of the decomposition products. In nitrogen the same pattern is found except for the lack of any significant exothermic process after decomposition. The occurrence of the same endothermic decomposition process suggests thermal depolymerization.

The DTA curves of fiber samples indicate significant changes from the bulk polymer which may involve the effects of the spinning process. The shape of the T_g is different in that no endothermal peak is present and the change in the base line is more gradual. The shape of the T_g in the DTA curve has been discussed by Wunderlich and Bodily[26] who have proposed

that the configuration of T_g is governed by the rate at which the polymer melt is cooled. The undrawn fiber shows the larger T_g change as might be expected on the basis that the drawn fiber should be partially crystalline thus reducing the magnitude of the T_g change. However, the drawn fiber curve shows no evidence of a melting peak so that this sample is indicated to have little or no crystalline structure. An exothermic process around 320°C is not found in the bulk polymer curve. The decomposition peak temperature (400°C.) is also significantly lower than that of (420°C.) the bulk polymer which may reflect chain damage during processing.

In Figure 12 the DTA (gas diffusion apparatus) curves of Teflon* bulk polymer and fiber are shown. Teflon is reported to have a transition at 327°C. that involves a loss in crystallinity.[27] Grassie[19] reports thermal degradation around 600°C and Madorsky and Strauss[28] found only 17% volatilization at 500°C. for 30 min. Various pyrolysis studies[19,28–30] have indicated depolymerization to monomer, C_2F_4, with subsequent formation of secondary reaction products C_3F_6 and C_4F_8.

The DTA curves show a sharp endotherm with a peak at 343°C. for the bulk polymer and a broad, asymmetric endotherm with a peak at 346°C. for the fiber. These transitions involve the loss of crystallinity and the asymmetric peak for the fiber may indicate a second reaction due to disorientation since Teflon fibers are said to be highly oriented. This transition is followed by an exothermic process with a major endothermic decomposition beginning about 530°C. with a peak around 560–570°C. due to free radical depolymerization of the polymer. This endotherm is followed by major exothermic reactions.

In the fiber case a small exothermic reaction is found at 585°C. with the main exotherm peaking at 616°C. The presence of exothermic reactions in an inert atmosphere suggests the formation of covalent bonds, e.g. the formation of new products. Thus, the DTA curves show exothermic peaks following depolymerization reflecting the formation of secondary reaction products described by Lewis and Naylor[29] and others.[19,28]

Conclusions

The results show that DTA is a highly useful method for the unambiguous characterization of synthetic fibers from low temperature transitions through decomposition. It is shown that DTA can detect changes resulting from the conversion of bulk polymers into fibers as well as reveal certain changes in fiber fine structure due to further processing.

A good correlation was found between DTA results and data on the thermal degradation behavior of fiber-forming polymers from more conventional methods. Thus, DTA can provide "thermal spectra" that not only serve as fiber "fingerprints" but are also interpretable in terms of molecular rearrangements, depolymerization, new product formation, and other chemical changes that occur during the thermal degradation of synthetic textile materials.

* Du Pont trademark.

It has also been shown that increasing the rate of heating from 1 to 10°C./min. causes the peak temperatures for polymer crystallization and decomposition to increase significantly whereas the glass transition and melting temperatures are not greatly affected although a tendency to increase somewhat at high rates of heating was observed.

The authors are grateful to Mr. Harold Lambert for assistance in the design and construction of DTA apparatus.

The support of this work by a group of Textile Research Institute member firms as sponsors of a project on thermoanalysis is gratefully acknowledged. Special thanks are due to the Du Pont Company, Allied Chemical Corp., and the Dow Chemical Co., for special fiber and polymer samples. The authors also thank Fabric Research Laboratories for samples of polycarbonate fiber.

References

1. Schwenker, R. F., Jr., L. R. Beck, Jr., and W. J. Kauzmann, Navy Contract N140-(132)57442B, Final Report, February 1960.
2. Schwenker, R. F., Jr., and L. R. Beck, Jr., *Textile Res. J.*, **30**, 624 (1960).
3. Schwenker, R. F., Jr., and J. H. Dusenbury, *Textile Res. J.*, **30**, 800 (1960).
4. Schwenker, R. F., Jr., L. R. Beck, Jr., and E. Pacsu, Div. of Cell. Chem., paper No. 42, abstracts of 138th ACS Mtg., New York, September 1960.
5. White, T. R., *Nature*, **175**, 895 (1955).
6. Keavney, J. J., and E. C. Eberlin, *J. Appl. Polymer Sci.*, **3**, 47 (1960).
7. Ke, B., in *Organic Analysis, Volume 4*, J. Mitchell, Jr., eds., Interscience, New York, 1960, p. 361.
8. Ke, B., *J. Appl. Polymer Sci.*, **6**, 624 (1962).
9. Hay, A., paper presented at the Eleventh Canadian High Polymer Forum, September 1962.
10. Gordon, S., and C. Campbell, *Anal. Chem.*, **27**, 1102 (1955).
11. Whitehead, W. L., and I. A. Breger, *Sci.*, **111**, 279 (1959).
12. Lodding, W., and L. Hammel, *Rev. Sci. Instr.*, **30**, 885 (1959).
13. Stone, R. L., *Anal. Chem.*, **32**, 1583 (1960).
14. Smothers, W. J., and Y. Chiang, *Differential Thermal Analysis*, Chemical Publishing Co., New York, 1958.
15. Vassallo, D. A., and J. C. Harden, *Anal. Chem.*, **34**, 132 (1962).
16. Mackenzie, R. C., and B. D. Mitchell, *Analyst*, **87**, 420 (1962).
17. Ward, I. M., *Textile Res. J.*, **31**, 650 (1962).
18. Hess, K., and E. Steurer, *Z. Physik Chem.*, **A193**, 234 (1944).
19. Grassie, N., *Chemistry of High Polymer Degradation Processes*, Interscience, New York, 1956, p. 110.
20. Schwenker, R. F., Jr., and J. C. Whitwell, *Textile Res. J.*, **23**, 804 (1953).
21. Strauss, S., and L. A. Wall, *J. Res. Natl. Bur. Std.*, **60**, 39 (1958).
22. Madorsky, S. L., S. Strauss, D. Thompson, and L. Williamson, *J. Polymer Sci.*, **4**, 639 (1949).
23. Christopher, W. F., *Plastics Engr. J.*, **14**, 31 (1958).
24. Freeman, H. I., and M. J. Coplan, *Some Properties of Polycarbonate Fibers*, paper presented at 33d Annual Meeting, Textile Research Institute, New York, March 1963.
25. Krum, F., and F. H. Müller, *Kolloid Z.*, **164**, 81 (1959).
26. Wunderlich, B., and D. M. Bodily, *J. Polymer Sci.*, **C6**, 137 (1964).
27. Roff, W. J., *Fibers, Plastic and Rubbers*, Butterworths, London, 1956.
28. Madorsky, S. L., and S. Strauss, *J. Res. Natl. Bur. Std.*, **66A**, 401 (1962).
29. Lewis, E. E., and M. A. Naylor, *J. Am. Chem. Soc.*, **69**, 1968 (1947).
30. Goldfarb, I., R. J. McHenry, and E. C. Penski, *J. Polymer Sci.*, **58**, 1283 (1962).

Résumé

On a étudié l'application de l'analyse différentielle thermique (DTA) à la caractérisation et à l'étude de la dégradation thermique de fibres synthétiques, y compris les fibres de polyester, nylon-6, le polypropylène et le polytétrafluoroéthylène. On a employé des appareils DTA, construits au laboratoire, dans le domaine de température de 50°C à 650°C. On discute les considérations et techniques expérimentales, et les variables comme la préparation et la grandeur de l'échantillon, le contrôle de l'atmosphère et la vitesse de chauffage ont été étudiés. On a trouvé que la technique conventionnelle d'écraser ou de moudre les échantillons DTA donne lieu à des changements significatifs pour certains échantillons, plus spécialement dans le cas de films non-étirés. Le contrôle de l'atmosphère de l'échantillon par un courant gazeux dynamique à travers de la cellule de l'échantillon, donne des pics qui sont, en général, plus nets et plus étroits que ceux trouvés lors du contrôle par diffusion gazeuse. On donne des résultats pour différentes transitions à basse température trouvées dans ces films. On a trouvé des différences significatives entre des transitions à basse température entre le polypropylène fibreux et le polymère en bloc et également pour les fibres de nylon-6 étirées et non-étirées. On discute l'interprétation des courbes DTA pour la décomposition et d'autres réactions à des températures élevées. Par le nylon-6 et le polypropylène, on ne constate que des réactions endothermiques, ce qui indique un processus de dépolymérisation, tandis que les autres fibres montrent dans le domaine de décomposition des réactions endothermiques et exothermiques.

Zusammenfassung

Die Anwendung der Differentialthermoanalyse (DTA) zur Charakterisierung des thermischen Abbaus von synthetischen Textilfasern, nämlich Polyester-, Nylon-6-, Polypropylen- und Polytetrafluoräthylenfasern, wurde untersucht. Der Temperaturbereich des im Laboratorium gebauten Apparates erstreckte sich von 50°C bis 650°C. Die experimentellen Grössen und Verfahren werden diskutiert und Probenbereitung, Gröss, Zellpackung, kontrollierte Atmosphäre und Erhitzungsgeschwindigkeit als Variable untersucht. Das übliche Verfahren des Zerreibens oder Mahlens von DTA-Proben ruft bei gewissen Proben, besonders bei nicht gereckten Fasern, wichtige Veränderungen hervor. Die Kontrolle der Probenatmosphäre durch dynamische Gasströmung durch die Probenzelle lieferte im allgemeinen schärfere und grössere Maxima als bei Kontrolle durch Gasdiffusion. Die Daten der verschiedenen in den Fasern festgestellten Tieftemperaturumwandlungen werden angegeben. Wichtige Unterschiede bei den Tieftemperaturumwandlungen ergaben sich zwischen der Polypropylenfaser und dem unverarbeiteten Polymeren sowie zwischen gereckten und ungereckten Nylon-6-Fasern. Die Interpretation der DTA-Kurven bei der Zersetzung und anderen Reaktionen bei erhöhter Temperatur wird diskutiert. Nylon-6 und Polypropylen zeigten lediglich endotherme, für Depolymerisationsprozesse charakteristische Reaktionen, während andere Fasern im Zersetzungsbereich endotherme und exotherme Reaktionen aufwiesen.

JOURNAL OF POLYMER SCIENCE: PART C NO. 6, PP. 17–25 (1964)

Differential Thermal Analysis of Linear Polyesters

R. M. SCHULKEN, JR., R. E. BOY, JR., and R. H. COX, *Research Laboratories, Tennessee Eastman Company, Division of Eastman Kodak Company, Kingsport, Tennessee*

Synopsis

Differential thermal analysis (DTA) was used to measure crystallization, melting, and glass transition temperatures of poly(ethylene terephthalate), poly-1,4-cyclohexylenedimethylene terephthalate, and some copolyesters. These values are affected in different ways by systematic changes in such factors as copolymerization, molecular block formation, crystal perfection, nucleation, thermal history, and orientation. At least two types of abnormally high melting structures were formed and identified. The stability of these polymers to thermal and oxidative degradation was studied by DTA.

Introduction

Differential thermal analysis (DTA) may be used to measure melting, crystallization, and glass transition temperatures of polyesters. Oxidative and thermal breakdown also may be measured. These thermal properties are affected by systematic variations in the molecular or crystalline structure of the polyester, which may be brought about by copolymerization, heat treatments, nucleation (by orientation or other means), or by rate of heating in the DTA measurement.

Polyethylene terephthalate (T2) and poly-1,4-cyclohexylenedimethylene terephthalate (T16) and a variety of copolyesters were studied by DTA to determine the effects of the above factors on these systems.* The basic repeating units are as follows:

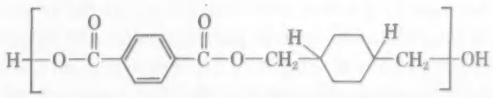

Poly 1,4-cyclohexylenedimethylene terephthalate (T16)

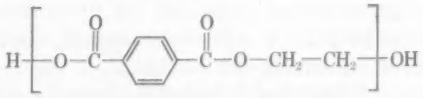

Polyethylene terephthalate (T2)

* We are indebted to C. J. Kibler and J. G. Smith, of these Laboratories, for the T2, T16, and copolyesters used in this work. The compositions of these resins were verified by NMR and infrared spectroscopy.

Ke[1] has studied some of these polymers, and the data are in good agreement where they overlap.

Experimental

The equipment used for this work has been described elsewhere by Boy, Schulken, and Tamblyn.[2] It permits the simultaneous analysis of five samples, which are usually in the form of a fine powder. Provision is made for evacuating the samples in place and for controlling the atmosphere over the samples. Sample temperatures may be accurately determined during a transition.

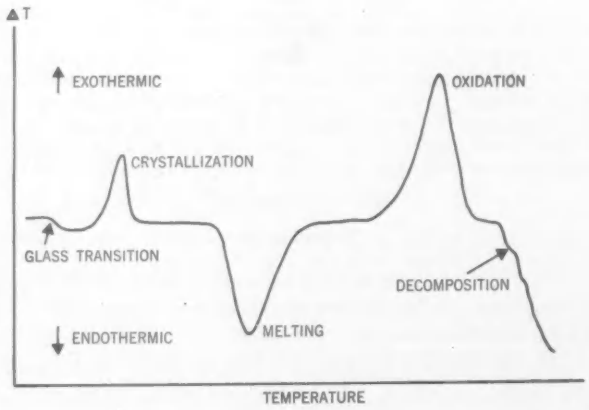

Fig. 1. Schematic DTA curve.

Figure 1 is a schematic differential thermogram which illustrates how the various thermal characteristics appear on a DTA curve. In actual practice, however, all of these characteristics are not revealed so well on a single curve. It is necessary to make slight variations in the procedure in order to show the thermal characteristic of particular interest to best advantage. Oxidation is measured on a sample of smaller than normal size, and the experiment is carried out in the presence of either oxygen or air. The other measurements are carried out in nitrogen or in vacuum. The equipment is designed for programmed cooling so that the crystallization temperature on cooling may be measured. For this measurement, obviously the cooling must be started before decomposition occurs.

The copolymers of T2 studied included the homologous series 3-, 4-, 5-, 6-, and 8-carbon linear glycols. Since the 1,4-cyclohexanedimethanol used in making T16 may exist in either a *cis* or *trans* configuration, variations in the *cis-trans* ratio were considered. Also, the effects of modification of the T16 system with isophthalic acid were studied.

Discussion of Results

Figure 2 shows how the thermal characteristics of T16 change with the variation in the *cis-trans* ratio of the glycol. T_m is the melting temperature, T_c is the crystallization temperature on cooling, $T_{c'}$ is the crystallization temperature on heating, and T_g is the glass transition temperature. For $T_{c'}$ the solid line represents values on well-quenched samples; the dotted line represents values on samples which were nucleated by orientation and hence crystallize more easily. Values for T2 are included in the margin at the right for comparison. All of these values were measured at a heating rate of 4.5°C./min. The distances between T_m and T_c and between T_g and $T_{c'}$ have been found to be qualitatively related to the nucleation or crystallization rate of the polymer. It will be observed that there is very little difference in crystallization rate throughout this range of composition.

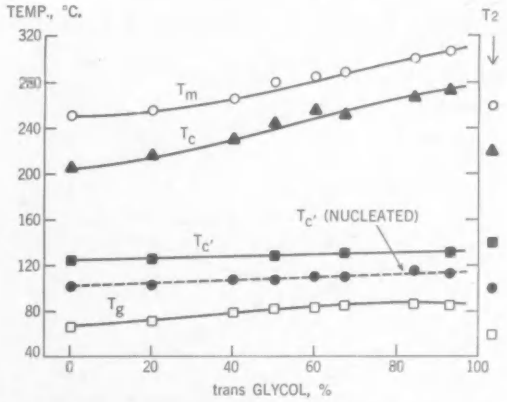

Fig. 2. Thermal properties of T16, variation in *cis-trans* ratio.

Also, there is no eutectic composition in the melting or crystallization curves. The temperature range in $T_{c'}$ and $T_{c'}$ (nucleated) for T2 is comparatively wide. Values for T_c were obtained on thoroughly melted samples which were not intentionally nucleated. To thoroughly melt, a sample must be heated well above its melting temperature. Failure to melt thoroughly may leave crystal nuclei which will raise the value of T_c.

Figure 3 shows the thermal properties of T16 modified with isophthalic acid. The T_g curve is almost horizontal, which shows that the compositions of this series of copolymers vary little with respect to the freedom of rotation of the chain. This also has been indicated by solution measurements.[3] However, the crystalline regularity of the system is greatly disturbed by the copolymerization of increased amounts of isophthalic acid. Isophthalic acid interrupts the packing efficiency of the molecules, thereby reducing crystallizability. As Figure 3 shows, on increasing the isophthalic content the melting temperature drops sharply, T_c diverges somewhat from

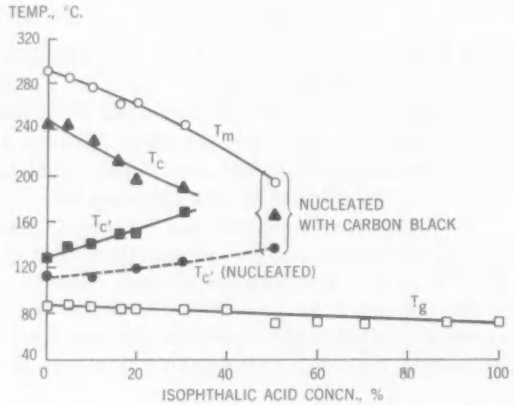

Fig. 3. Thermal properties of T16 modified with isophthalic acid.

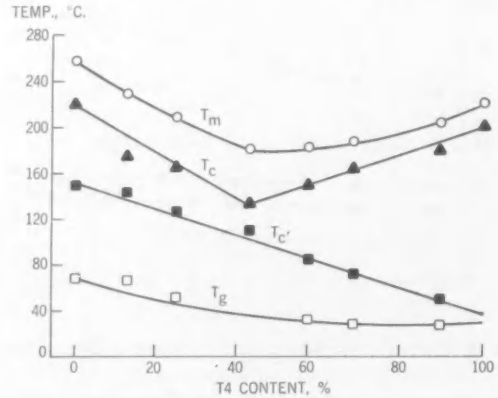

Fig. 4. Thermal properties of T2-T4 copolyesters.

T_m and $T_{c'}$ diverges from T_g. If the copolymer contains more that 35% isophthalic acid, crystallization can be obtained only by artificial nucleation techniques. We have used specialized nucleation techniques to obtain crystallization in copolymers of T16 containing up to 70% isophthalic acid. Isophthalic acid has a similar effect when copolymerized with T2 except that an equal amount produces a greater effect on T2. Copolymers of T2 with isophthalic acid do not crystallize normally if the isophthalic acid content is greater than 25%.

Figure 4 shows the thermal properties of T2 modified with 1,4-butanediol. There is an eutectic in the T_m and T_c curves in the copolymer containing polytetramethylene terephthalate (T4) at about 45% T4. T4 appears to crystallize more rapidly than T2 although T2 melts at a higher temperature.

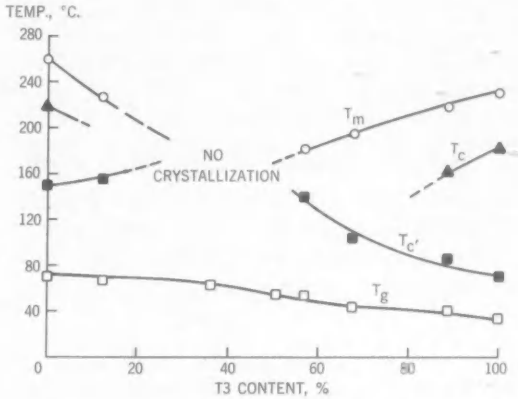

Fig. 5. Thermal properties of T2-T3 copolyesters.

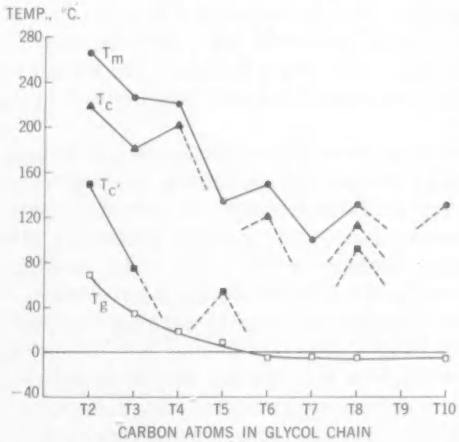

Fig. 6. Thermal properties of polymers of terephthalic acid and a homologous series of glycols.

Note that crystallization occurs readily throughout the range of compositions.

Figure 5 shows the thermal properties of T2 and 1,3-propanediol co polyesters. Polytrimethylene terephthalate (T3) has less effect on the T_g curve than T4. However, the odd numbered carbon atom segment in the 1,3-propanediol apparently does not fit the crystal lattice of T2 and thus has a very marked effect on the crystallization of the copolymers. T3 itself crystallizes very readily, but in the range of 20 to 50% T3 no crystallization occurs. Copolymers of T2 and T16 also do not crystallize in the middle ranges of composition.

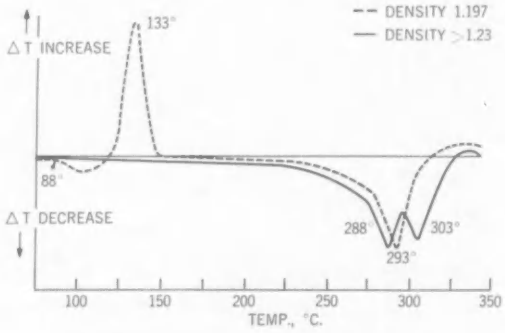

Fig. 7. Thermogram of T16 (70% *trans*).

Figure 6 shows the thermal properties of polymers of terephthalic acid and a homologous series of glycols. T_g decreases monotonically with increasing chain length of the glycol though it tends to level off for the higher glycols. Other thermal properties also decrease with increasing chain length of the glycol but in a zig-zag fashion. The T4 and polyhexamethylene terephthalate (T6) crystallized even when quenched rapidly from the melt.

Table I shows the effect of heating rate on the DTA curve of T16. T_g is sensitive to heating rate only at fast rates of heating, whereas T_m is sensitive to heating rates only at extremely slow rates of heating. $T_{c'}$ is very sensitive to heating rates, showing that nucleation is very definitely a rate phenomenon within the time required for running a DTA curve. T_c was also found to be sensitive to the heating rate. Low molecular weight polymers crystallize more rapidly than high molecular weight polymers. T_m increases at a very slow heating rate because the polymer anneals spontaneously to a more perfect crystal structure (the crystalline structure has fewer defects) with a high melting point.[4]

Figure 7 shows the beginning of the formation of such an improved crystal structure for T16 (70% *trans*). The sample showing the twin melting peak had been annealed for a short time at 289°C. (slightly below the normal T_m). By using a longer heating time or by very slowly heating up to 295°C., the lower peak was completely eliminated and the upper peak was increased in size and temperature. Melting temperatures have been in-

TABLE I
Effect of Heating Rate on DTA of T16

Heating rate, °C./min.	T_g, °C.	$T_{c'}$, °C.	T_m, °C.
10	85	140	291
4.5	82	128	291
1	80	120	294

creased to over 310°C. by such a technique. Actually two different types of changes in the polymer structure which produce a very marked increase in the normal melting temperature of the polymer have been found.

In Table II the characteristics of these abnormally high melting polymers of T16 are compared with those of a normal polymer. The improved crystal-type polymer is generally produced by heating at a temperature close to the melting point of the polymer. The block polymer is somewhat more difficult to produce and involves the heating of a polymer containing an active catalyst at a temperature slightly above or below the melting temperature. The block polymer molecule has appreciable amounts of long blocks of *trans* T16 instead of the normal random sequence of *trans* and *cis* units.

TABLE II
Characteristics of Abnormally High Melting Crystals of T16

	Melting point, °C.				
	First cycle	Second cycle	Density	Precipitation solubility	X-ray sharpness
Normal polymer	292	293	1.23	30.2	Moderate
Block polymer	311	310	1.25	25.3	High
Improved crystal polymer	310	293	1.25	30.3	High

Both types of polymer have abnormally high melting points, abnormally high densities, and high x-ray diffraction pattern sharpness. The differences in density are very significant. They correspond to an increase in degree of crystallinity from 45% in the normal polymer to 65% in the the high-melting variety. The actual differences in these polymers have been deduced by extensive studies which will not be reported here. However, two simple methods for differentiating these two types of polymers are shown in Table II: (*1*) the melting point of the improved crystal-type polymer is reduced to a normal value on the second cycle DTA curve, whereas the block polymer is unchanged by melting if the catalyst is inactive, and (*2*) a precipitation-solubility method[5] shows that the chemical structure of the improved crystal-type polymer is similar to that of a normal polymer, whereas the structure of the block polymer is different. The block polymer retains its high melting point even after thorough melting, whereas the improved crystal-type polymer reverts to the normal type. The precipitation solubility is determined by dissolving the polymer in a suitable solvent and then adding nonsolvent until it precipitates. Numbers shown in Table II are arbitrary figures denoting the amounts of precipitant required to cause the polymer to precipitate. The solvent-precipitant system was especially chosen to show composition differences, not molecular weight differences. These values show that the normal polymer and improved crystal polymer are identical chemically. The block polymer is less soluble than these two polymers. Heating the block poly-

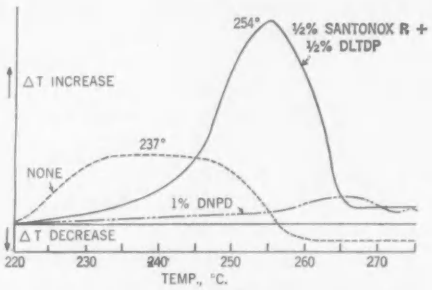

Fig. 8. Oxidative stability of stabilized T16.

mer under ester-interchange conditions changes its precipitation behavior and melting temperature to those of the normal polymer. This involves heating the polyester with an active catalyst.

Abnormally high melting materials of the improved crystal type have been observed in all crystalline polymers we have studied, including polyesters, polyolefins, isotactic polystyrene, and polyamides. Some polyamides appear to produce the widest range of melt temperatures (over 40°C.) and to form the high-melting variety most easily. However, a given sample of T2 with a normal melting point of 252°C. has produced polymers melting from 245 to 280°C. Low molecular weight polymers are particularly susceptible to formation of high-melting crystals.

Figure 8 shows how the oxidative stability of T16 may be studied. Data are shown for the unstabilized polymer and for two stabilized compositions. These curves were obtained on samples analyzed in oxygen with the temperature increased at a rate of 2°C./min. Note the different shapes of the curves and the marked improvement in oxidation resistance imparted by the *N,N'*-di-2-naphthyl-*p*-phenylenediamine (DNPD). DLTDP is dilauryl 3,3'-thiodipropionate.

The studies reported in this paper show how differential thermal analysis may be used to measure a variety of thermal characteristics of polymers. These properties are important in determining processing techniques and the uses of the polymer. Thermal analyses may be used to elucidate molecular and crystal structure problems also. However, certain precautions are necessary to assure reliable interpretation of results.

References

1. Ke, B., *J. Appl. Polymer Sci.*, **6**, 624 (1962).

2. Boy, R. E., R. M. Schulken, Jr., and J. W. Tamblyn, *Crystallinity in Secondary Cellulose Esters*, paper presented at the 142nd National Meeting of the American Chemical Society, Atlantic City, N. J., Sept. 9–14, 1962.

3. Moore, L. D., *Comparison of Solution Properties of Polyethylene terephthalate and Poly-1,4-cyclohexylenedimethylene terephthalate*, paper presented at the 137th National Meeting of the American Chemical Society, Cleveland, Ohio, April, 1960; and private communication.

4. Coste, J., *Ind. Plastiques Mod.* (*Paris*), **9**, 37 (1957).
5. Morey, D. R., and J. W. Tamblyn, *J. Appl. Phys.*, **16**, 419 (1945).

Résumé

L'analyse thermique différentielle (DTA) a été employée pour mesurer les températures de cristallisation, de fusion et de transition vitreuse du poly(éthylène-téréphtalate) du poly(1,4-cyclohexylène-diméthylène téréphtalate), et de quelques copolyesters. Ces valeurs sont affectées de différentes manières en apportant des changements systématiques dans des facteurs comme la copolymérisation, la formation de blocs moléculaires la perfection du cristal, le phénomène d'initiation du cristal, l'histoire thermique et l'orientation. Au moins deux types de structures à point de fusion anormalement élevé, ont été formés et identifiés. La stabilité de ces polymères du point de vue de la dégradation thermique et par oxydation a été étudiée par DTA.

Zusammenfassung

Differentialthermoanalyse (DTA) wurde zur Messung der Kristallisations-, Schmelz- und Glasunwandlungstemperaturen von Polyäthylenterephthalat, Poly-1,4-cyclohexylendimethylenterephthalat und einigen Copolyestern angewendet. Die Werte werden durch systematische Änderungen einiger Faktoren, wie Copolymerisation, Molekülblockbildung, Kristallvollkommenheit, Keimbildung, thermische Vorgeschichte und Orientierung in verschiedener Weise beeinflusst. Mindestens zwei abnormal hoch schmelzende Strukturtypen wurden gebildet und identifiziert. Die Beständigkeit der Polymeren gegen thermischen und oxydativen Abbau wurde mittels DTA untersucht.

JOURNAL OF POLYMER SCIENCE: PART C NO. 6, PP. 27–32 (1964)

Thermal Analysis of Polyurethane Elastomers

PHILIP E. SLADE, JR., and LLOYD T. JENKINS,
Chemstrand Research Center, Inc., Durham, North Carolina

Synopsis

Differential thermal analysis and thermogravimetric analysis were used to evaluate the thermal properties of several types of polyurethane elastomers. The composition of the polymers investigated was changed by varying the substrate, or soft segment, diisocyanate and extender. The data indicated that within the limits of the compositions under study, polyurethanes were thermally stable to their melting points, however, above the melt they were susceptible to oxidation unless stabilized by the addition of an antioxidant. On the differential thermograms the absence of a pronounced endothermic peak at the melting point, characteristic of non-crystalline polymers, was observed. The decomposition of polymers made with 4,4′-diphenylmethane diisocyanate (MDI) occurred above 400°C. and was at least a two-step process, while the decomposition of polymers containing toluene diisocyanate (TDI) occurred below 400°C. and appeared to be a one-step reaction.

Although the number of literature reports on the thermal analysis of polymers has increased rapidly during the past few years, these techniques have not been frequently used to study synthetic elastomers. Differential thermal analysis has been utilized to investigate the state of cure,[1] ethylene–propylene elastomers,[2] and fluoroelastomer systems.[3]

However, there is no reported thermal data on polyurethanes, either differential thermal analysis (DTA) or thermogravimetric analysis (TGA).

In this paper both DTA and TGA data for five typical polyurethane systems is presented, where composition has been changed by varying substrate, isocyanate and extender.

The general method[4] of preparing the type of polymer used in this study is to react a polyester or polyether with a diisocyanate, either in solution or in bulk, to form a prepolymer, or as the case may be, a "capped" polyester or polyether. That is, the terminal positions would be occupied by an isocyanate. This prepolymer is then "extended" into a polyurethane by reaction with either a diamine or diol. It is believed that the commercial polymers used in this study were prepared by this method.

All of the equipment used in this work was designed and built at the Chemstrand Research Center. The DTA unit utilizes a Leeds and Northrup Speedomax X-Y recorder, a F & M Model 40 temperature programmer and a Leeds and Northrup Model 9835-A stabilized dc microvolt amplifier as a preamplifier between the differential thermocouple and the x input of

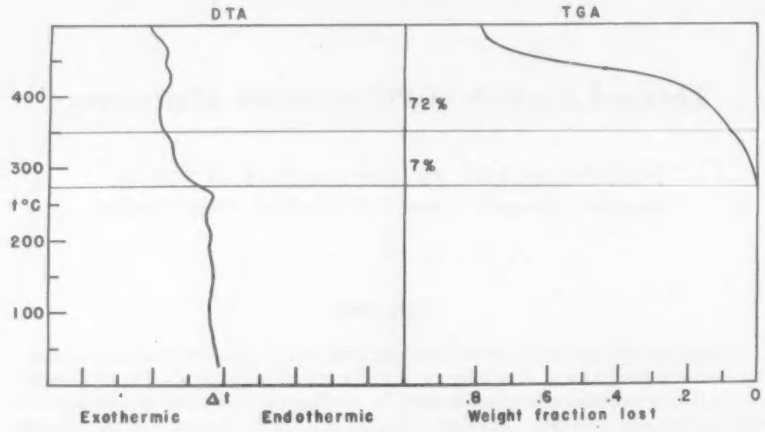

Fig. 1. Thermograms for a polyurethane of the composition: polyether-MDI-aliphatic diamine.

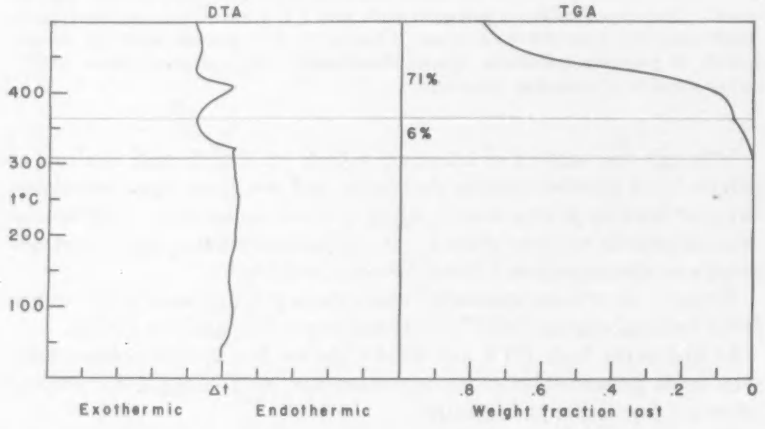

Fig. 2. Thermograms for a polyurethane of the composition: polyester-MDI-aromatic diamine.

the recorder. A Hoskins tube furnace is used as the heater. The use of two furnaces was helpful in eliminating cool down times.

Nickel cells with $^3/_8$ in. diameter sample wells were employed. About 150 mg. of sample, in fiber form, was cut into lengths not exceeding $^1/_8$ in. and mixed with powdered quartz as a diluent. Quartz, also used in the reference well, was selected as the inert material because its particle size tends to suspend fiber samples more uniformly than alumina. Inert atmosphere was maintained by flushing the furnace cavity with nitrogen at a rate of about six liters per minute. The heating rate was 11°C./min.

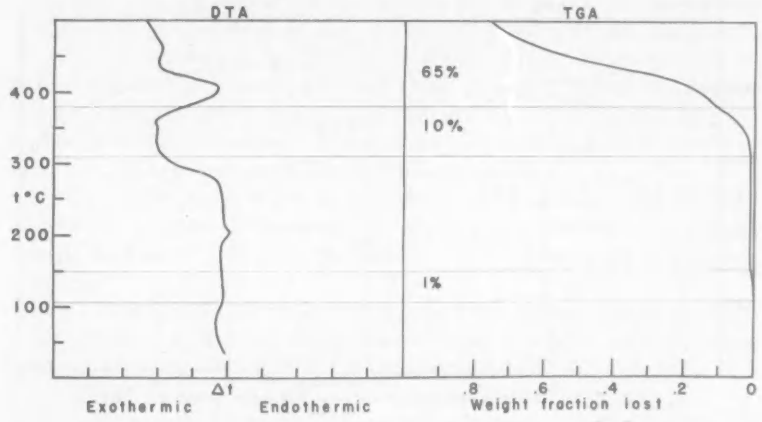

Fig. 3. Thermograms for a polyurethane of the composition: polyester-MDI-diol.

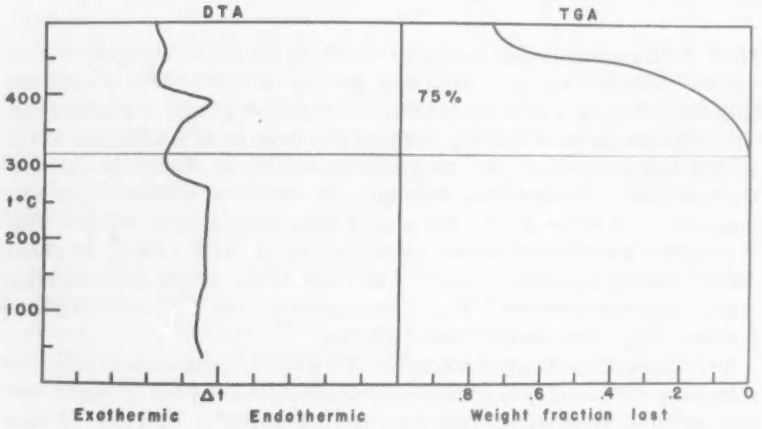

Fig. 4. Thermograms for a polyurethane of the composition: polyester-TDI-aromatic diamine.

The TGA apparatus also uses a L & N X-Y recorder and a F & M Model 40 programmer. Weight change was observed with a Minnesota Instrument Co. electronic balance. A stainless steel rod was inserted into a tube provided in the balance and extends into the furnace. The fiber samples of about 1 g. each were placed in a small quartz tube that fits a cup atop the stainless rod. A Vicor jacket protected the furnace windings and provided a means for collecting off gases from the decomposition reaction.

Comparative DTA and TGA data are presented by Figure 1 for a composition consisting of a polyether substrate, or soft segment, 4,4′-diphenylmethane diisocyanate (MDI) and an aliphatic diamine extender. The

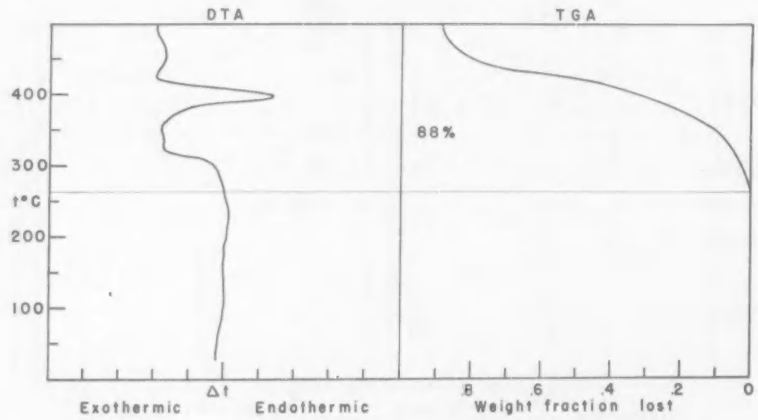

Fig. 5. Thermograms for a polyurethane of the composition: polyester-TDI-aromatic diamine.

DTA thermogram shows two very small endothermic changes, one at 150°C. which has not been identified, and one at 205°C. that is identical with the softening or stick temperature observed on a thermal gradient bar. This polymer melts at 260°C., and probably because of residual air in the sample wells, some oxidative degradation occurs, as shown by the exothermic drift. Weight loss, beginning at 280°C. is attributed to this oxidation. At about 325°C., the second decomposition step begins. This is probably due initially to the decomposition of MDI. Later, at about 400°C., depolymerization begins, with most of the weight loss occurring above that temperature. The percentages on the TGA thermograms indicate the per cent weight loss in each step.

On Figure 2, the thermal properties of a polymer containing a polyester substrate, MDI, and an aromatic diamine extender are shown. Again, two very small endothermic changes are seen, one at 100°C. that has not been identified (although one would suspect that this was loss of adsorbed water, TGA shows no weight loss in this region) and a very gradual change with the maximum deflection occurring at about 250°C. This, too, corresponds with polymer softening. The polymer melts at 320°C., with the same type of oxidative degradation seen after melting. Initial weight loss, beginning at about 310°C. is again believed to be due to oxidation. The second decomposition step started at 365°C. and is thought to be similar to that process described for the polymer shown in Figure 1, that is, isocyanate decomposition followed by depolymerization at temperatures above 400°C.

On Figure 3, thermograms for a polymer of slightly different compositions is shown. A polyester and MDI were used to prepare the prepolymer, but it was extended with a diol instead of a diamine. Only one small endotherm is present below the melting point. at 110°C. Since this cor-

responds with a 1% weight loss as shown by the TGA, it is probably due to vaporization of adsorbed water. The melting point of this polymer is 203°C., but it differs in its behavior in the melt from the other samples, as oxidation does not start until it is heated to about 75° above the melting point. This polymer, however, contained an antioxidant, which accounts for the observed differences. The same two-step decomposition, shown by Figures 1 and 2, is again exhibited by this composition.

Two other samples were investigated, where another diisocyanate, toluene diisocyanate (TDI) was used. The compositions were very similar, that is, both were made with polyesters, TDI, and aromatic diamine extenders.

Figure 4 indicates that there were no significant changes below the melt, which occurred at 265°C. Weight loss begins at 320°C., with only one apparent decomposition step and with the principal DTA depolymerization below 400°C., in contrast with the polymers made with MDI.

The next polymer, Figure 5, shows no well defined melting point, but softens at about 250°C., and begins to lose weight at once, at 260°C. Again, the main decomposition occurs below 400°C. and is a one step process.

Several conclusions may readily be made on inspection of the thermograms. The slight increase in thermal stability of the MDI based polymers is seen on both DTA and TGA. The depolymerization endotherms for all of these samples (Fig. 1, 2, and 3) are above 400°, while the depolymerization of the polymers containing TDI is below that temperature. This is in agreement with the decomposition of the isocyanates alone, TDI decomposing at a lower temperature than MDI.

The effect of extender is most noticeable when contrasting aliphatic and aromatic compounds. Although these materials exhibit no crystallinity, as determined by x-ray diffraction patterns on film, some degree of order is shown by the areas of the DTA melting point endotherms on Figures 1 and 3. These compositions, both with aliphatic extenders, have larger peak areas than the aromatic extended polymers.

The value of DTA as a technique for evaluating stabilizers has also been observed. The greatly increased melt stability of the compound of Figure 3, which contained an antioxidant, is shown very clearly.

In summary, five different compositions of elastomeric polyurethanes have been investigated by DTA and TGA. The results indicate that polymers made with MDI decompose in a two-step reaction while those prepared using TDI have a one-step decomposition that occurs at a slightly lower temperature than the MDI samples. The effect of stabilizers on polymer melt was also observed.

References

1. Bhaunik, M. L., A. K. Sircar, and D. Banerjee, *J. Appl. Polymer Sci.*, **4**, 366 (1960).

2. Knox, J. R., paper presented at the 140th Meeting, American Chemical Society, Chicago, September, 1961.

3. Paciorek, K. L., W. G. Lajiness, and C. T. Lenk, *J. Polymer Sci.*, **60**, 114 (1962).
4. Rinke, H., *Chimia*, **16**, 93 (1962).

Résumé

Des analyses thermiques différentielles et thermogravimétriques ont été utilisées pour évaluer les propriétés thermiques de divers types d'élastomères de polyuréthanne. La composition des polymères examinés a été modifiée en variant le substrat, ou segment mou, le diisocyanate et l'extenseur. Les résultats indiquaient que dans les limites de composition étudiées, les polyuréthannes étaient thermiquement stables jusqu'à leur point de fusion, tandis qu'au-dessus de la fusion, ils étaient susceptibles d'être oxydés à moins qu'ils ne soient stabilisés par l'adjonction d'un antioxydant. On a noté dans les thermogrammes différentiel l'absence, au point de fusion, d'un pic endothermique, caractéristique des polymères noncristallins. La décomposition des polymères effectuée sur le diisocyanate de 4,4′-diphényl-éthane (MDI) a eu lieu au-dessus de 400°C et procédait par deux étapes au moins, tandis que pour les polymères contenant le diisocyanate de toluène (TDI) elle avait lieu au-dessous de 400°C et semblait procéder par une réaction eu une étape.

Zusammenfassung

Zur Ermittlung der thermischen Eigenschaften einiger Polyurethanelastomertypen wurde die Differentialthermoanalyse sowie die thermogravimetrische Analyse herangezogen. Die Zusammensetzung der untersuchten Polymeren wurde durch Variierung des Substrats, oder weichen Segments, des Diisocyanats und des Extenders verändert. Innerhalb des untersuchten Zusammensetzungsbereiches erwiesen sich die Polyurethane bis zu ihrem Schmelzpunkt als thermisch stabil, oberhalb des Schmelzens waren sie jedoch, ausser bei Stabilisierung durch Zusatz eines Antioxydans, gegen Oxydation empfindlich. Bei den Differentialthermogrammen fehlte, wie es für nichtkristalline Polymere charakteristisch ist, ein deutliches endothermes Maximum. Die Zersetzung der mit 4,4′-Diphenylmethandiisocyanat (MDI) hergestellten Polymeren trat oberhalb 400°C ein und war zumindest ein Zweistufenprozess, während die Zerstzung von Toluoldiisocyanat (TDI) enthaltenden Polymeren unterhalb 400°C ablief und eine Einstufenreaktion zu sein scheint.

JOURNAL OF POLYMER SCIENCE: PART C NO. 6, PP. 33–41 (1964)

The Specific Heat of Poly-1-butene

H. WILSKI and T. GREWER, *Farbwerke Hoechst AG., vormals Meister Lucius & Brüning, Frankfurt/Main-Hoechst, Germany*

Synopsis

The specific heat and the specific volume of the different crystal modifications of poly-1-butene were investigated. Modification III, the crystalline structure of which is still unknown, was obtained by precipitating the benzene solution with methyl acetate. At 101°C. it is transformed into the tetragonal phase which melts at 121.5°C. The specific heat of the rhombohedric structure, which was obtained from the melt by cooling and storage over a long period, increased evenly with a rise in temperature up to its melting point; by immediately measuring a freshly cooled melt, the specific heat of the tetragonal modification (at least above 80°C.) was obtained. A predominantly atactic material which had been stored for a long period, indicated the melting at 87°C. of the small fraction of the rhombohedric crystals. The investigations were supplemented by dilatometric measurements. By means of the degree of crystallinity thus obtained, the heats of fusion were calculated and compared with values from measurements conducted on the melting point depression of mixtures.

Introduction

Isotactic poly-1-butene has recently been the subject of numerous investigations.[1–7] In certain solvents poly-1-butene crystallizes in a yet unclarified form III. On cooling, the melt of the pure poly-1-butene at first forms a tetragonal crystalline structure which is to some extent stable only above 80°C. and below −20°C. At room temperature the tetragonal form is rearranged into a more densely packed rhombohedric modification. This process takes place as a first order reaction at 20°C. and has a half-life of about 4 hr. in the case of well formed crystals (cooled slowly), and about 7 hr. for poorly formed crystals (quenched in ice water) (Table I).[6]

TABLE I
Half-Life (hr.) of Poly-1-butene Rearrangement at 20°C.

Method of measurement	Well crystallized	Poorly crystallized
X-ray	3.8	7.0
Dilatometric	4.1	6.3

The tetragonal modification is very sensitive to mechanical action; by applying pressure or stress at any temperature, it can momentarily be rearranged into the rhombohedric phase. In this paper the dependency

of the specific heats of the different crystal modifications on the temperature will be examined.

Experimental

The specific heats were measured with an adiabatic calorimeter similar to that of Nölting.[11] Instead of using silver dishes for the polymer, an aluminium block with many holes was employed.[12] The polybutene was filled into these holes. In order to extend the measurements to lower temperatures, a cooling jacket was fitted in place of the heating jacket. The refrigerant used was methanol from a low temperature thermostat. All measurements were taken under pure nitrogen at a pressure of 20 mm. Hg.

The specific volumes were measured by dilatometers similar to those of Ueberreiter and Kanig,[13] and Wilski.[14] Only two days were needed to obtain a volume curve.

A polarizing microscope with heating stage (Leitz/Wetzlar) served for the melting point determinations of certain mixtures. The heating rate was 1°C./10 min. The solvents used were highly purified α-chloronaphthalene and dibutyl maleate. For the determination of the heat of fusion by the method of Flory and Mandelkern,[15] mixtures of appropriate composition were fused together under nitrogen at 150°C. and were then slowly cooled in a block of diatomaceous earth previously heated to 150°C.

The isotactic poly-1-butene was made with Ziegler catalysts in hexane.[8] The raw product was purified by dissolving it at 130°C. in isoamyl acetate (with 0.1% phenyl-β-naphthylamine) under nitrogen. By cooling to 20°C., the pure product is separated; it was then washed several times in methanol and hexane and dried *in vacuo*. The molecular weight of the product thus obtained was relatively high. The reduced viscosity measured in decahydronaphthalene was found to be $\eta_{spec}/c = 3.69$ dl./g. (at 135°C. and 0.1 g./dl.).

A mixture of rhombohedric and modification III crystals is obtained from isoamyl acetate. To obtain modification III in the pure state, the polybutene was dissolved in benzene and then precipitated with methyl acetate. The x-ray spectrum of the pure modification III obtained in this way conforms to Figure 3 of reference (1).

For the purpose of the calorimetric measurement, the polybutene III powder was placed into the calorimeter under slight pressure. During this process a partial transition into the rhombohedric modification took place. The transformation had progressed somewhat further during the pressing of the sheet at 20°C. which was to be used for the dilatometric determination.

The atactic poly-1-butene was polymerized with a special Ziegler catalyst (titanium tetrachloride and aluminium triisobutyl).[9] For purification the raw product was dissolved in boiling hexane, and the crystalline constituents which are separated on cooling were centrifuged. The isotactic material remaining in solution was precipitated by the addition of methyl acetate. The separated solution was evaporated to dryness. The poly-1-

butene thus obtained consists of the greater part of atactic material, but the isotactic (crystallizable) fraction could not be entirely removed. The molecular weight was relatively low, $\eta_{spec}/c = 0.66$ dl./g.[10]

Results

Calorimetric Measurements

The state of the poly-1-butene powder (from benzene/methyl acetate) which is pressed into the calorimeter was not precisely known. The x-ray diagram permits a rough estimation which indicates that the crystalline fraction consists of equal parts of the rhombohedric and modification III crystals. A statement regarding the mass of the amorphous fraction is not possible. Determination of the density, which was very difficult indeed, gave values around 0.94 g./cm.^{3} ($\pm 1\%$) at 20°C.

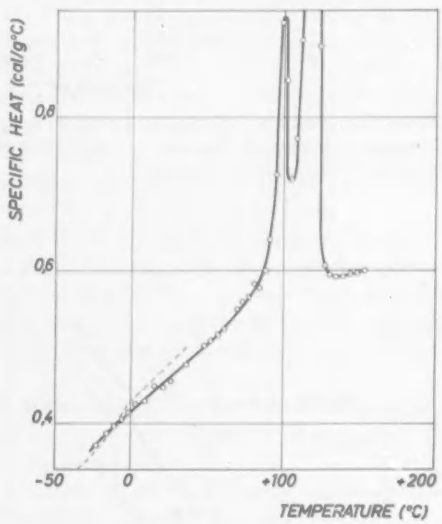

Fig. 1. Specific heat of poly-1-butene. The crystalline fraction of the sample consists in equal parts of the rhombohedric structure and the unknown modification III (at 20° C., rough estimate). Dotted curve.[2]

Figure 1 shows the result of the specific heat measurement. After a slight indication of glass transition below 0°C., the specific heat rises evenly with the temperature until 101°C. is reached. At this temperature, a transition of modification III into the tetragonal modification takes place. The height of the maximum is a measure of the magnitude of the heat of transition which can, however, not be evaluated quantitatively for the above mentioned reasons. The tetragonal modification begins to melt just above the temperature of transition. The graph by Dainton et al.,[2]

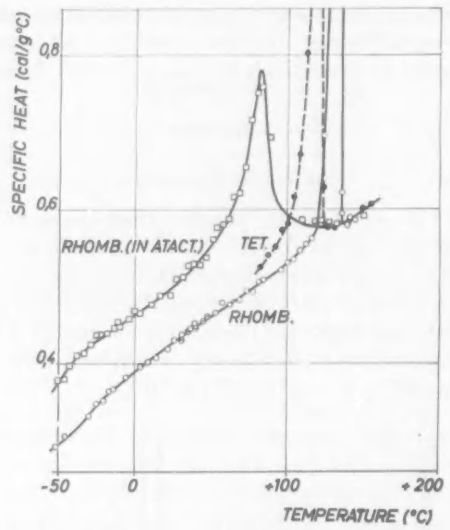

Fig. 2. Specific heat of poly-1-butene: (○) highly crystalline samples of exclusively rhombohedric; (●) exclusively tetragonal structure; (□) predominantly atactic sample containing small crystalline (rhombohedric) fraction.

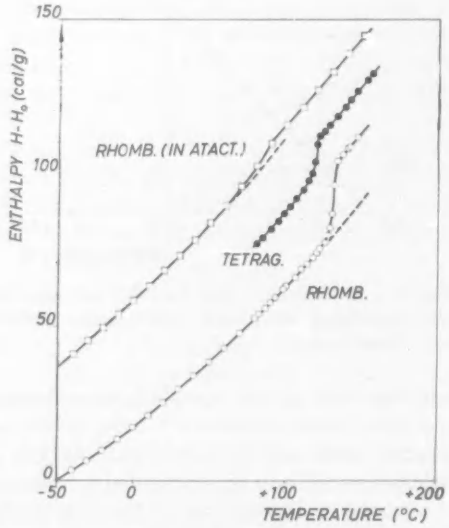

Fig. 3. Enthalpy of poly-1-butene, samples and symbols as in Figure 2. The curves have been displaced parallelly so that the graphs are all visible at a glance (dotted lines are calculated values).

which is given for comparison, agrees with ours; one may, therefore, suppose that the polybutene available to these authors was available in a modification similar to ours.

After the last measurement had been conducted on the melt, the calorimeter was switched off and allowed to cool.

Crystallization mainly took place in the slow-cooling apparatus at 98°C. After a waiting time of 150 hr. at 20°C., the temperature was reduced to −50°C. and the specific heat of the rhombohedric modification thus formed was measured. Figure 2 shows that below 0°C. a glass transition apparently takes place; however, the exact transition point cannot be determined from our measurements. A maximum in the vicinity of room temperature, which was expected in accordance with the polypropylene results[16–18] did not appear. The melting interval is remarkably clear-cut.

After the measurements conducted on the melt, the calorimeter was allowed to cool in the same way as before, but only to 80°C. Thereupon the specific heat of the tetragonal modification obtained in this way was immediately determined. This modification melts at lower temperatures than the rhombohedric form.

For comparison, the specific heat of the predominantly atactic material was also measured (Fig. 2) (sample heated to 150°C., slowly cooled as before, and aged for 150 hr. at 20°C.). This sample also did not show a low temperature maximum but only a peak at 87°C., which is explained by the melting of the crystalline rhombohedric fraction.

The enthalpies of the three samples examined were determined by graphic integration and also by summation of the electrical energy input. The results are shown in Figure 3; the zero point was chosen arbitrarily. The values for the heats of fusion given in Table II are derived from Figure 3. In this case only the value for the rhombohedric form can claim greater accuracy.

Extrapolation of the enthalpy curves was fitted to second degree polynomials determined by the method of least squares (Fig. 3, dotted line).

Rhombohedric material: $H - H_0 = 17.21 + 0.385t + 0.752 \times 10^{-3}t^2$. Rhombohedric modification chiefly in atactic material: $H - H_0 = 21.24 + 0.463t + 0.747 \times 10^{-3}t^2$. For the tetragonal modification the extrapolation was made only graphically.

TABLE II
Results with Poly-1-butene

Structure	Density at 20°C., g./cm.³	Cryst. fraction, %	Heat of fusion		Melting point, °C.
			Cal./g. of sample	Cal./monomer unit	
Rhombohedral	0.9294	76.0	22.7	1675	134.7
Rhombohedral (in atactic)	0.8795	13.0	3.6	1554	87.0
Tetragonal	0.8745	76.0[6]	13.2	974	121.5

Specific Volume Measurements

The dilatometric examination of a pressed sheet is shown in Figure 4. Its crystalline constituent was present partly in modification III and partly in rhombohedric structure. The transition is readily recognized by a distinct bend in the volume curve. A second bend at 121.5°C. indicates the melting of the tetragonal modification. A quantitative evaluation of the graph is unfortunately not possible, since the weight fractions of the various crystalline components are unknown.

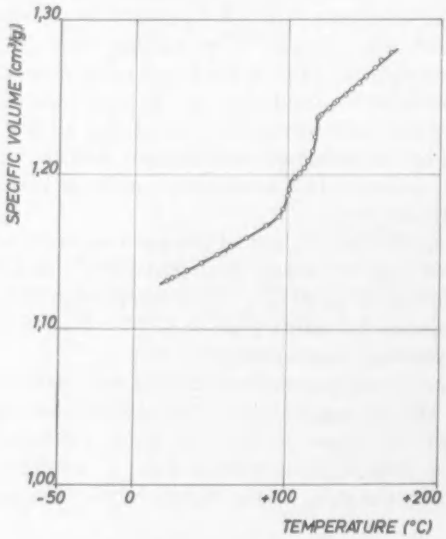

Fig. 4. Specific volume of a pressed sheet of poly-1-butene III (pressing has caused partial transition into the rhombohedric structure).

The result of the dilatometric examination of the other samples is shown in Figure 5. The samples were pretreated in the same way as for the calorimetric measurements. The crystalline fraction of the polybutene can be calculated from the volume curves in Figure 5. The specific volume of the amorphous polybutene was obtained by extrapolation of the liquid line with a second degree polynomial.[14] The specific volume of the pure crystal was taken from curve V_c in Figure 5 which was drawn from a value reported by Danusso et al. (at 30°C.).[19] Although a degree of randomness was involved in the choice of this curve, the result (Figure 6) is nevertheless quite reliable. The crystalline fraction of the poly-1-butene in its rhombohedric modification is constant over a very wide temperature range, and the melt interval is unusually narrow. Taking a value of 76% (independent of the temperature) for the crystalline fraction, the heat of fusion of the com-

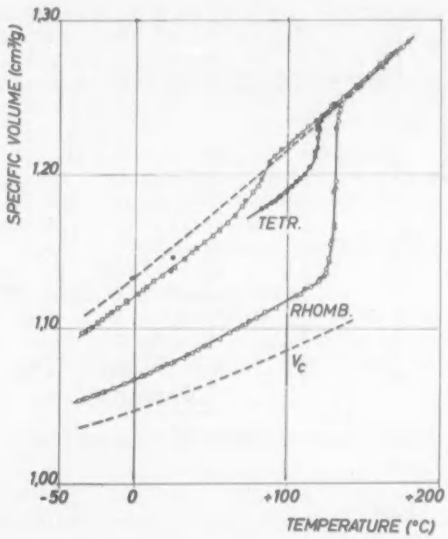

Fig. 5. Specific volume of poly-1-butene, samples as in Fig. 2 (different symbols denote different series of readings; dotted lines are calculated values).

pletely crystalline substance is calculated to be $\Delta H_u = 1675$ cal./monomer unit.

The value is substantiated by measuring the melting point depression. According to a theory of Flory and Mandelkern,[15] the equation for the relationship between the melting point of mixtures and their chemical composition is as follows

$$\frac{\frac{1}{T_m} - \frac{1}{T_m^0}}{v_l} = \frac{R}{\Delta H_u}\frac{V_u}{V_l}\left(1 - \frac{BV_l}{R}\frac{v_l}{T_m}\right)$$

where T_m = melting point of the mixture; T_m^0 = melting point of the high polymer; R = gas constant; ΔH_u = heat of fusion of the high polymer (calculated on 1 mole monomer); V_u = molecular volume of the monomer unit (at T_m^0); V_l = molecular volume of the solvent (at T_m^0); v_l = volume fraction of the solvent (at T_m); and B = constant.

Extrapolation of the data in accordance with the equation given above (Fig. 7) results in the heat of fusion of the rhombohedric form as follows

$$\Delta H_u = 1730 \text{ cal./mono (using } \alpha\text{-chloronaphthalene)}$$

$$\Delta H_u = 1576 \text{ cal./mono (using dibutyl maleate)}$$

It should be noted that the pure rhombohedric modification can only be obtained by using dibutyl maleate. When using α-chloronaphthalene, a

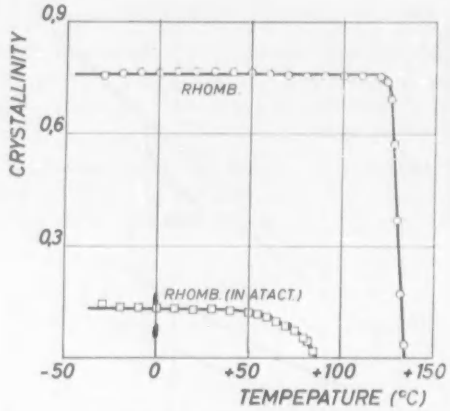

Fig. 6. Crystallinity (mass fraction) of poly-1-butene calculated from the values in Fig. 5.

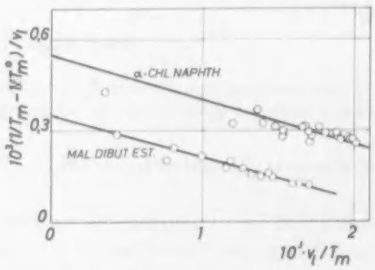

Fig. 7. Determination of the heat of fusion of poly-1-butene from melting point depression by the addition of α-chloronaphthalene or dibutyl maleate respectively.

more or less greater fraction of modification III always crystallizes out. Agreement of the various values of heat of fusion indicates that the heat of fusion of modification III is of similar magnitude as that of the rhombohedric modification.

The heat of transformation (rhombohedric → tetragonal) is 1675 − 974 = 701 cal./monomer unit.

The authors would like to express their gratitude to Dr. A. Pebler for the numerous x-ray photographs.

References

1. Zannetti, R., P. Manaresi, and G. C. Buzzoni, *Chim. Ind.*, **43**, 735 (1961).
2. Dainton, F. S., D. M. Evans, F. E. Hoare, and T. P. Melia, *Polymer*, **3**, 286 (1962).
3. Danusso, F., and G. Gianotti, *Makromol. Chem.*, **61**, 139 (1963).
4. Boor, J., and J. C. Mitchell, *J. Polymer Sci.*, **62**, S73 (1962).
5. Boor, J., and J. C. Mitchell, *J. Polymer Sci.*, **A1**, 59 (1963).

6. Herre, F., E. Prinz, and H. Wilski, Wandel in der Chemischen Technik (editor: Farbwerke Hoechst), 1963, p. 380.
7. Pebler, A., and G. Reichert, in press.
8. Prepared by Dr. H. G. Kirschner after French Pat. 1203848 (1958).
9. Prepared by Dr. E. Junghanns.
10. Purified by Dr. O. Fuchs.
11. Nölting, J., *Ber. Bunsenges, Phys. Chem.*, **67**, 172 (1963).
12. West, E. D., and D. C. Ginnings, *J. Res. Natl. Bur. Std.*, **60**, 309 (1958).
13. Ueberreiter, K., and G. Kanig, *Glas- und Hochvakuum-technik*, **2**, 218 (1953).
14. Wilski, H., *Kunststoffe-Plastics*, **54**, 10 (1964).
15. Flory, P. J., *Principles of Polymer Chemistry*, Cornell Univ. Press, Ithaca, 1953; L. Mandelkern, *Chem. Rev.*, **56**, 903 (1956).
16. Wilski, H., *Kunststoffe-Plastics*, **50**, 335 (1960).
17. Wilkinson, R. W., and M. Dole, *J. Polymer Sci.*, **58**, 1089 (1962).
18. Passaglia, E., and H. K. Kevorkian, *J. Appl. Phys.*, **34**, 90 (1963).
19. Danusso, F., G. Moraglio, and G. Natta, *Ind. Plastiques Mod. (Paris)*, **10**, 43 (1958).

Résumé

On a étudié la chaleur spécifique et le volume spécifique des différentes variétés cristallines de polybutène-1. La variété III dont la structure cristalline est encore inconnue a été obtenue par précipitation de la solution benzénique dans l'acétate de méthyle. A 101°C, elle se transforme en phase tétragonale fondant à 121°5C. La chaleur spécifique de la variété rhomboédrique, qui a été obtenue à partir du polymère fondu par refroidissement, suivi d'une conservation prolongée augmente régulièrement avec la température jusqu'au point de fusion. Par des mesures immédiates effectuées sur du polymère fondu et récemment refroidi, on a obtenu la chaleur spécifique de la variété tétragonale (du moins au-dessus de 80°C). Un produit fortement atactique, qui a été conservé durant une longue période, possède une petite fraction de cristaux rhomboedriques fondant à 87°C. Cette étude a été complétée par des mesures dilatométriques. Partant des degrés de cristallinité ainsi obtenus, on a calculé les chaleurs de fusion et on les a comparées avec les valeurs provenant de mesure d'abaissement du point de fusion des mélanges.

Zusammenfassung

Es wurde die spezifische Wärme und das spezifische Volumen der verschiedenen Kristallformen von Polybuten-1 untersucht. Die aus Benzol durch Ausfällen mit Methylacetat erhaltene, in ihrer Kristallstruktur noch unbekannte Form III zeigte bei 101°C eine Umwandlung in die tetragonale Struktur, die bei 121,5°C schmilzt. Die aus der Schmelze durch Abkühlen und langes Lagern erhaltene rhomboedrische Struktur zeigte einen monotonen Anstieg der spezifischen Wärme bis zum Schmelzpunkt; durch sofortige Messung eine frisch abgekühlten Schmelze konnte auch die spezifische Wärme der tetragonalen Form (wenigstens oberhalb +80°C) erhalten werden. Ein vorwiegend ataktisches, lange gelagertes Material zeigte bei 87°C das Aufschmelzen der geringen, rhomboedrisch kristallisierten Beimengung. Die Untersuchungen wurden durch dilatometrische Messungen ergänzt. Mit Hilfe des so gewonnenen Kristallinitätsgrades wurden die Schmelzwärmen berechnet und mit Werten verglichen, die sich aus Messungen der Schmelzpunktsdepression von Gemischen ergeben.

JOURNAL OF POLYMER SCIENCE: PART C NO. 6, PP. 43-51 (1964)

Differential Thermal Analysis of Polybutene-1

BERT H. CLAMPITT and RICHARD H. HUGHES, *Research and Development Department, Spencer Chemical Company, Merriam, Kansas*

Synopsis

The three polymorphic forms of polybutene-1 may be easily characterized by DTA: Form I has a DTA peak near 132°C.; Form II has a peak near 118°C.; and Form III has doublet peaks at 104° and 118°C. The kinetics of the room temperature transformation of Form II to Form I have been qualitatively investigated by DTA. The results indicate: (*1*) the thinner the film the faster the conversion rate and (*2*) the greater the catalysis residue in the system, the faster the conversion to Form I. The doublet in the Form III thermogram is due to the fact that the 104°C. transition corresponds to a phase change III to II with the 118°C. transition merely being the normal melting transition of Form II. Indeed, it is possible to heat Form III polybutene to 110°C., quench; and on standing it is found that the product has reverted to Form I.

Introduction

Polybutene-1 (PB) is unique among the polyolefins in that it exists in three polymorphic forms. This polymorphic behavior of PB was first reported by Natta et al.,[1] and the x-ray and density properties of the various crystal forms of PB were subsequently studied by Zannetti et al.[2] Recently Boor and Mitchell[3] further characterized two of the polymorphic forms of PB by several techniques including infrared (IR) and differential thermal analysis (DTA). The results presented in the present paper generally confirm the data of previous workers, but extend the DTA and IR measurements to include all of the crystal forms of PB, and indicate several new aspects of the kinetics of the various polymorphic transformations.

Following the nomenclature of previous workers, the three crystal forms of PB may be prepared as follows: (*1*) Form I: This form is apparently the thermodynamically most stable form and can be prepared by melting a PB sample, cooling, and allowing the sample to stand for a long time at room temperature; (*2*) Form II: This is an unstable form of PB and is the form that is first present when a sample is quenched from the molten state. (*3*) Form III: This is also a very stable form of PB and is prepared by precipitating PB from solution.

Experimental

Materials

The PB samples used in this research were experimental resins prepared with a Ziegler type catalyst system and possessing the characteristics listed in Table I.

TABLE I
Physical Properties of Polybutene Samples

Sample	Density (g./cc.)[a]	Log viscosity no.
1488	0.9156	3.437
1272	0.9254	2.071
1275	0.9404	2.912

[a] Measured 10 days after preparation of sample.

Apparatus

A Perkin Elmer Model 221 spectrophotometer was used in all the IR investigations.

DTA Apparatus: The construction of the DTA apparatus used in these experiments was described previously.[4] A heating rate of 2.4°C./min. was used, and the sample size was 0.7 g. in all cases.

Sample Preparation

Three types of samples were used in this study: cast, film, and powder samples. The cast samples were prepared by placing a sample in the sample holder (described in reference 4); melting at 190°C. for 10 min., and compressing by hand with a Teflon plunger. This gave a compact, bubble-free sample which was reheated for 5 min. at 190°C. prior to placing the thermocouple in the molten polymer. The system was then rapidly cooled to room temperature by placing the sample holder in the cool DTA block.

Film samples were used in both IR and DTA studies. In the case of the DTA studies, the films were tightly wrapped directly around the thermocouple and then placed in the sample tube. Form III films were prepared by dissolving PB in trichloroethane (5 g./100 cc.) and laying down a film on a glass plate which was allowed to air dry at room temperature. After evaporation of the solvent, the film was removed from the glass plate. This gave an opaque film which had the characteristic Form III x-ray pattern. Form II films were made by heating a sample, contained between mylar, to 150°C. and applying 20,000 psi pressure. The pressure was released while the polymer was still molten and the mylar was removed from the press and allowed to rapidly cool to room temperature. Form I films were Form II films which had been allowed to stand at room temperature for a week.

As received the samples used in these studies were powders. (If, however, the material is not a powder, it may easily be obtained in this condition by dissolving the PB in benzene and adding methanol to precipitate the sample.) Powdered samples were compressed directly in the DTA sample tube with a Teflon plunger and the cold thermocouple inserted directly in them.

Results and Discussion

The IR curves of the various forms of PB are given in Figures 1 through 3. Of particular note in Figure 1 are the bands at 12.5, 11.8, 10.85, and the 7.5 μ doublet, all of which appear to be specific to Form I. The Form II spectra shown in Figure 2 do not contain the bands listed previously, but do show a new band at 11.05 μ which appear to distinguish it from Form I PB. The difference between the Form III spectra, shown in Figure 3, and the other forms is more subtle. Nevertheless, the triplet near 7.5 μ and the absence of a band 10.0 μ, appear to be peculiar to Form III. The intensities of the 7.75 and 9.82 μ bands are stronger than in the other forms. It is sufficient here to point out that differences in the IR spectra of the three forms do exist, and that it is possible to identify which form of PB is present from the IR spectra of the sample.

The other method used to identify the various forms of PB is DTA, with thermograms of the various forms being depicted in Figures 4 and 5. In Figure 4, the 118°C. peak is characteristic of PB in Form II; whereas the 131°C. peak is characteristic of Form I. The thermogram of pure Form

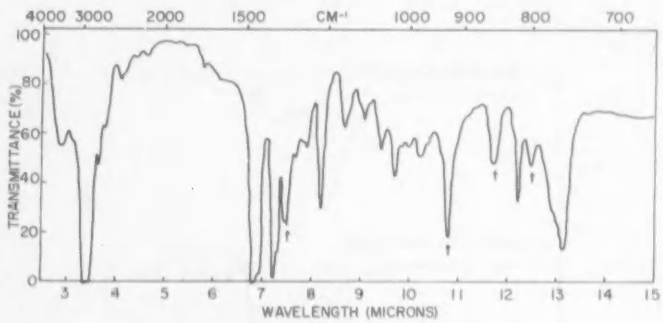

Fig. 1. IR spectra of Form I polybutene.

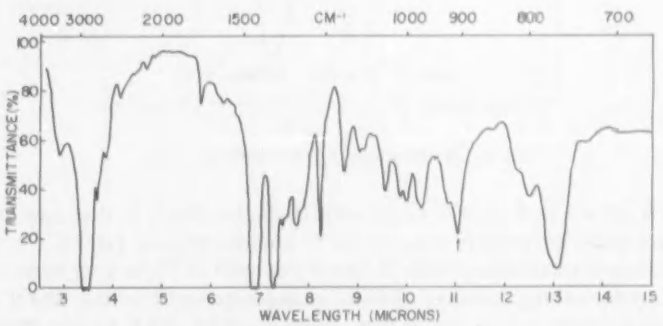

Fig. 2. IR spectra of Form II polybutene.

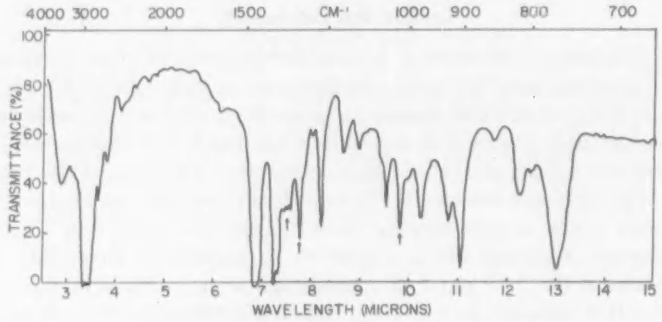

Fig. 3. IR spectra of Form III polybutene.

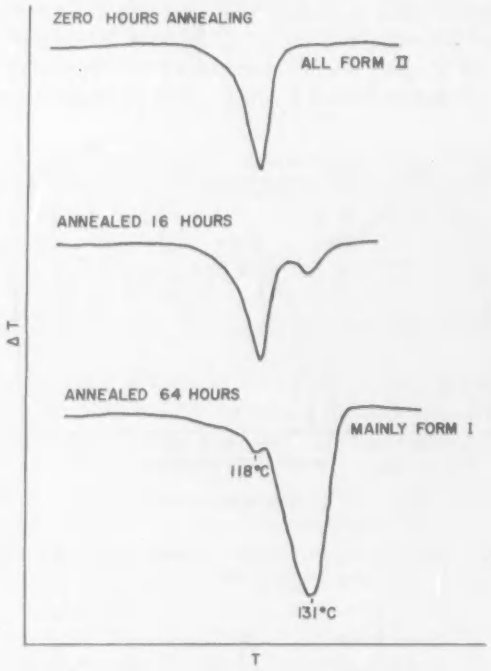

Fig. 4. Thermograms of polybutene no. 1272.

III PB, shown in Figure 5, is different from the others in that two endothermic peaks are present—one at 104°C. and the other at 118°C.

As Figure 4 indicates, Form II slowly converts to Form I on room temperature annealing; however, it soon became apparent that the rate of conversion as measured by IR on film samples and by DTA on cast samples were not the same. The question then arose as to the cause of the different

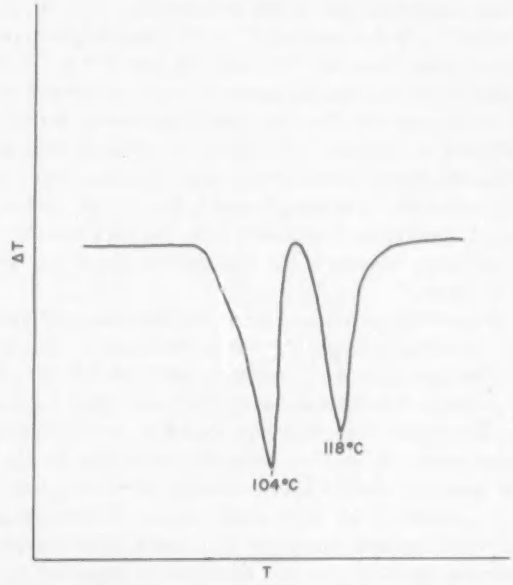

Fig. 5. Thermograms of Form III polybutene no. 1272.

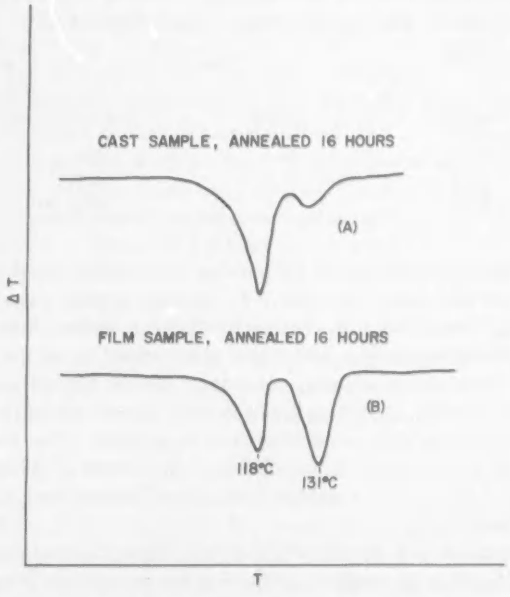

Fig. 6. Thermogram of polybutene no. 1272.

rates, and it was suggested that it was perhaps due to the thickness of the sample. In order to check this possibility, film samples were prepared and the rate of conversion measured by both IR and DTA. The measured rates on the film samples were the same by both methods and clearly indicated that the thinner the film, the faster the conversion rate. Indeed, this was confirmed by further IR studies on films of various thickness. The effect of film thickness on conversion rate is perhaps best seen in Figure 6 where DTA curves of a cast sample and a film sample both annealed for 16 hr. at room temperature are shown. In the cast sample, the 131°C. peak is barely present; whereas in the film sample, the 131°C. peak is larger than the 118°C. peak.

Boor and Mitchell[3] reported somewhat similar effects of film thickness; however, they felt that it might be due to orientation effects. As all of our samples, film and cast, were heated to at least 150°C. and were not cooled under pressure, it is difficult to see how orientation could be of major importance. This point was, however, checked by examining the films through crossed polaroids and by polarization studies on the IR instrument. These results indicated slight orientation in the plane of the film, but the extent appears to be very small, and to be independent of film thickness. It would appear, therefore, that the kinetic changes associated with film thickness are more complex than can be explained by orientation phenomena alone.

Another interesting aspect of the conversion of Form II to Form I became apparent in the study of the conversion rates of different PB samples. Indeed, it was found that the conversion rate is dependent on the amount of ash in the sample.

Sample	% Ash	Conversion rate
1488	0	slow
1272	1.2	fast
1275	2.6	very fast

From these data it appears that the greater the catalyst residue in the system, the faster the conversion rate. It does not appear that the catalyst residue acts as crystallization centers for the conversion, because various amounts of aluminum oxide (100 mesh) were added to sample 1488 without altering the conversion rate. It might also be argued the molecular weight of the sample is causing the observed kinetic effects with the catalysis residues being only an artifact of the system. The viscosity data given in Table I eliminate this possibility. At present it is not clear what the function of the catalyst residue is or even if it is primarily responsible for the observed phenomenon.

The thermogram of Form III PB shown in Figure 5 is unique in that it is the only DTA curve of an alpha olefin that has more than one peak. The thermogram is independent of whether the sample is run as a powder or a

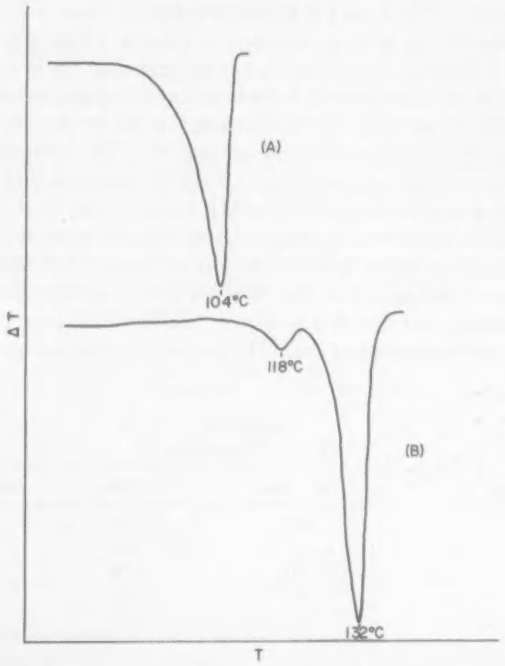

Fig. 7. Thermogram of powdered polybutene no. 1272.

film, both as to the position and size of the endotherms. The 104°C. peak is presumably characteristic of Form III; while the 118°C. peak has been previously identified as characteristic of Form II. It is difficult to believe that part of the sample exists as Form II since it should all decay to Form I. It therefore seems possible that the 104°C. transition corresponds to a phase transition of III to II which then melts at its normal temperature of 118°C. Because of the rapid heating rate, Form II does not have time to decay to the most stable form (i.e., Form I). To give some support to this hypothesis, the experiment depicted in Figure 7 was carried out. In this experiment a Form III sample was heated until the 104°C. transition was completed, and at this point the sample was quenched and let stand at room temperature for a week. It was then rerun and the 104°C. peak was not observed; the Form II 118°C. peak was greatly reduced; and a new peak at 132°C., the Form I peak, became the major peak. These results give strong support to the hypothesis that the Form II peak is observed in solution precipitated samples only because it is formed from the decomposition of Form III. Similarly, IR results on samples heated to 110°C. show only Form II to be present; while visual observation of the samples heated to 110°C. indicate that the samples do not melt and indeed no visible change occurs at this temperature.

The area under a DTA peak is proportional to the heat of transition, and values for some of the systems depicted in Figures 4 through 7 have been tabulated in Table II. From Figure 4 it appears that Form I has a higher heat of transition than Form II. It is not clear at present whether this means the system is more crystalline when it all reverts to Form I, or whether the two states have the same crystallinity but different heats of fusion for the various pure crystal forms. Table II indicates that Form II PB made by the decomposition of Form III has a higher heat of transition than the same crystal form prepared by quenching molten PB. This is further reflected in higher heats of fusion of Form I PB derived from a Form III source as opposed to that derived from a molten source. These results apparently indicate that a more crystalline PB Form I state can be derived from decomposition of Form III than can be derived by cooling from the melt.

TABLE II
Heats of Transition

Figure no.	PB form	T (°C.)	ΔH (cal./gm.)
4A	II	118	11
4C	I	131	21
5	III	104	20
	II	118	15
7B	I	131	26

The authors wish to express their appreciation to Mr. Nathan Scarritt and Mr. Charles Harris for much of the experimental work. Thanks are also expressed to Mr. Dale German for stimulating discussion of the results and to Dr. H. D. Anspon for encouragement in this program.

References

1. Natta, G., P. Corradini, and I. W. Bassi, *Nuovo Cimento*, **15**, special number 1, 52 (1960).
2. Zannetti, R., P. Manaresi, and G. C. Buzzoni, *Chim. Ind.*, **43**, 735 (1961).
3. Boor, J., and J. C. Mitchell, *J. Poly. Sci.*, **A1**, 59 (1963).
4. Clampitt, B. H., *Anal. Chem.*, **35**, 577 (1963).

Résumé

Les trois formes polymorphes du polybutène-1 peuvent aisément être caractérisées par DTA: la forme I possède un pic DTA vers 132°C; la forme II a un pic ver 118°C et la forme III possède un doublet à 104° et 118°C. Les cinétiques de transformation à température de chambre de la forme II en forme I ont été étudiées qualitativement par DTA. Les résultats montrent: (*1*) plus le film est mince, plus rapide est la vitesse de conversion et (*2*) plus le résidu de catalyseur dans le système est grand, plus la conversion dans la forme I se fait rapidement. Le doublet dans le thermogramme de la forme III est dû au fait que la transition à 104°C correspond à un changement de phase de la forme III en II, la transition à 118°C étant simplement la transition de fusion normale de la forme II. En effet il est possible de chauffer à 110°C la forme III du polybutène; en la refroidissant et en la laissant reposer on trouve que le produit s'est retransformé en forme I.

Zusammenfassung

Die drei polymorphen Formen von Polybuten-1 können mittels DTA leicht charakterisiert werden: Form I besitzt ein Maximum in der Nähe von 132°C, Form II in der Nähe von 118°C und Form III hat ein Doppelmaximum bei 104° und 118°C. Die Kinetik der Raumtemperaturumwandlung von Form II in Form I wurde qualitativ mit DTA untersucht. Die Ergebnisse zeigen, dass (*1*) die Umwandlungsgeschwindigkeit um so grösser, je dünner der Film und (*2*) je grösser der Katalyserückstand im System, um so rascher die Umwandlung zu Form I ist. Das Dublett im Thermogramm der Form III kommt dadurch zustande, dass bei 104°C die Phasenumwandlung von III zu II und bei 118°C die normale Schmelzumwandlung von Form II stattfindet. Es ist tatsächlich möglich Polybuten, Form III, auf 110°C zu erhitzen und abzuschrecken, wobei beim Stehen sich das Produkt als rückgebildt zu Form I erweist.

JOURNAL OF POLYMER SCIENCE: PART C NO. 6, PP. 53-64 (1964)

A Differential Thermal Analysis Study of the Effects of Thermal History on Polyethylene

H. W. HOLDEN, *Central Research Laboratory, Canadian Industries Limited, McMasterville, Quebec, Canada*

Synopsis

The melting and crystallization behavior of polyethylene samples has been investigated by differential thermal analysis (DTA), with special emphasis on the effects of thermal conditioning on the crystalline state of the sample. Techniques are outlined for impressing a wide variety of thermal histories on the sample in the DTA cell. In particular, the use of an annealing procedure is shown to provide a significant evaluation of the extrapolated value of the equilibrium melting temperature, combined with a rapidity not possible by the dilatometric method. Theoretical implications of the various procedures and results are briefly discussed. Critical examination of the fine structure observed in the melting thermograms leads to the conclusion that under certain conditions crystallites originating from both heterogeneous and homogeneous nucleation can be detected. The temperature rise associated with very fast crystallization is considered to influence the subsequent melting temperature more significantly than the effects of recrystallization during the actual melting cycle. Some illustrations are given of the general usefulness of the conditioning procedures in clarifying phenomena observed with various samples.

Introduction

Differential thermal analysis (DTA) has been used extensively to study the melting behavior of semicrystalline polymers.[1-6] The importance of thermal history on the crystalline state of such polymers is well known and its detection by DTA has been demonstrated by Coste[1] and more recently by Ke[3] and Wyckoff.[4] Studies in this laboratory have been carried out on a range of polymers, with thermal history and its influence on physical properties primarily in mind.

Experimental

The characteristic feature of the present apparatus design is a cell holder which can be readily subjected to a variety of heating and cooling operations.

In addition, attention was given to the following factors in thermocouple design: since rigidity for symmetry and reproducibility took precedence over signal sensitivity (which was more than adequate with the Liston-Becker Model 14 preamplifier used), 22 gage bare chromel and alumel wire was selected; since fast response time was necessary for high resolution, the thermocouple junction was confined to the area produced by spot-

welding the singly-crossed wires and grinding off all excess metal. With a cell containing the typical charge of 20 mg. of sample and 200 mg. of diluent, heated at 3°C./min., the return-to-baseline after detecting a first-order transition occurred in less than a minute. Thus in a favorable case (sharp-melting components) the system is capable of separating peak maxima about 1°C. apart.

Because of variations in the use of the term, it is necessary to define annealing, as used in this paper, as exposure of the sample to a temperature program which (as interpreted by subsequent melting behavior) does not cause a total disappearance of measurable crystallinity at the maximum conditioning temperature. The annealing operations in the early stages of this work were carried out by manual adjustment of an autotransformer input to an oven which was constructed from a thick cylindrical tube of brass. Rapid-response corrections could be made by adjusting the position of the cell along the vertical axis of the oven. As the method developed, a linear-drive auto-transformer power source was installed to give essentially linear heating rates, and a thermoregulator unit was included to permit switching over from linear heating to constant-temperature operation without overshoot. The whole thermal history of the sample is directly recorded by means of the sample thermocouple which is part of both the differential and cold-junction measuring circuits. This thermocouple was calibrated against a secondary standard, permitting temperatures to be reported to an accuracy of ±0.1°C.

The cell holder, essentially that described by Rudin, Schreiber, and Waldman,[7] was particularly well-suited for impressing various cooling histories on the samples. The natural cooling rate of the furnace assembly is about 3°C./min., but by reversing the motor driving the autotransformer supplying the furnace power, rates as low as 0.1°C./min. were obtained. By plunging the hot cell holder into chipped ice, cooling rates of 150–180°C./min. were consistently recorded through the freezing range of the samples.

Results and Discussion

Figure 1 shows some representative thermograms obtained with a two-pen record of T and $(-\Delta T)$ versus time, arising from samples with various thermal histories. Dotriacontane is included to indicate the resolution attainable with the apparatus.

An interesting feature of this study is the occurrence of reproducible fine structure in a great number of the thermograms. When polymer P (a Phillips-type linear polyethylene having $\bar{M}_n$ 12,000, $\bar{M}_w$ 90,000) was pressed in a frame 0.010 in. thick and shock-cooled from 150°C. in ice-water, the resulting sample (pulverized on a Wiley mill with a large excess of solid CO_2) gave rise to a double peak (shown in Figure 1*b*). The resolution of the two features was somewhat reduced when the rapid cooling was carried out in the cell itself, probably because of less efficient heat-transfer; nevertheless the fact that both peaks were obtained by even

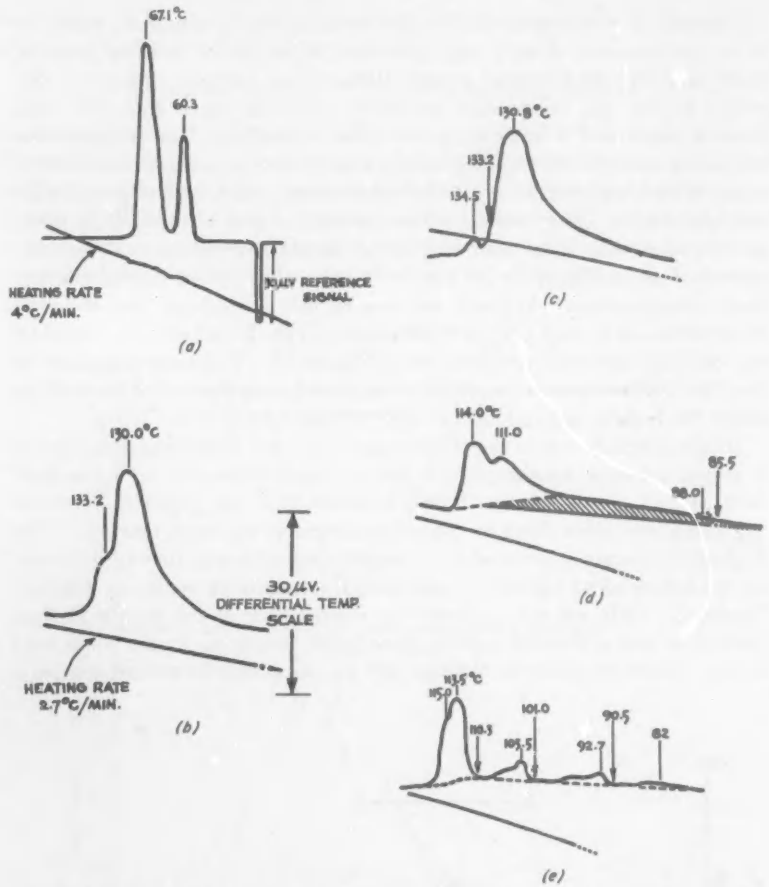

Fig. 1. Representative thermograms for melting runs. ΔT and T records versus time are shown (arrows correspond to upper temperature limits of preceding annealing cycles): (*a*) Dotriacontane (thermocouples uncalibrated); (*b*) polymer P; (*c*) polymer P; (*d*) polymer Q; (*e*) polymer Q.

the latter method in two different environments (i.e., with two different diluents) indicates that it is a property of the polymer resin rather than of any interfacial nucleation sites.

The small, fully-resolved peak of Figure 1*c* is an extreme illustration of the effect of annealing (at a temperature corresponding to that marked by the arrow), followed by quenching of polymer P in the cell. The temperature was raised from 130 to 133.2°C. over a period of 23 min., then rapidly cooled; that portion of the sample which was liquid at the end of that period crystallized at a lower temperature because of the competition in rates of cooling and crystallization.

Polymer Q which gave rise to the thermograms in Figures 1*d* and 1*e* is an intermediate density high-pressure polyethylene molding resin of melt index 20 (19.3 methyl groups/1000 carbon atoms). When rapidly cooled in the cell, the sample produced a melting curve with two well-defined peaks and a large apparent shift in baseline. Low-temperature annealing changed the thermograms in such a way as to confirm the occurrence of melting over a very wide temperature range, and to reveal that the long sloping featureless region was actually a part of the melting peak, and not baseline. The course of actual baseline variation could be demonstrated as in Figure 1*e* by a series of annealing cycles at successively lower temperatures. Without the use of this procedure, heat-of-fusion determinations of such polymers are subject to the large errors indicated by the hatched area under the curve in Figure 1*d*. The largest amount of baseline shift is observed, as might be expected, near the end of the melting where the highest rate of loss of sample crystallinity occurs.

In the investigation of the annealing phenomena, annealing time showed a strong influence on the relative areas of peaks observed on subsequent melting, as expected; it was found, however, that the duration of annealing had a low-order effect on the temperatures of the peak maxima. The highest temperature attained in a conditioning cycle can therefore be used as the independent variable in a graphical summary of results, as shown in Figure 2. Data are also included for conditioning of the sample at temperatures well above the melting point (not annealing in the sense used in this paper), to show the lack of any effects except in a short tempera-

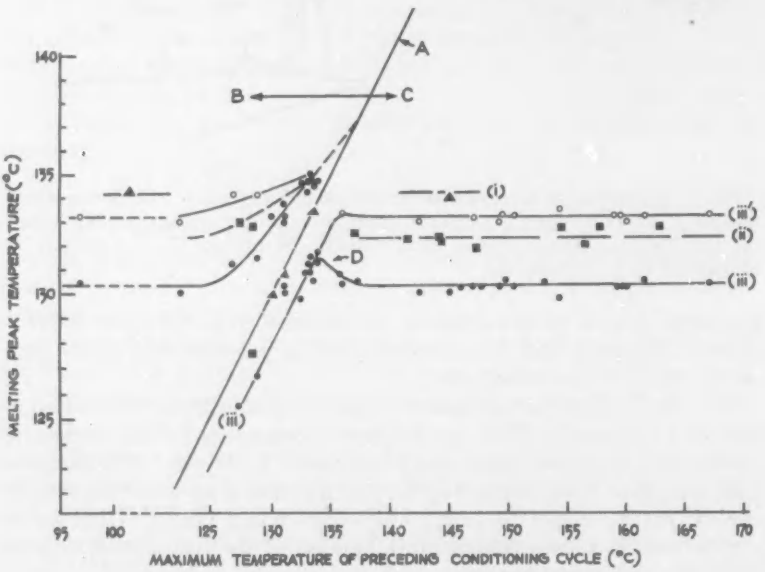

(*a*)

ture range B–C near the melting point. The reference line A plotted in Figure 2*a* and 2*b* is defined by the relation

$$T \text{ (melting peak)} = T \text{ (conditioning temperature)}$$

Annealing followed by quench cooling frequently led to the resolution of two peaks producing a point above and a point below this line (Fig. 1*c*).

Finally, the results are grouped according to the distinct differences produced by different rates of cooling, both from the melt and at the end of annealing. The study of samples cooled at the maximum rate was more extensive than for slower rates of cooling because of the better resolution of

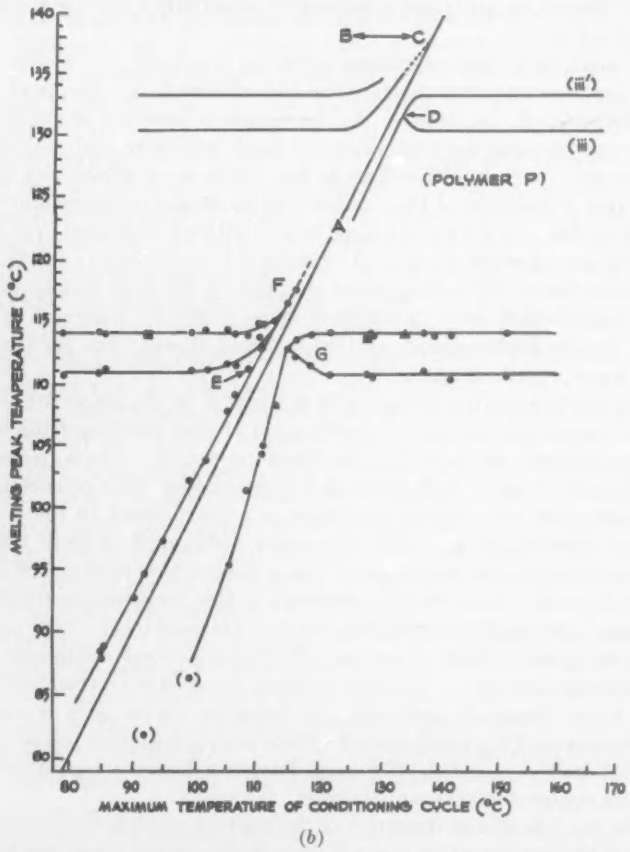

(*b*)

Fig. 2. Influence of thermal conditioning on melting peak temperatures: (*a*) Polymer P: (i) (▲) melt cooled at 0.3–0.5°C./min.; (ii) (■) melt cooled at 2.7–3.3°C./min.; (iii) (●) melt cooled at 150–180°C./min., principal peak; (iii′) (○) melt cooled at 150–180°C./min.; minor peak; (*b*) polymer Q (with curves (iii) and (iii′) for polymer P recopied). Experimental points coded as in Fig. 2*a*. Since the components of the double peak were of comparable size, both are plotted as principal peaks.

detail and the shorter times required. The temperature of the principal peak for polymer P shifts 3.8°C. with extremes of cooling rate; on the other hand that for polymer Q remains virtually independent of cooling rate even though the actual peak shape changes very markedly.

The temperature coefficient of the rate of crystallization of linear polyethylene is so large, that shifts in peak temperature due to annealing are confined to a five-degree temperature range—a situation which taxed the precision of the manual procedures to its limit. Only those measurements based on quenched samples are numerous enough to permit an estimate of the equilibrium melting point by extrapolation, and they show enough scatter to introduce considerable uncertainty, giving a value of 137.3 ± 0.7°C.

The peak temperatures corresponding to maximum differential signal at the thermocouple cannot strictly be identified with the disappearance of the last crystals in the sample. As the sample is annealed at higher temperatures, the surviving crystallites are more and more uniform, and the discrepancy vanishes. The effect of any discrepancy would be a slightly high value of the slope of the line through the points corresponding to annealing-peaks. As drawn the slope is 0.62 with an estimated uncertainty of ±0.1 (compared to a reported value of 0.5, as quoted in ref. 4). The sparse results for the melting peaks obtained by different sample pretreatment suggest that lines of different slope might be generated, as predicted by the kinetic theory of Hoffman and Weeks,[8] but further work would be required to confirm this.

The cooling following annealing of polymer P in the temperature range *B–C* brings about the rapid crystallization of that portion of the sample which was liquid at the end of the annealing period. The corresponding melting peak is fairly well resolved for the highest rates of cooling; for slow cooling the only observable feature is a sharp break in the curve of the main melting peak. After formalized assignment of peak temperatures in the latter case, it is apparent that a much weaker dependence of peak temperature on cooling rate is obtained in this temperature range than elsewhere. Presumably crystallization is accelerated by the large numbers of surviving nuclei which shows that primary nucleation is a rate-controlling crystallization process. The most extreme example is represented by the point *D* on Figure 2, produced by annealing cycles with a top temperature near 134°C., which show no peaks to signify the survival of crystallites, but only a single melting peak having a higher temperature than normally obtained following quenching.

Using the operational definition of the melting point as the temperature at which the last detectible trace of crystals disappears,[9] then the conventional interpretation of DTA curves would indicate that no crystallinity was detected in this sample above 135°C. The portion of the curve at *D*, however, represents a less conventional way in which the survival of crystallites *is in fact detectible* up to temperatures above 137°, with a mini-

mum of extrapolation required. The extrapolation procedure[9] is to be preferred on a theoretical basis for establishing a thermodynamic equilibrium point, but the curve at *D* supplies further strong experimental justification for the procedure.

Curves *i*, *ii*, and *iii* extend only a short distance along the line *A*, since the polymer is chemically quite uniform. Fractionated samples of polymer P have been obtained and studied briefly. The lowest molecular weight fraction ($\overline{M}_n$ approximately 3600) generated a double melting peak with characteristic temperatures (following crystallization at 150°C./min.) of about 111 and 125°C. Since these peaks are not greatly modified by different modes of cooling, it is likely that they represent chemically different species, present in small amounts in the parent polymer.

One high molecular-weight fraction was studied ($\overline{M}_w$ by light scattering in α-chloronaphthalene at 140°C.: 400,000) which indicated, in the manner described above, the survival of crystallites above 140°C. (cf. refs. 10 and 11), although the highest melting crystallites obtained in measurable quantity by annealing melted at 137.3°C. The melting peaks exhibited much of the doublet structure previously described, during melting and crystallization runs even at 3–4°C./min. In melting runs following quenching, the doublet as well separated. The greatly increased breadth of the peak following quenching (and perhaps the other effects also) can be related to the low chain mobility in the very viscous melt.

The contrast with high-pressure polyethylene is brought out once more in Figure 2*b*, by the more gradual changes which are indicated for the curves of polymer Q. The maxima resulting directly from annealing generate a line which intersects the reference line *A* only after a long extrapolation beyond the point *F*. (The point *E* is anomalous only in that it represents a broad unresolved pair of peaks belonging to the adjacent curves.) Since the peak represented by *F* was very small, it is likely that crystallites could be obtained at a higher temperature only with great difficulty. On the other hand the comparatively long curved section at *G* suggests that some crystallite nuclei survive up to temperatures of 121°C. but are readily destroyed beyond this temperature.

The equilibrium melting temperature defined from the extrapolated line is probably the same as for linear polyethylenes. The difficulties encountered with kinetic analysis of crystallization rates of branched polyethylenes lie in establishing the amount of supercooling in relation to a real or a fictitious equilibrium process. The results presented here suggest that this process is identical with that for completely unbranched polyethylene, and gives conceptual support for the imperfect crystal model in preference to the two-phase model of low-melting polyethylene.[12]

The nature of the fine structure exhibited in the melting curves must be examined critically. There are a number of experimental facts which all but rule out the possibility of instrument interference. In the first place the relative importance of the peaks varies greatly from resin to resin (of several dozen examined), but remains remarkably reproducible for

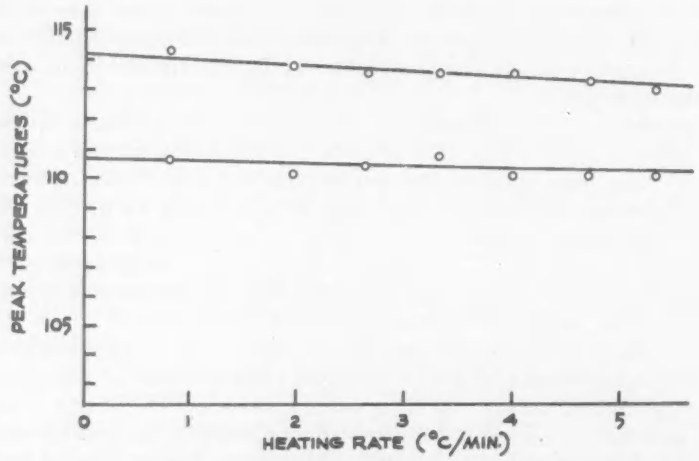

Fig. 3. Influence of heating rate on peak temperatures (polymer Q; melt cooled at 150–180°C./min.).

repeated samplings of each. Polymers P and Q were studied using 45–60 mesh borosilicate glass and Dow Corning Silastic Gum 400 as diluent, with essentially identical results; this would indicate that the diluent does not play a significant part in the nucleation of crystallization.

The shape of polymer Q melting curves suggests the possible explanation that the low-melting crystallites undergo rapid recrystallization to produce the minimum before the high-melting peak. If this were the case, the peak temperature could be expected to show a strong dependence of the heating rate; at slow rates the recrystallization would take place sooner causing the false low-melting peak to be shifted to a much lower temperature because of the simultaneous exothermic reaction. Figure 3 shows that the experiments do not support this hypothesis; all changes in the appearance of the compound peak could be attributed to the fixed thermal relaxation time (time to return to baseline at the end of the exothermic process) of the instrument while the very small variations in peak temperatures show the opposite trend to that predicted.

It is reasonable to conclude that the fine structure observed is characteristic of the sample, and that when it is observable only after a very rapid cooling of the melt it is brought about by the occurrence of two types of crystallization process. Under such crystallization conditions it is unlikely that differences in chemical species could account for the effect. The extensive evidence for crystal nucleation at heterogeneities[13–16] gains further support from the present results. The stability of the sites is confirmed by the apparent invariance of crystallization behavior even when the melts are kept at elevated temperatures for long intervals before crystallization. The presence of doublet peaks, however, indicates that in

the non-isothermal crystallization of rapid cooling, two mechanisms occur either simultaneously or consecutively. It seems reasonable to identify these mechanisms with heterogeneous and homogeneous nucleation, in agreement with the recent work of Cormia, Price, and Turnbull.[16] The temperature spread (130.3–133.3°C) for the two peaks in quenched polymer P is the same as that reported by them for the melting of the two types of spherulitic structures, and by Wunderlich and Kashdan[5] for bulk-crystallized and solution-crystallized linear polyethylene (129 and 132°C.).

The crystallization following homogeneous nucleation with high supercooling takes place extremely rapidly. It is possible to calculate from published data that the latent heat released by the adiabatic crystallization of supercooled polyethylene is sufficient to heat the sample 50–80°. Thus experiments carried out by quenching or under nominally isothermal conditions with large supercooling will produce crystallites in a very rapidly rising local temperature environment. This could account for the fact that the crystals nucleated at a low temperature T_c do not melt at the low temperature theoretically predicted for complete crystallization at T_c. Such an explanation is more acceptable, at least in the bulk crystallization case, than the idea of melting and recrystallization during the heating DTA run, since experiments showed that significant variations in the shape of the low temperature side of the DTA peaks could be "annealed in" reproducibly at temperatures below 120°C. At a lower temperature any recrystallization of melt produced from very imperfect crystallinity would be so rapid that an exothermic signal would be expected because of the higher stability of the new crystals formed.

Other Applications of Sample Conditioning in the DTA Cell

Apart from the straightforward use of the annealing procedure to confirm the existence and estimate the intensity of very diffuse melting peaks, two examples will serve to illustrate more specialized applications. Figure 4 shows melting curves for a 1:1 blend of a Ziegler-type and a low-density polyethylene before and after annealing (continuous and dashed curves respectively). The high-temperature peak is 30% narrower (at half-height) and lies at a temperature 3–4°C. lower than that of the undiluted component. Below the normal melting temperature of the linear polyethylene the melt system may be considered as a supersaturated solution with the low melting constituent acting as solvent; thus the greater amount of supercooling necessary for crystallization leads to lower-melting crystallites.[8] These show evidence, however, of a greater uniformity because of the greater mobility of the chains during this stage of the crystallization.

The low-temperature peak, on the other hand, is severely modified by the residues of late crystallizing linear polymer. The melting transformation, furthermore, takes place in the complete temperature interval between the normal melting ranges of unmixed constituents. By the use of the annealing cycle in this temperature interval, subsidiary peaks (of a type completely absent in high-density polyethylene alone) can be gen-

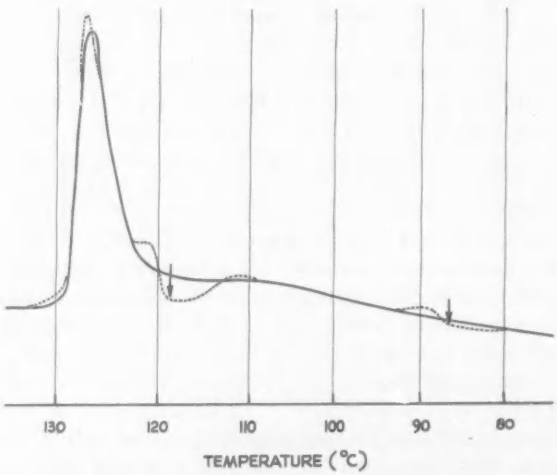

Fig. 4. Thermogram for 1:1 blend of Ziegler-type and low-density polyethylenes. Melt cooled at 3°C./min.; dashed curve shows changes produced by annealing at temperatures indicated by the arrows.

erated. While it is impossible to speak of an equilibrium process at the annealing temperature, it is clear that crystallization has occurred during annealing to a more highly ordered and stable state, while nevertheless incorporating into the crystal structure a proportion of the highly branched molecules which cannot be obtained unmelted at that temperature except when blended. (This conclusion is at variance with the interpretation of Clampitt.[6]) In any practical process involving finite cooling rates, this spectrum of mixed crystal structures will play an important part in determining the physical properties of the blend.

In plastics technology, the testing of semicrystalline materials is complicated by the lack of reproducibility of samples, largely due to the strong influence of thermal history on the crystallite morphology. While annealing would appear to offer a reliable way of standardizing the results, examination of DTA annealing results for low density polyethylenes leads to the very opposite conclusion. ASTM test method D1693–59T requires the sample to be conditioned for one hour at 100°C. in water or steam, but in practice the procedure is to use boiling water regardless of atmospheric pressure variations. DTA shows that depending on the nearness of the main melting peak to 100°C., and on the normal variations of the boiling point, the crystallite distribution of one resin or a group of resins may be affected to a small or to a very great extent. Furthermore since the melting peak of high pressure polyethylenes is in practice at least a few degrees above 100°C. the annealing procedure is incapable of influencing that proportion of crystallites which may most strongly reflect uncontrolled variations in the original crystallization. Therefore, a more recently adopted

conditioning procedure (ASTM D1928-62T) of cooling the sample molding according to a strictly regulated schedule from a temperature well above its melting point, offers a preferred means of standardizing the crystal texture of semicrystalline specimens.

Appendix: The Use of DTA for Calorimetric Measurements

The analysis of Boersma[17] which assumes attainment of a high degree of symmetry in the DTA cell (cf. ref. 18) predicts a loss of sensitivity, without loss of detail, in the case where the thermocouple leads provide a significant path for the conduction of heat into the centre of the sample. When adapted to the present apparatus, the treatment leads to the following formula for peak area (of the ΔT versus time curve):

$$A = K_q/(k\lambda + m\Lambda)$$

where K is a geometrical coefficient, q is the heat absorbed per unit volume, and $k\lambda$ and $m\Lambda$ are terms dealing with the relative proportions of heat conducted by the powdered sample-diluent and the thermocouple leads, respectively. It is estimated for the present cell-thermocouple system that about 60% of the heat conducted to the thermocouple junction comes through its leads.

Any attempt to calibrate the system with a calorimetric standard will involve predictable shifts in thermal conductivity λ, and *uncontrolled* variation of the packing coefficient k, since the texture of highly crystalline standards varies widely, and is quite unlike representative polymer samples. Therefore, one approach to cell-design for measuring heats of transition by peak area would eliminate as far as possible the importance of conduction through the sample. This would account for the relative success of early attempts to perform calorimetric measurements, where bulk polymer samples and relatively massive thermocouple assemblies were used. With the growth of interest in instruments of high resolution and short response time, where a more faithful representation of the temperature-dependence of the melting process is sought, great care must be exercised to be sure that the boundary conditions of the heat-flow equations are reliably known, both during and after the melting process.

The author is pleased to acknowledge the many helpful discussions with Dr. A. Rudin during the course of this work.

References

1. Coste, J., *Ind. Plastiques Mod.*, 37 (April 1957).
2. Ke, B., *J. Polymer Sci.*, **42**, 15 (1960).
3. Ke, B., *J. Polymer Sci.*, **61**, 47 (1962).
4. Wyckoff, H. W., *J. Polymer Sci.*, **62**, 83 (1962).
5. Wunderlich, B., and W. H. Kashdan, *J. Polymer Sci.*, **50**, 71 (1961).
6. Clampitt, B. H., *Anal. Chem.*, **35**, 577 (1963).
7. Rudin, A., H. P. Schreiber, and M. H. Waldman, *Ind. Eng. Chem.*, **53**, 137 (1961).

8. Hoffman, J. D., and J. J. Weeks, *J. Rest. Natl. Bur. Std.*, **64A**, 73 (1960).
9. Hoffman, J. D., and J. J. Weeks, *J. Rest. Natl. Bur. Std.*, **66A**, 13 (1962).
10. Broadhurst, M. G., *J. Chem. Phys.*, **36**, 2578 (1962).
11. Chiang, R., and P. J. Flory, *J. Am. Chem. Soc.*, **83**, 2857 (1961).
12. Berger, M., *J. Polymer Sci.*, **62**, S145 (1962).
13. Rabesiaka, J., and A. J. Kovacs, *J. Appl. Phys.*, **32**, 2314 (1961).
14. Banks, W., J. N. Hay, A. Sharples, and G. Thomson, *Nature*, **194**, 542 (1962).
15. Sharples, A., *Polymer*, **3**, 250 (1962).
16. Cormia, R. L., F. P. Price, and D. Turnbull, *J. Chem. Phys.*, **37**, 1333 (1962).
17. Boersma, J., *J. Am. Ceram. Soc.*, **38**, 281 (1955).
18. Barrall, E. M., and L. B. Rogers, *Anal. Chem.*, **34**, 1101, 1106 (1962).

Résumé

On a étudié le comportement à la fusion et à la cristallisation d'échantillons de polyéthylène par analyse thermique différentielle (DTA) en examinant spécialement les effets du conditionnement thermique sur l'état cristallin de l'échantillon. On a développé des techniques en vue d'appliquer une large variété de traitements thermiques à l'échantillon dans la cellule DTA. En particulier on a montré que l'emploi d'un procédé de recuit fournit une évaluation significative de la valeur extrapolée de la température de fusion à l'équilibre, combinée avec une rapidité qui est impossible par la méthode dilatométrique. Des données théoriques des différents procédés et des résultats ont été brièvement discutées. L'examen critique de la structure fine, observée dans les thermogrammes de fusion, conduit à la conclusion que sous certaines conditions on peut détecter des cristallites provenant d'une formation de noyau hétérogène et homogène. On considère que l'élévation de température associée à une cristallisation très rapide influence la température de fusion subséquente d'une façon plus importante que les effets de cristallisation pendant le cycle de fusion. Quelques illustrations sont données de l'utilité générale des procédés de conditionnement en clarifiant les phénomènes observées pour divers échantillons.

Zusammenfassung

Das Schmelz- und Kristallisationsverhalten von Polyäthylenproben wurde mittels Differentialthermoanalyse (DTA) mit besonderer Berücksichtigung der Einflüsse der thermischen Konditionierung auf den kristallinen Zustand der Probe untersucht. Verfahren zum Versehen der Proben in der DTA-Zelle mit verschiedenartigen thermischen Vorgeschichten werden beschrieben. Im besonderen wird gezeigt, dass ein Temperungsverfahren eine Ermittlung des extrapolierten Wertes der Gleichgewichtsschmelztemperatur mit einer bei der dilatometrischen Methode nicht möglichen Geschwindigkeit gestattet. Die theoretischen Folgerungen aus den verschiedenen Verfahren und Ergebnissen werden kurz diskutiert. Eine kritische Überprüfung der in den Schmelzthermogrammen beobachteten Feinstruktur führt zu dem Schluss, dass unter gewissen Bedingugen sowohl durch heterogene als auch homogene Keimbildung entstandene Kristallite festgestellt werden könne. Der mit einer sehr raschen Kristallisation verbundene Temperaturanstieg scheint die darauffolgende Schmelztemperatur charakteristischer zu beeinflussen als die Rekristallisationseffekte während des tatsächlichen Schmelzcyklus. Einige Beispiele für die Brauchbarkeit der Konditionierungsverfahren bei der Klärung der an verschiedenen Proben beobachteten Erscheinungen werden gegeben.

JOURNAL OF POLYMER SCIENCE: PART C NO. 6, PP. 65–81 (1964)

Effect of Flame Retardants on Pyrolysis and Combustion of α-Cellulose

WALTER K. TANG, *Forest Products Laboratory,* Forest Service, U. S. Department of Agriculture,* and WAYNE K. NEILL, *Chemical Engineering Department, University of Wisconsin, Madison, Wisconsin*

Synopsis

In the combustion of wood, the α-cellulose fraction contributes most of the flaming; the lignin fraction supports the major part of the glowing. In the present study, thermogravimetric and differential thermal analyses were conducted to determine the effect of low concentrations of flame retardants on the kinetics of pyrolysis and phenomena of combustion of α-cellulose. The flame retardants investigated—sodium tetraborate, aluminum chloride, potassium bicarbonate, and ammonium phosphate—were found to lower the active pyrolysis temperatures and increase the yield of chars. The kinetic data obtained by thermogravimetric analysis of the treated α-cellulose in vacuum suggest that at least two mechanisms are involved. The early stage is controlled by pseudo-zero-order and the late stage is of pseudo-first-order. Sodium tetraborate and aluminum chloride caused little reduction in activation energies. Ammonium phosphate decreased the activation energy mostly in the early stage. Potassium bicarbonate lowered activation energies of both stages. Further thermal analysis in helium and oxygen showed that flaming combustion of α-cellulose was substantially reduced by treatment, and its exothermic peak occurred near the end of pyrolytic volatilization. The heat of pyrolysis was reduced significantly by treatment. The heat of combustion is distributed to a wider temperature range, and the maximum intensity of flaming was much reduced by treatment.

Introduction

The use of many interior finish products in the construction of public and institutional buildings is restricted because the products are flammable. Therefore, the wood and wood products industry is becoming increasingly interested in the flammability of wood, and how chemical treatment can prevent or retard it.

Thermal analysis techniques have been applied at the Forest Products Laboratory to determine the effectiveness of various chemicals as fire retardants for wood.[1–3] Differential thermal analyses of wood and its constituents in air and in inert atmospheres have been made also by several other investigators[4–6] by both qualitative and quantitative procedures. Our current studies show that, as wood burns, the cellulose fraction contributes most the flaming combustion, whereas the lignin fraction supports

* Maintained at Madison, Wis., in cooperation with the University of Wisconsin.

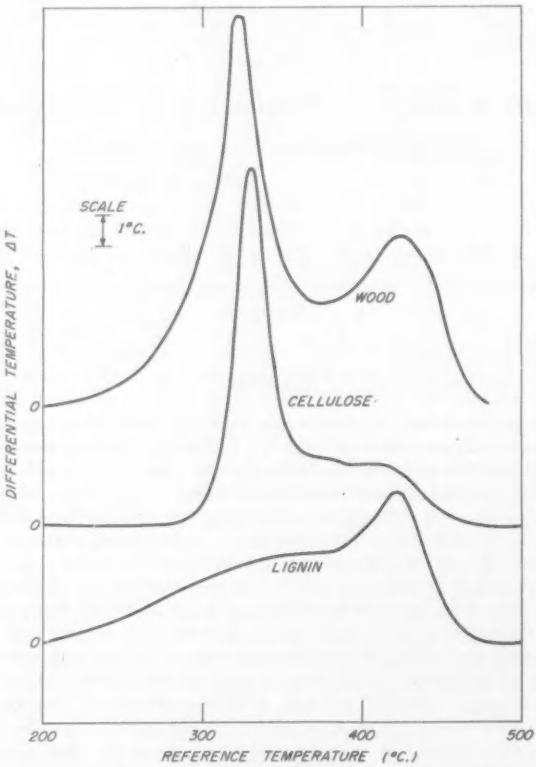

Fig. 1. Differential thermograms of combustion of wood, cellulose, and lignin in oxygen.

most of the subsequent glowing combustion. This is shown by differential thermal analysis data in Figure 1. The sharp peaks near 300°C. are attributed to flaming of volatile products of the initial pyrolysis; the flatter peaks beyond 400°C. are due to glowing combustion of the residual char.

It has been found by several investigators that the principal product in the early depolymerization of α-cellulose is levoglucosan. Levoglucosan reacts further to form char, tars, volatiles, and water.[7–13] Flame retardants increase the percentage of char and water and decrease the percentage of tars in the total product yield.[1,7,8,10,12,14,15] Kinetics of pyrolysis of cellulose have been studied by Akita,[16] Stamm,[17] and Madorsky et al.[10,11] Differential thermal analysis also was used for pyrolysis and combustion of cellulose by several investigators.[5,6,15,18,19]

Such information is insufficient for the comprehensive study of the action of fire-retardant chemicals in changing the pyrolysis and combustion reactions of wood. Current research, which is a part of a continuing program at the Forest Products Laboratory, was begun to study the kinetics of the pyrolysis and thermal analysis of pyrolysis and combustion of untreated and treated α-cellulose by thermogravimetric (TGA) and differential thermal (DTA) analysis.

Experimental Procedure

Four flame retardants were selected for investigation in this study. They are monobasic ammonium phosphate, aluminum chloride hydrate, sodium tetraborate decahydrate, and potassium bicarbonate—all believed to operate by different mechanisms for reducing the production of tars. The concentration of these inorganic salts used in this study was considerably lower than normally used in commercial fire-retardant treatments. However, the low concentration was used to give a better indication of the function of flame-retardant action without complications from excess salts.

The α-cellulose samples used in TGA were Whatman grade 1 chromatography paper, and for DTA, Whatman cellulose powder. Both contain at least 99.3% α-cellulose. The treated samples were prepared by soaking cellulose in solutions of various salts so that the samples retained 2% of the salts when dried and conditioned at 27°C. and 30% relative humidity. A set of samples with 8% $NH_4H_2PO_4$ also was studied. A sample weight of 100 mg. was used for all experiments.

Dynamic TGA technique was applied to obtain the threshold decomposition temperature, the kinetic data, and the char yield. DTA technique was used to find the temperatures for endothermic pyrolysis reaction and exothermic combustion reaction and their intensity. DTA thermograms were also obtained for estimating the heats of pyrolysis and combustion using the calibration factors of known heats of fusion for benzoic acid, potassium nitrate and silver nitrate, and heat of vaporization of ammonium chloride.

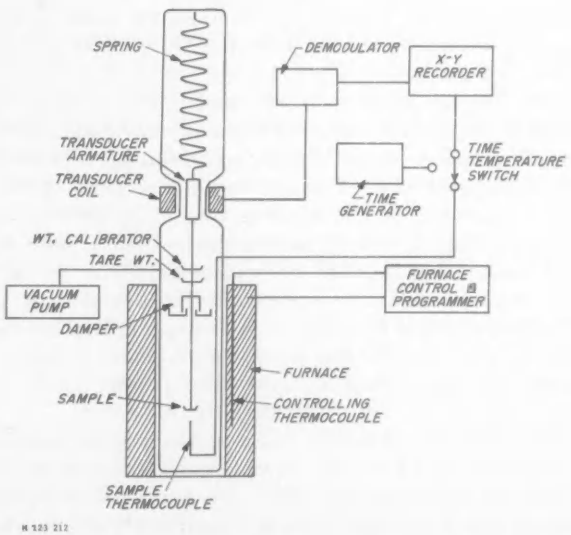

Fig. 2. Schematic diagram of the thermogravimetric balance.

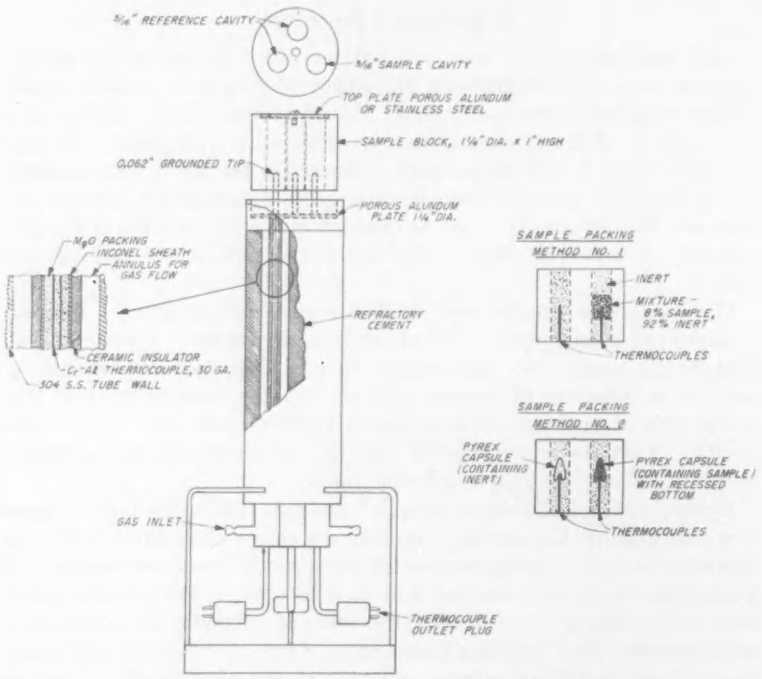

Fig. 3. Sample holder for differential thermal analysis.

A spring-type deflection balance, the Thermograv, made by the American Instrument Company, was used for the TGA. The schematic diagram is shown in Figure 2.

This balance was also modified for the use in DTA by designing a DTA sample holder to be placed within its furnace. The e.m.f. from the differential thermocouple of the holder was applied through a Leeds-Northrup d.c. microvolt amplifier to the Y-axis of the X-Y recorder of the balance. The sample holder (Fig. 3) was made to contain 20–100 mg. of sample, sandwich packed (Fig. 3, sample packing method No. 1) with Minnesota Mining and Manufacturing micro glass beads (0.03 mm. in diameter) in the dynamic gas experiments.[20] A gas (O_2 or He) flowed at the same rate through the packed beads of reference and sample cells. For the heat of pyrolysis study the reference and sample were placed in pyrex capsules (Fig. 3, sample packing method No. 2).[21] The recorder for DTA differential temperature had a sensitivity of 0.25 to 5°C./in.

In the TGA experiments for the study of kinetics, the sample was exposed to a heating rate of 3°C./min. in a vacuum of 0.3 mm. Hg abs.

Other auxiliary TGA and all DTA runs were performed at atmospheric pressure with a flow rate of 30 ml./min. (27°C.) of a gas, except the DTA for heats of pyrolysis with 5 ml./min. gas flow. The heating rate was 12°C./min. The sensitivity of the recorder for differential temperature

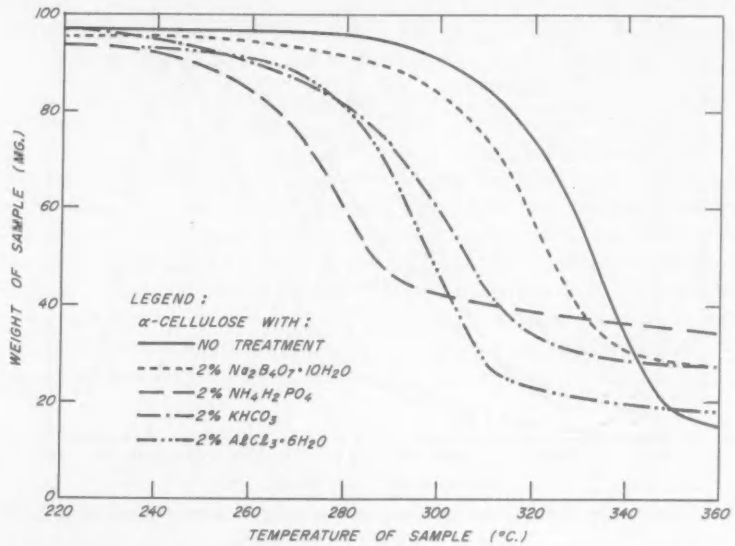

Fig. 4. Thermogravimetric curves of α-cellulose untreated and treated with flame retardants (in vacuum).

was 0.5°C./in. for pyrolysis in inert atmospheres and 5°C./in. for combustion in O_2. All runs were made in triplicate.

Results and Discussion

The thermograms (Fig. 4) from TGA in vacuum show that the α-cellulose with no treatment had the highest threshold temperature for active pyrolysis at 270°C. and lowest char yield of 14 mg. at 360°C. The 2% $NH_4H_2PO_4$ sample indicated a low threshold decomposition temperature of 230°C. with a high char yield of 34 mg. at 360°C. The 2% $Na_2B_4O_7 \cdot 10H_2O$ sample showed threshold decomposition temperature only slightly below that for the untreated cellulose, but char yield substantially higher than that for untreated cellulose although lower than that for the phosphate-treated cellulose. The 2% $AlCl_3 \cdot 6H_2O$ sample and the $KHCO_3$ sample revealed low threshold decomposition temperatures close to that for the $NH_4H_2PO_4$ sample, but the $KHCO_3$ sample left about the same amount of char as the $Na_2B_4O_7 \cdot 10H_2O$ sample whereas the $AlCl_3 \cdot 6H_2O$ sample left little more char than did the untreated cellulose. The differential TGA curves (Fig. 5) also show early decomposition for the treatments with $NH_4H_2PO_4$, $KHCO_3$, and $AlCl_3 \cdot 6H_2O$. The rate of loss in weight reaches sharp maximums of 5.2 mg./min. near 280°C. for $NH_4H_2PO_4$ treatment, 7.5 mg./min. near 300°C. for $AlCl_3 \cdot 6H_2O$ treatment, and 5.6 mg./min. near 305°C. for $KHCO_3$ treatment. For $Na_2B_4O_7 \cdot 10H_2O$ treatment the maximum rate of 7.0 mg./min. near 325°C. is not far from that of 7.4 mg./min. near 335°C. for the untreated cellulose.

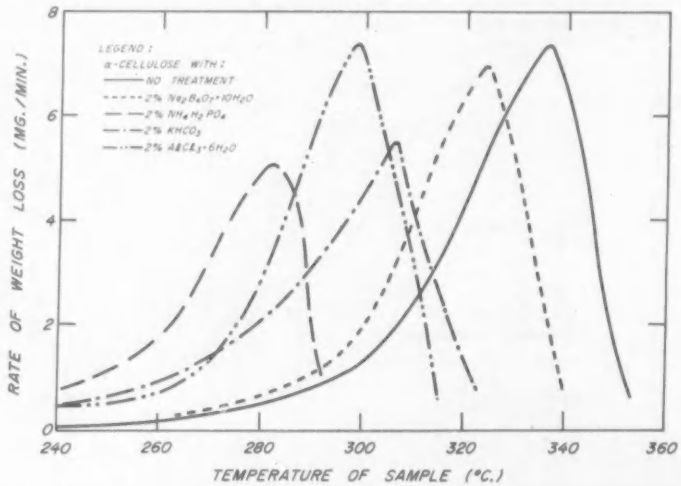

Fig. 5. Differential thermogravimetric curves of α-cellulose untreated and treated with flame retardants (in vacuum).

Kinetics

Because of their low salt concentration, the pyrolysis reaction for these samples was treated as a pseudo-single chemical reaction. The kinetics of pyrolysis of the samples was examined by the difference method (so called by Farmer[22]) of Freeman and Carroll[23] and Anderson and Freeman[24] who derived the equation:

$$\frac{\frac{-E}{2.3R}\Delta\,(T^{-1})}{\Delta \log W_r} = -n + \frac{\Delta \log\,(dw/dt)}{\Delta \log W_r}$$

where E = the activation energy of the reaction, cal./mole; n = the kinetic order of the reaction; T = the absolute temperature, °K.; and R = the gas constant, 1.987 cal./°K. mole and $W_r = W_c - W$, where W_c is the weight loss at the completion of the reaction and W the total weight loss up to time t. A plot of

$$\frac{\Delta \log\,(dw/dt)}{\Delta \log W_r} \text{ versus } \frac{\Delta(T^{-1})}{\Delta \log W_r}$$

should result in a linear plot having a slope of $-E/2.3R$ and an intercept corresponding to n. The results (Fig. 6) illustrate that a pseudo-first-order reaction took place during most of the pyrolysis; however, the data for the initial stage did not conform to the plot. The scattering of data points in the initial stage may be attributed to two factors: (*a*) The initial stage has a different reaction mechanism, and (*b*) the difference method has magnified the possible small errors in the initial stage where weight loss

is small. When those data for the initial stage were plotted (Fig. 7) according to a pseudo-zero-order reaction, excellent conformity was obtained. It is apparent that there are two mechanisms involved. When a plot of

$$\log \frac{(dw/dt)}{W_r} \text{ versus } 1/T$$

was made from the data instead of following the difference method, the initial stage of pyrolysis showed a fair correlation as a pseudo-first-order reaction but not so good a fit as a pseudo-zero-order reaction. The activation energies from this plot were a little higher than those by the difference method. Thus the results suggest that the initial stage is controlled by pseudo-zero-order kinetics and the final stage is pseudo-first-order controlled. The temperature range, percentage of total weight loss in each stage, and the activation energies for each stage are shown in Table I.

TABLE I
Energies of Activation for Pyrolysis of α-Cellulose

α-Cellulose with	Initial stage (0 to 1st order)			Final stage (1st order)		
	Temp., °C.	%	E, kcal./mole	Temp., °C.	%	E, kcal./mole
No treatment	240–310	15	33.1–35.2	310–360	85	53.1–55.7
2% $Na_2B_4O_7 \cdot 10H_2O$	230–285	11	29.8–31.9	285–345	89	50.7–54.0
2% $AlCl_3 \cdot 6H_2O$	210–265	10	32.8–33.4	265–320	90	53.0–55.0
2% $KHCO_3$	200–270	20	19.3–21.0	270–330	80	38.2–42.0
2% $NH_4H_2PO_4$	190–255	20	16.9–19.0	255–300	80	51.8–54.5

Auxiliary TGA and DTA

To assist the interpretation of the kinetic results, a series of TGA was performed in He and a series of DTA was carried out in O_2 and in He. The thermograms of the results are shown in Figure 8.

The initial stage of pyrolysis of untreated α-cellulose was an endothermic reaction of loss of moisture near 100°C. At 200–270°C. (Fig. 8*A*) depolymerization took place without further loss of weight. Depolymerization continued beyond 270°C. where the TGA curve began to show significant weight loss. It possible involved volatilization of monomeric levoglucosan in the initial stage of pyrolysis. In the final stage, the endotherm reached its nadir at 335°C. where the weight loss also reached its maximum rate (Fig. 5) and the exotherm of combustion reached a flaming peak from the combustion of volatile tars. At a temperature near 360°C., the endotherm and weight loss in pyrolysis show that the active pyrolysis with evolution of low molecular weight flammable tars was nearly completed. In combustion in O_2, however, an exotherm continued because the higher molecular weight chars were being consumed by glowing until about 460°C., where the entire sample had been consumed. For the mechanism of flame

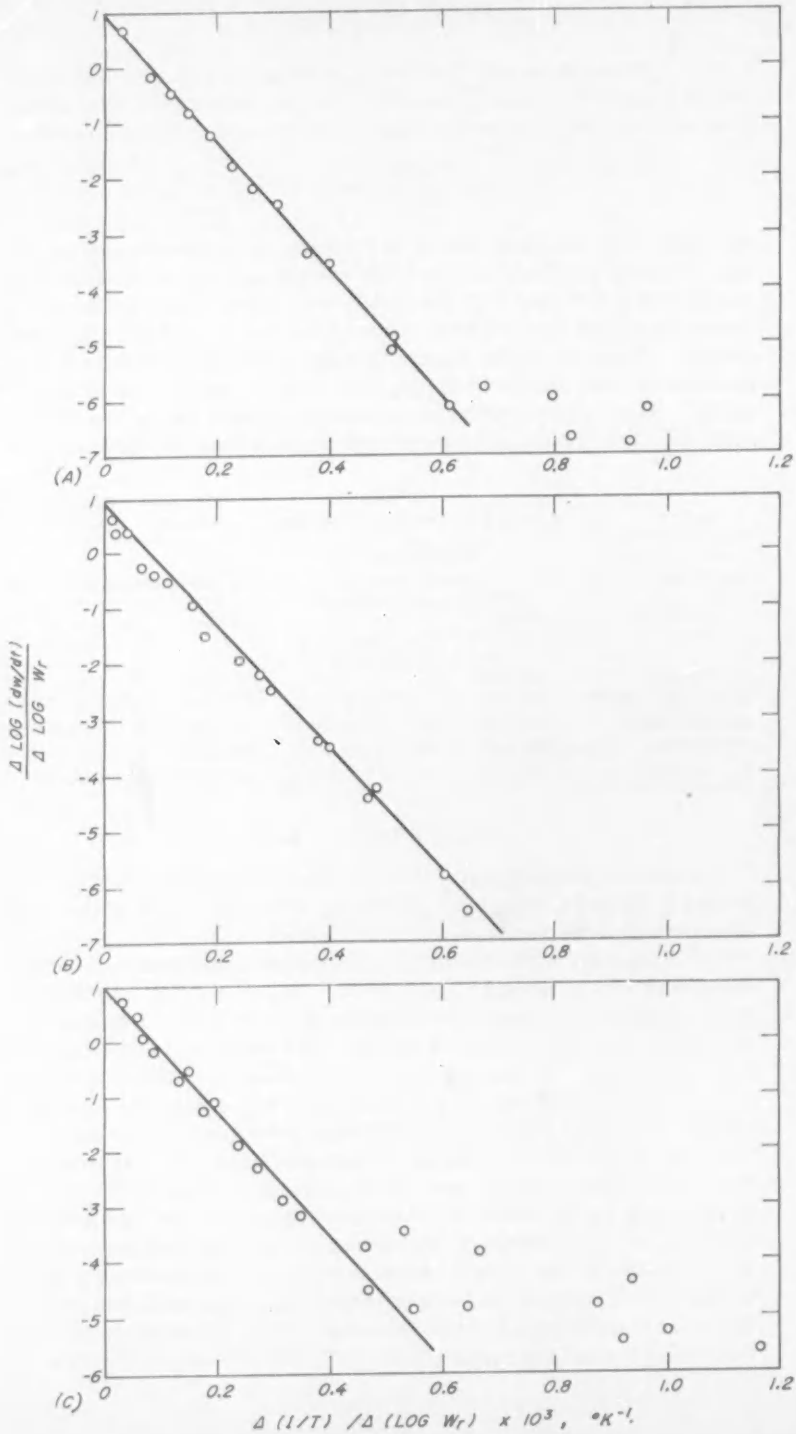
(A)
(B)
(C)
Δ LOG (dw/dt) / Δ LOG Wr
Δ (1/T) / Δ (LOG Wr) x 10³, °K⁻¹.

retardance by $Na_2B_4O_7$ it may be postulated that the depolymerized low molecular weight fragments of α-cellulose were catalyzed to form more char and less tar[9] by polymerization and aromatization. As a result, the endotherm (Fig. 8*B*) shows that the endothermic heat of pyrolysis was less than that of untreated α-cellulose. These reactions ceased sharply at 345°C. as shown also by the weight-loss curve. In combustion, therefore, the intensity of flaming was definitely reduced because less tar was made available. Glowing combustion, however, continued and contributed an increased amount of heat because of the greater yield of char. The temperature range of glowing combustion was also extended to 500°C., about 40°C. higher than that for untreated α-cellulose.

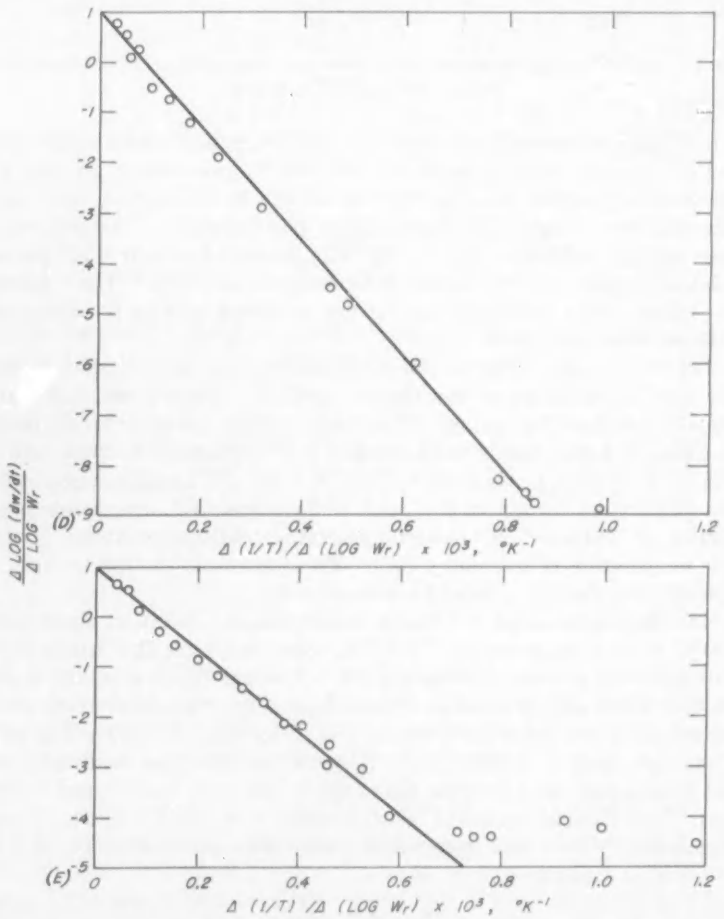

Fig. 6. Kinetics of the pyrolysis of α-cellulose(in vacuum): (*A*) untreated; (*B*) treated with 2% $Na_2B_4O_7 \cdot 10H_2O$; (*C*) treated with 2% $NH_4H_2PO_4$; (*D*) 2% $AlCl_3 \cdot 6H_2O$; (*E*) 2% $KHCO_3$.

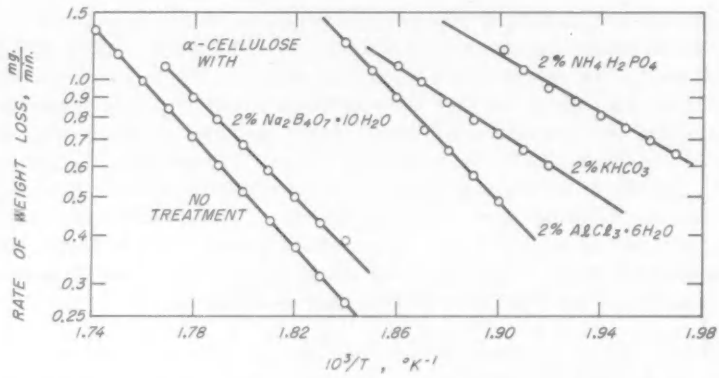

Fig. 7. Temperature dependency of low temperature range pyrolysis of untreated and treated α-cellulose (in vacuum).

In the case of α-cellulose treated with $KHCO_3$,[25] an increased weight loss and endothermic effect between 100 and 200°C. presumably was due to reactions initiated by decomposition of $KHCO_3$ to K_2CO_3, CO_2, and H_2O. The endotherm (Fig. 8*C*) indicates that a possible series of complex reactions took place between 200 and 350°C. It reached a nadir when loss of volatiles by active pyrolysis was nearly complete at 350°C. The combustion curve shows decreased flaming but increased glowing as compared with untreated α-cellulose.

The DTA curves (Fig. 8*D*) of $AlCl_3 \cdot 6H_2O$ treated samples show a similar trend of reduction of endothermic nadir for pyrolysis and reduction of exothermic peak in flaming. Hydrate of aluminum chloride breaks down to Al_2O_3, HCl, and H_2O between 100 and 180°C. (from TGA data). $AlCl_3$ and Al_2O_3 are both Lewis acids.[14] The TGA and DTA results suggest that the dehydration mechanism of a Lewis acid was initiated during decomposition of $AlCl_3 \cdot 6H_2O$. This catalytic process is sustained by Al_2O_3. Pyrolysis temperature is lowered by HCl. These reactions showed no noticeable effect on the rate of weight loss of cellulose.

The decomposition of $NH_4H_2PO_4$ yields NH_3 and H_3PO_4 at about 170–200°C. in the treated sample. The NH_3 volatilizes, while H_3PO_4 may react with hydroxyl groups of glucosan units.[1] The endotherm (Fig. 8*E*) shows that there probably is a change of some kind in the mechanism of the process at 245°C. for 2% $NH_4H_2PO_4$ and 225°C. for 8% $NH_4H_2PO_4$ (Fig. 8*F*). The combustion for the 2% $NH_4H_2PO_4$ again indicates that the flaming did not reach a peak until near the end of the endothermic reaction and weight loss. The flaming peak and glowing peak were 125°C. apart. These phenomena became still more marked when the concentration of $NH_4H_2PO_4$ was increased to 8%.

Heat of Pyrolysis

For the purpose of estimating the heat of pyrolysis, thermograms of pyrolysis were obtained by DTA of samples placed in pyrex capsules. This

technique would reduce the convective losses in He stream and give more nearly quantitative results. The area under the curve integrated graphically was used to calculate the heat of pyrolysis by the relation:[6,26]

$$(\Delta H)_s = \frac{A_s m_k}{A_k m_s} (\Delta H)_k$$

where $(\Delta H)_s$ = heat of reaction of sample, cal./g.; $(\Delta H)_k$ = known heat of reaction of a reference substance, cal./g., m_s, m_k = weight of sample and a reference substance, g.; and A_s, A_k = integrated area under DTA curve, cm.^{2}.

Heats of fusion of $AgNO_3$, benzoic acid, and KNO_3 were used as the calibration standard. The DTA curves of the compounds were obtained under the same experimental conditions as those of the cellulose samples. The calibration values are shown in Table II.

TABLE II
Calorimetric Calibration Factors for DTA

Compound	Melting point, °C.	Heat of fusion, cal./g.	$\frac{m_k(\Delta H)_k}{A_k}$, $\frac{\text{cal.}}{\text{cm.}^2}$
Benzoic acid	122	33.9	0.304
$AgNO_3$	208	17.7	0.292
KNO_3	308	25.4	0.290

The values of heats of pyrolysis of untreated and treated α-cellulose estimated under these conditions are listed in Table III.

TABLE III

α-Cellulose with:	Heat of pyrolysis, cal./g.
No treatment	88 ± 3.6
2% $Na_2B_4O_7 \cdot 10H_2O$	58 ± 2.4
2% $AlCl_3 \cdot 6H_2O$	87 ± 3.4
2% $KHCO_3$	72 ± 3.0
2% $NH_4H_2PO_4$	78 ± 3.2
8% $NH_4H_2PO_4$	64 ± 2.6

These values indicate that the treated samples have lower heats of pyrolysis than that of untreated samples. It suggests that the endothermic depolymerization and dehydration of cellulose is counteracted by the exothermic polymerization and aromatization of pyrolysis product.

Heat of Combustion

If combustion goes to completion, the heat of combustion of treated samples of α-cellulose corrected for any heat effect due to change in the treating chemical present must be the same as the heat of combustion of untreated α-cellulose. The reason is that in complete combustion the end products

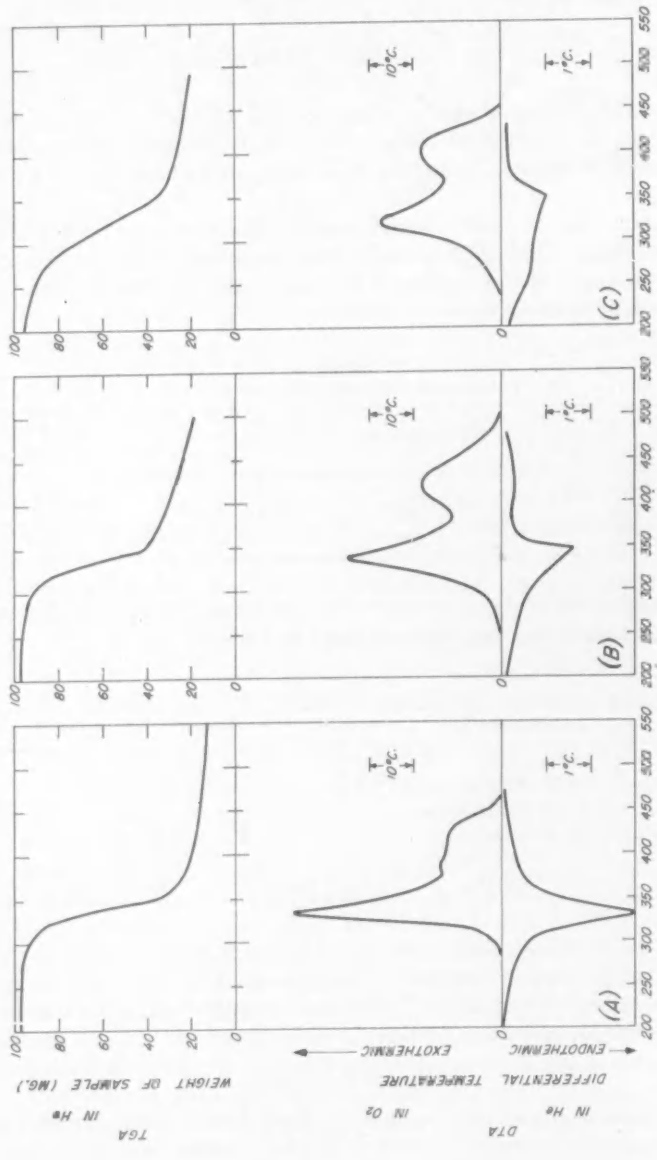
TGA
IN He
WEIGHT OF SAMPLE (MG.)
DTA
IN O2
IN He
DIFFERENTIAL TEMPERATURE
EXOTHERMIC
ENDOTHERMIC
(A)
(B)
(C)

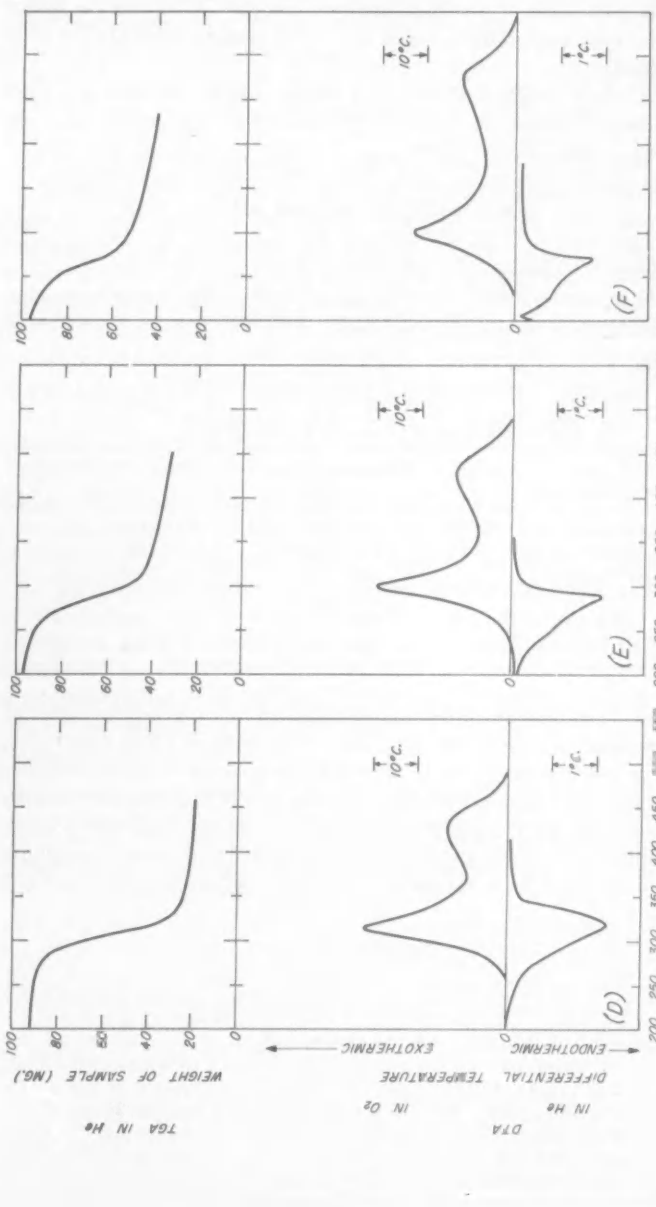

Fig. 8. TGA and DTA results on α-cellulose with different treatments: (*A*) no treatment; (*B*) 2% $Na_2B_4O_7 \cdot 10H_2O$; (*C*) 2% $KHCO_3$; (*D*) 2% $AlCl_3 \cdot 6H_2O$; (*E*) $\frac{1}{2}$% $NH_4H_2PO_4$; (*F*) 8% $NH_4H_2PO_4$.

of α-cellulose are the same for both untreated and treated samples. The effect of inorganic chemicals on the total heat of combustion in these cases will be small.

Ammonium chloride was used in the dynamic gas DTA, and the latent heat of vaporization of ammonium chloride was used to calibrate the heat of combustion.

The DTA was carried out on NH_4Cl in flowing nitrogen instead of oxygen with all other conditions the same as in the DTA of combustion of α-cellulose. The factor

$$\frac{m_k (\Delta H)_k}{A_k} = 2.2 \text{ cal./cm.}^2 \text{ for } NH_4Cl$$

where $(\Delta H)_k = 39.6$ kcal./mole or 740 cal./g.[27]

The heats of combustion of treated and untreated α-cellulose calculated from this factor and the integrated area of the thermograms are shown in Table IV.

TABLE IV
Calibrated Heats of Combustion of α-Cellulose

α-Cellulose with:	Integrated area, cm.²/g.	Heat of combustion, cal./g.
No treatment	1610 ± 64	−3540 ± 140
2% $Na_2B_4O_7 \cdot 10H_2O$	1650 ± 66	−3630 ± 146
2% $AlCl_3 \cdot 6H_2O$	1620 ± 64	−3560 ± 142
2% $KHCO_3$	1590 ± 64	−3500 ± 140
2% $NH_4H_2PO_4$	1600 ± 64	−3520 ± 140
8% $NH_4H_2PO_4$	1600 ± 64	−3520 ± 140

The heat of combustion of α-cellulose obtained by oxygen-bomb calorimeter has a value of −4030 cal./g. The value from DTA is about 12% lower. The possible reason for the low value is a loss of unburned volatiles in the gas stream. If it is assumed that the loss of combustible volatiles is proportional to the heat evolution and corrections are made accordingly, the maximum rate of heat generation for untreated and treated α-cellulose may be estimated. These values under these conditions are given in Table V.

TABLE V

α-Cellulose with:	Maximum rate of heat generation, cal./g. min.
No treatment	870 ± 35
2% $Na_2B_4O_7 \cdot 10H_2O$	730 ± 29
2% $AlCl_3 \cdot 6H_2O$	665 ± 27
2% $KHCO_3$	588 ± 24
2% $NH_4H_2PO_4$	635 ± 25
8% $NH_4H_2PO_4$	498 ± 20

These results show a definite suppression of maximum rate of heat generation by flame retardants in the flaming of α-cellulose. However, the degree of suppression by the several retardants does not indicate their relative effectiveness, because they cannot be compared properly on the weight percent basis.

Conclusions

In general, thermogravimetric analysis shows that flame retardants lower the threshold temperature of pyrolysis for α-cellulose and raise the char yield in the products. Differential thermal analysis in O_2 demonstrates that flame retardants reduce flaming but may extend glowing. In other words, the heat of combustion of untreated α-cellulose, which is concentrated in intensity in a narrow temperature range, is actually redistributed by the effect of flame retardant to a wider temperature range with a lower maximum intensity. The results of depolymerization and dehydration of cellulose and polymerization and aromatization of pyrolysis products gave a reduced heat of pyrolysis for many of the treated α-celluloses. The maximum intensity of the heat of pyrolysis also was reduced.

Specifically the $KHCO_3$, even at low concentration, seems to be able to change the pyrolysis kinetics, both in the initial and final stages. On the other hand, $NH_4H_2PO_4$ at low concentration affects only the initial stage of pyrolysis, but further effect may be expected with higher concentration. This may also be true for $AlCl_3 \cdot 6H_2O$ samples. $Na_2B_4O_7 \cdot 10H_2O$ after losing water at 200°C. seems to behave in a manner different from the other three and is expected to be stable even above the pyrolysis temperatures of cellulose. Although none of the four flame retardants may react stoichiometrically with α-cellulose, the availability of these molecules for catalysis is important. For this reason, higher concentration is needed to assure their effectiveness.

The authors wish to thank Mr. H. W. Eickner, in charge of research of Fire Performance of Wood at the Forest Products Laboratory, and Dr. F. L. Browne for their valuable suggestions. This study is a continuation of a study begun under a grant by National Science Foundation with Dr. Browne as principal investigator, and aided further by the Koppers Company, Incorporated.

References

1. Browne, F. L., *U. S. Dept. Agr., Forest Serv., Forest Prod. Lab. Rpt.*, **2136** (1958).
2. Browne, F. L., and W. K. Tang, *Fire Res. Abstr. Rev.*, **4**, 76 (1962).
3. Browne, F. L., and W. K. Tang, *U. S. Dept. Agr., Forest Serv., Res. Paper*, **6** (1963).
4. Arseneau, D. F., *Can. J. Chem.*, **39**, 1915 (1961).
5. Damansky, R., and F. Rendos, *Holz Roh- Werkstoff*, **20**, 473 (1962).
6. Keylwerth, R., and N. Christoph, *Deutsche Verband Materialprüfung, Materialprüf*, **2**, 281 (1960).
7. Berkowitz-Mattuck, J. B., and T. Noguchi, *J. Appl. Polymer Sci.*, **7**, 709 (1963).
8. Holmes, F. H., and C. J. G. Shaw, *J. Appl. Chem.*, **11**, 210 (1961).

9. Honeyman, J., The British Cotton Industry Research Association, Progress Report (1959–1960). The Cotton, Silk, and Man-made Fibres Research Association Progress Report (1960–1962).

10. Madorsky, S. L., V. E. Hart, and S. Straus, *J. Res. Natl. Bur. Std.*, **56**, 343 (1956).

11. Madorsky, S. L., V. E. Hart, and S. Straus, *J. Res. Natl. Bur. Std.*, **60**, 343 (1958).

12. Pascu, E., and R. F. Schwenker, Pyrolytic Degradation of Cellulose and Chemical Modification of Cellulose for Flame and Glow Resistance, Contract DA-18-129-QM-122, U.S. Army Quartermaster Corps, (1954–1957).

13. Schwenker, R. F., and E. Pascu, *Ind. Eng. Chem.*, **2**, 83 (1957).

14. Schuyten, H. A., J. W. Weaver, and J. D. Reid, *Am. Chem. Soc. Adv.-Chem. Ser.*, **9**, 7 (1954).

15. Schwenker, R. F., L. R. Beck, and E. Pascu, *Am. Chem. Soc. Abstr. Papers*, **17E** (1960).

16. Akita, K., *Rept. Fire Res. Inst. Japan*, **9**, (1959).

17. Stamm, A. J., *Ind. Eng. Chem.*, **48**, 413 (1956).

18. Berkowitz, N., *Fuel*, **36**, 355 (1957).

19. Morita, H., and H. Rice, *Anal. Chem.*, **27**, (3), 336 (1955).

20. Stone, R. L., *Anal. Chem.*, **32**, 1582 (1960).

21. Bollin, E. M., and P. F. Kerr, *Am. Mineralogist*, **46**, 823 (1961).

22. Farmer, R. W., U. S. Air Force Aeronautical Systems Division Rpt., ASD-TDR-62-1043 (1963).

23. Freeman, E. S., and B. Carroll, *J. Phys. Chem.*, **62**, 394 (1958).

24. Anderson, D. A., and E. S. Freeman, *J. Polymer Sci.*, **54**, 253 (1961).

25. Broido, A., and S. Martin, *Fire Res. Abstr. Rev.*, **3**, 193 (1961).

26. Smothers, W. J., and Y. Chiang, *Differential Thermal Analysis: Theory and Practice*, Chemical Publishing Company, New York, 1958.

27. *Handbook of Chemistry and Physics*, 44th Ed., Chemical Rubber Publishing Company, Cleveland, 1962–1963.

Résumé

Dans la combustion du bois, c'est principalement la fraction constituée d'alpha-cellulose qui contribue à la formation de flammes, tandis que la fraction constituée de lignine est responsable, en majeure partie, de l'incandescence. Dans cette étude, on a effectué des analyses différentielles thermiques et thermogravimétriques pour déterminer l'effet de petites concentrations de substances retardant l'apparition des flammes, sur la cinétique de pyrolyse et sur les phénomènes de combustion de l'alpha-cellulose. Les retardateurs de flamme étudiés (tétraborate de sodium, chlorure d'aluminium, bicarbonate de potassium et phosphate d'ammonium) abaissent la température de pyrolyse active et augmentent la carbonisation. Les données cinétiques obtenues par analyse thermogravimétrique, sous vide de l'alpha-cellulose, suggère l'existence d'au moins deux mécanismes. La première étape répond à un ordre nul apparent et la dernière étape présente un ordre 1 apparent. Le tétraborate de sodium et le chlorure d'aluminium ne produisent qu'un faible abaissement des énergies d'activation. Le phosphate d'ammonium abaisse surtout l'énergie d'activation de la premipre étape. Le bicarbonate de potassium abaisse les énergies d'activation des deux étapes. Des analyses thermiques ultérieures effectuées dans l'hélium et dans l'oxygène, montrent que la combustion vive de l'alpha-cellulose est sensiblement réduite par le traitement et que son pic exothermique apparaît vers la fin de la volatilisation pyrolytique. La chaleur de pyrolyse a été réduite de façon importante par ce traitement. La chaleur de combustion s'étend sur un domaine de température plus large et le maximum d'intensité dans l'apparition des flammes a été fortement réduit par ce traitement.

Zusammenfassung

Bei der Verbrennung von Holz trägt die α-Cellulosefraktion den grössten Teil der Flammenbildung bei; die Ligninfraktion unterhält den Hauptteil des Glühens. In der vorliegenden Untersuchung wurden thermogravimetrische Messungen und Differentialthermoanalysen zur Bestimmung des Einflusses kleiner Konzentrationen von Flammenschutzstoffen auf Pyrolysenkinetik und Verbrennungserscheinungen von α-Cellulose durchgeführt. Die untersuchten Flammenschutzstoffe—Natriumtetraborat, Aluminiumchlorid, Kaliumbikarbonat und Ammonium-phosphat—setzten die aktive Pyrolysentemperatur herab und erhöhten die Ausbeute an Verkohlungsprodukten. Die durch thermogravimetrische Analyse der behandelten α-Cellulose im Vakuum erhaltenen kinetischen Daten sprechen dafür, dass mindestens zwei Mechanismen wirksam sind. Die frühe Phase ist pseudo-nullter Ordnung und die späte Phase pseudo-erster Ordnung. Natriumtetraborat und Aluminiumchlorid lieferten eine unwesentliche Verminderung der Aktivierungsenergie. Ammoniumphosphat setzte die Aktivierungsenergie hauptsächlich in der frühen Phase herab. Kaliumbikarbonat erniedrigte die Aktivierungsenergie beider Phasen. Weitere Thermoanalysen unter Helium und Sauerstoff zeigten, dass die Flammenverbrennung von α-Cellulose durch die Behandlung wesentlich reduziert wurde und dass die exotherme Spitze nahe dem Ende der pyrolytischen Verflüchtigung auftrat. Die Pyrolysenwärme wurde durch die Behandlung typisch reduziert. Die Verbrennungswärme wird über einen weiteren Temperaturbereich verteilt und die maximale Flammungsintensität durch die Behandlung stark reduziert.

JOURNAL OF POLYMER SCIENCE: PART C NO. 6, PP. 83-91

Kalorimetrische Messungen der Kristallisations- und Schmelzvorgänge an Polymeren

F. H. MÜLLER und H. MARTIN, *Institut für Polymere, Phillips Universität, Marburg/Lahn, West Germany*

Synopsis

Crystallizing and melting of polymers as a function of sample history is investigated by means of a differential thermal analytic method developed for quantitative evaluation. Crystallization and the subsequent melting of the same polymer occur at temperatures differing by 12 to 18°C. The melt temperature and the time of keeping the sample in the molten state, the cooling rate and the course of cooling have a reproducible effect on the subsequent melting. The crystallization is followed at constant temperature, and the crystallization rate is evaluated. Application of the Avrami method gives agreement with similar density and refractive index measurements.

Umwandlungserscheinungen in Polymeren, insbesondere Kristallisations- und Schmelzvorgänge, werden heute vielfach mit einfacher Differentialthermoanalyse (DTA) untersucht. Die DTA-Methode kann jedoch im wesentlichen nur Informationen über die Temperaturbereiche liefern, in denen Vorgänge ablaufen, und nur gewisse *qualitative* Aussagen über die Umwandlungswärmen.[1] Für *quantitative* Aussagen ist die Kenntnis der "spezifischen Wärme," die Wärmeaufnahme, als Funktion der Temperatur erforderlich.

Feste Polymere befinden sich zudem im allgemeinen nicht im thermodynamischen Gleichgewicht. Das bedeutet, das die "spezifische Wärme" mit der Vorbehandlung variieren kann. Es tritt also das Problem auf, wie man *quantitative* c_p-Messungen reproduzierbar erhalten kann. Dabei ist zu beachten, dass die Probe auch noch während der Messung selbst einer Vorbehandlung unterliegt. Bei den Punkt-für-Punkt-Messungen, etwa im adiabatischen Kalorimeter, besteht die Gefahr, dass wegen der Wartezeiten zum Temperaturausgleich an jedem Messpunkt die "Vorbehandlung" in Hinblick auf das Zeitverhalten der Substanz verschieden ist.[2]

Definierter, jedenfalls wegen dieser Zeiteffekte leichter analysierbar, erscheinen uns daher Messungen mit zeitlich linear geführter Aufheizung. Solche quasistationären Messungen sind erreichbar, wenn man die Methode der Differentialthermoanalyse in quantitativer Richtung ausbaut. Das haben wir getan.[3]

Inzwischen wurde diese Apparatur in ihrer Empfindlichkeit und Eichfähigkeit noch weiter ausgebaut.[4] In einer theoretischen Untersuchung

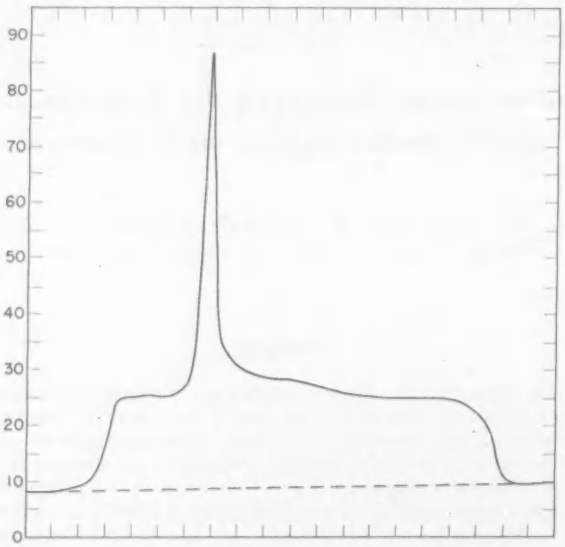

Abb. 1. Unmittelbare Wiedergabe einer Registrierkurve des Temperaturganges der spezifischen Wärme in der Umgebung des Klärpunktes an einer reinsten Substanzprobe von 0,5 g *p,p'*-Azoxyanisol unter Stickstoff.

des Messprinzips konnten wir ferner zeigen, dass sich aus den Registrierkurven durch Entzerrung der Verlauf der specifischen Wärme mit der Temperatur exakt ermitteln lässt,[5] und zwar sowohl bei Aufheizung als auch bei Abkühlung.[6]

Als charakteristisches Beispiel für die Leistungsfähigkeit sei hier eine Messung an *p,p'*-Azoxyanisol gezeigt,[7] und zwar der Übergang von kristallin-flüssig zu amorph-flüssig. Abb. 1 gibt eine Registrierkurve wieder. Die scharfe Spitze entspricht nach Entzerrung einer latenten Umwandlungswärme von 0,53 cal/g ± 6% bei einer Temperatur von 132°C. Dieser scharfen Umwandlung vorgelagert im Bereich zwischen 128–132° zeigt sich eine verwaschene Umwandlung mit einer Enthalpiedifferenz von 0,16 cal/g. Die Summe beider Werte stimmt überein mit früheren Messungen aus der Literatur,[8] wobei sich zeigte, dass die—übrigens schon von anderer Seite angezweifelten–Werte von Kreutzer[9] 1,79 cal/g falsch sein müssen. Interessant ist, dass die Existenz einer vorgelagerten Ordnungs-Unordnungsumwandlung sich nach W. Maier, Freiburg/Br.[10] auch aus dielektrischen und Kernresonanzmessungen vermuten liess und hiermit kalorisch bestätigt werden konnte.*

Die Messungen selbst wurden an $^1/_4$ g der unter Stickstoff eingeschmol

* Wie inzwischen im Gespräch gehört, sind unsere Werte in exakter Übereinstimmung mit neuren Messungen von Dr. R. S. Porter, California Research Corporation Institute, Richmond, Calif.

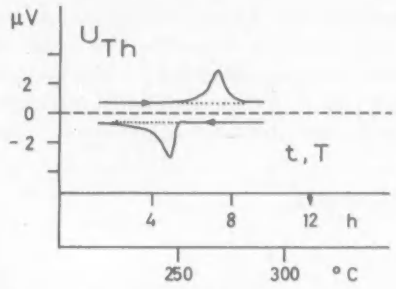

Abb. 2. Kristallisations- und Schmelzkurve von 0,6 g Terylen (Poly-äthylenglykolterephthalat). Aufgetragen ist die Thermospannung zwischen Mess- und Vergleichsröhrchen ($U_{Th} \backsim c_p$ + konst.) gegen die Temperatur der Probe (T) und die Versuchszeit (t). Messgeschwindigkeit: 1 °C/6 min.

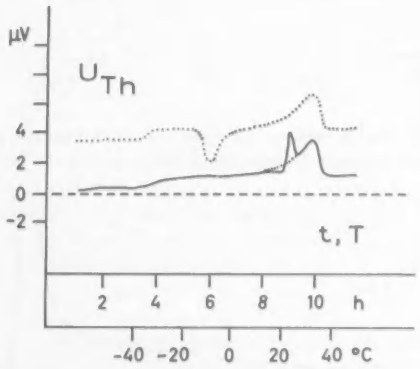

Abb. 3. Aufheizmessung an 0,5 g isozyanatvernetztem Polyurethan. Punktiert: nach oben verschobene Kurve für aufgeschmolzene, auf −60° abgeschreckte Probe; ausgezogen: Aufheizung der ebenso behandelten Probe, bei 20° für 24 Stunden konstant gehalten, erneut abgekühlt auf −60° und nun gemessen. Es verschwindet das Kristallisationsminimum, es erscheint ein Doppelmaximum des Schmelzens. Auch die Stufe des Einfrierintervalls bei −40° ändert sich in der Form.

zenen extrem reinen Substanz getätigt und waren reproduzierbar, sowohl bei Aufheizung als bei Abkühlung.

Eine allgemeine charakteristische Eigenschaft kristallisierender Polymerer scheint zu sein, dass bei gleicher Abkühl- und Aufheizgeschwindigkeit das Maximum des Aufschmelzens stets um ungefähr 12–18° C höher als das der Kristallisation liegt. Dies ist sowohl an Polyäthylenen als auch an Polyäthylenglykolterephthalat (Abb. 2), aber auch an Polyamiden usw. zu beobachten.

Bekanntlich müssen zur Kristallisation bei einer bestimmten Temperatur die Keime eine bestimmte *kritische Lange* besitzen, *wenn* sie *wachstumsfähig* sein sollen. Mandelkern, Hoffman, und Lauritzen[11] haben diese kritische

Keimlänge für bündelförmige Keime berechnet. *Andererseits* hängt die *Schmelztemperatur* des einzelnen Kristallits von seiner *Kristallitlänge* ab, für die Flory eine Beziehung abgeleitet hat.[12] Ein Vergleichbeider Formeln lässt erkennen, dass unter bestimmten Voraussetzungen (vor allem die, dass der Schmelzpunkt der Kristalle nur von deren "Länge" abhängt) bei

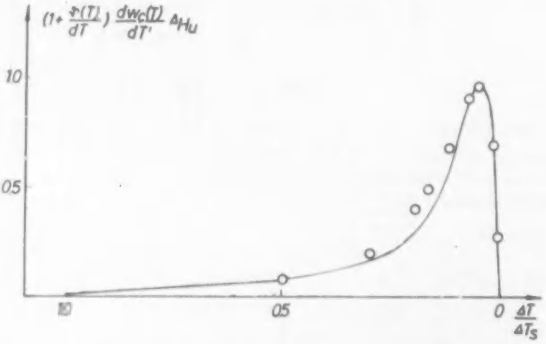

Abb. 4. Normierte Auftragung von $c_p{}^+$ für eine chlorierte Polyäthylenprobe (3 Mol% Chlor), ausgezogen die berechnete Kurve, Kreise die Messung.

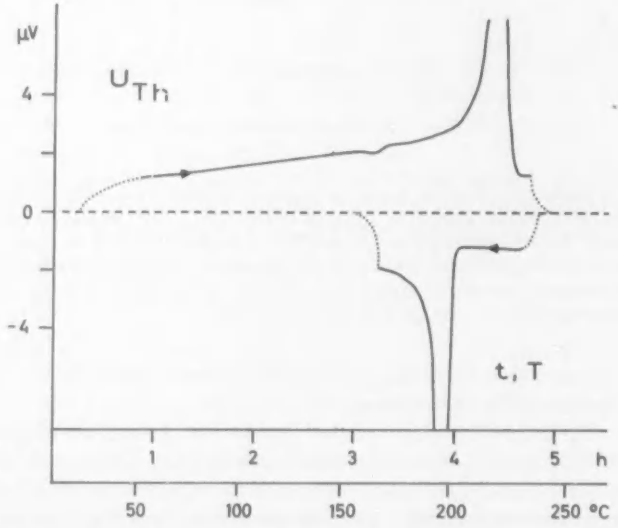

Abb. 5. Kristallisations- und Schmelzkurve von 0,5 g Polycaprolactam (6-Nylon). Aufgetragen ist die Thermospannung zwischen Mess- und Vergleichsröhrchen ($U_{Th} \backsim c_p$ + konst.) gegen die Temperatur der Probe (T) und die Versuchszeit (t). Messgeschwindigkeit: 1 °C/2 min. (Die Einlaufvorgänge sind punktiert eingezeichnet.) Beim Einlaufvorgang während der Abkühlmessung in der Nähe von 160° erscheint bei der Aufheizmessung eine Wellung (Minimum-Maximum).

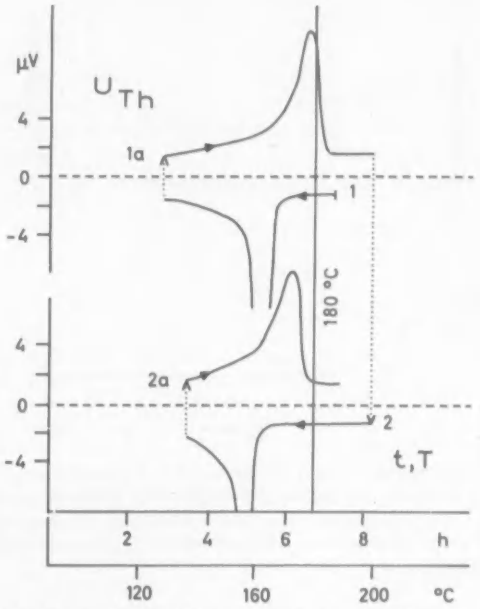

Abb. 6. Kristallisations- und Schmelzkurven von 0,79 g 4,6-Polyurethan. Aufgetragen ist die Thermospannung zwischen Mess- und Vergleichsröhrchen ($U_{Th} \backsim c_p$ + konst.) gegen die Temperatur der Probe (T) und die Versuchszeit (t). Messgeschwindigkeit: 1°C/4,5 min. (Die Abkühlmessung 1 wurde von 185 °C aus begonnen, die Abkühlmessung 2 von 200 °C).

der Temperatur des Kristallisationsbeginns beim Abkühlen gerade Kristalle der halben Länge (der Faktor "halb" ist nicht streng, sondern nur der Grössenordnung nach zutreffend, je nach den Voraussetzungen für die Keimform) zum Schmelzen zu bringen sind. Der Schmelzpunkt von Kristalliten einer bestimmten Grösse kann nach diesen Betrachtungen nicht mit der Temperatur, bei der Kristallite dieser Grösse entstehen, zusammenfallen.

Wenn man eine Substanz in dem Bereich zwischen Kristallisations- und Schmelzmaximum lagert, dann treten Umordnungen dergestalt auf, dass ausser dem Schmelzmaximum noch ein Vormaximum entsteht, das bei genügend langer Lagerung wieder in das eigentliche Schmelzmaximum hineinwandert (Abb. 3).[13] Die Erklärung ist, dass kleinere Kristallite schneller zu etwas grösseren zusammenwachsen als grössere zu noch grösseren. Auf diese Weise ändert sich die Kristallitgrössenverteilung im Material zeitlich, und letztere spiegelt sich in der Schmelzkurve wieder (s.w.u.).

Nicht nur Lagerung bei geeigneten Temperaturen, auch Abschrecken und Verstrecken verändern die Aufschmelzkurven bzw. den Verlauf der spezifischen Wärme. Bei Polytetrafluoräthylen lässt sicht aus dem c_p-

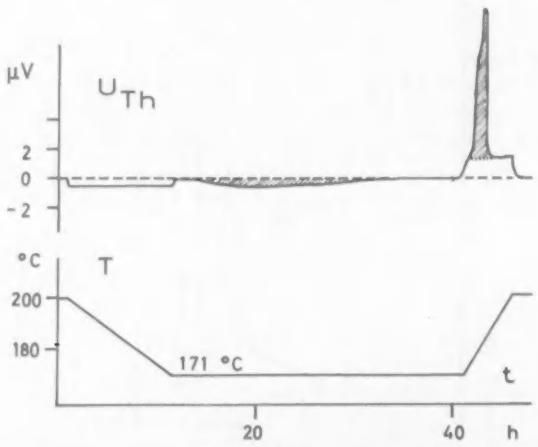

Abb. 7. Messung der isothermen Kristallisation von Polyurethan. Die untere Kurve gibt das Temperaturprogramm, die obere die registrierte Thermospannung in Abhängigkeit von der Zeit. Die schraffierte Fläche in der Mitte gestattet den zeitlichen Kristallisationsablauf bei 171 °C zu berechnen. Die schraffierte Fläche rechts dient zur Kontrolle der Gesamtkristallisation.

Verlauf der bekannten Umwandlungen bei Zimmertemperatur[14] schliessen, dass sowohl die Güte der kristallinen Ordnung als auch die Verteilung der Kristallitgrössen beeinflusst wird, und zwar ähnlich durch Verstrecken wie durch Abschrecken.[15] Dass in erster Näherung aus der "Form" der Aufschmelzkurve auf die Kristallitgrössenverteilung geschlossen werden kann, konnten wir aus anderen Untersuchungen schliessen.

Diese Analyse lässt sich quantitativ so weit durchentwickeln, dass verschiedene Kristallitgrössenverteilungen (z.B. Verteilungen bei linearen und verzweigten Polyäthylenen bzw. von in bekannter Menge chlorierten Polyäthylenen) einerseits aus statistischen Betrachtungen über die Verteilung kristallisationsfähiger Sequenzen abgeleitet und daraus der Verlauf des Aufschmelzens mit Hilfe einer modifizierten bzw. ergänzten Theorie von Flory vorausberechnet wurde und sich dann diese berechnete c_p-Kurve experimentell bestätigen lässt (Abb. 4).*

Jedes Tempern für einige Zeit bei einer bestimmten Temperatur zeigt sich in der späteren Aufheizkurve als eine kleine Wellung (Abb. 5), und selbst eine unterschiedliche Temperatur der Schmelze wirkt sich mit Änderung der Lage des Kristallisations- und des Schmelzmaximums aus (Abb. 6). Das hängt mit der Art und Verteilung der Kristallkeime in der Schmelze zusammen.†

* Im einzelnen hierzu: Kilian, Hellmuth, und F. H. Müller, dieses Symposium.

† Interessant sind auch Messungen an PVC und an reinen amorphen Substanzen wie PMMA. Darauf will ich im einzelnen hier nicht eingehen (Vergl. Wunderlich, dieses Symposium).

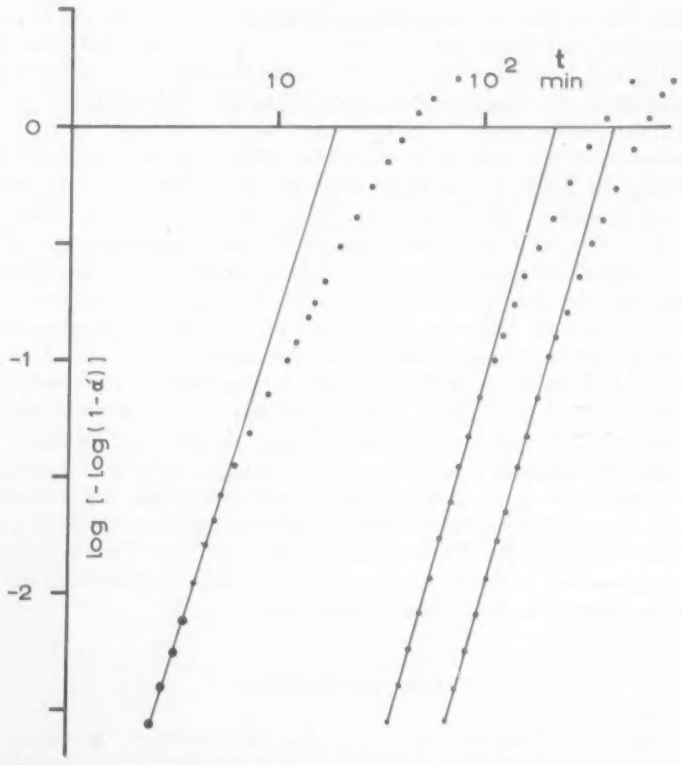

Abb. 8. Avrami-Auftragung der Auswertungen für die Temperaturen 125°C (linke Gerade), 126,5°C und 127°C (rechte Gerade) bei Linearem Polyäthylen.

Da unser Gerät ein willkürlich wählbares Temperatur-Zeit-Programm erlaubt, lassen sich durch geeignete Führung des Temperaturverlaufs, d.h. durch Anhalten der Temperatur auf einen Wert dicht unter der Kristallisationstemperatur, auch Kristallisationsgeschwindigkeiten bestimmen. Derartige Messungen haben wir an 4,6-Polyurethan (Abb. 7) und Polyäthylen (Marlex 50) durchgeführt und nach AVRAMI[16] (Abb. 8) ausgewertet.

Durch eine Gegenbelastung des zweiten Probenröhrchens lässt sich der Effekt der spezifischen Wärme* so weitgehend kompensieren, dass die Empfindlichkeit der Apparatur voll ausgenutzt werden kann. Man erkennt nach Einstellung der konstanten Temperatur von 171°C (Abb. 7) im Anschluss an den raschen Rückgang des wegen nicht exakter Kompensation verbliebenen kleinen Ausschlages auf die Nullinie nach einer "Initialzeit" die *Entwicklung der Kristallisationswärme*. Integriert man die

* d.h. die Stufe während der absinkenden Temperatur.

Flächen jeweils bis zu verschiedenen Zeiten und vergleicht sie mit der Gesamtfläche, so stellt diese Kurve $F(t)/F_0$ gegen t die zeitliche Entwicklung der Kristallisation dar. Die anschliessende Aufheizung dient lediglich dazu, die Gesamtkristallisation nochmals zu kontrollieren: beide schraffierte Flächen sollen übereinstimmen.

Insbesondere die Messungen an Polyäthylen ergaben weitgehende Bestätigung der Werte für die Konstanten aus der Avrami-Formel mit den aus der Literatur auf Grund von Dichtemessungen bisher bekannten Werten.[17] Unsere Messungen zeigen die in der Avrami-Auftragung aus Dichten ebenfalls bekannten systematischen Abweichungen vom linearen Verlauf mit der Zeit (mit wachsendem Gehalt an Kristallisiertem), die einige Autoren als Hohlraumbildung bei fortschreitender Kristallisation diskutiert haben. Unsere kalorischen Messungen bestätigen nun die allein durch Hohlraum- und Rissbildungen bedingt sind (was ja eine falsche Dichtebestimmung verursachen würde und damit eine nur vorgetäuschte Abweichung bedeuten würde), sondern dass sie offenbar spezifisch für das Kristallwachstum Polymerer sind. Sie beginnen zudem schon bei relativ niedrigen Kristallisationsgraden, bei denen sich die Kristallite noch kaum berühren dürften, und sie treten bei umso kleineren Werten auf, je tiefer die gewählte Kristallisationstemperatur ist. Der Vorteil der kalorimetrischen Methode scheint in ihrer hohen Empfindlichkeit vor allem im Beginn der Kristallisation zu liegen.

Literaturverzeichnis

1. Man vergleiche hierzu die verschiedensten Arbeiten auf *diesem* Symposium.
2. Die Frage der Wartezeiten wird diskutiert in den Arbeiten von M. Dole and Mitarbeitern.
3. Martin, H., und F. H. Müller, *Kolloid-Z.*, **172**, 97 (1960).
4. Verbesserte Apparatur noch nicht veröffentlicht.
5. Adam, G., und F. H. Müller, *Kolloid-Z.*, **192**, in Erscheinen.
6. Martin, H., und F. H. Müller, *Kolloid-Z.*, **191**, 1 (1963).
7. Müller, F. H., und H. Martin, *Kolloid-Z.*, **187**, 107 (1963).
8. Schenk, R., *Kristalline Flüssigkeiten*, pp. 84–89, Leipzig, Germany, 1905.
9. Kreutzer, H., *Ann. Phys.*, **33**, 192 (1938).
10. Maier, W., und Alfred Saupe, Zs. Naturforsch., **15A**, 287 (1960); *ibid.*, **16A**, 816 (1961).
11. Mandelkern, L., *J. Appl. Phys.*, **26**, 443 (1955); L. Mandelkern, F. A. Quinn, und P. J. Flory, *J. Appl. Phys.*, **25**, 830 (1954); J. I. Lauritzen und J. D. Hoffman, *J. Res. Natl. Bur. Res.*, **64A**, 73 (1959).
12. Flory, P. J., *J. Chem. Phys.*, **17**, 119 (1960).
13. Müller, F. H., und H. Martin, *Kolloid-Z.*, **171**, 119 (1960).
14. Müller, F. H., und H. Martin, *Kolloid-Z.*, **188**, 19 (1963).
15. Kilian, H. G., und E. Jenckel, Zs. Elektrochem. **63**, 951 (1959).
16. Avrami, M., *J. Chem. Phys.*, **7**, 1103 (1939); *ibid.*, **8**, 212 (1940); *ibid.*, **9**, 177 (1941).
17. Rohleder, J., und H. A. Stuart, *Makromol. Chem.*, **41**, 111 (1960); L. Mandelkern, F. A. Quinn, und P. J. Flory, *J. Appl. Phys.*, **25**, 830 (1954); J. Rabesiaka und A. J. Kovacs, *J. Appl. Phys.*, **32**, 2314 (1961).

Zusammenfassung

Kristallisieren und Schmelzen von Polymeren lässt sich mit einer für quantitative Auswertungen weiterentwickelten Differentialthermoanalyse als Funktion der Vorgeschichte untersuchen. Die Kristallisation und das anschliessend durchgeführte Schmelzen desselben Polymeren erfolgt bei Temperaturen, die sich um 12 bis 18°C unterscheiden. Die Temperatur der Schmelze und die Zeitdauer des aufgeschmolzenen Zustandes, die Geschwindigkeit und der zeitliche Verlauf der Abkühlung beeinflussen den nachfolgend gemessenen Schmelzverlauf in reproduzierbarer Weise. Aus der Verfolgung der Kristallisation bei konstanter Temperatur lassen sich Kristallisationsgeschwindigkeiten ermitteln, deren Auswertung nach Avrami in Übereinstimmung mit analogen Messungen an Dichte und Brechungsindex stehen.

Résumé

La cristallisation et la fusion des polymères peuvent être étudiées comme une fonction des traitements antérieurs sur la base d'une analyse thermique différentielle développée pour permettre une évaluation quantitative. La cristallisation et la fusion consécutive de ce même polymère ont lieu à des températures qui se différencient par un écart de 12 à 18°C. La température de la masse en fusion et la durée de vie de l'état de fusion, la vitesse et le cours du refroidissement en fonction du temps influencent de manière reproductible le déroulement de la fusion mesurè par la suite. En suivant le déroulement de la cristallisation à température constante, on peut déterminer des vitesses de cristallisation dont les calculs suivant Avrami sous en accord avec des mesures analogues de densité et d'indice de réfraction.

JOURNAL OF POLYMER SCIENCE: PART C NO. 6, PP. 93–99

Crystallization of Polypropylene Measured by Differential Thermal Analysis

H. J. DONALD, E. S. HUMES, and L. W. WHITE, *Saginaw Bay Research Department, The Dow Chemical Company, Midland, Michigan*

Synopsis

The crystallization of polypropylene has been studied by DTA in a linear thermal gradient type furnace. The crystallization rate was found to be linear with temperature, and the rate data were correlated on an Arrhenius type plot. The rate of crystallization of the low molecular weight fraction was lower at the same temperature than the rate for a higher molecular weight fraction.

Introduction

Differential thermal analysis (DTA) has become of recent years a useful and popular tool for the characterization of polymers in regard to their thermal properties, e.g., melting points, second order transition temperature, freezing points, and intrapolymer reactions. The estimation of the degree of crystallization of a polymer has been made by measuring the area between a base line and the curve produced during an analysis. This area can be converted to crystallinity percentage, if the heat of fusion of the polymer is known and a suitable heat equivalent to area has been established.

The usual DTA has been measured during the heating cycle of the sample since reproducible heating patterns seem to be more easily controlled than cooling patterns. The introduction of a linear temperature gradient furnace has made it possible to obtain linear heating and cooling patterns by controlling the speed (lineal) that a sample moves into or out of the furnace. A typical assembly is shown in Figure 1. This equipment consists of a linear temperature gradient tube through which a sample is raised or lowered by means of a wire wrapped around a pulley which can be rotated at various speeds. The temperature gradient is maintained by heating one end of the tube to a controlled temperature of 400°C. and cooling the opposite end with water at 20°C.

A typical DTA curve is shown in Figure 2; the upper portion of the curve moving to the left is the heating curve and the lower portion of the curve moving to the right is the cooling curve. The vertical spread between the base lines of the two curves is a result of the difference in heat conductivity of the reference and the sample. The difference in the melting

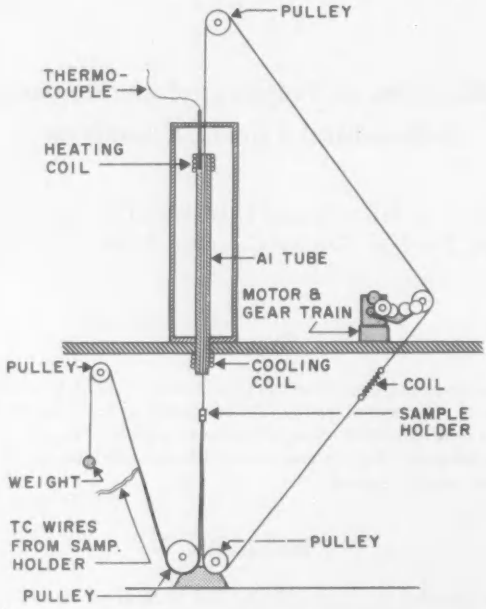

Fig. 1. Schematic of DTA apparatus.

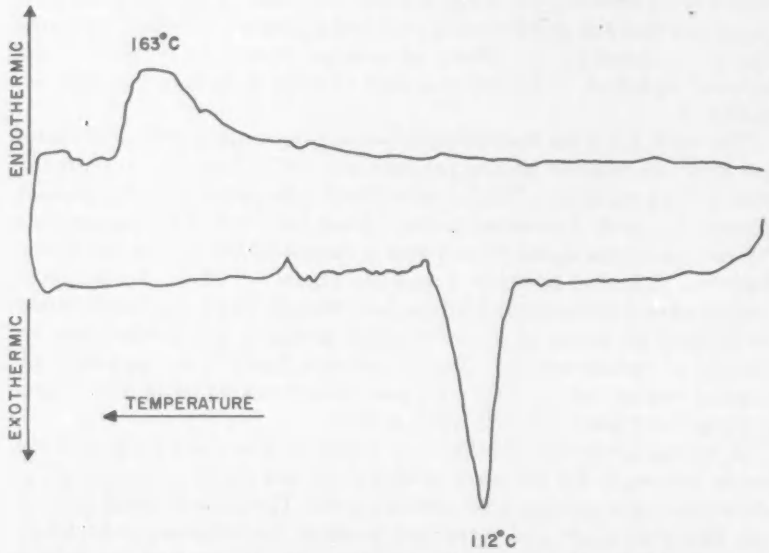

Fig. 2. Typical DTA curve for polypropylene showing both heating and cooling curves.

and freezing points as indicated in this curve is a result of the degree of supercooling a sample must be submitted to before an appreciable enthalpy difference can be measured. The large difference between the freezing and

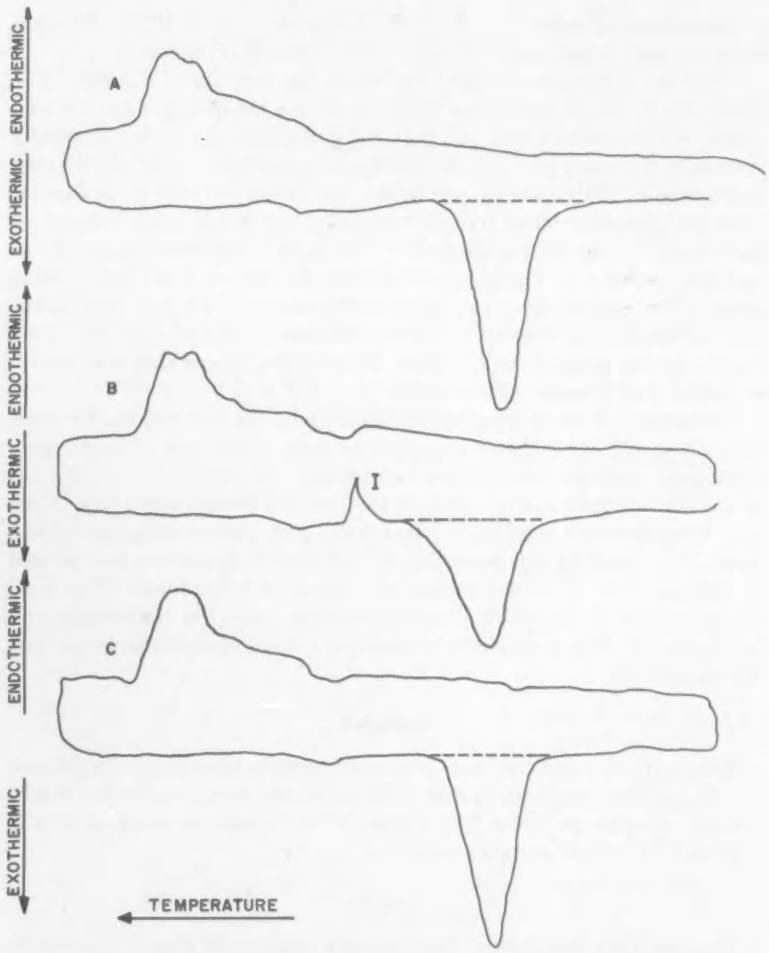

Fig. 3. Typical curves used to determine rate data: (*a*) first; (*b*) second; (*c*) third heating and cooling cycles. *I* is the point at which the sample was maintained at constant temperature.

melting points of polypropylene prompted this study of crystallization rates by thermal measurements. Previous crystallization rate measurements have been made by observing dilatometrically the volume change of the sample and by measuring the spherulite growth rate[1] under micro-

scopic examination. Each method has its own limitation and the technique described herewith is not without qualifications.

Procedure

Crystallization rates were determined from a series of DTA runs on a sample of polypropylene which were made in the following manner.

A 40 mg. pellet was prepared by fusing the polymer in a mold. The pellet was placed in the sample holder in such a manner that the thermocouple was in contact with the polymer and aluminum oxide completely surrounds the sample. The sample holder was drawn into the furnace and heated to 180°C., the sample holder was then drawn out of the furnace until the sample reached room temperature. A DTA curve (similar to that shown in Fig. 2) was obtained. The sample was reheated to 180°C. and then cooled to a temperature between the melting point and freezing point. The sample was held at this temperature for a preset interval before continuing the run to room temperature. A third run was made similar to the original run. Figure 3 shows the curves obtained from a sequence of runs made in this manner.

Consistency of the determinations is shown by the first and third curves, and the second curve shows a marked decrease in the area of the freezing point peak from that of the other two curves. The difference in the areas of the freezing point curves between the first and second curve was, therefore, a measure of crystallinity which had taken place during the holding time. By repeating this procedure for different temperatures and periods of time, a series of crystallization rate curves were obtained. The third curve was run to determine if any appreciable change in the sample may have occurred during the heat treatment as a result of oxidation or thermal decomposition.

Samples

Two polypropylene fractions were used to show the effect of molecular weight on the crystallization rate. The number-average molecular weight for these samples are 1.96×10^5 and 6.06×10^5 for samples designated LCE 5–16 and LCE 5–24, respectively.

Results

The rate data obtained on the fractions of polypropylene are shown in Figures 4 and 5. The surprising result is that the rate of crystallization appears to remain constant with time at the temperature studied. Lower temperatures were impossible to study as a result of the high rates of crystallization encountered. Measurement of higher per cent crystallinities were limited by the small differences and the precision of the technique.

Figure 4 shows the data on a low molecular weight fraction of polypropylene and indicates the linearity of per cent crystallization with time at

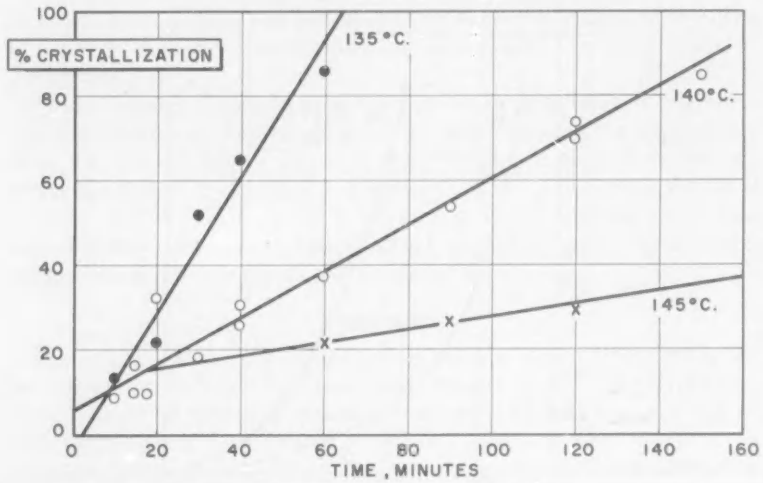

Fig. 4. Crystallization rate data for low molecular weight fraction (LCE 5-16) polypropylene.

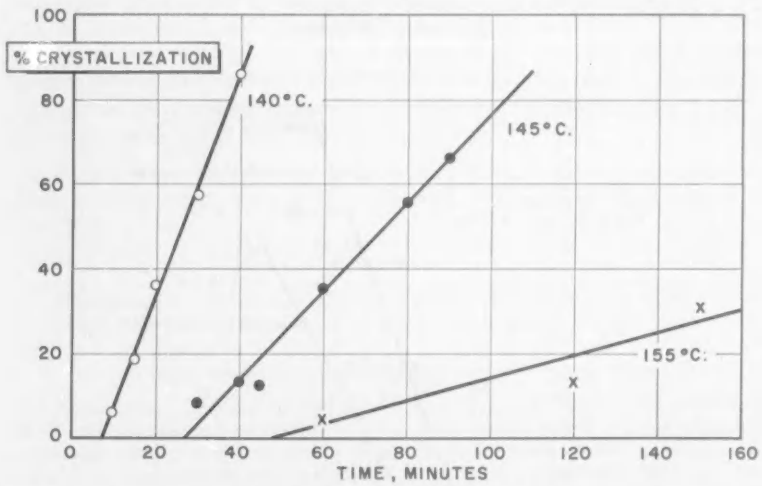

Fig. 5. Crystallization rate data for high molecular weight fraction (LCE 5-24) polypropylene.

constant temperature. Figure 5 is a plot of the data for a high molecular weight fraction and shows a similar trend with time.

Figure 6 is a plot of rates of crystallization (obtained from the slopes of the curves shown in Figs. 4 and 5) as a function of temperature, and shows the rapid increase in rate as the temperature is lowered. This lower temperature appears to be the temperature at which the large exotherm ap-

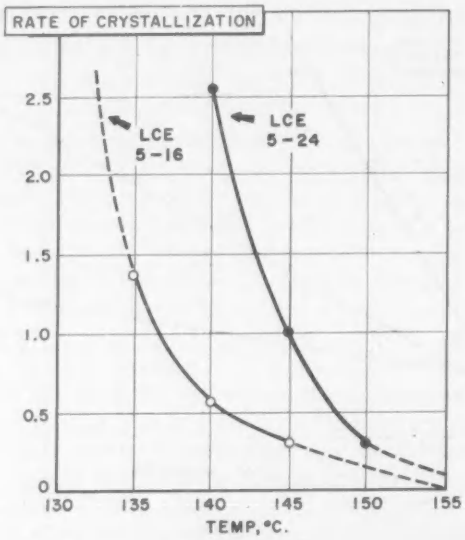

Fig. 6. Crystallization rate as a function of temperature on two molecular weight fractions of polypropylene.

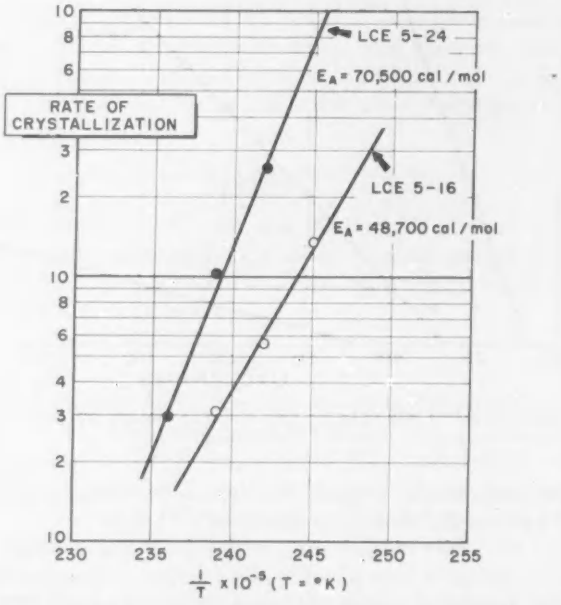

Fig. 7. Arrhenius type plot of crystallization rates from data shown in Figs. 4 and 5.

pears in the DTA curve and perhaps may be considered as the temperature at which spontaneous crystallization or homogeneous nucleation occurs in this system.

Figure 7 shows Arrhenius plots for the two samples used in this work. Linearity again was obtained but may be expected since the temperature range was not too large. The activation energies obtained for these two curves are indicated on graph and were calculated with a gas constant R equal to 1.987 cal./mole. The significance of the activation energy term may be of little importance as such but is a convenient value for expressing crystallization rate as a function of temperature.

Discussion

The results of this work do not appear to be in agreement with the dilatometric rate data published on crystallization or with the linear rate data obtained on spherulite diameter change. The data suggests that at these temperatures the degree of nucleation remains constant and that the crystallization must proceed independent of concentration but dependent upon number of nucleation sites. This observation is supported by the data on spherulite growth rate obtained by Gogos[2] who observed the number of spherulite nuclei remained constant after nucleation had occurred.

This technique of analysis allows the calculation of crystallization rates by the measurement of the heat of fusion of the samples, and provides another procedure for determining crystallization rate data. The procedure can be used to determine differences between various samples of polymers which may result from their preparation.

The authors would like to express thanks to Dr. T. Davis for the fractions of polypropylene used in this study and to the Dow Chemical Company for permission to publish these results.

References

1. Mandelkern, L., *Growth & Perfection of Crystals*, Wiley, New York, 1958.
2. Gogos, G. C., Master of Science Thesis, Princeton University, 1962.

Résumé

La cristallisation du polypropylène a été étudiée par DTA dans un four caractérisé par un gradient linéaire de température. On a trouvé que la vitesse de la cristallisation varie linéairement avec la température, et les données de vitesse ont été mises en correlation avec un diagramme du type Arrhénius. La vitesse de cristallisation de la fraction de faible poids moléculaire était plus faible pour la même température que la vitesse de la fraction de poids moléculaire plus élevé.

Zusammenfassung

Die Kristallisation von Polypropylen wurde mittels DTA in einem Ofen mit linearem Temperaturgradienten untersucht. Die Kristallisationsgeschwindigkeit zeigt eine lineare Temperaturabhängigkeit; die Geschwindigkeitsdaten wurden in einem Arrhenins-diagramm dargestellt. Die Kristallisationsgeschwindigkeit der niedermolekularen Fraktion war bei der gleichen Temperatur niedriger als die Geschwindigkeit einer höhermolekularen Fraktion.

JOURNAL OF POLYMER SCIENCE: PART C NO. 6, PP. 101–108

Differentialkalorimetrische Messungen an verschieden verzweigten und verschieden chlorierten Polyäthylenen in Verbindung mit Röntgenmessungen

E. HELLMUTH, H. G. KILIAN, und F. H. MÜLLER,
Institut für Polymere, Philipps Universität Marburg/Lahn, West Germany

Synopsis

Branched or partially chlorinated polyethylenes may be considered as copolymers, the branching or chlorinated sites forming the noncrystallizing components. Melting curves are calculated according to Flory and compared to experimental curves on well annealed samples. A normalized conversion (fitting) function is obtained which is largely independent of the nature and concentration of the noncrystallizing component. By means of the fitting function conclusions are possible on the deviation from thermodynamic equilibrium, on the crystallite size distribution and on the heterogeneous small angle scattering behavior.

Die maximalen Kristallanteile verschiedenster linearer Copolymer des Äthylens können in Anlehnung an die Florysche Theorie des Schmelzens von Copolymeren[1] mit der Hilfe von zwei weiteren. aus Messgrössen ableitbaren Parametern richtig berechnet werden:[2] Es wurde erstens angenommen, dass es eine kleinste Kristallitlänge[3] gibt. Die Kristalle sollten hiernach in der Richtung, in welcher die Molekülängsachsen liegen, nicht kürzer als 10–30 A. werden. Diese Grenzlänge erweist sich als unabhängig von der Art der nichtkristallisierbaren Copolymereneinheit (*B*-Einheit) und in weitem Mass auch unabhängig von der Konzentration an *B*-Einheiten. Zur Berechnung der maximalen Kristallanteile ist es zweitens notwendig, die analytisch bestimmte Konzentration der *B*-Einheiten durch eine stets grössere "fiktive" Konzentration X'_B zu ersetzen. Diese letztere ergibt sich aus der Anpassung der berechneten Kristallanteile in der unmittelbaren Umgebung des Schmelz-punktes. X'_B hängt damit noch von der Grösse der longitudinalen Grenzflächenenergie ab—ein Problem, das wir hier nicht weiter verfolgen wollen. Die fiktive Konzentration erfasst in jedem Fall Abweichungen vom hypothetischen Grenzfall des Gleichgewichts, die den maximalen Kristallanteil mitbestimmen und schon in den Anfängen der Kristallisation auftreten.

Unter diesen Voraussetzungen—also mit zwei zusätzlichen empirisch gewonnenen Parametern—lässt sich mit einer entsprechend modifizierten Flory-Gleichung jedoch noch nicht exakt berechnen, wie der Kristallanteil mit steigender Temperatur bis zum Schmelzpunkt hin

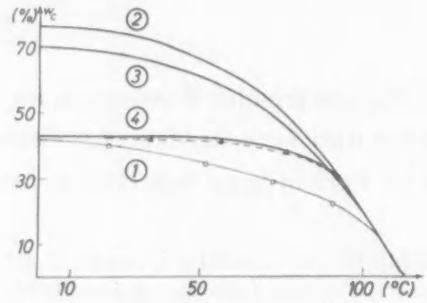

Abb. 1. Kristallanteile W_c als Funktion der Temperatur T von verzweigtem Polyäthylen: (*1*) Experiment (Massenanteil); (*2*) Flory (molar); (*3*) Flory (Massenanteil); and (*4*) diese Arbeit mit Anpassung durch kleinste Kristallitlange nach Flory berechneten Verlauf.

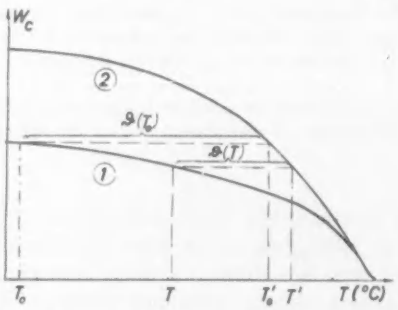

Abb. 2. Schematische Darstellung der Ermittlung der Anpassungsfunktion $\vartheta(T) = T' - T$.

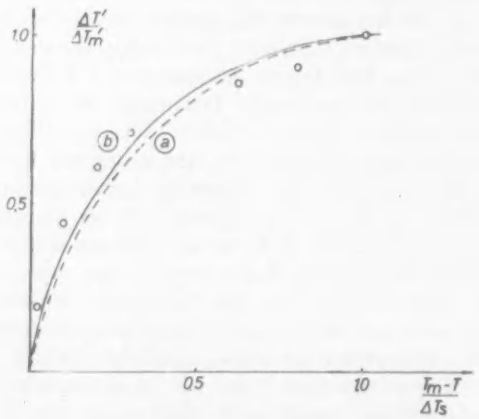

Abb. 3. Reduzierte und normierte Anpassungsfunktion ϑ. Ermittelt gemäss Abb. 2.

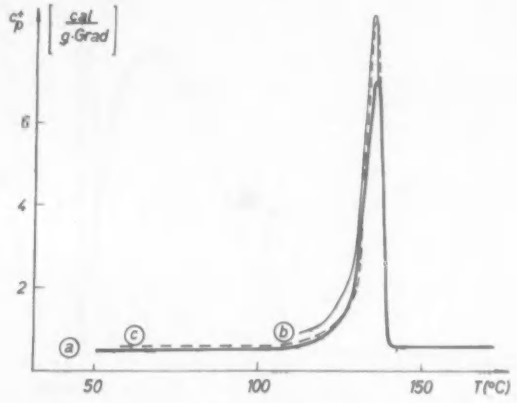

Abb. 4. Vergleich zwischen gemessenen (*a*) und berechneten c_p*-Kurven von linearem Polyäthylen (*b*) Gleichgewichtstheorie von Flory (*c*) diese Arbeit.

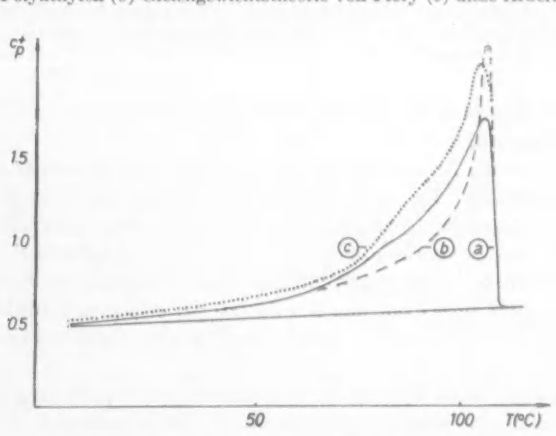

Abb. 5. Dasselbe wie in Abb. 4 für (*a*) verzweigtes Polyäthylen, jedoch (*b*) Anpassung mit kürzester Kristallitlänge, (*c*) mittels ϑ.

abnimmt. Dies erkennt man aus dem Vergleich der beiden Kurven (*1*) und (*4*) in Abb. 1. Die Abweichungen des Experiments von der Rechnung nach Flory (Kurve (*3*)) wurden deshalb nunmehr sozusagen "punktweise" für jede Temperatur erfasst, wie es in Abb. 2 schematisch gezeichnet ist, d.h.—statt durch die Parameter der kleinsten kritischen Länge bei tiefer und hoher Temperatur—durch eine Funktion. Durch Projektion der Messwerte auf die berechnete Kurve (*2*) erhält man die Funktion $\vartheta(T)$, die jedem Messwert einen Wert der Flory-Kurve mit gleich grossen berechenbarem Kristallanteil zuordnet. Die Anpassungsfunktion $\vartheta(T)$ charakterisiert somit die komplizierten Nichtgleichgewichtszustände partiell kristallisierender Copolymerer durch die Abweichungen vom Gleichge-

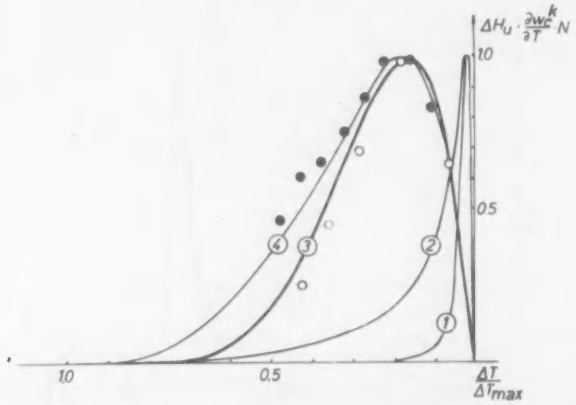

Abb. 6. Normierte, reduzierte Auftragung der Schmelzkurven c_p^* verschiedener Copolymerer des Äthylens. Kurve 3 und 4 umgerechnete Messungen von Wunderlich und Poland. Ausgezogen: berechnete Kurven. Copolymere des Aethylens mit seitständigen Methylgruppen: X_A:—(*3*) 0,840, nach Wunderlich; (*4*) 0,880; nach Wunderlich; (*2*) 0,937; (*1*) 1,000.

wichtskonzept (wobei wir im Augenblick die Bestimmung von X'_B ausser Acht lassen wollen).

In Abb. 3 ist die Anpassungsfunktion, bezogen auf den Abstand von der Schmelztemperatur T_M und normiert in bezug auf die Breite des "Schmelzvorgangs," aufgetragen. In dieser reduzierten Form ist die Funktion für verschieden verzweigte Polyäthylene praktisch identisch. Auch ist sie unempfindlich auf die longitudinale Grenzflächenenergie. Vergrössert man deren Wert (etwa auf das Fünffache), so ergibt sich praktisch derselbe Verlauf, wie es in Abb. 3 aus der gestrichelten Kurve zu entnehmen ist.

Man kann bekanntlich aus der Gleichgewichtsformulierung von Flory unter bestimmten Voraussetzungen auch die spezifische Wärme im Schmelzintervall berechnen.[4] Die so errechnete Kurve der spezifischen Wärme als Funktion der Temperatur stimmt im Habitus, aber nicht im ganzen Verlauf, gleich wie man die verfügbaren Parameter wählt. Aus den Abbildungen 4 und 5 erkennt man jedoch, dass sich der experimentelle Verlauf von $c_p^*(T)$ für verschieden verzweigte Polyäthylene richtig wiedergeben lässt, wenn man hierbei die oben beschriebenen Abweichungen mittels $\vartheta(T)$ vom Gleichgewichtskonzept berücksichtigt. Abb. 6 zeigt den Vergleich analog berechneter, normiert aufgetragener Kurven der Wärmeaufnahme mit Messungen an verschieden konzentrierten Copolymeren das Äthylens mit seitständigen CH_3-Gruppen, die von Wunderlich und Poland[5] stammen. Die gute Übereinstimmung von Experiment und Rechnung wird auch durch das in Abb. 7 aufgeführte Beispiel einer Messung an chloriertem linearem Polyäthylen belegt.[6] Die Veränderungen in der Kurvenform der Wärmeaufnahme an verschieden konzentrier-

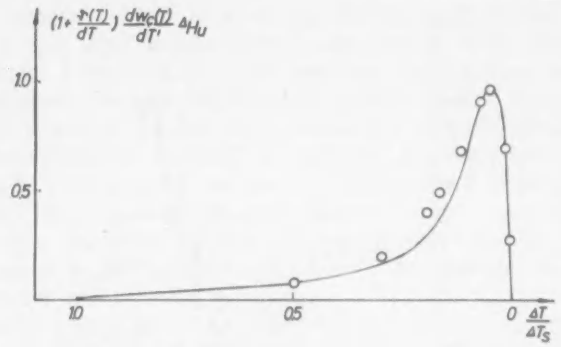

Abb. 7. Normierte, für die Abszisse reduzierte Auftragung der Schmelzkurven c_p^* einer chlorierten Polyäthylenprobe. Die ausgezogene Kurve ist also aus unserer Rechnung gewonnen worden. Die Messpunkte schmiegen sich gut an.

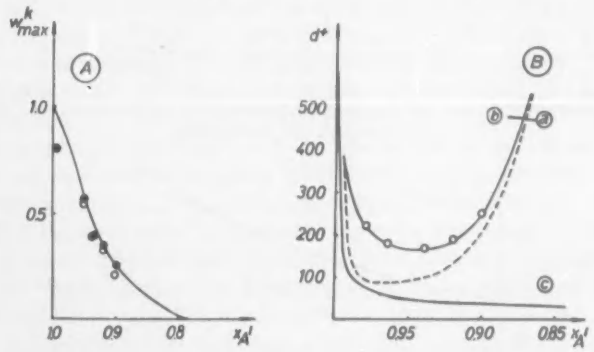

Abb. 8. (*A*) Die berechneten maximalen Kristallanteile verschieden chlorierter Polyäthylenproben als Funktion des Molenbruchs der kristallisationsfähigen *A*-Einheiten im Vergleich mit den gemessenen; (*B*)Dasselbe für die Langperiode: Kurve (*c*) gibt die berechnete mittlere Kristallitlänge als Funktion von X'_A an.

ten Copolymeren werden durch die Rechnung offensichtlich richtig wiedergegeben.

Sieht man von der Bestimmung der fiktiven Konzentration $X'_B > X_B$ (X_B = molare Konzentration der *B*-Einheiten nach der Analyse) ab, so folgt aus den obigen Beispielen, dass die *Abweichungen vom Gleichgewichtskonzept für verschiedene Copolymere des Äethylens* ohne Rücksicht auf die besondere *Bauart der B-Copolymereneinheit untereinander ähnlich sind.* Dies muss offensichtlich auf einem unspezifischen Effekt beruhen. Es ist wahrscheinlich auf die *Kristallvernetzung* zurückzuführen, die dadurch entsteht, dass Teile eines Makromoleküls in verschiedene Kristalle eingebaut werden: Schon in den ersten Stadien der Kristallisation werden hierdurch—offensichtlich in einer entsprechend unspezifischen Weise—

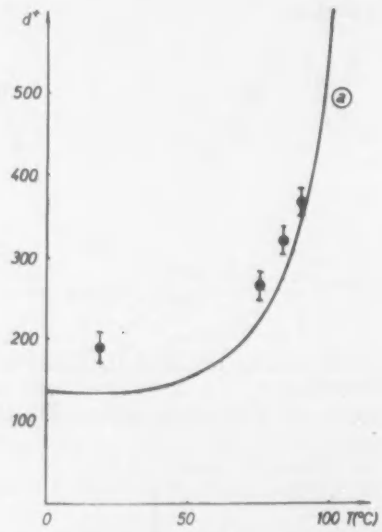

Abb. 9. Berechnete (——) und gemessene Langperioden vom verzweigten Polyäthylen als Funktion der Temperatur.

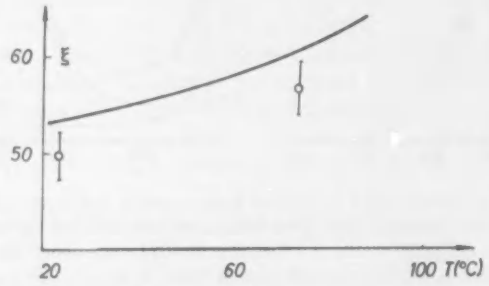

Abb. 10. Berechnete und aus Kleinstwinkelaufnahmen ermittelte mittlere Partikelgrösse vom verzweigten Polyäthylen als Funktion von der Temperatur.

erst bei weiterer Abkühlung auffindbare Abweichungen vom Gleichgewichtskonzept festgelegt. Man denke etwa an immer vorhandene Fehlordnungen mit Hinsicht auf die trans-Konformation in den Kristallen. Solche Fehlordnungen werden in den Molekülteilen zwischen zwei schon gebildeten Kristallen "konserviert." Sie machen sich beim weiteren Ablauf der Kristallisation in zunehmendem Masse bemerkbar und bewirken die wachsende Abweichung vom Gleichgewichtskonzept. Bei der Kristallisation von Copolymeren wird dies besonders evident, weil hier zusätzlich eine passende Zuordnung der kristallisierbaren Sequenzen verschiedenster Länge erfolgen muss.[1]

Gerade diese der Länge nach richtige Zuordnung der kristallisierbaren Folgen ist aber auch für die Bildung der grössten möglichen Kristalle entscheidend: Hier treten die esten impliziten Abweichungen vom Gleichgewichtskonzept auf, weil die längsten kristallisierbaren Folgen in kleinere Kristallite eingebaut werden. Der "unendlich grosse" Kristall wird ein immer unerreichbarer Grenzfall, je höher die Konzentration der *B*-Einheiten ist.[6] Das entspricht in der oben gegebenen Näherung der Tatsache, dass zur Anpassung am "Schmelzpunkt" eine fiktive Konzentration X'_B gewählt werden musste, die konsequenterweise mit steigender Konzentration an *B*-Einheiten sich immer mehr von der analytischen Konzentration unterscheidet.

Wesentlich scheint uns, dass obige Überlegungen sich auch in anderer unabhängiger Weise rechtfertigen: Die oben gegebene Charakterisierung der Nichtgleichgewichte partiell kristallisierter Copolymerer gestattet eine Vorausberechnung der Langperiode in Abhängigkeit von der Konzentration der *B*-Einheiten und von der Temperatur. Der Rechnung entnimmt man, dass die Langperiode als Funktion von der Konzentration der *B*-Einheiten einen Minimalwert durchlaufen sollte [Abb. 8, Kurve (1)]. Das Minimum prägt sich besonders deutlich aus, wenn man die Rechnung für Schichtkristalle ausführt. In diesem Modell liegen die amorphen Zwischenbereiche zwischen den (001)-Flächen der Kristalle. Der Minimalwert ergibt sich deshalb, weil mit kleiner werdender Kristallitdicke (die dem asymptotischen kleinsten Wert zustrebt) gleichzeitig der Kristallanteil rapide sinkt,[2] Hierdurch werden die mittleren Abstände zwischen den Kristallen von einer bestimmten Konzentration an *B*-Einheiten an wieder grösser: Die Langperiode muss erneut zunehmen. Andeutungen zu einem Wiederanstieg der Langperiode sind aus den Messungen an verschieden chlorierten Proben zu entnehmen [Abb. 8, Kurve (*b*)].

Abb. 9 zeigt schliesslich den Vergleich zwischen berechneten und gemessenen Langperioden von verzweigtem Polyäthylen als Funktion der Temperatur. Der sehr starke Anstieg der Langperiode bei hoheren Temperaturen lässt sich durch die Rechnung nur dann wiedergeben, wenn das Schichtkristallmodell zugrunde gelegt wird. Dies bestätigt sich auch an hand weiterer, hier noch nicht wiedergegebener Messungen an Copolymeren des Äethylens.[7]

Aus der Linienbreite der Kleinwinkelinterferenz kann man für verzweigtes Polyäthylen bis zu etwa 70°C die "Partikelgrösse" bestimmen.[8] Hier liegen flüssigkeitsähnliche Interferenzen vor, für die die Abstände zwischen den Streuzentren um mehr als 30% schwanken. Diese Partikelgrösse *wächst* mit steigender Temperatur (Abb. 10). Genau diese Abhängigkeit ergibt sich aber auch aus der Berechnung der Kristallitlänge unter Einbeziehung der diskutierten Abweichungen vom Gleichgewichtskonzept. Dem *selektiven Aufschmelzen* der Gleichgewichtsformulierung entspricht es, dass offenbar beim Aufheizen tatsächlich zunächst die kleinsten Kristallite verschwinden, vorausgesetzt natürlich, dass die Proben hinreichend gut getempert worden sind, so dass eine Vergrösserung

der Partikel bzw. der Kristallite durch Umkristallisation ausgeschlossen werden kann.

Literatur Verzeichnis

1. Flory, P. J., *Trans. Faraday Soc.*, **51**, 848 (1955).
2. Kilian, H. G., *Kolloid-Z.*, **189**, 23 (1962).
3. Wunderlich, B. J., *J. Chem. Phys.*, **29**, 1395 (1958).
4. Dole, M., *Fortschr. Hochpolymer. Forsch.*, **2**, 221 (1960).
5. Wunderlich, B., und D. Poland, *J. Polymer Sci.*, **A1**, 357 (1963).
6. Kilian, H. G., und F. H. Müller, *Kolloid-Z.*, **192**, 134 (1963).
7. Kilian, H. G., F. H. Müller, und H. Ringsdorf, in Vorbereitung.
8. Bonart, R., und R. Hosemann, *Kolloid-Z.*, **186**, 16 (1962).

Zusammenfassung

Verzweigte oder teilweise chlorierte Polyäthylene kann man als Copolymerisate auffassen, in denen die Verzweigungs- oder chlorierten Stellen die nichtkristallisierbare Komponente darstellen. Berechnet man die Schmelzkurven nach Flory und vergleicht sie mit den gemessenen Kurven an gut getemperten Proben, so ergibt sich eine Umrechnungs-(Anpassungs-) Funktion. Diese ist in normiert reduzierter Form weitgehend unabhängig von der Natur und der Konzentration der nichtkristallisierbaren Komponente. Mit Hilfe der Anpassungsfunktion lassen sich Schlüsse auf die Abweichung vom thermodynamischen Gleichgewicht, die Verteilung der Kristallitgrössen und das Verhalten der heterogenen Kleinwinkelstreuung (Langperiode) ziehen.

Résumé

Des polyèthylènes ramifiès ou partiellement chlorès peuvent être considèrès comme des copolymèrisats où les sites de ramification ou de chloration représentent les composants non-cristallisables. Si l'on calcule les cour bes de fusion d'après Flory et si on les compare aux courbes expèrimentales obtenues à partir d'èchantillons parfaitement recuits, on obtient une fonction de transformation (fonction d'adaptation). Cette dernière sous sa forme rèduite est en plus grande partie indèpendante de la nature et de la concentration des composantes non cristallisables. A l'aide de la fonction d'adaptation on peut tirer des conclusions en ce qui concerne l'écart de l'équilibre thermodynamique, la distribution des grandeurs des cristallites, le comportement de la diffusion hétérogène aux petits angles.

JOURNAL OF POLYMER SCIENCE: PART C NO. 6, PP. 109–115

Thermodynamic Properties of Lexan Polycarbonate from 110–560°K.

JAMES M. O'REILLY, FRANK E. KARASZ, and HARVEY E. BAIR,
General Electric Research Laboratory, Schenectady, New York

Synopsis

The heat capacity of Lexan polycarbonate has been accurately measured on samples of different degrees of crystallinity. No low temperature transitions are observed in C_p. The usual discontinuity in C_p at the glass temperature is observed at 142° C. for a completely amorphous sample. In semicrystalline samples the change in C_p at T_g is greatly suppressed by the presence of crystallites. The crystalline regions of the polymer exhibit melting over the range 200–250°C. and a latent heat accompanies the melting process. From the magnitude of this latent heat the per cent crystallinity has been calculated as 17% (powder sample) and 24% (solvent crystallized sample). Upon slow cooling from the melt a completely amorphous sample is obtained.

Introduction

High polymers in general exhibit marked changes in physical properties as a function of temperature. These transitions in physical properties occur at more or less well defined temperatures and can be observed by a wide variety of experimental techniques such as volumetric or dielectric measurements, dynamic mechanical measurements, nuclear magnetic resonance spectroscopy and many others. Since polymers are usually made up of an amorphous and a crystalline phase, a given transition may result from the presence of either phase. Most measurements only locate the transition temperature and do not directly specify the nature of the transition. In some cases experiments on samples of various compositions (i.e., various degrees of crystallinity) allow one to specify the phase responsible for the transition. The calorimetric method detects the transition temperature and also distinguishes between an amorphous and crystalline transition from the shape of the C_p curve.

In the case of poly(4,4′-dioxy diphenyl-2,2-propane carbonate), results of dielectric,[1] mechanical,[2] and volumetric[3] measurements have indicated at least three transition regions: (*a*) a low temperature transition observed by mechanical and dielectric measurements at ~170°K.; (*b*) a glass transition at 415°K.; and (*c*) a crystal melting point at 500–530°K.

For this polymer, the crystalline phase is difficult to obtain under normal conditions and the amount of crystallinity in quenched samples has been the subject of some speculation. Crystallization can be induced by sol-

vent treatment but again quantitative results have been lacking. The glass transition is evident in all three experimental methods and seems normal. The fact that the polycarbonate is ductile at room temperature (even considerably below room temperature) has led to speculation that the glass transition behavior is anomalous. The possibility of another transition in the region between 25 and 140°C. was also considered and recently Hellwege has reported anomalous behavior of the volumetric[3] and heat capacity[4] measurements in this region.

Experimental

Heat capacities were determined using a precision adiabatic calorimeter[5] in the temperature range 80–570°K. The absolute accuracy has been assessed by measuring the heat capacity of a standard NBS sample of aluminum oxide. Our measurements agree with the NBS results of Furukawa et al.[6] to within 0.1% at low temperatures and 0.4% at the highest temperatures. Reproducibility on a given sample is somewhat better than this. Temperature intervals of 5 to 10° were used with heating rates of 10 to 20°/hr. In the region of a transition, smaller temperature intervals were used.

The sample used in this study was a Lexan* polycarbonate powder sample obtained by precipitating the polymer from solution. The molecular weight of the sample from viscosity measurements was 4×10^4. Samples were dried at 110°C. in a vacuum oven for at least 24 hr. to remove water and volatiles. A crystalline sample was prepared by slowly evaporating the solvent from a methylene chloride solution of the powder on a clean mercury surface. Experiments indicate that it is difficult to remove the last traces of methylene chloride from the crystallized material even under vacuum at 110°C. The final sample could contain as much as 0.1% by weight of methylene chloride.

The powder sample consisted of particles with a maximum size of a millimeter and the powder occupied approximately 75 cc. (21.599 g.). The white crystalline sample was in the form of irregular large pieces and weighed 25.263 g.

Results

a. Powder

The heat capacity of the powder sample is nearly a linear function of temperature from 80 to 400°K. as shown in Figure 1. No evidence of a transition near 170°K. is found, and it is estimated that a change of several parts in a thousand in the heat capacity would be perceptible.

In the neighborhood of 410°K. a slight upward curvature is observed in C_p as shown in Figure 2, and large positive temperature drifts in the calorimeter are observed. This is the glass transition region, but the

* General Electric Company trademark.

magnitude of ΔC_p (C_p liquid $-$ C_p glass) is much smaller than expected of a slightly crystalline sample. Positive drifts indicate that an exothermic process is occurring in the calorimeter and is attributed to the crystalliza-

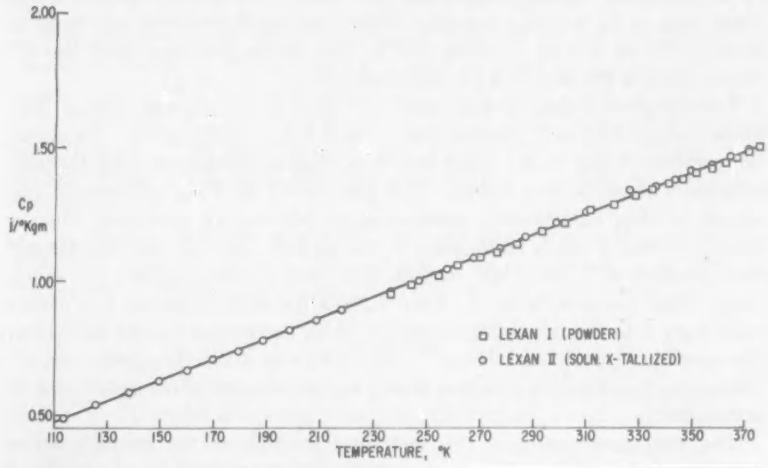

Fig. 1. Low temperature heat capacity of Lexan (powder and solution crystallized sample).

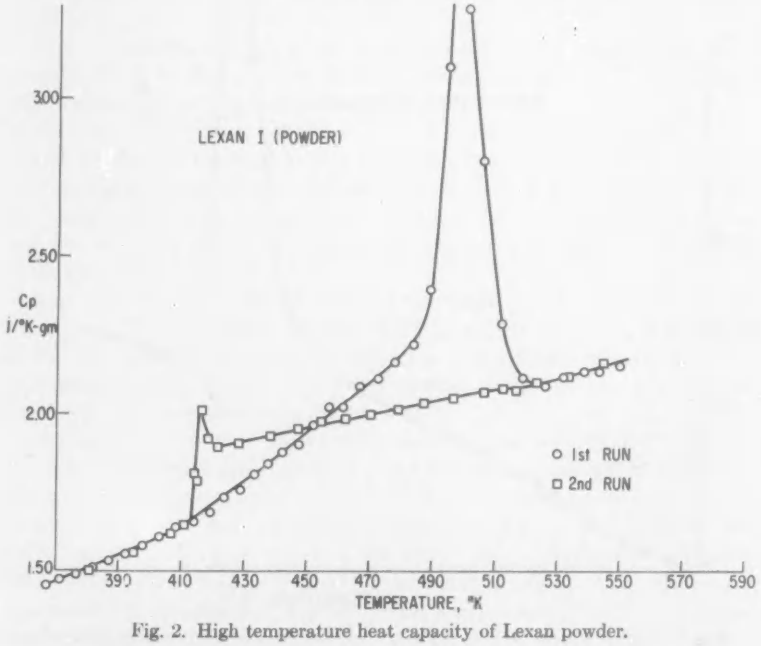

Fig. 2. High temperature heat capacity of Lexan powder.

tion of the polymer. The heat liberated by the crystallization tends to reduce C_p and therefore ΔC_p. The small amount of recrystallization which occurs is not enough to depress C_p to the observed level. At 450–460°K. C_p is increasing rapidly indicating now that crystals are melting. The usual peak in C_p during a crystal melting process is observed and melting is complete at 520°K. Above 520°K. the drifts disappear and the C_p curve exhibits the expected liquidlike behavior.

The sample was then cooled slowly (15°/hr.) to 320°K. and rerun. The usual change in C_p at T_g is now observed and $\Delta C_p = .25$ j./g.°K. Negative temperature drifts in the glass transition region are due to long thermal relaxation times in this region. The peak in C_p at T_g is not usually observed in slow calorimetric measurements but can be observed when a sample is heated much faster than it was cooled. In this case the sample was annealed at T_g overnight so that effectively the heating rate was much faster than the cooling rate. The reasons for this effect are intimately connected with the relaxation processes which occur near T_g and have been discussed by Davies and Jones.[7] Above T_g the drifts disappear and C_p rises with temperature into the liquid region without showing a trace of crystallinity.

The heat accompanying the melting transition of the initial powder sample is 5.54 cal./g. The heat of fusion of the polycarbonate has been

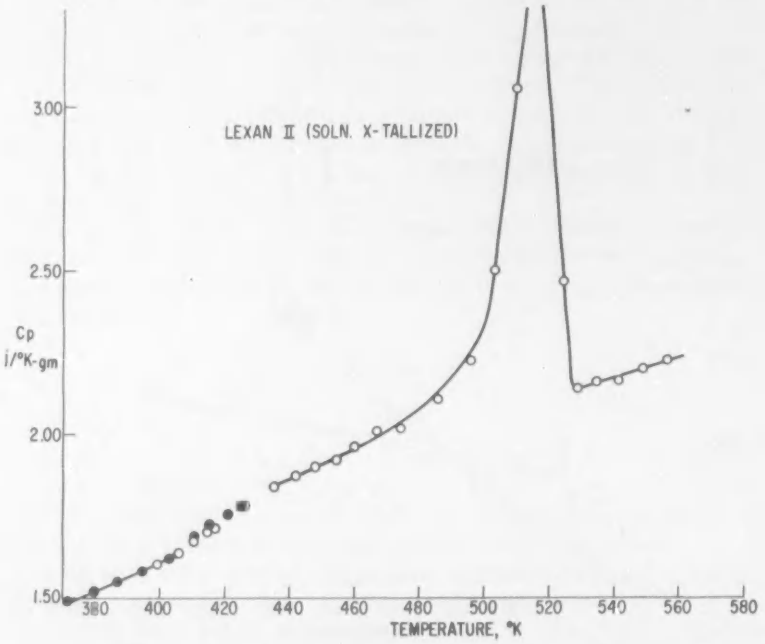

Fig. 3. High temperature heat capacity of Lexan (solution crystallized sample).

estimated as 32 cal./g. ± 10% by Wineman[8] from diluent measurements which gives a per cent crystallinity of 17%.

b. Solvent Crystallized Sample

This sample shows the same general behavior as the powder sample shown in Figure 3. After heating to 425°K. (solid points in Fig. 3) the sample was cooled to below 400°K. and then rerun (open points in Fig. 3). The small ΔC_p is only a fraction of what a 75% amorphous sample should show. Also positive drifts are not observed until a higher temperature, 460°K., so that crystallization does not interfere with the ΔC_p measurement.

The melting behavior is sharper than the powder sample as would be expected from the sample preparation. This sample gives a heat of transition of 7.74 cal./g., equivalent to 24% crystallinity.

Discussion

The absence of a transition in C_p at low temperatures implies that the change in the mode of motion is very subtle and does not contribute significantly to C_p. A transition in C_p could in principle be due to at least two causes since $C_p = C_v + TV\alpha^2/\beta$, where C_p = specific heat at constant pressure, C_v = specific heat at constant volume, T = absolute temperature, V = specific volume, α = volume expansion coefficient, and β = compressibility.

First, a transition in C_v could occur because of a change in the vibrational motion of the polymer which might also appear as a transition in the mechanical or dielectric properties. Secondly, a transition in C_p could result from a transition in α or β. A transition in the compressibility would be directly observable as a transition in mechanical measurements. The second term contributes several per cent to C_p at low temperature and increases rapidly with temperature. Usually the low temperature transitions in mechanical and dielectric properties are quite broad (100–200°K. in the case of the polycarbonate).

Since the transition occurs over a large temperature interval, it is possible that a C_p transition is masked by the normal temperature dependence of C_p. At present the nature of these low temperature transitions is not well understood. When more experimental data become available at least empirical correlations can be attempted.

The data reported here do not show the flattening out of the C_p curve at 110–135°C. reported by Hellwege.[4] Hellwege used a sample of Makrolon (Bayer polycarbonate), and the difference in results may be due to the different samples. Also we see no peculiarities in C_p in the region of 70–110°C. where Hellwege[3] reports a transition in the expansion coefficient for a Lexan polycarbonate sample. It is worth noting that measurements of first order properties (i.e., volume) to 0.1% is less sensitive than measurements of second order properties (i.e., heat capacity) to the same accuracy.

Therefore the observed change of approximately 10% in the expansion coefficient should be readily observable in the heat capacity measurements.

The observed ΔC_p at T_g is not proportional to the per cent amorphicity as would be expected on the basis of a two phase model. Independent measurements of crystallinity by x-ray and density methods confirm that the heat of fusion estimate of crystallinity is at least within 10% of the actual value. Even allowing for an error in the per cent crystallinity, the observed ΔC_p is much too low. This means that a small amount of crystallinity restricts the polymer chains from attaining their liquid-like amorphous configurations and the accompanying liquid-like C_p above T_g. A similar behavior has been noted by Dole[9] for polyethylene terephthalate. Investigation of this phenomena would no doubt lead to a better understanding of the interactions between the phases in semicrystalline polymers.

The T_g/T_m ratio for the polycarbonate is 0.79 which is slightly larger than rule of thumb value, $0.5 < T_g/T_m < 0.67$. The fact that the polycarbonate shows no trace of crystallinity after slow cooling from the melt indicates that ordinary molded samples of Lexan are completely amorphous.

References

1. Müller, F. H., and F. Krum, *Kolloid-Z.*, **164**, 81 (1959).
2. Illers, K. H., and H. Breuer, *Kolloid-Z.*, **176**, 110 (1961).
3. Hellwege, K. H., J. Hennig, and W. Knappe, *Kolloid-Z.*, **186**, 29 (1962).
4. Hellwege, K. H., W. Knappe, and W. Wetzel, *Kolloid-Z.*, **180**, 126 (1962).
5. Karasz, F. E., and J. M. O'Reilly, to be published.
6. Furukawa, G. T., T. B. Douglas, R. E. McCaskey, and D. C. Ginnings, *J. Res. Natl. Bur. Std.*, **57**, 67 (1956).
7. Davies, R. O., and G. O. Jones, *Advan. Phys.*, **2**, 370 (1953).
8. Wineman, P., private communication.
9. Dole, M., *Kolloid-Z.*, **165**, 40 (1959).

Résumé

La capacitè thermique du polycarbonate Lexan a ètè mesurèe exactement sur de èchantillons de degrès diffèrents de cristallinitè. A basse température, on n'a pas observé de transition dans le C_p. Pour un échantillon complètement amorphe, l'habituelle discontinuité de C_p à la température de transition vitreuse se situe à 142°C. Dans les échantillons semi-cristallins, le changement de C_p à T_g est fortement diminué parsuite de la présence des cristallites. Les régions cristallines du polymère fondent entre 200 et 250°C; une chaleur latente accompagne le processus de fusion. À partir de la grandeur de cette chaleur, le pourcentage de cristallinité a été calculé; on a trouvé un pourcentage de 17 (échantillon en poudre) et 24 (échantillon cristallisé dans un solvant). Un échantillon complètement amorphe est obtenu par refroidissement lent du polymère fondu.

Zusammenfassung

Die Wärmekapazität von Lexan-Polykarbonat wurde an Proben mit verschiedenem Kristallinitätsgrad genau gemessen. Am C_p werden keine Tieftemperaturumwandlungen beobachtet. Die übliche Diskontinuität in C_p bei der Glastemperatur wird an einer vollständig amorphen Probe bei 142°C beobachtet. Bei halbkristallinen Proben wird

die C_p-Änderung bei T_g durch die Gegenwart von Kristalliten grossen Teils unterdrückt. Die kristallinen Bereiche des Polymeren schmelzen im Bereich von 200 bis 250°C und eine latente Wärme begleitet den Schmelzprozess. Aus der Grösse dieser latenten Wärme wurde die prozentuelle Kristallinität zu 17% (Pulverprobe) und 24% (lösungsmittel-kristallisierte Probe) berechnet. Bei langsamer Abkühlung aus der Schmelze wird eine völlig amorphe Probe erhalten.

JOURNAL OF POLYMER SCIENCE: PART C NO. 6, PP. 117–124

Kalorimetrische Messungen von Wärmeeffekten bei Verstreckung

F. H. MÜLLER und N. WEIMANN, *Institut für Polymere, Philipps Universität, Marburg/Lahn, West Germany*

Synopsis

Heat effects and the work in stretching a polycarbonate are measured in a wide range of stretching rates and at two different temperatures. Conclusions are drawn on the enthalpy increase during the stretching process. Indirect conclusions on the entropy variation during stretching seem to be possible. The effect of temperature balance is confirmed and the strain relaxation of the stretched material seems also to be coupled with heat production.

Kalorimetrische Messungen der Wärmeproduktion während der Deformation werden von uns in Marburg nun seit mehr als 10 Jahren durchgeführt.[1] Die Problematik ging aus der Feststellung hervor, dass bei Kaltverstreckung eines Materials die Fliesszone meist eine merklich erhöhte Temperatur besitzt. Wir wollten die Konsequenzen, die aus dem Nachweis dieser Temperaturerhöhung der Fliesszone mit Thermoelement[2] und temperaturempfindlichen Fluoreszens-stoffen[3] zu ziehen sind, noch durch unmittelbare Messungen der Wärmeentwicklung während der Verstreckung erhärten.

So entstand seinerzeit ein sehr empfindliches Kalorimeter, das an kleinen Messproben (weniger als 1 g) die kalorischen Effekte während der Deformation zu verfolgen erlaubt. Hierüber wurde schon vor Jahren ausführlich berichtet,[4] unter anderem auch auf der Gordon-Research-Konferenz über Polymere (1960).[5] Das Gerät wurde inzwischen in seiner Empfindlichkeit und vor allem in seiner Nullpunktskonstanz wesentlich verbessert.[6] Im übrigen ist in Verwendung unserer Erfahrung und Weiterentwicklung unserer Konstruktion nun ein analoges Gerät von Benner und Foster bei der Firma Du Pont entwickelt worden.[7]

Das gleiche Messprinzip lässt sich auch anwenden, um Lösungswärmen zu bestimmen.[8] Da wir bei den Verstreckungsexperimenten fanden, dass die bei Deformation einer Probe aufgewendete Arbeit grösser ist als die auftretende Wärmemenge, folgt nach dem ersten Hauptsatz der Thermodynamik, dass die Enthalpie des Materials sich entsprechend erhöht haben muss. Die Enthalpiedifferenz zwischen dem verformten und dem Ausgangsmaterial, sofern das Verformte eine bleibende Deformation

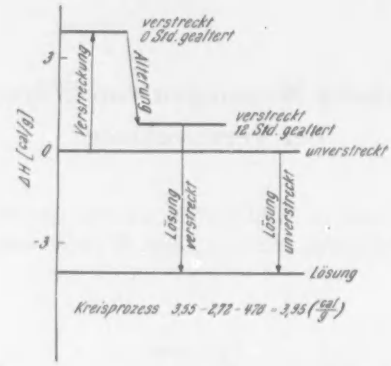

Abb. 1. Das Schema lässt erkennen, dass die Äenderungen der Enthalpie bei Verstreckung mit der Differenz der Lösungswärmen von Unverstrecktem und Verstrecktem nur durch Zwischenschalten eines Umwandlungsvorgangs (Alterung) nach der Verstreckung vereinbart werden kann.

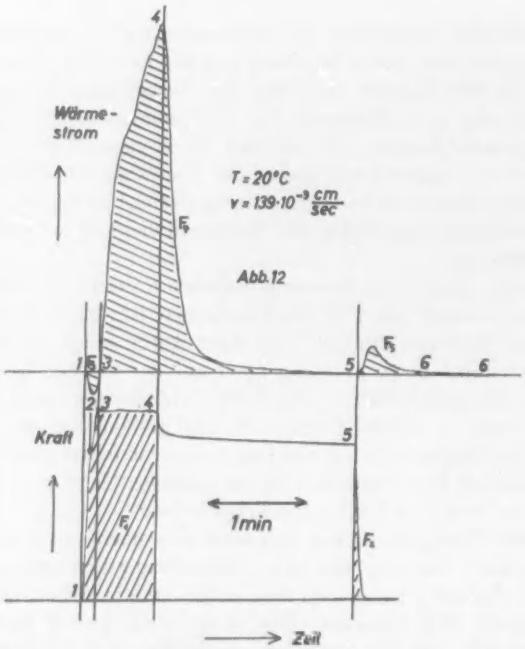

Abb. 2. Wiedergabe einer Registrierung mit dem neuen Kalorimeter; untere Kurve Kraft als Funktion der Zeit, obere Kurve zugehöriger Wärmestrom als Funktion der Zeit.

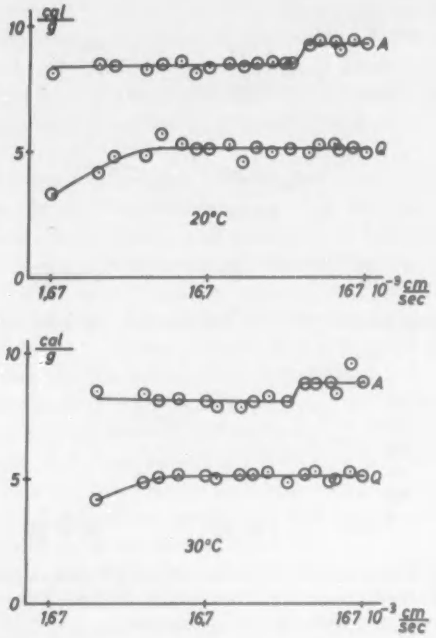

Abb. 3. Wärme Q und Arbeit A als Funktion der Streckgeschwindigkeit bei 20° und bei 30°C gemessen für Polycarbonat. Je ein Punktepaar Q und A folgt aus der Auswertung einer Registrierung gemäss Abb. 2.

besitzt, sollte sich jedoch auch aus der Differenz der Lösungswärmen bei gleicher Endkonzentration ermitteln lassen.

In der Diskussion der kalorischen Erscheinungen bei der Verstreckung spielt ausserdem die spezifische Wärme als Funktion der Temperatur und der Verstreckung eine Rolle. Deshalb bauten wir auf Weiterentwicklung der Differential-thermoanalyse eine empfindliche quantitative Methode auf, die diese Daten liefert und von denen an anderer Stelle einiges berichtet wurde.[9]

Zwei Punkte seien hier behandelt:

(*a*) Man sollte erwarten, dass die Erhöhung der Enthalpie eines Materials beim Verstrecken, wie sie im Verstreckungskalorimeter unmittelbar während des Vorgangs bestimmt wird, die gleiche ist, die man anschliessend aus der Differenz der Lösungswärmen von unverstrecktem und verstrecktem Material feststellt. Das ist nicht der Fall. Letztere Differenz ist kleiner.[10]

Die einzig mögliche Erklärung hierfür ist, dass im Anschluss an eine Verstreckung Nacheffekte, langsame weitere Umordnungen der Moleküle, stattfinden, die mit einer Abnahme der freien Enthalpie verbunden sind. D.h. sowohl die Enthalpie als auch die Entropie des Materials verändern

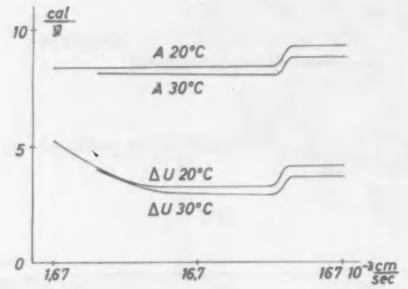

Abb. 4. Berechnung aus Abb. 3 für die Differenz ΔU (ΔH) der Innerern Energien.

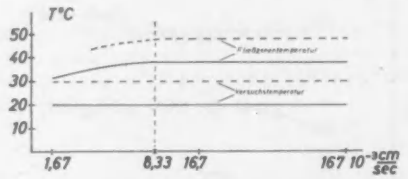

Abb. 5. Die Auswertung für die Uebertemperatur der Fliesszone (gekrümmte Kurven) im Vergleich zur Versuchstemperatur (Geraden bei 20° und 30°). Die ausgezogenen und die gestrichelten Kurven gehören jeweils zusammen.

sich anschliessend an eine Verstreckung. Derartige Nacheffekte sind aus technischen Prozessen bekannt, und man sucht sie durch "Alterung," z.B., Tempern im feuchten Zustand unter Zug, zu beschleunigen. Im übrigen dokumentieren sie sich zum Teil auch in der Spannungsrelaxation.

Nun war, um das für unsere Lösungsmessungen erforderliche Material von etwa $^1/_2$ g herzustellen, eine gewisse Zeit notwendig, zu der die Zeit der Thermostatisierung im Lösungskalorimeter hinzukommt. Während dieser Zeit von im Mittel 12 Stunden bis zur Messung wird also durchaus mit einer Veränderung der Enthalpie des verstreckten Materials zu rechnen sein. Man kann eine Art Termschema aufstellen, hier für Polyvinylchlorid (Abb. 1), aus dem deutlich zu erkennen ist, wie durch Kombination von Messungen mit dem Verstreckungskalorimeter und solchen mit dem Lösungskalorimeter quantitative Werte gefunden werden können. Diese Experimente sollten noch in Abhängigkeit von den Lagerungsbedingungen nach der Verstreckung, insbesondere von Lagerungszeit und -temperatur weiter analysiert werden.

(*b*) Die zweite Frage, die ich hier behandeln will, ist die, in wieweit sich die "vollständige" Energiebilanz, d.h. die Deformationsarbeit und die bei dieser Deformation entstehende Wärme als Funktion der Deformationsgeschwindigkeit verändert.[6]

Hierzu schien das Polycarbonat ein besonders geeignetes Material, da es bei praktisch konstantem Streckverhältnis von 2,24 über alle anwendbaren

Geschwindigkeiten von extrem langsam bis zu der, bei der es gerade noch nicht reisst, sich stets mit Fliesszone verstreckt. Die scharfe Fliesszone ist geometrisch sehr gut ausmessbar und in ihrer Form ebenfalls unabhängig von der angewendeten Geschwindigkeit. Es verändert sich also der äussere Ablauf der Verformung mit der Geschwindigkeit nicht.

Abb. 2 zeigt eine Messkurve mit dem neuen Gerät.

Abb. 3 zeigt den Verlauf der Deformationsarbeit und der zugehörigen Wärmetönung für die Verstreckung von 1 g Material als Funktion der Geschwindigkeit. Die Kurven bei 20 und bei 30°C Verstreckungstemperatur zeigen innerhalb der Messgenauigkeit für die Wärme denselben Verlauf, während die Arbeit bei 20° etwas höher liegt. Dementsprechend ist die Zunahme der Enthalpie (Abb. 4) für eine Verstreckung bei 20° im Bereich konstanter Wärmeentwicklung überall einige Prozent höher als bei 30°. Auffällig ist, dass die Arbeit bei einer bestimmten, sehr scharf definierten Geschwindigkeit in einer Stufe ansteigt, während sich für die Wärme nichts erkennen lässt. Schliesslich fällt auf, dass nach kleinen Geschwindigkeiten hin bei konstant bleibender Arbeit die Wärmeentwicklung absinkt.

Aus diesen Kurven ergibt sich ferner, dass oberhalb der Stufe die Enthalpieerhöhung des Verstreckten grösser ist und dass sie ferner nach kleinen Geschwindigkeiten zu stark ansteigt (Abb. 4).

Das Absinken der Wärmeproduktion nach kleiner werdenden Geschwindigkeiten zu wird zweifellos mit der Abnahme der Energiedissipation durch innere Reibung mit sinkender Geschwindigkeit zusammenhängen: Es zeichnet sich der Übergang von einer Verstreckung mit thermischer zur isothermen Fliesszone ab.[11] Wenn man nämlich die Wärmeproduktion mit dem Volumen der Fliesszone kombiniert, lässt sich die Fliesszonenübertemperatur abschätzen (Abb. 5). Sie sinkt in gleicher Weise wie die Wärmeproduktion nach langsamen Geschwindigkeiten zu ab. Der gleichzeitige Anstieg der Enthalpie nach langsamen Verformungen hin muss auf einer Veränderung des Umordnungsmechanismus der Molekülsegmente zueinander beruhen.

Die Deutung der Stufe in der mechanischen Arbeit erscheint schwieriger. Man kann aus der Streckgeschwindigkeit die Zeit abschätzen, während der die Fliesszone um die eigene Breite weiterwandert. Das Reziproke dieser Zeit entspricht einer Frequenz und sollte—so könnte man vermuten—mit der Frequenzlage eines Relaxationsmaximums der mechanischen Dämpfung in Zusammenhang stehen. Man findet zwar bei nicht vollkommen ausgetempertem Polycarbonat im dielektrischen Verlust ein Maximum, das umgerechnet auf 1 Hz entsprechend liegt, das jedoch mit der Temperatur seine Lage stark verschiebt und ausserdem relativ breit ist. Somit lässt sich auf diese Art weder die Tatsache, dass die Stufe steil ist, noch die Unempfindlichkeit der Lage der Stufe auf Variation der Strecktemperatur verstehen.

Es scheint deshalb einer etwas anderen Deutung der Vorzug zu gebühren, bei der die Temperaturleitfähigkeit des Materials mit hinzugezogen wird. Nach der Seite des unverstreckten Materials zu ist ein relativ steiler Tem-

peraturgradient während der Verstreckung vorhanden (Abb. 6). Dieser verursacht, dass die bei der Streckung im Fliesszonenbereich produzierte Wärme jeweils bevorzugt in das Gebiet geführt wird, das sich im nächsten Augenblick verformen muss. Wenn jedoch die Fliesszone rascher über das Material fortwandert (höhere Streckgeschwindigkeit), als die Temperaturleitfähigkeit ein Ausbreiten der erhöhten Temperatur gestattet, wird sich der Temperaturgradient aufsteilen (Abb. 6*b*). Das von der Verformung im nächsten Augenblick erfasste Material wird nicht mehr wie bei langsamen Verstreckgeschwindigkeiten um die Fliesszonenübertemperatur wärmer sein. Es muss also bei der tieferen Strecktemperatur verformt werden, und der Aufwand an mechanischer Arbeit wird deshalb höher sein. Das könnte wegen der Versteilung der Temperaturgradienten sehr scharf bei einer bestimmten Streckgeschwindigkeit einsetzen. Tatsächlich entspricht die Höhe der Stufe etwa dem Doppelten der Erhöhung der Arbeit beim Übergang der Versuchstemperatur von 20° auf 30°C, also einer Änderung um 20°, während für die Fliesszonenübertemperatur 18°C ermittelt wurden.

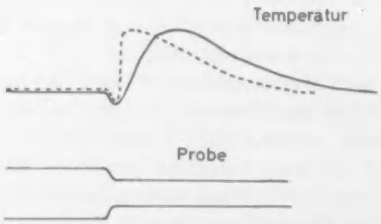

Abb. 6. Schematischer Verlauf der Uebertemperatur über die Fliesszone, ausgezogen bei langsamer, gestrichelt bei schneller Streckung, unter- und oberhalb der Stufe.

Die Art der Umlagerung wird sich entsprechend wie bei kälterem Material verändern. Somit erklärt sich sowohl die Stufe in der Arbeit wie in der Enthalpie. Und die Unabhängigkeit von der Verstreckungstemperatur resultiert aus der geringen Abhängigkeit der Temperaturleitfähigkeit von der Temperatur. Um weitere Bestätigung zu erhalten, wird es notwendig sein, nunmehr den bei der Entlastung der Proben auftretenden Wärmeeffekten mehr Aufmerksamkeit zu widmen, insbesondere die bei Spannungsrelaxation zu vermutenden abzutrennen.[12]

Schlieslich sei noch eine Abschätzung mitgeteilt, die sich auf zweierlei Weise über den Fliesswiderstand des Materials im Bereich der Fliesszone während der Verstreckung treffen lässt. Sowohl eine geeignet umgeformte Beziehung für die Ermittlung einer "Viskosität" von Stefan-Trouton für die Kraft als Funktion der Streckgeschwindigkeit[13] als auch die Berechnung einer "Viskosität" des Materials aus der pro Sekunde und Volumeneinheit entwickelten Wärme während der Verstreckung im Bereich der Fliesszone unter Zuhilfenahme einer Abschätzung des Schergefälles führt zu Formeln, nach denen der Fliesswiderstand umgekehrt proportional zur Streckge-

TABELLE I

Viskosität in der Fliesszone

aus Reibungswärme:

$$\left[\dot{Q} = \eta \times \left(\frac{dv}{dy}\right)^2\right] \qquad \eta = \frac{2}{3} \times \frac{Q \times B}{\Delta l(\lambda + 1)^2} \times \frac{1}{v}$$

von Stefan:

$$\eta = \frac{2}{3} \times \frac{\sigma_B B^3 \times 2\pi(\lambda - 1)}{q_F(\lambda + 1)} \times \frac{1}{v}$$

Geschätzte Werte der "Viskosität" η in der Fliesszone

Streckgeschwindigkeit, cm/sec	η_1, poise	η_2, poise
$v = 8 \times 10^{-3}$	$2{,}8 \times 10^7$	$0{,}9 \times 10^7$
$v = 1{,}7 \times 10^{-3}$	$1{,}4 \times 10^7$	$0{,}46 \times 10^7$

schwindigkeit laufen muss. (Tab. I). Das entspricht einer von Lazurkin schon erwähnten Tatsache.[14]

Die aus der Geometrie der Fliesszone und den Näherungen über Schergefälle ermittelten Werte liegen jedoch im ersten Falle höher als im zweiten (Tab. I). Den absoluten Werten nach liegen sie stets weit unter den Viskositätswerten von Gläsern im Einfrierbereich (5 Zehnerpotenzen). Daraus folgt zunächst die Bestätigung, dass das Auftreten der Fliesszone auf einem nichtlinearen Verhalten beruht:[11] bei höheren Verformungsgeschwindigkeiten bzw. -Kräften sinkt der Fliesswiderstand stark ab.[12]

Die höheren Werte für die "Viskosität," die man aus der Wärmeproduktion erhält, können jedoch darauf hinweisen, dass nur ein Teil der gemessenen Wärme durch Entropieerzeugung, d.h. als Reibungswärme, entsteht, ein anderer Teil jedoch aus einer Entropieverminderung während der Verstreckung resultiert.

Sollten die angewendeten Formeln genügend gute Näherungen darstellen, so wäre damit ein Weg gegeben, um ausser über die Enthalpieänderung bei Verstreckung, die nach dem ersten Haupsatz exakt aus Differenz von Arbeit und Wärme folgt, *auch etwas über die Entropieänderung bei einer Deformation* aussagen zu können. Dafür besteht bisher keine Möglichkeit,[17] und es wäre sehr interessant, wenn sich hiermit ein Weg zu diesen Aussagen eröffnen liesse.

Literaturverzeichnis

1. *Erste Veröffentlichung*, Müller, F. H., und Ad. Engelter, *Kolloid-Z.*, **149**, 126 (1956); Ausführlich: Dissertation Engelter, *Kolloid-Z.*, **157**, 89 (1958) und *Rheologica Acta*, **1**, 39 (1958); Dissertation Dick, *Kolloid-Z.*, **172**, 1 (1960).
2. Dissertation Jäckel, *Kolloid-Z.*, **137**, 130 (1954).
3. Brauer, P., und F. H. Müller, *Kolloid-Z.*, **135**, 65 (1954).
4. Engelter, Ad., und F. H. Müller, *Rheologica Acta*, **1**, 39 (1958).
5. Vortrag auf der Gordon-Research-Konferenz, 4–8, Juli 1960.
6. Diplomarbeit N. Weimann 1963, Veröffentlichlung demnächst in der *Kolloid-Z.*
7. Foster, H. O., und R. E. Benner, Vortrag auf dem IV. Internationalen Kongress für Rheologie, Brown University, Providence, Rhode Island, 26–30, August 1963.

8. Müller, F. H., und Ad. Engelter, Sitzungsberichte der Gesellschaft zur Beförderung der gesamten Naturwissenschaften zu Marburg, **83, 84,** Band, 487 (1962).
9. siehe Vortrag Müller-Martin auf diesem Symposium.
10. Müller, F. H., *Österr. Chemiker-Z.*, **63,** 158 (1962).
11. Müller, F. H., und G. Binder, *Kolloid-Z.*, **183,** 120 (1962).
12. Versuche im Gang.
13. Stefan, J., *Sitzungsber. Akad. Wiss. Wien II*, **69,** 713 (1874); F. T. Trouton, *Proc. Roy. Soc. (London)*, **77,** 426 (1906).
14. Prandtl, L., *Z. Angew. Math. Med.*, **8,** 85 (1928); S. Glasstone, K. J. Laidler, und H. Eyring, *The Theory of Rate Processes*, McGraw-Hill, New York–London, 1941, pp. 477.
15. Müller, F. H., *Kolloid-Z.*, **165,** 96 (1959).

Zusammenfassung

Aus der Messung der Wärmeeffekte und der Arbeit bei Verstreckung von Polycarbonat mit grosser Variation der Streckgeschwindigkeit und bei zwei verschiedenen Temperaturen, ergeben sich Folgerungen über die bei der Verstreckung auftretende Enthalpiezunahme. Auf die Entropieänderung beim Verstrecken scheinen indirekte Schlüsse möglich zu sein. Der Einfluss von Temperaturausgleichsvorgängen wird bestätigt, und es scheint auch die Spannungsrelaxation des verstreckten Materials mit einer Wärmeentwicklung gekoppeltzusein.

Résumé

La measure des effets thermiques et du travail d'éntirement sur le polycarbonate pour de grandes variations de la vitesse d'étirement et pour deux températures différentes, permet de tirer des conclusions sur l'augmentation d'enthalpie résultant de l'étirement. Il semble qu'en ce qui concerne le changement d'entropie lors de l'étirement, on puisse déduire des conclusions indirectes. De plus des données au sujet de l'influence d'effets de compensation de la température se trouvent confirmées; de même il semble que le relâchement de la tension du matériel étiré puisse être couplé avec un dégagement de chaleur.

JOURNAL OF POLYMER SCIENCE: PART C NO. 6, PP. 125–136

Studies of the Thermal Behavior of Polymers by Torsional Braid Analysis*

JOHN K. GILLHAM and ARMAND F. LEWIS, *Stamford Research Laboratories, American Cyanamid Company, Stamford, Connecticut*

Synopsis

The application of the torsional braid technique to the thermal analysis of polymers (and monomers) is demonstrated. Included in this work are details of a visual method for estimating the dynamic mechanical damping factor of a freely oscillating system. Studies of a thermoplastic polymer and a thermosetting resin are presented in which their thermal behavior is demonstrated with respect to first and second order transitions, cure, thermal crosslinking and degradation. Isotactic polypropylene is studied as an example of a semicrystalline thermoplastic polymer. The monomer 1,3,5-triacrylylhexahydro-s-triazine represents an example of a thermosetting material. The dynamic mechanical data are compared with the results obtained by differential thermal analysis, thermogravimetric analysis, and infrared spectroscopy.

Introduction

The current report demonstrates the interrelationship of the results of the various techniques which are used in the thermal analysis of polymers. It will be apparent that no one technique should serve as *the* tool for even a preliminary examination. Degradation can occur without loss of weight, without apparent changes in infrared spectra, without apparent changes in electrical and mechanical properties, and without measurable changes in heat content. Unfortunately a technique of general applicability which uses a mechanical property as an index for the measurement of thermal stability has been lacking. Torsional braid analysis represents an attempt to fill this gap in the preliminary screening of polymers.

Torsional braid analysis[1] (TBA) is a dynamic mechanical method for the investigation of polymers. The technique is based on the fact that changes in dynamic mechanical behavior with temperature (or other variables) of a composite made up of a mechanically inert substrate (the braid) and a polymer can be attributed to changes in the polymer. In contrast with classical methods of dynamic mechanical spectroscopy, for which geometrical specimens are fabricated, the present technique permits the investigation of any type of polymer (or chemical compound)

* This paper is the third in a series[2,4] on the subject "Dynamic Mechanical Properties of Supported Polymers."

which can be deposited or synthesized on the braid. The current communication relates the status of the technique and exemplifies its utility in the thermal analysis of polymers. Polypropylene, as an example of a thermoplastic semicrystalline polymer, was examined in the expectation of being able to detect both the second order transition of the amorphous region of the polymer (glass transition) and the first order transition associated with the crystalline region (melting point). As an example of a thermosetting material the monomer 1,3,5-triacrylylhexahydro-*s*-triazine was investigated. The simplicity of its structure permitted changes in mechanical properties to be correlated with the results of other methods of thermal analysis. These latter include thermogravimetric analysis and differential thermal analysis. Complementary examination by infrared spectroscopy is essential in order to be able to correlate the results with specific chemical processes.

Procedure

A. Rigidity Determination

The torsional pendulum of previous publications[1-5] was employed throughout these studies. The shaft of the pendulum consists of a loose braid of glass fibers[4] which is impregnated with the polymer to be studied. The mechanical properties of the composite are ascertained by observation of the sinusoidal torsional oscillations of an inertial mass which is suspended by the shaft. Free oscillations are induced into the system from time to time, in the manner which has been described.[1] Two parameters are currently used in an attempt to obtain a measure of rigidity and damping. The relative rigidity[1] and damping index[5] correspond to the real part of the complex modulus and to the logarithmic decrement, respectively. The relative rigidity, G_t/G_0, refers the rigidity at time t relative to that at an arbitrary time t_0 in the same experiment, and is calculated from the period P of the oscillations. $G_t/G_0 = (P_0/P_t)^2$. Subscript T is employed when temperature rather than time is variable.

B. Visual Determination of Dynamic Mechanical Damping

The damping index, which is designated $1/n$, is determined by a visual method. This consists in counting the number of oscillations n which the eye can discern upon induction of free, damping vibrations. The approach supplies reproducible data and has a physical basis. An analysis of the relationship between the damping index $1/n$, and the logarithmic decrement Δ, follows.

In general Δ may be defined thus:

$$\Delta = \ln (A_0/A_1) = \ln (A_1/A_2) = \ln (A_2/A_3) \ldots = \ln (A_{n-1}/A_n) \quad (1)$$

where A_{n-1} and A_n refer to successive peaks in amplitude of a time- amplitude decay curve (damped sine wave). There are several ways of

evaluating Δ from such a curve. When a trace of the time-amplitude decay curve is available, Δ is obtained directly from the slope of the straight line which results from plotting ln A_n versus the cycle number. The method is tedious. Another way of determining the logarithmic decrement is to establish the cycle number at which the initial amplitude A_0 decays to a predetermined factor, say fA_0, of the original amplitude.[6] Such a procedure offers the possibility of a "one point" determination of Δ. This is the basis for the visually determined damping index $1/n$. The technique was conceived from the observation that in highly damped regions, only one or two swings of the pendulum could be obtained no matter how vigorously the pendulum was impulse-activated. In a weakly damped region, under the same degree of activation, hundreds of swings could be counted. From a mathematical analysis of this behavior the logarithmic decrement may now be defined as:

$$\Delta = 1/n \ln (A_0/A_n) \tag{2}$$

If A_n is set equal to fA_0 the equation takes the form:

$$\Delta = 1/n \ln (1/f) \tag{3}$$

where f is the fraction of the original amplitude one can distinguish visually during the course of the free vibration. This coefficient may be called the motion perceptivity factor for free vibration. From eq. (3) for a constant initial amplitude and an assumed constancy in f, the value of $1/n$ may be considered to be directly proportional to the logarithmic decrement. This term $1/n$ may be called the mechanical damping index.

The mechanical damping index has been tested as a means for measuring damping in torsional braid experiments. In all cases where measurements were compared with experimental data obtained by conventional (absolute) methods, the qualitative behavior of the mechanical damping index, $1/n$, paralleled that of the logarithmic decrement, Δ. Under some conditions the relative levels of $1/n$ and Δ were displaced. This led to the suspicion that f may not be constant. The nature of f was therefore investigated in greater detail.

The determination of f was accomplished by a procedure which was based on the linearity of the following equation:

$$\ln (1/f_t) = \Delta n_t \tag{4}$$

where f_t is the fraction of the original amplitude remaining, A_t/A_0, at cycle number n_t. Values of A_t at constant A_0 were obtained by following visually the behavior of the time-amplitude decay curve on the torsional braid apparatus. This was accomplished by marking off on a sheet of polar graph paper which was located beneath the oscillating pendulum, the peaks of the decaying curve at various cycle numbers. Plots of ln (A_t/A_0) versus n_t were found to be linear. An extrapolation of this straight line to n yielded an estimate of ln $(1/f)$. Such an experimental procedure was carried out for a number of values of n (by using the dif-

ferent materials of Table I) while estimates in the errors in determining n were also made. The results presented in Table I show some experimental characteristics of this visual method for estimating the logarithmic decrement. Of immediate interest is the fact that f is not constant in the region where n has values below about 30. Secondly for high values of n the estimation of n by (uncontrolled A_0) impulse activation of the pendulum is as good as the value of n obtained when A_0 is controlled. (In this latter case A_0 represents stressing 90° from equilibrium.) From these data, an estimate of the errors was made. It appears that for high values of n the logarithmic decrement Δ can be obtained with precision and accuracy using this visual method. At lower values of n, say below thirty, errors in reading n are apparent. Here errors of over 10% are encountered. Furthermore from this analysis, at very high damping, errors of 50% in the determination of Δ may arise. If the variation of ln $(1/f)$ with n is taken into account, the errors in Δ for low values of n are greatly lessened. Unfortunately ln $(1/f)$ is difficult to determine for low values of n.

TABLE I

Estimation of Errors Involved in the Visual Method for Obtaining Mechanical Damping as Applied to Torsional Braid Analysis

Material	Frequency, cps	n I Impulse activated	n II Stressed to 90°	ln $(1/f)$	Δ (based on II)	% error in $1/n$ A[a]	B[b]	Sum
Epoxy resin[7] on glass fibers	1.38	90.0	90	6.40	0.072	0	0	0
Polymethyl methacrylate[8] rod	2.07	25.0	30	6.40	0.213[c]	20	0	20
Cotton thread	0.12	19.0	16	5.86	0.366	16	10	26
PMMA-benzene solution coated on cotton thread[9]	0.32	3.5	4	4.82	1.205	14	33	47

[a] Possible error in $1/n$ due to non-constant A_0.

[b] Possible error in assuming ln $(1/f)$ is constant (6.40).

[c] Value (ref. 8) for PMMA at room temperature is 0.25 (torsional pendulum). Therefore, the absolute error in the method could be about 12%.

In regard to the measurement of logarithmic decrement by more absolute schemes, the values of Δ for high damping are usually subject to errors from inherent sources. For example, eqs. (1) and (2) are valid only for low damping levels and errors up to 15% exist in these regions. Nevertheless, logarithmic decrement curves in free vibration are still considered interpretable in a qualitative sense. It is therefore felt that although visual determination of Δ by the method analyzed herein does not produce absolute values of Δ, especially when ln $(1/f)$ is assumed constant, the value of mechanical damping reflected by $1/n$ is sufficiently adequate for qualitative interpretation of the data.

There is no doubt that analysis of a polymer in terms of the concurrently determined relative rigidity and damping index parameters provides an excellent basis for the investigation of changes which occur in polymers. This is due in large measure to the range of values which the parameters cover in the present experimental procedure. The relative rigidity extends over four to five, and damping index over more than three, orders of magnitude. Instrumentation of the torsional braid apparatus will permit an accurate measure of damping to be made for the composite.

C. General Procedures

Studies of polymers from room temperature to 500°C. were conducted in an apparatus[4] which used an air-fluidized bed of silica gel as the heat-transfer medium. Studies from −100°C. to room temperature employed liquid nitrogen as the initial coolant for the fluidized bed. In the complementary techniques of differential thermal analysis (DTA) and thermogravimetric analysis (TGA) the rate of temperature increase is rarely programmed at less than two degrees per minute. A slower rate of heating would not alter resolution of the cumulative parameter, loss of weight, in TGA; however, in DTA the discrete exo- and endothermic processes would be obscured with a much slower rate of rise of temperature. In this communication the results of TGA and DTA are for a programmed rate of five degrees rise per minute. A faster rate is less harmful to the sensitivity of the relative rigidity than to the damping index. This is because of the finite time required for a reading (e.g., with a period of 1 sec., 300 discerned oscillations would take 5 min. for completion). The graphical plots of the mechanical properties as a function of temperature incorporate a time scale. In attempted correlations between TGA, DTA, and TBA, transformations should occur at about the same temperature. Small variations may be attributed to differences in the rate of increasing temperature and to the influence of frequency and possibly filler on dynamic transition behavior.[2] The frequency of the free vibrations lies within the range 0.1–2.5 cps. Unless stated to the contrary, experiments were conducted in an atmosphere of nitrogen as described earlier.[4,5] Each experiment in TBA used about 0.1 g. while those in DTA and TGA used about 0.02 g. of material.

Thermal Analyses

Polypropylene

Polypropylene was powdered in a Wiley mill at −78°C., extracted with acetone for 72 hr. in a Soxhlet apparatus and was dried and stored *in vacuo*. An infrared spectrum corresponded[10] with that of a specimen of predominantly isotatic polypropylene.

The following procedure was used for the preparation of solvent-free polypropylene-impregnated braid. A hot solution of polypropylene

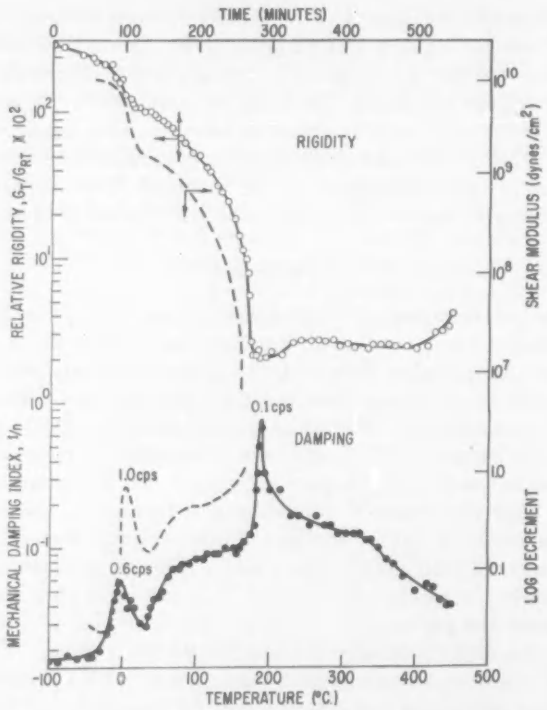

Fig. 1. Thermo-mechanical behavior of polypropylene: (——)T BA; (- - -) conventional free vibration technique (ref. 11).

(10%) in tetrahydronaphthalene was applied to the braid by dipping. The pendulum was then inserted into the jacket of the torsional braid apparatus, air was displaced by nitrogen, and the temperature was raised to 180°C. under normal pressure. To insure removal of tetrahydronaphthalene (bp 210°C.) low pressure (0.25 mm. Hg) was applied for three hours at 180°C. before cooling slowly *in vacuo*. The subsequent experiment was performed at 0.25 mm. Hg pressure.

The thermo-mechanical behavior of the glass braid-polypropylene composite is presented in Figure 1. Dynamic mechanical data[11] for an unfilled rod of highly crystalline polypropylene are included in the figure. A comparison of the data demonstrates the extent of agreement between TBA and classical methods. Furthermore, it is apparent that TBA extends the range of temperatures capable of investigation by dynamic mechanical methods.

The two distinct damping maxima (about 0°C. and 190°C.) correspond respectively to a second order transition[8,12,13] of the amorphous region of polypropylene and to the first order transition[12,13] due to melting of the

crystalline regions of the polymer. It is evident that for a melting transition, as well as for glass transitions, a decrease in rigidity accompanies a damping maximum. Incidentally with classical (unsupported) dynamic mechanical techniques, the detection of first order transitions is rarely observed in consequence of limitations in dimensional stability of the specimens at temperatures approaching those of a melting transition.

Analyses by thermogravimetric and differential thermal analyses are presented in Figure 2. That the response of DTA to the first order transition (at about 170°C.) is greater than to the secondary (at about

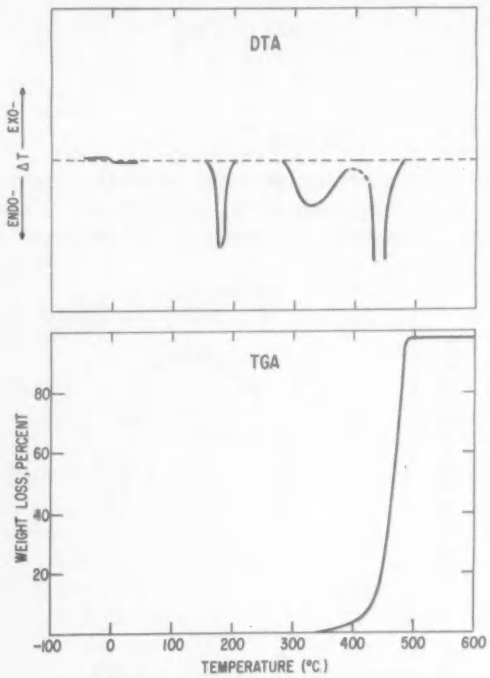

Fig. 2. Thermal analysis of polypropylene.

−10°C.) is a consequence of an energy term for fusion. Above the melting point at least two discrete processes occur, the endotherm at the higher temperature being accompanied by loss of weight. More complete studies[14,15] of the degradation of polypropylene revealed the occurrence of at least two distinct processes. One involves no loss of weight, has a lower activation energy and occurs at a lower temperature than the other which with a higher activation energy becomes dominant at a higher temperature and involves a more complete breakdown of the polymer to volatile fragments. The process with lower activation energy has been attributed[14] to hydroperoxides which were formed as part of the pre-

history of the specimen. A similar explanation would be plausible for the present studies.

Poly(1,3,5-triacrylylhexahydro-s-triazine)

1,3,5-Triacrylylhexahydro-*s*-triazine is a trifunctional vinyl monomer[16,17] with a structure represented thus:

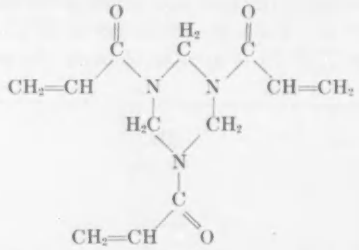

In the absence of an inhibitor, attempts to obtain a melting point are accompanied by the formation of an insoluble and infusible polymer. This complication presented a challenge to the technique since impreg-

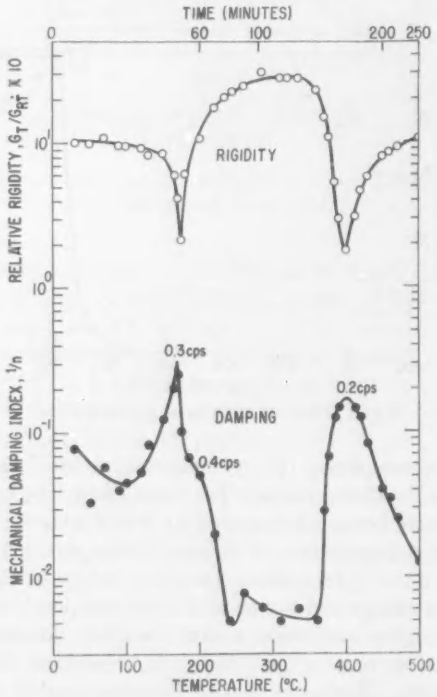

Fig. 3. Thermo-mechanical behavior of 1,3,5-triacrylylhexahydro-*s*-triazine.

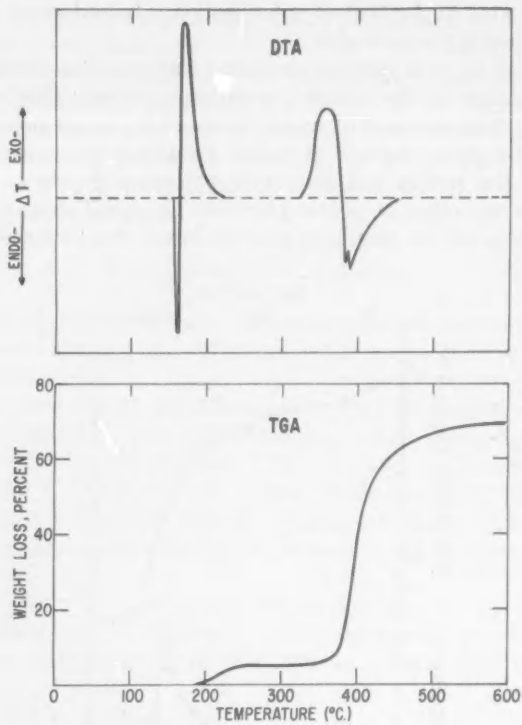

Fig. 4. Thermal analysis of 1,3,5-triacrylylhexahydro-s-triazine.

nation of the polymer onto the braid is not possible. Hence crystals of monomer were deposited on the braid by brushing with a solution (5%) of the monomer in chloroform, and allowing the solvent to evaporate. This monomer-impregnated braid formed the sample for the thermal softening experiment, the results of which are presented in Figure 3. An interpretation is aided (Fig. 4) by complementary examination of the monomer by TGA and DTA.

Melting (158°C.) is accompanied by an endotherm, a maximum in damping and a decrease in rigidity. Polymerization is detected immediately after melting by the increase in rigidity and the exotherm. The damping maximum in the vicinity of the melting point shows some dispersion and appears to be resolved partially into two peaks. The lower and sharper maximum is attributable to the melting region itself while the subsequent shoulder is probably the maximum in damping which is associated[7,18] with the curing process. The polymer appears to be thermally stable to about 350°C. after which a decrease in rigidity occurs with a concurrent exotherm. A subsequent increase in rigidity is accompanied by loss of weight and an endotherm. The latter might

well be accounted for by heat of volatilization. Indeed an oil condensed in the cooler part of the apparatus.

Parallel analysis by infrared spectroscopy supported the interpretations. The only changes in the infrared spectrum to about 350°C. were attributable to disappearance of unsaturation in the vinyl polymerization process. Subsequent changes at higher temperatures showed that the structure of the residue had lost amide-absorbing groups and had approached the structure of polyacrylonitrile pyrolyzed similarly to 400–500°C. This is not too surprising since the hexahydro-*s*-triazine monomer

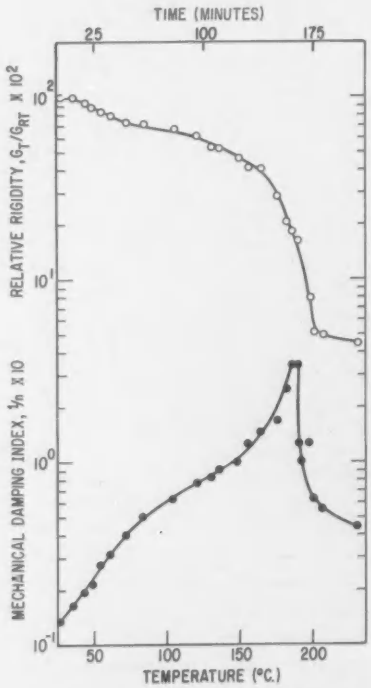

Fig. 5. Thermo-mechanical behavior of diphenyl terephthalate.

can be synthesized from acrylonitrile and formaldehyde. On the other hand the condensate (about 50% yield) consisted of saturated primary amides. Further analysis of the oil by gas phase chromatography demonstrated the presence of at least a dozen constituents. Since the purposes of this research are to show how torsional braid analysis fits into a scheme of polymer analysis further investigations concerning the specific chemical processes are not reported here.

In the thermal analysis two processes would require further study for complete correlation. The loss of weight and maximum in damping

which are apparent in the range 200–300°C. might well be attributed to volatilization of free unincorporated monomer. The damping maximum at about 400°C. is associated with the degradative processes which occur during the pyrolysis. Performing thermo-mechanical experiments at different heating rates may help to delineate these. The existence of a pyrolyzed continuum (indicated with TBA by an increase in rigidity) may well be shown by measuring the change in electrical resistance of the braid during the heating.[4]

Transformations in Monomers

The examples which have been considered demonstrate that a melting transition is accompanied by a maximum in damping and a drop in rigidity with rise of temperature. Particularly interesting was the observation that this occurred during the melting of a crystalline monomer on the glass braid. Results for a crystalline monomer which does not polymerize on melting are presented in Figure 5. The monomer was diphenyl terephthalate (mp 190°C.). Crystals were formed on the braid by evaporation of chloroform from an applied solution. Again, decreasing rigidity and a maximum in damping occur as the temperature is raised through the first order transition.

Other transformations of monomers are accompanied by changes in rigidity and damping. Studies on monomers and model compounds should facilitate the interpretation of the dynamic mechanical spectra of polymers.

Conclusions

It is apparent that preliminary thermal analysis of a polymer should involve several complementary techniques. No one technique responds to all the transitions and transformations which occur in a polymer system. Furthermore the magnitude of response of a technique to a change will differ with technique and type of change. It is apparent too that torsional braid analysis makes an important contribution in relating not only changes but also the mechanical state of a polymer. The present report includes several new aspects of the technique. Among these are an analysis of a visual method for estimating damping in free vibration and the detection of first order transitions in polymers and monomers by the dynamic mechanical method. It is suggested that correlations exist between relaxations of model compounds and of polymers which could be used to facilitate interpretation of dynamic mechanical spectra of polymers.

The authors wish to thank Mr. J. R. Murray for the results of TGA, Miss E. C. Eberlin for results and discussions concerning DTA, and Mr. N. B. Colthup for results and interpretative advice concerning the infrared spectra. Their gratitude extends too to Dr. R. E. Spalding for discussions pertinent to the presentation, and to Miss M. Wilson for drawing the figures.

References

1. Lewis, A. F., and J. K. Gillham, *J. Appl. Polymer Sci.*, **6**, 422 (1962).
2. Lewis, A. F., and J. K. Gillham, *J. Appl. Polymer Sci.*, **7**, 685 (1963).
3. Gillham, J. K., and A. F. Lewis, *Nature*, **195**, 1199 (1962).
4. Gillham, J. K., and A. F. Lewis, *J. Appl. Polymer Sci.*, **7**, 2293 (1963).
5. Gillham, J. K., *Science*, **139**, 494 (1963).
6. Thurn, H., *Kolloid-Z.*, **173**, 71 (1961).
7. Lewis, A. F., *SPE Trans.*, **3**, 201 (1963).
8. Lewis, A. F., and M. C. Tobin, *SPE Trans.*, **1**, 177 (1961).
9. Lewis, A. F., and M. C. Tobin, *Trans. Soc. Rheol.*, **6**, 27 (1962).
10. Clampitt, B. H., and R. H. Hughes, *J. Polymer Sci.*, **C6**, 43 (1964).
11. Miller, R. L., *Polymer*, **1**, 135 (1960).
12. Newman, S., and W. P. Cox, *J. Polymer Sci.*, **46**, 29 (1960).
13. Passaglia, E., and H. K. Kevorkian, *J. Appl. Physics*, **34**, 90 (1963).
14. Schooten, J. V., and P. W. O. Wijga, *Soc. Chem. Ind. (London)*, Monograph No. **13**, p. 432 (1961).
15. Schott, H., and W. S. Kaghan, *SPE Trans.*, **3**, 145 (1963).
16. Smolin, E. M., and L. Rapoport, *s-Triazines and Derivatives*, Interscience Publishers Inc., New York, 1959, p. 535.
17. American Cyanamid Co., Wayne, N. J., *The Chemistry of Acrylonitrile*, second ed., 1959, p. 69.
18. Drumm, M. F., C. W. H. Dodge, and L. E. Nielsen, *Ind. Eng. Chem.*, **48**, 76 (1956).

Résumé

On démontre le procédé de torsion de tresses (torsional braid technique) l'analyse thermique des polymères (et monomères). On donne, dans ce travail, des détails concernant une méthode visuelle pour l'estimation du facteur dynamique d'amortissement mécanique et d'un système d'oscillation libre. On présente les études sur un polymère thermoplastique et une résine thermodurcissable dont le comportement thermique est démontré en fonction des transitions du premier et du second ordre, du traitement thermique, du pontage thermique et de la dégradation. On a étudié le polypropylène isotactique comme échantillon d'un polymère thermoplastique semi-cristallin. Le monomère 1,3,5-triacrylyldecahydro-*s*-triazine représente un échantillon du matériel thermodurcissable. Les données dynamiques concernant les propriétés mécaniques sont comparées aux résultats obtenus par analyse thermique différentielle, analyse thermogravimétrique et spectroscopie infra-rouge.

Zusammenfassung

Das Schnurtorsionsverfahren (torsional braid technique) wird zur thermischen Analyse von Polymeren (und Monomeren) verwendet. Die vorliegende Arbeit gibt auch Einzelheiten einer visuellen Methode zur Bestimmung des dynamisch-mechanischen Dämpfungsfaktors eines frei oszillierenden Systems an. Ein thermoplastisches Polymeres und ein wärmehärtendes Harz werden in Hinblick auf ihr thermisches Verhalten bei Umwandlungen erster und zweiter Ordnung, thermischer Vernetzung und thermischem Abbau untersucht. Als Beispiel für ein semi-kristallines thermoplastisches Polymeres wird isotaktisches Polypropylen gewählt. Monomeres 1,3,5-Triacrylylhexahydro-*s*-triazin bildet ein Beispiel für einen wärmehärtenden Stoff. Die dynamisch-mechanischen Daten werden mit den Ergebnissen der Differentialthermoanalyse, der thermogravimetrischen Analyse und der Infrarotspektroskopie verglichen.

JOURNAL OF POLYMER SCIENCE: PART C NO. 6, PP. 137–148

Dynamic Differential Thermal Analysis of the Glass Transition Interval

BERNHARD WUNDERLICH* and DAVID M. BODILY,† *Department of Chemistry, Cornell University, Ithaca, New York*

Synopsis

Dynamic differential thermal analysis (DDTA) will be described and its application to the study of the glass transition interval of polystyrene will be discussed. The mode of operation involves reproducible cooling from the molten state through the glass transition interval and subsequent heating, both at reproducible linear rates of temperature change. Data on the temperature of half-freezing on cooling and on the temperature of the peak and (or) minimum in the heat capacity have been collected and will be compared with theoretical expressions derived on the basis of the hole theory of liquids. From the half-freezing temperature on cooling; which is taken to be a mean fictive temperature, properties of a mean hole are calculated for polystyrene. (Mean molar hole volume = 21.9 cm.^{3}, energy 1600 cal., activation energy 157,600 cal.; relaxation time at the fictive temperature 5.5 min.) DDTA will be shown to be applicable to the determination of the second freezing-in process of polystyrene which occurs over a range of 230 to 350°K. and is thought to involve the librational motion of the phenyl rings.

Introduction

The first detailed investigation by thermal methods of the glass transition interval with respect to the time variable was done by Tool and Eichlin[1] in 1930. Measurements similar to DTA revealed differences in properties between glasses obtained by quenching and by annealing. The main result was that depending on the rate of cooling through the glass transition interval, different behavior on subsequent heating was experienced. To describe the experimental results Tool used a fictive temperature.[2] Above the glass transition interval the fictive and true temperature are identical. Below the glass transition region the fictive temperature is constant and has a higher value than the true temperature, giving an indication of the frozen-in conformations of the different glasses.

A better understanding of the fictive temperature is gained in terms of the hole theory.[3,4] In its latest form this hole theory has been extended to describe the glass transition.[5,6] Each hole is characterized by its molar volume v_h, and the molar excess energy over the no hole situation, ϵ_h.

* Present address: Department of Chemistry, Rensselaer Polytechnic Institute, Troy, New York.

† Present address: Department of Chemistry, Northwestern University, Evanston, Illinois.

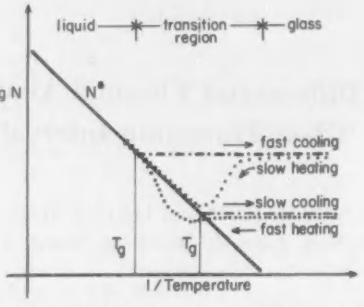

Fig. 1. Change of N with temperature: (——) calculated for equilibrium (eq. 1); (- · -) change on fast or slow cooling; (. . .) change on subsequent heating. T_g denotes the glass-transition or fictive temperature.

Other parameters of interest are the activation energy for the disappearance of a hole ϵ_j, the partition function of the holes Q^h, and the partition function of the activated state $Q\ddagger$. The process of disappearance of a hole is thought to create elastic strain, which propagates to the surface with the velocity of elastic waves. The excess energy is taken up by the changed liquid lattice. If the hole-equilibrium is frozen-in, the material is in the glassy state.

The equilibrium number of moles of holes, N_h^*, has been expressed as[5,6]

$$N_h^* = N_0\left(\frac{v_0}{v_h}\right)e^{-\epsilon_h/RT} \tag{1}$$

N_0 and v_0 are the number of moles of repeating units in question and the molar volume per repeating unit.

The number of frozen-in holes below the glass transition interval is called N_a and related to the fictive temperature T_x, in the following way:

$$N_a = N_0\left(\frac{v_0}{v_h}\right)e^{-\epsilon_h/RT_x} \tag{2}$$

Figure 1 describes qualitatively the two main situations which can arise on cooling a melt through the transition region to a glass followed by subsequent heating. (*a*) On *slow cooling* a relatively small number of holes, N_a, are frozen-in. On subsequent *fast heating*, the equilibrium number of holes N_h^* is overshot since there is not enough time for equilibration, and the glass returns to the equilibrium condition via a path which appears endothermic, giving rise to a maximum in the specific heat at the point of inflection of the curve in Figure 1. (*b*) On *fast cooling* on the other hand, a relatively large number of holes N_a are frozen-in. On subsequent *slow heating*, equilibrium is approached before the N^* curve is reached giving rise to a minimum in the specific heat at the point of inflection of the appropriate curve in Figure 1. This minimum is also present, in case (*a*), however, its magnitude is small and it is hard to detect experimentally.

Dynamic Differential Thermal Analysis (DDTA)

In order to investigate the kinetic effects in the glass transition interval it is thus necessary to observe the sample during a complete cycle of cooling from above the glass transition temperature T_g through T_g and then heating up through T_g from low temperatures. For this purpose differential thermal analysis[7] was modified to allow the dynamic measurements involving complete heating and cooling cycles.

A schematic diagram of the dynamic differential thermal analysis apparatus is shown in Figure 2.

The heating chamber consists of a $1^1/_2$ in. by 5 in. cylindrical brass block. Two $^7/_{16}$ in. holes are symmetrically drilled about a plane through the cylinder axis. The holes are $^9/_{32}$ in. from the center of the cylinder. A $^7/_{16}$ in. by 2 in. brass rod is placed in the bottom of each hole. The sample and reference holders are located in the holes on top of the rods, thus bringing the sample and reference material near the center of the brass block. The brass block is wrapped uniformly with a glass-fiber-shielded heating

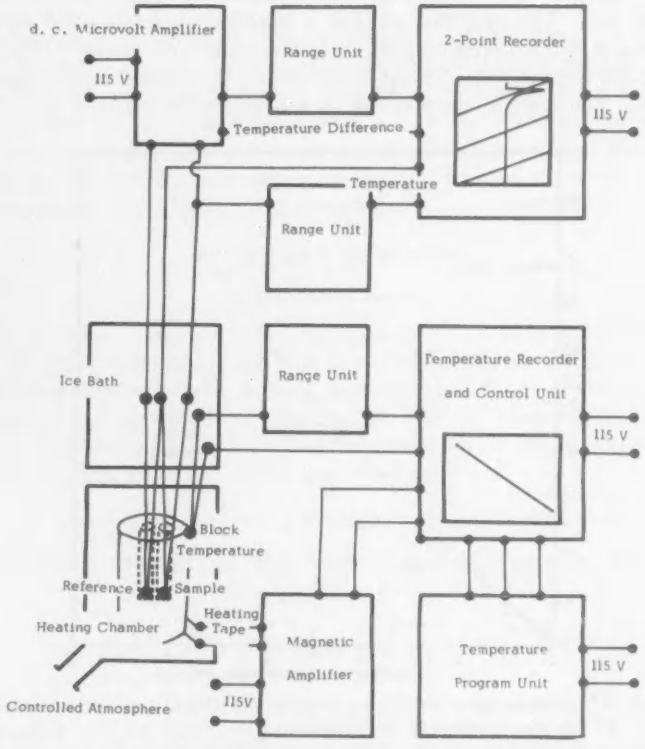

Fig. 2. Schematic diagram of the DDTA-set-up.

tape and the tape is insulated uniformly with asbestos. The entire chamber is contained in a 1000 ml. vessel which can be evacuated or kept under a nitrogen atmosphere.

The sample and reference holders contain typically 0.5 g. material and are 1 in. by $^7/_{16}$ in. brass vials. The thickness of the vial walls is $^1/_{16}$ in.

Iron-constantan thermocouples are used to measure the temperature of the sample and the temperature difference between the sample and the reference. The thermocouples are stainless-steel sheathed, insulated by magnesium oxide (Aero Research Instrument Company, Inc.) with an over-all diameter of $^1/_{16}$ in. They are centered in the heating chamber by asbestos cement discs. The thermocouples were calibrated by measuring the melting point of a number of compounds that melt in the temperature range of interest. The melting points could be measured with a precision of ±0.2°C.

The voltage difference between the two thermocouples can be amplified by a factor of from 1 to 200 by a d.c. microvolt amplifier (Leeds and Northrup 9835b). Range changes are generally made by adding a potential using a millivolt potentiometer which has a reproducibility of ±0.005 mv. The amplified voltage is recorded on a two-point recorder (Leeds and Northrup Speedomax G). The print cycle is 4 sec. The output of the thermocouple placed in the sample is recorded on the same recorder. The span of the recorder is two millivolts, but the potentiom-

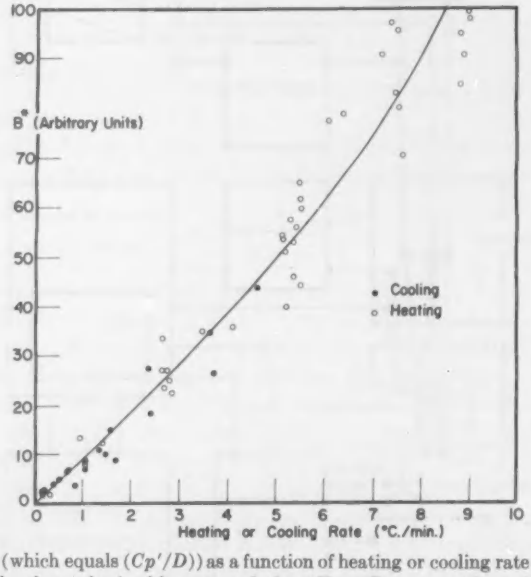

Fig. 3. B^* (which equals (Cp'/D)) as a function of heating or cooling rate q, (see eqs. 3 and 9). B^* has been obtained by extrapolating $(T_r - T_s)_{melt} - (T_r - T_s)_{glass}$ to the temperature of half-change in Cp'. Filled points, cooling; circles, heating. Drawn out curve: $q = 0.1161, B^* - 3.1372 \times 10^{-4} B^{*2}$.

eters allow the zero to be shifted to the desired value for each recorded voltage.

The temperature of the brass block is measured by an iron-constantan or chromel-alumel thermocouple placed between the heating tape and the brass block. The voltage is recorded by a strip chart recorder with a span of 10 mv. The temperature can be controlled at a constant value, varied manually or varied automatically (Leeds and Northrup series 60 3-action control unit). Automatic programing is accomplished by means of a motor-driven cam, cut to the desired program (Leeds and Northrup program control unit 10170). The maximum rate of temperature change is 7.44°C./min. with the iron-constantan thermocouple. The chromel-alumel thermocouple allows rates up to 9.84°C./min. The control unit governs a magnetic amplifier whose output is sent through the 192 watt heating tape.

The specific heat of the sample can be set equal to

$$c_s \approx D(T_r - T_s) + K \tag{3}$$

D and K are functions which vary only slowly with temperature for linear heating rates, and $T_r - T_s$ is the recorded difference in temperature between reference and sample. For the discussion of the part of the specific heats due to the change in hole equilibrium, extrapolation of the $(T_r - T_s)$-curve from temperatures below the glass transition establishes a zero base line and fixes K. An estimation of D as a function of heating rate can be obtained by comparison of the increase in $T_r - T_s$ in going from the glassy region to the equilibrium melt with calorimetrically measured ΔC_p's.[6] Figure 3 shows such a comparison using 4.7 cal./deg. mole for ΔC_p.

Application to Polystyrene

1. Qualitative Results

Figures 4 and 5 show a series of uncorrected DDTA-traces of the heating cycle of quickly quenched and slowly cooled polystyrene samples. The polystyrene had a weight average molecular weight of about 350,000. The initial cooling cycle was begun about 420°K. Case (*a*) and (*b*) of Figure 1 are clearly demonstrated by the maxima of the slowly cooled samples and the minima of the quickly quenched polymers.

2. Quantitative Analysis of Peaks for Constant Cooling Rates

For quantitative analysis the following general expression has been derived[8] for the apparent heat capacity at constant pressure C_p':

$$C_p' = \frac{\epsilon_h}{q\tau_h} e^{-\varphi(T)} \left[N_h^*(T_a) - N_a + \int_{N_h^*(T_a)}^{N_h^*(T)} e^{\varphi(T)}\, dN_h^*(T) \right] \tag{4}$$

where

$$\varphi(T) = \int_{T_a}^{T} \left(\frac{dT'}{q\tau_h} \right) \tag{5}$$

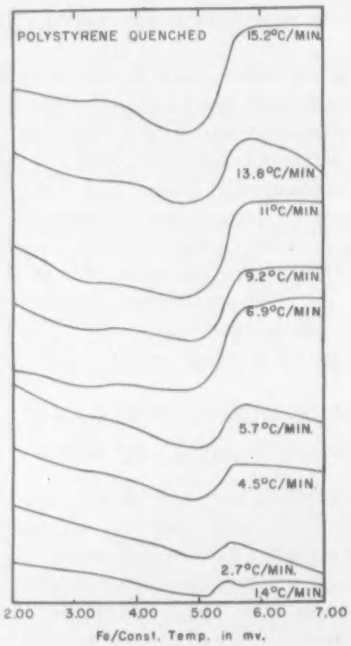

Fig. 4. DDTA traces for different heating cycles after quenching from above 420°K.

τ_h is the relaxation time for the disappearance of holes[5]

$$\tau_h = \left(\frac{h}{kT}\right)\left(\frac{Q^h}{Q\ddagger}\right)e^{\epsilon_f/RT} \tag{6}$$

q is the heating rate

$$q = \left|\frac{dT}{dt}\right| \tag{7}$$

The apparent heat capacity C_p' is the contribution to the heat capacity due to the change in hole concentration. Below the glass transition interval

$$C_p' = 0 \tag{8}$$

above the glass transition interval

$$C_p' = \left(\frac{\partial N_h^*}{\partial T}\right)\epsilon_h \tag{9}$$

while eq. 4 expresses the non-equilibrium apparent contribution determined by the cooling rate (through N_a) and the heating rate q.

Reevaluating the equilibrium C_p' due to holes (eq. 9) using recent tabulations[9] and measurements[10] gave an estimate of 4.7 cal./mole repeating

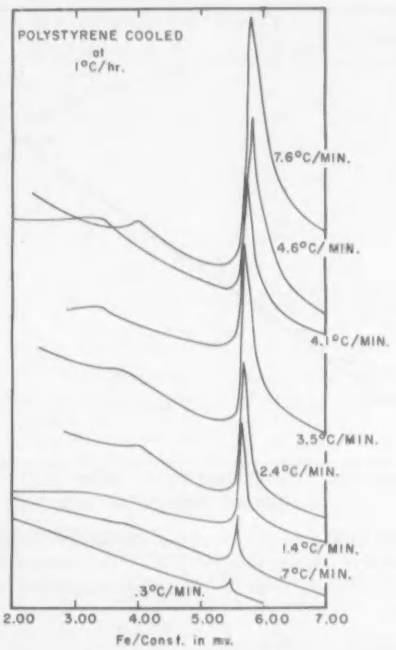

Fig. 5. DDTA traces for different heating cycles after slow cooling from above 420°K

units at 355°K. Employing the previously described methods,[6] ϵ_h has been evaluated to be 1600 cal./mole repeating units while the ratio of repeating unit volume to hole volume is 4.7. If the total hole volume is loosely equated to free volume, a free volume of 10% results at the glass transition region. This value of 10% is close to the estimate of Simha and Boyer[11] who extrapolate the liquid volume to 0°K. and call the excess volume above the liquid volume at 0°K. and free volume. Apparently, both free volume concepts are related.

With these data, an exact calculation of C_p' is possible using the above equations. These calculations were performed using an electronic computer. Figure 6 shows the peak temperatures as a function of heating rates thus calculated for the 1°C./hr. cooling. The resulting exact curve (broken line) is almost a straight line and represents the experimental points well.

Over the limited range of 4 decades, the position of the maximum can be approximated by an explicit expression for the temperature of the maximum of C_p' at the heating rate q:

$$\log q = A - \frac{B}{T_m} \tag{10}$$

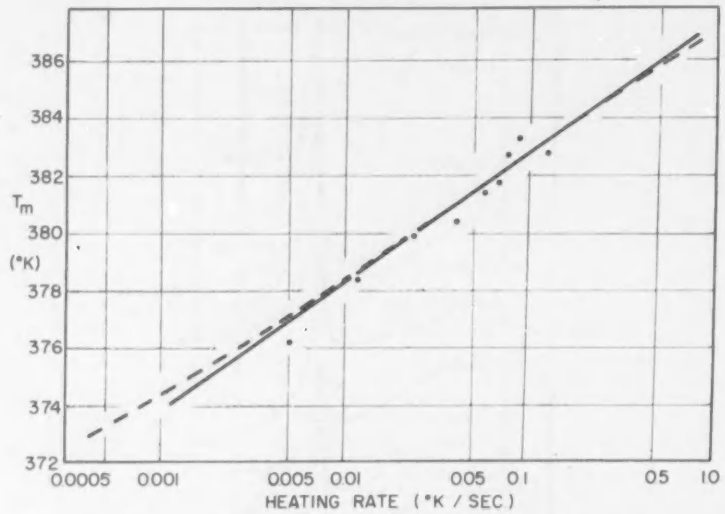

Fig. 6. Temperature of the maximum of C_p' versus the logarithm of the heating rate q for glasses of fictive temperature 365.5°K. (- - -) computer curve obtained by evaluating eq. 4. (——) eq. 13. Points are experimental values.

with A an approximate constant

$$A = \log\left(R\bar{T}_m^3 - \frac{\epsilon_h^2 \bar{N}_h^* \bar{T}_m}{C_p'}\right) - \log\frac{h.Q^h}{kQ^\ddagger}(\epsilon_j + R\bar{T}_m) \qquad (11)$$

and

$$B = 0.4343\,(\epsilon_j/R) \qquad (12)$$

All quantities to be evaluated at the respective maxima and averaged in the region of interest. Using the data derived above, taking as averages the values calculated at 381°K., the following expression is obtained:

$$\log q = 82.634 - (32014/T_m) \qquad (13)$$

The difference between q calculated using eq. 13 and q from the exact expression eq. 4 is 50% at rates of 10^{-4}°C./sec., goes to zero at the point of fit ($\sim 0.4 \times 10^{-2}$°C./sec.) and decreases to −6% for rates of 1°C./sec. This presents an easy procedure to evaluate ϵ_j from peak positions measured at different heating rates. Plotting log q versus $1/T_m$ gives a slope of $-(0.4343/R)\,(\epsilon_j)$.

3. *Quantitative Analysis of Cooling Cycle*

Following the freezing-in process by DDTA on cooling lead to Figure 7. The sensitivity of the DDTA allowed observation of the temperature of half-freezing for cooling rates from 0.08° C./sec. down to 0.002° C./sec.

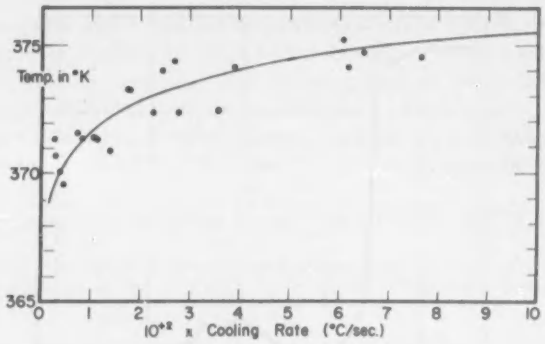

Fig. 7. Temperature of half-change in the temperature difference of DDTA traces during the cooling cycle. Corresponds to the "fictive temperature" of eq. 2. Drawn out curve: $\log q = 90.6852 - 3.4444 \cdot 10^4/T_g$.

The analytic form of Figure 7 suggests that the temperature of half-freezing, which is identical to Tool's fictive temperature (eq. 2) and should thus determine N_a, occurs at constant $q\tau_h$:

$$q\tau_h = \text{Const.} = \left(\frac{hq}{kT}\right)\left(\frac{Q^h}{Q^\ddagger}\right)e^{\epsilon_j/RT} \tag{14}$$

$$\log q = \log \text{Const.} + \log\left(\frac{kT}{h}\frac{Q^\ddagger}{Q^h}\right) - (\epsilon_j/RT)\log e \tag{15}$$

or

$$\log q = \text{Const.}' - 0.4343(\epsilon_j/RT) \tag{16}$$

Comparison with experiments assigns ϵ_j a value of 157.6 kcal./mole. Comparison of this activation energy with those obtained from the peak position of heating runs, which give different ϵ_j's for different cooling rates, shows agreement for cooling rates of 0.004°C./sec. (which corresponds to a freezing temperature of 370°K.).

A provisional conclusion from these results is that there exists a hole size distribution, characterized by different activation energies and relaxation time spectra. The half-freezing temperature would determine something like the activation energy of the mean hole.

TABLE I
Properties of a Mean Hole in Polystyrene

Size (v_h) = 21.9 cm.^{3}/mole of holes
Energy (ϵ_h) = 1600 cal./mole of holes
Activation energy (ϵ_j) = 157,600 cal./mole of holes
$\frac{hQ^h}{hQ^\ddagger} = 1.96 \times 10^{-87}$ sec. deg.
$q\tau_h$ = constant at freezing temperature = 6.6°

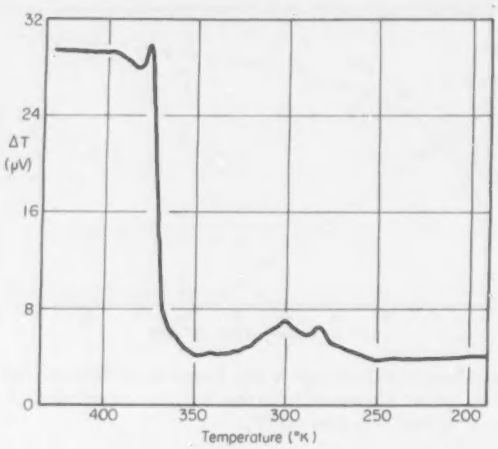

Fig. 8. Direct copy of a DDTA-trace of polystyrene through the temperature range of the primary and the secondary transition. A ΔT of 20 μv is approximately equal to 5 cal./deg. mole.

Assuming the mean hole can be characterized in this fashion, on cooling it would have the properties given in Table I.

The half-freezing temperature allows a comparison with glass transition temperatures, which are measured volumetrically. Fox and Loshaek[12] report 373°K. for the glass temperature of polystyrene of infinite chain length. This temperature corresponds, according to Figure 7, to a cooling rate of 0.02°C./sec. Since $q\tau_h$ at this temperature must be 6.6°, the relaxation time at 373°K. for the mean hole can be calculated to be 5.5 min., the order of magnitude suggested by Kauzmann.[13]

4. Measurements of Secondary Freezing-in Processes by DDTA

As has been known for a long time,[14,15] polystyrene shows secondary freezing-in processes below the glass transition temperature which have before only been observed by mechanical or related techniques.[16] Figure 8 shows a particularly good DDTA heating trace of the primary freezing-in process of holes (glass transition) and the secondary freezing-in process[16] (attributed to freezing-in of phenyl group librational motion).

Summary

Dynamic Differential Thermal Analysis (DDTA) (Fig. 4) has been described and used to study the glass transition region of polystyrene on cooling from above T_g and subsequent heating at reproducible linear rates.

Data on the temperature of half-freezing (Fig. 7) on cooling, and on the temperature of the maximum and minimum of C_p' on heating were collected.

Agreement with exact and approximate theoretical expressions for the peak temperature on heating could be achieved for constant slow cooling followed by variable heating. For different cooling rates different activation energies and entropies are needed.

From the half-freezing temperatures on cooling, which is taken to be a mean fictive temperature (eq. 2) properties of a mean hole, are calculated (Table I).

Secondary feeezing-in processes are also detectable by DDTA.

Financial help from the Advanced Research Projects Agency is gratefully acknowledged. Programming and operation of the computer were done by the Cornell Computing Center.

References

1. Tool, A. Q., and C. G. Eichlin, *J. Res. Natl. Bur. Std.*, **6**, 523 (1930).
2. Tool, A. Q., *J. Am. Ceramic Soc.*, **29**, 240 (1946).
3. Eyring, H., *J. Chem. Phys.*, **4**, 283 (1936).
4. Frenkel, J., *Kinetic Theory of Liquids*, Clarendon, Oxford, 1946.
5. Hirai, N., and H. Eyring, *J. Appl. Phys.*, **29**, 810 (1958); *J. Polymer Sci.*, **37**, 51 (1959).
6. Wunderlich, B., *J. Phys. Chem.*, **64**, 1052 (1960).
7. For general references see: W. J. Smothers, and Yao Chiang, *Differential Thermal Analysis, Theory and Practice*, Chemical Pub. Co., New York, 1958.
8. Wunderlich, B., D. M. Bodily, and M. H. Kaplan, *J. Appl. Phys.*, **35**, 95 (1964).
9. Warfield, R. W., and M. C. Petree, *J. Polymer Sci.*, **55**, 497 (1961).
10. Dainton, F. S., D. M. Evans, F. E. Hoare, and T. P. Melia, *Polymer*, **3**, 263 (1962).
11. Simha, R., and R. F. Boyer, *J. Chem. Phys.*, **37**, 1003 (1962).
12. Fox, T. G., and S. Loshaek, *J. Polymer Sci.*, **15**, 371 (1955).
13. Kauzmann, W., *Chem. Rev.*, **43**, 219 (1948).
14. Tammann, G., *Der Glaszustand*, Leopold Voss, Leipzig, 1933.
15. Tammann, G., and A. Pape, *Z. Anorg. Allgem. Chem.*, **200**, 113 (1931).
16. Wunderlich, B., M. Jaffe, and M. L. Stahl, *Kolloid-Z.*, **185**, 65 (1962); B. Wunderlich and D. Bodily, *J. Appl. Phys.*, **35**, 103 (1964).

Résumé

On décrit l'analyse thermique dynamique différentielle DDTA et on discute de son application à l'étude de l'intervalle de la transition vitreuse du polystyrène. Le mode opératoire comprend un refroidissement reproductible à partir de l'état fondu en passant par l'intervalle de transition vitreuse, suivi par un échauffement, les deux à des vitesses linéaires reproductibles de changement de température. On a réuni des données sur la température de demi-congélation, sur le refroidissement et sur la tempèrature du maximum et/ou du minimum de la capacité calorifique, et on les compare avec les expressions théoriques déduites de la théorie des lacunes des liquides. A partir de la température de demi-congélation, prise comme température fictive moyenne, on a calculé les propriétés d'une lacune moyenne pour le polystyréne (le volume molaire moyen de la lacune = 21.9 cm^3, l'énergie: 1600 cal., l'énergie activation: 157.600 cal., le temps de relaxation à la température fictive: 5.5 min.). On montre que le DDTA peut être appliqué pour déterminer le second processus de congélation du polystyréne, ce qui se passe de 230°K à 350°K, et on pense que cela implique le mouvement libre des noyaux phényles.

Zusammenfassung

Die dynamische Differentialthermoanalyse wird beschrieben und ihre Anwendung auf die Untersuchung des Glasumwandlungsintervalls von Polystyrol diskutiert. Die Arbeitsweise besteht in einer reproduzierbaren Abkühlung vom geschmolzenen Zustand durch das Glasumwandlungsintervall und darauffolgendem Erhitzen, beides mit reproduzierbarer linearer Geschwindigkeit der Temperaturänderung. Daten über die Halb-Gefrier-Temperatur beim Abkühlen und über die Maximums- und Minimumstemperatur in der Wärmekapazität wurden gesammelt und werden mit theoretischen Ausdrücken auf Grundlage der Löchertheorie der Flüssigkeiten verglichen. Aus der Halb-Gefrier-Temperatur, die als eine "mittlere fiktive Temperatur" angenommen wird, werden die Eigenschaften eines mittleren Loches in Polystyrol berechnet. (Mittleres Lochvolumen = 21.9 cm^3, Energie 1600 cal, Aktivierungsenergie 157.600 cal, Relaxationszeit bei der fiktiven Temperatur 5,5 min). DTA ist zur Bestimmung des zweiten Einfrierprozesses in Polystyrol anwendbar, der im Bereich von 230°K bis 350°K auftritt und, wie angenommen wird, der Librationsbewegung der Phenylringe entspricht.

JOURNAL OF POLYMER SCIENCE: PART C NO. 6, PP. 149–155

Specific Heat of Synthetic High Polymers. XI. The Glass Transition in Isotactic Polypropylene*

ISMAT ABU-ISA, V. A. CRAWFORD,† A. R. HALY,‡ and MALCOLM DOLE, *Department of Chemistry and Materials Research Center, Northwestern University, Evanston, Illinois*

Synopsis

The specific heat of various samples of isotactic polypropylene has been measured over the glass transition range from 230 to 310°K. A glass transition has been found, the magnitude of which is roughly proportional to the amorphous content of the sample. In highly crystalline samples the rise in c_p with temperature over the glass transition range is probably partly caused by an increase in the number of modes of vibration that become active in this temperature range. A new thermodynamic name, the encraty, has been given to the function c_p/T (equals $(dS/dT)_p$ or $-d^2G/dT^2$). The encraty is abnormally low for quenched isotactic polypropylene for reasons for which speculations only can be given at this time. Negative temperature drifts were observed below about 270°K.

I. Introduction

In a previous study[1] of the specific heat of atactic and isotactic polypropylene a pronounced glass transition occurring over the temperature range −30 to 0°C. was observed in atactic polypropylene, but no transition was detectable in the isotactic sample. Since this result was in apparent disagreement with later specific heat researches of Passaglia and Kevorkian[2] and of Dainton, Evans, Hoare, and Melia,[3] it seemed worthwhile to carry out a more complete calorimetric investigation of the glass transition range in isotactic polypropylene.

By means of volume-temperature and stiffness-temperature measurements Reding[4] found a glass transition in isotactic polypropylene at −18°C.

II. Experimental

The isotactic polypropylene sample, ESCON 114, used in this research was supplied by the Esso Research and Engineering Company through the kind offices of Dr. John Rehner, Jr. The properties of this material are summarized in Table I.

* The previous paper of this series is given in ref. 1.

† Materials Research Center Summer Research Participant 1963. Present address, Department of Chemistry, Rockford College, Rockford, Illinois.

‡ Visiting Research Scholar 1963. Present address, Wool Research Laboratories, C.S.I.R.O., Ryde, N.S.W., Australia.

TABLE I
Properties of Esso Polypropylene. Lot No. 1625, CD-2

Melt index	Heptane insoluble fraction	Stabilizer (phenolic-type)	Metal fatty acid salt
3.3 (230°C.)	0.947	<0.2%	<0.05%

Total ash (ex additives)	Density values, g., cm.$^{-3}$		
	As received	Quenched	Quenched, slightly annealed
0.01%	0.913	0.889	0.893

The quenched polypropylene was prepared by melting it in an atmosphere of helium in a glass cylinder held in an electric oven at about 260°C. and then forcing it under helium pressure through an orifice of 2.5 mm. diameter into liquid nitrogen. The polypropylene froze to a solid rod which was then wrapped in cloth while still cold and broken into small pieces so as to fit into the calorimeter. It was then allowed to warm up to room temperature and to remain at room temperature for about 48 hr. when it was loaded into the calorimeter. The density measurement of the quenched polymer given in Table I was made after 24 hr. at room temperature. The density measurement of the slightly annealed sample was made after the quenched material had been heated to 38°C. in the calorimeter. After loading the calorimeter with the quenched sample, it was then cooled slowly over a period of about 13 hr. and the specific heat measurements started.

The calorimetric techniques were the same as those previously described.[1]

III. Results

The data are illustrated in the form of the function c_p/T which thermodynamically is equal to the temperature coefficient of the entropy $(dS/dT)_p$ or to the negative of the second derivative of the free energy with respect to the temperature, $-(d^2G/dT^2)_p$. This important function has no name and we propose to call it the encraty after the Greek word crasis, mixture, and to give it the symbol L. In Figure 1*a*, open circles, the encraty is given for the isotactic polypropylene of initial density 0.913. Our previous values[1] for atactic polypropylene, solid circles, are also shown in Figure 1*a* as well as similar values for isotactic polypropylene, crosses. The old values for the isotactic encraty are seen to agree fairly well with the new, probably as well as could be expected in view of the difference in the sample density. Also given in Figures 1*b* and *c* are encraty values obtained by Dainton[3] and co-workers and by Passaglia and Kevorkian.[2] These encraty values were calculated from the actual specific heat data and not from smoothed values.

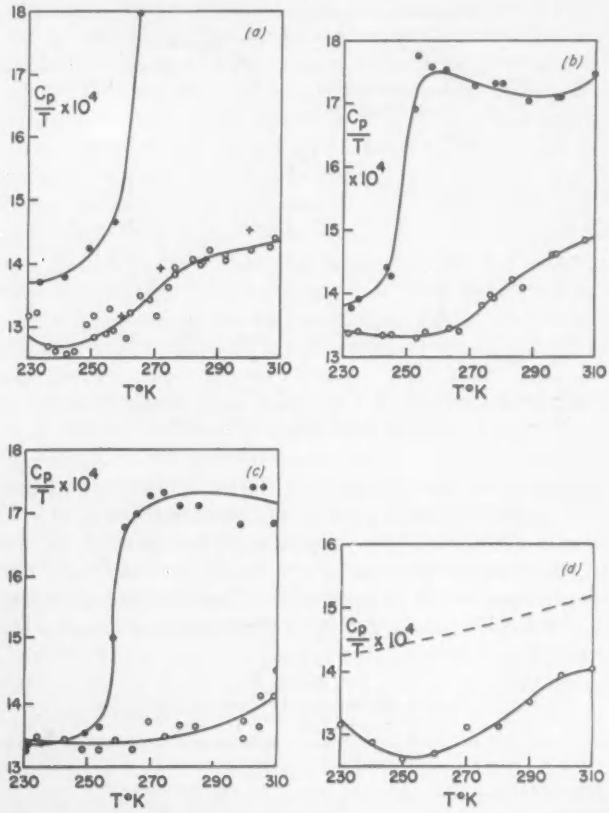

Fig. 1. (*a*) Encraty values obtained in this work for: (○) isotactic polypropylene; previous data from Wilkinson and Dole[1] are also shown, (●) atactic polypropylene; (×) isotactic; (*b*) encraty values obtained by Dainton and co-workers;[3] (*c*) encraty values obtained by Passaglia and Kevorkian;[2] (*d*) encraty values for 100% crystalline polyethylene, calculated from specific heats estimated by Wunderlich.[7] The dotted line illustrates actual data for Marlex-50 polyethylene obtained by Dainton[3] et al. All encraty data are in units of cal. deg.$^{-2}$ g.$^{-1}$ × 10^4.

In Figure 2 the encraty data for the quenched isotactic polypropylene are given, open circles, and for the quenched material on its second heating, solid circles. It will be noted that the encraty values of the quenched material are very low at the low temperatures, around 11.0 × 10^{-4} cal. deg.$^{-2}$ g.$^{-1}$ as compared to a more normal value of 13 × 10^{-4}. We believe that these abnormally low values are correct experimentally, because we also observed them in studying the specific heat of a 5n–50 mixture of atactic and isotactic polypropylene.

The data illustrated in Figures 1*a* and *b* demonstrate the existence of a glass transition in isotactic polypropylene, but necessarily of a smaller

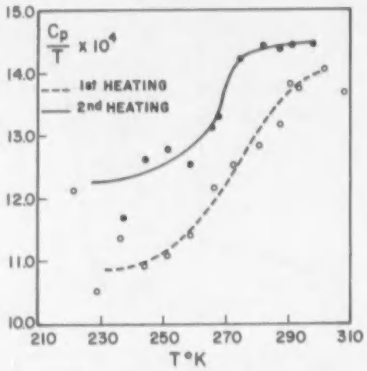

Fig. 2. Encraty values for quenched isotactic polypropylene. All encraty data are in units of cal. deg.$^{-2}$ g.$^{-1}$ $\times$ 10^4.

order of magnitude than the glass transition in atactic polypropylene because of the partial crystalline nature of the isotactic samples. The maximum increase in the encraty over the temperature range of the glass transition, ΔL, the roughly estimated T_g values defined as the temperature at which the increase in the encraty during the glass transition has reached half of its total value and the density of the samples are given in Table II.

TABLE II
Values for the Increase in Encraty During the Glass to Liquid Transition

Polypropylene sample	T_g, °C.	ΔL, cal. g.$^{-1}$ deg.$^{-2}$ $\times$ 10^4	ρ_l, g. cm.$^{-3}$
Atactic			
Dainton et al.[3]	−25	3.8	
Dole et al.[3]	−11	4.5	0.868
Passaglia et al.[2]	−15	3.8	
Wunderlich's rule		4.8 ± 0.8	
Isotactic			
As received	−1	1.2	0.913
Quenched			
1st heating	0	3.1	.889
2nd heating	−5	1.9	.893

IV. Discussion

First of all, we discuss the question of the existence of a glass transition in the amorphous regions of the isotactic sample. We had previously[1] found no glass transition, but by reference to Figure 1*a* this can be seen to have been due to not working over a large enough temperature range and to the

high crystallinity of the material. Our new data coupled with those of Dainton et al.[3] definitely show a rise in the encraty over the temperature range 250–290°K. and an increase in ΔL with decrease in crystallinity of the samples (Table II). However, even in completely crystalline polymers the encraty function will go through a minimum at about this temperature because of the increase in the number of modes of vibration that come into play as the temperature is raised, as has already been discussed by Dole and Wunderlich.[6] In fact if one plots the encraty of completely crystalline polyethylene using for this calculation the specific heat data estimated by Wunderlich[7] for 100% crystalline polyethylene, a rise in the encraty with temperature occurs, Figure 1*d* a rise which is remarkably similar to that shown by the most crystalline polypropylene, Figure 1*a*. Inasmuch as there can be no glass transition in a completely crystalline polymer, one might conclude that there was none in isotactic polypropylene. However, we reject this conclusion for the following two reasons: First, the increase in encraty is greater, the less crystalline the sample (Table II). Second, the measurements of the thermal conductance of isotactic polypropylene carried out by Eiermann[8] indicate that the thermal conductance passes through a very broad maximum at 0 to 50°C. Eiermann and Hellwege[9] had previously shown a correlation between T_g and the maximum in the thermal conductance-temperature curve. Crystalline polyethylene shows no such maximum, but a continual decrease in the thermal conductance with rise of temperature from −150 to 75°C. (A maximum will exist, but below −150°.) Thus, from the standpoint of thermal conductance, isotactic polypropylene is more like amorphous atactic polypropylene than it is like crystalline polyethylene. In Figure 1*d* we also have plotted encraty values calculated from the low temperature specific heat data of Dainton et al.[3] No sharp rise in the encraty can be seen; hence, there is some question concerning the validity of using Wunderlich's extrapolated values for the comparison of encraty in this temperature range.

The existence of a glass transition in amorphous isotactic polypropylene is more clearly demonstrated in Figure 2 where we have plotted the encraty values for the quenched polypropylene sample. A considerable rise in the encraty occurs over the temperature interval 250–280°K., and this rise is greater the lower the density of the sample as would be expected. In fact a plot of ΔL versus the specific volume yields roughly a linear plot extrapolating at 100% amorphous content to approximately the value adopted by Wunderlich[5] as the average value for many substances.

Although we conclude that a glass transition in amorphous isotactic polypropylene does exist, it is very difficult to estimate how much of the rise in the encraty at T_g is due to the glass to liquid transition and how much to the normal increase in the number of vibration modes coming into play over the glass transition temperature range.

Dainton and co-workers[3] discovered slow temperature drifts with time in their atactic samples as a function of pretreatment and temperature. In general they found downward drifts up to about 240°K. and then positive

drifts above this temperature. However, if they cooled their atactic polypropylene rapidly to only 273°K., then a downward drift was observed from 273 to 303°K. They suggest that the downward drifts may be the result of a time delay in the transmission of heat through the polymer granules during the heating period. It is doubtful that this is the explanation because there is only about a 50% greater thermal conductance in isotactic polypropylene than in the atactic. No pronounced temperature drifts were observed by Dainton et al.[3] in their studies of isotactic polypropylene. A calculation of the difference in temperature as a function of time in cylindrical polymer rods when the surface is suddenly heated by an amount ΔT shows that for a rod of unit radius, the difference between surface and actual temperatures has decreased to within 1% of zero in ten minutes. For a rod of 0.1 cm. radius, the time for 99% decrease in ΔT is reduced to 0.1 min.

We observed pronounced downward temperature drifts in the quenched isotactic sample which had been cooled over a 13 hr. period to 222°K. These drifts became very much smaller in magnitude about 255°K. and were slightly positive above 300°K. During the second series of specific heat measurements after the material had been again cooled to −235°K. (but at an initially slower rate) the negative drifts were about one-seventh as large as during the first series of measurements. Unless the quenched polypropylene has a considerably reduced thermal conductance as compared to the initial material, we believe that the temperature drifts are real and represent very slow transformations occurring in the polymer. It might be noted that in our work the temperature of the calorimeter was usually followed for an hour or more after the heating period in contrast to the seven minutes employed by Dainton and co-workers.[3]

A negative temperature drift requires that the process producing it, if real, must have a positive entropy increment. Positive entropy effects could be produced by a slow incorporation of holes into the amorphous regions of the solid, or by a slow reorganization of polymer into a more random configuration of the chains. Inasmuch as the heat effect is endothermic, the process would have to have a positive enthalpy increment. Actually, the heat effects are very minute; the largest negative temperature drift observed, amounting to about 0.008°C. min.$^{-1}$, corresponds to only 0.0024 cal. g.$^{-1}$ min.$^{-1}$

Finally, we wish to comment on the unexpectedly low encraty values exhibited by the quenched isotactic polypropylene at low temperatures. If any crystallization had occurred during a specific heat measurement, then the calculated specific heat would have been abnormally low; but this seems unlikely to have happened in the present case inasmuch as the post-heating period drifts were negative. A slow crystallization would have produced positive drifts. Incorporation of holes during the heating period, like melting, would have increased the measured specific heat. A low value of c_p and the encraty, if real, must be the result of restriction of chain oscillations or motions due to the rapid quenching.

This research was supported by the Advanced Research Projects Agency of the United States Department of Defense through the Northwestern University Materials Research Center. The gift of the isotactic polypropylene from the Esso Research and Engineering Company is gratefully acknowledged.

References

1. Wilkinson, R. W., and M. Dole, *J. Polymer Sci.*, **58**, 1089 (1962).
2. Passaglia, E., and H. K. Kevorkian, *J. Appl. Phys.*, **34**, 90 (1963).
3. Dainton, F. S., D. M. Evans, F. E. Hoare, and T. P. Melia, *Polymer*, **3**, 286 (1962).
4. Reding, F. P., *J. Polymer Sci.*, **21**, 547 (1956).
5. Wunderlich, B., *J. Phys. Chem.*, **64**, 1052 (1960).
6. Dole, M., and B. Wunderlich, *Makromol. Chem.*, **34**, 29 (1959).
7. Wunderlich, B., *J. Chem. Phys.*, **37**, 1203 (1962).
8. Eiermann, K., Paper presented before the Polymer Division, 144th Meeting of the Am. Chem. Soc., New York, September 1963.
9. Eiermann, K., and K. H. Hellwege, *J. Polymer Sci.*, **57**, 99 (1962).

Résumé

On a measuré la chaleur spécifique de différents échantillons de polypropylènes-isotactiques dans le domaine de la température de transition vitreuse de 230 à 310°K. On trouve une température de transition vitreuse dont la grandeur est approximativement proportionnelle à la teneur en quantité amorphe de l'échantillon. Dans les échantillons hautement cristallins, l'augmentation de c_p avec la température dans le domaine de transition vitreuse est sans doute partiellement causée par une augmentation du nombre de vibrations qui deviennent actives dans ce domaine de température. On donne une nouvelle dénomination thermodynamique, l'encratie, à la fonction c_p/T égale (dS/dt ou d^2G/dT^2). L'encratie est anormalement basse pour des polypropylènes refroidis; seules des spéculations peuvent expliquer actuellement ce phènomène. On observe des changements négatifs avec la température en-dessous de 270°K.

Zusammenfassung

Die spezifische Wärme verschiedener isotaktischer Polypropylenproben wurde im Glasumwandlungsbereich von 230 bis 310°K gemessen. Es wurde eine Glasumwandlung gefunden, deren Grösse ungefähr dem Gehalt der Probe an amorpher Substanz proportional ist. Bei hochgradig kristallinen Proben ist der Anstieg von c_p mit der Temperatur im Glasumwandlungsbereich wahrscheinlich zum Teil durch eine Zunahme der Zahl der Schwingungsfreiheitsgrade, die in diesem Temperaturbereich aktiv werden, bedingt. Eine neue thermodynamische Bezeichnung, nämlich Enkratie, wurde für die Funktion c_p/T (identisch mit $(dS/dT)_p$ oder $-d^2G/dT^2$) gewählt. Die Enkratie ist für abgeschrecktes isotaktisches Polypropylen abnorm niedrig; über Gründe für dieses Verhalten können derzeit nur Vermutungen angestellt werden. Unterhalb etwa 270°K wurde eine negative Temperaturabhängigkeit beobachtet.

JOURNAL OF POLYMER SCIENCE: PART C NO. 6, PP. 157–165

Thermal Conductivity of High Polymers

K. EIERMANN, *Deutsches Kunststoff-Institut, Darmstadt, Germany*

Synopsis

The thermal conductivity of several high polymers was measured in the temperature range from −190 to 90°C. with an automatic apparatus. In amorphous polymers a break has been found in the thermal conductivity at the glass transition temperature. This break can be explained by a model conception, which coordinates an elementary thermal resistance to every bond and which is also able to interpret the anisotropy of the thermal conductivity of stretched amorphous polymers. Even a rather universal relation between the anisotropies of the thermal expansion and the thermal conductivity can be derived. In partially crystalline polymers the thermal conductivity of the amorphous and the crystalline phases can be calculated from values measured with specimens of different crystallinities. The thermal conductivity of the crystalline phase of polyethylene shows the T^{-1}-law, valid for low molecular crystals. In other polymers we find a different behavior: the thermal conductivity of the crystalline phase is similar to that of the amorphous phase; we find that it can be described and calculated by means of the model derived from amorphous polymers. This model permits also to interpret the course of thermal conductivity at first-order transition points.

The thermal conductivity of several high polymers was measured in the temperature range from −190 to 90°C. with an automatic apparatus.[1] Relations between thermal conductivity, structure, and temperature of high polymers could be derived from the results of measurement. Finally, these relations could be interpreted by means of model conceptions. Characteristic differences exist between thermal conductivity of amorphous and partially crystalline polymers.

In amorphous polymers a break[2,3] occurs in the thermal conductivity at the glass-transition temperature (e.g., Fig. 1). This break was observed in all amorphous polymers tested: natural rubber,[2] Vulkollan (a polyurethane),[2] polyisobutylene,[2] atactic polypropylene,[4] polyvinyl chloride with different plasticizer contents,[2] and polychlorotrifluoroethylene.[5] Shoulberg and Shetter[6] recently also found the break in polymethyl methacrylate. Therefore, such a break probably exists in all amorphous polymers that show glass transitions.

To explain this break, we constructed the following model conception,[5] which is generally valid for all amorphous substances. It can be shown that in an amorphous substance each bond between adjacent atoms is equivalent to a thermal resistance, called elementary thermal resistance R_{We}. The thermal resistance of a macroscopic amorphous specimen consists of a network of elementary thermal resistances with the atoms as the

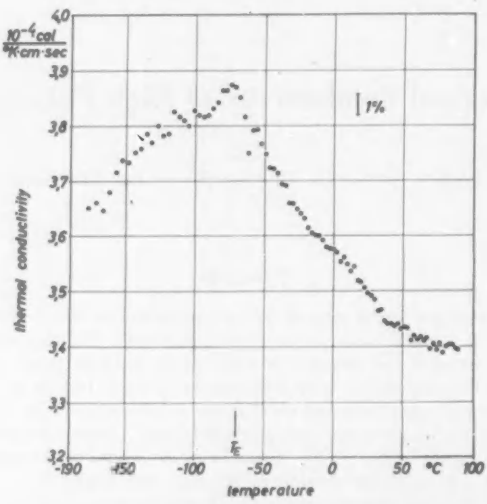

Fig. 1. Thermal conductivity of natural rubber.

points of junction. The elementary thermal resistance is dependent on the bond force. It decreases with increasing spring constant C_B of the bond. Therefore a primary valence, for instance, is equivalent to a small thermal resistance; a van der Waals bond, to a large one. There is:

$$R_{We} = \frac{1}{\text{const} \times k_A} \sqrt{\frac{m_A}{C_B}} \tag{1}$$

m_A is the arithmetical mean of the masses of the two atoms joined by the bond; k_A is the (formal) heat capacity per atom and the const. is approximately unity.

Amorphous high polymers expand more above glass-transition temperature than below; therefore, in the volume-temperature curve a break exists at the glass-transition temperature. The spring constant of the bonds is dependent on the space between the atoms. Therefore the break in the volume-temperature curve is transmitted to the spring constant and to the curve of thermal conductivity.

It has been shown[5] that the thermal conductivity of the amorphous high polymers is mainly determined by the behavior of the van der Waals bonds. From the force equation for the van der Waals bond the following relation between the break in the thermal conductivity and in the volume temperature curve can be derived:

$$\Delta\left[\left(\frac{1}{\lambda}\right)\left(\frac{d\lambda}{dT}\right)\right] = -5.8\Delta\alpha \tag{2}$$

TABLE I

Substance	$\Delta\left(\frac{1}{\lambda}\right)\left(\frac{d\lambda}{dT}\right)$ Measured, % °C.$^{-1}$	$\Delta\left(\frac{1}{\lambda}\right)\left(\frac{d\lambda}{dT}\right)$ Calculated, % °C.$^{-1}$
Natural rubber	−1.6	
Vulkollan	−1.6	
Polyisobutylene	−1.5	
Atactic polypropylene	−1.7	
PVC with 40% plasticizer	−1.7	−1.74
PVC " 20% "	−1.2	
PVC " 10% "	−1.3	
Polychlorotrifluoroethylene	−1.3	

$\Delta((1/\lambda)(d\lambda/dT))$ is the increment of the relative temperature coefficient of the thermal conductivity and $\Delta\alpha$ is the increment of the coefficient of cubic thermal expansion at the second-order transition temperature. This relation is independent of the substance and of the temperature. It agrees satisfactorily with the experiment, as shown in Table I (the calculated value is valid for all polymers in the Table).

When amorphous polymers are stretched, there is an increase of thermal conductivity in the direction of stretch and a decrease perpendicular to it.[2,7]

This effect can be explained thus. In the stretched polymer the chain molecules are orientated in the direction of stretch, so that in the network of bonds the primary valences with small thermal resistance are chiefly arranged in the direction of stretch and the van der Waals bonds with large thermal resistance are chiefly perpendicular to it.

From the model, the following equation can be derived:[5]

$$\frac{1}{\lambda_{\parallel}} + \frac{2}{\lambda_{\perp}} = \frac{3}{\lambda_{iso}} \tag{3}$$

$\lambda_{\parallel}$ = thermal conductivity in the direction of stretch; $\lambda_{\perp}$ = thermal conductivity perpendicular to it; and λ_{iso} = thermal conductivity of the unstretched specimen. This equation was tested by thermal conductivity measurements of polymethylmethacrylate over a wide temperature range[2,5] and of several amorphous polymers at room temperature;[7] the deviations were always smaller than 2%. From this model of the stretched network we could, in addition, calculate the following universal relation between the anisotropy of the thermal conductivity and the anisotropy of the linear thermal expansion of stretched amorphous high polymers:[5]

$$\frac{\lambda_{iso}}{\lambda_{\parallel}} = 0.8\left(\frac{\beta_{\parallel}}{\beta_{iso}}\right) + 0.2 \tag{4}$$

$$\frac{\lambda_{iso}}{\lambda_{\perp}} = 0.8\left(\frac{\beta_{\perp}}{\beta_{iso}}\right) + 0.2 \tag{5}$$

$\beta_{\parallel}$ = coefficient of linear expansion in the direction of stretch; $\beta_{\perp}$ = coefficient of linear expansion perpendicular to it; and β_{iso} = coefficient of linear expansion of the unstretched specimen. With these equations we

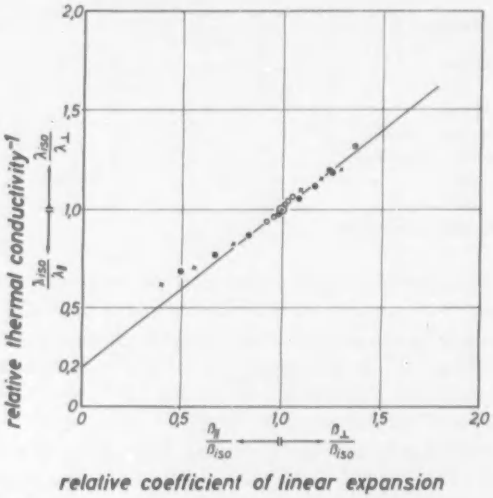

Fig. 2. Correlation between anisotropy of thermal conductivity and linear thermal expansion at stretched amorphous polymers; measured data by Hellwege et al.[7]: (●) polymethyl methacrylate; (×) polyvinyl chloride; (○) polystyrene; (◑) polycarbonate.

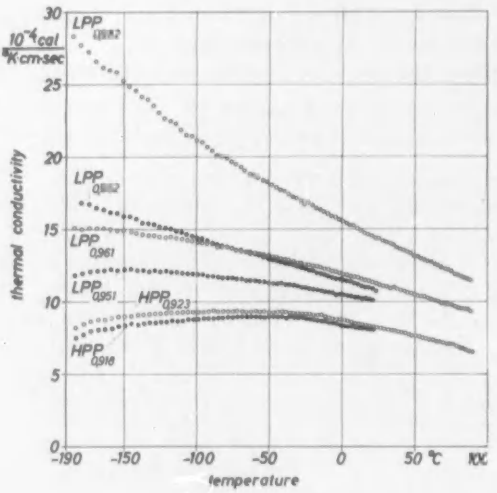

Fig. 3. Thermal conductivity of polyethylene LPP = low pressure polyethylene; HPP = high pressure polyethylene. The numbers signify the density of the specimen in g./cm.^{3}.

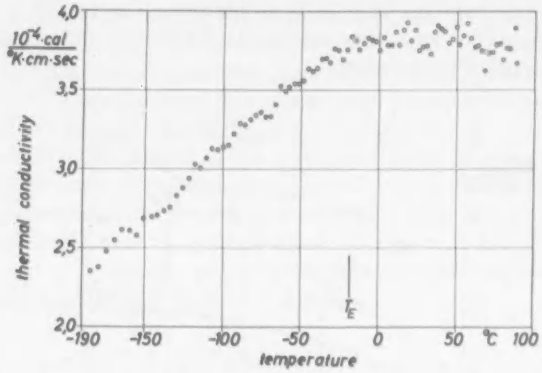

Fig. 4. Thermal conductivity of the amorphous phase of polyethylene.

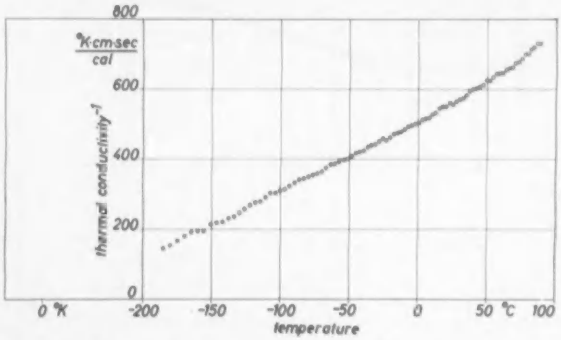

Fig. 5. Reciprocal thermal conductivity of the crystalline phase of polyethylene.

could predict the course of curve in Figure 2, the relation between the anisotropy of thermal expansion and thermal conductivity, measured by Hellwege et al.[7]

The behavior of the thermal conductivity of partially crystalline polymers is not uniform. Two classes can be distinguished. One class, to which belong polyethylene and polyoxymethylene, shows a decrease of thermal conductivity with increasing temperature. The thermal conductivity of the other class increases with increasing temperature: polyethylene terephthalate, isotactic polypropylene, polychlorotrifluoroethylene, and polytetrafluoroethylene.

The thermal conductivity of several polyethylene specimens with different densities is plotted in Figure 3. It increases with increasing density and therefore increasing degree of crystallinity. Moreover the shape of the curves changes. This behavior can be explained by means of the two-phase model, if the amorphous and the crystalline regions have a different thermal conductivity and these conductivities are additive in the

partially crystalline specimen as in a mixture. Conversely the thermal conductivity of the two components can be determined from measurements of partially crystalline samples.

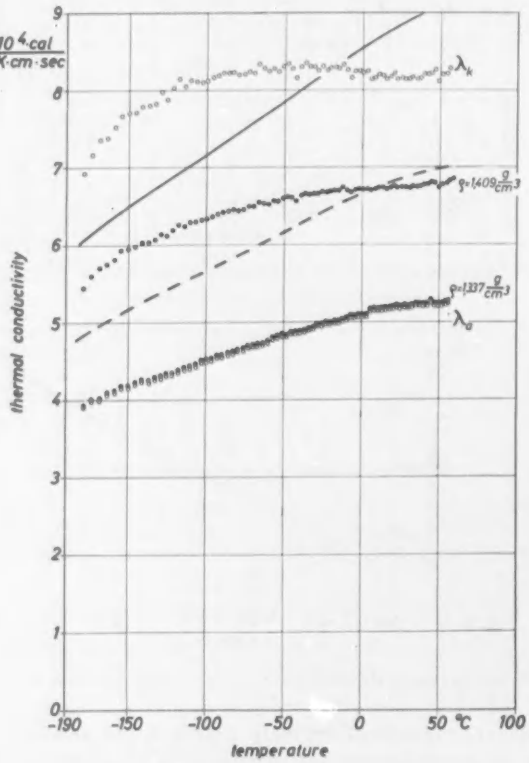

Fig. 6. Thermal conductivity of polyethylene terephthalate.

The Maxwell equation[8,9] for the conductivity of mixtures was used. For our problem it takes the form:[4,5]

$$\lambda = \frac{2\lambda_a + \lambda_k + 2\gamma(\lambda_k - \lambda_a)}{2\lambda_a + \lambda_k - \gamma\,(\lambda_k - \lambda_a)}\,\lambda_a \tag{6}$$

λ = thermal conductivity of the partially crystalline specimen; λ_k = thermal conductivity of the crystalline phase; λ_a = thermal conductivity of the amorphous phase; and γ = degree of volume crystallinity.

From the curves measured with two partially crystalline specimens, of which the degrees of crystallinity is known, the thermal conductivity of the

two phases can be calculated by means of eq. (6). For the amorphous phase the curve in Figure 4 was obtained. At −20°C. we find a break, as expected, because a break in the volume-temperature curve of polyethylene is observed at −20°C.,[10] and this break must cause, as shown above, a break in the thermal conductivity.

The thermal conductivity of the crystalline phase of polyethylene decreases sharply with increasing temperature. Figure 5 shows the reciprocal thermal conductivity plotted against temperature; we get a straight line approximately passing through the absolute zero. The thermal conductivity of the crystalline polyethylene is thus following the T^{-1}-law, found by Eucken[11] for low molecular crystals.

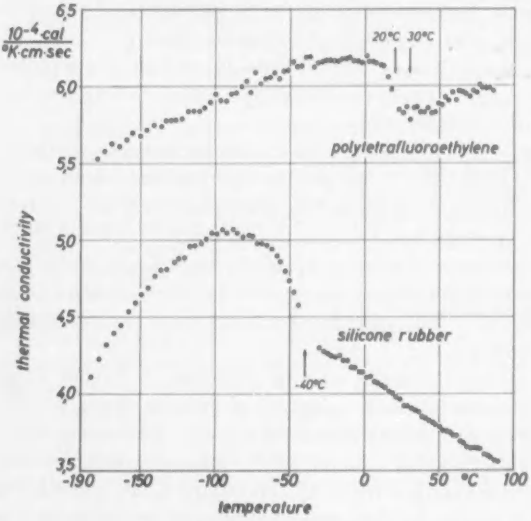

Fig. 7. Thermal conductivity of silicone rubber and polytetrafluoro ethylene.

To illustrate the second class of partially crystalline polymers, the thermal conductivity of two polyethylene terephthalate specimens of different density and degree of crystallinity is plotted in Figure 6. The measured values are plotted in the shape of filled circles. The specimen with the lower density was almost completely amorphous; the other specimen was about 50% crystalline. From the measured values the thermal conductivity in the amorphous (λ_a, open circles) and in the crystalline (λ_k, open circles) phase was calculated in the manner described above.

Contrary to that of polyethylene, the thermal conductivity of the crystalline phase of polyethylene terephthalate increases with increasing temperature, like that of the amorphous phase below the glass-transition temperature.

In an earlier work[5] we found that the heat conduction in the crystalline phase of polyethylene terephthalate (and of all the other substances of the second class) can be described by the network of elementary thermal resistances that is valid for amorphous substances. The higher thermal conductivity of the crystalline phase was found to be caused by the higher density and therefore higher spring constant of the bonds. The relation can be described by the following equation:

$$d\lambda/\lambda = 5.8\ (d\rho/\rho) \tag{7}$$

($d\lambda/\lambda$ = relative change of thermal conductivity and $(d\rho/\rho)$ = relative change of density. By means of this equation we calculated the thermal conductivity of the crystalline phase of polyethylene terephthalate from the thermal conductivity of the amorphous phase (curve λ_a) and the density of two phases. The calculated thermal conductivity is plotted in Figure 6 as a drawn line. The curve agrees approximately with the curve λ_k (open circles).

Surprisingly, eq. (7) is also valid[5] for a heterogeneous partially crystalline specimen, namely, the difference of the thermal conductivities of two partially crystalline samples can be calculated from the difference of densities without knowing any value of the amorphous or crystalline phase. In this way the thermal conductivity of the partially crystalline specimen in Figure 6 was calculated from the curve of the amorphous substance (dashed curve in Fig. 6). The calculated curve agrees approximately with the measured values.

Equation (7) also permits an interpretation of thermal conductivity at first-order transition points. Figure 7 shows the thermal conductivity of silicone rubber and polytetrafluoroethylene. The sharp decrease of the thermal conductivity of silicone rubber below −40°C. is caused by the melting of the crystalline regions. The shape of the curve in this temperature range is similar to the curve of degree of crystallinity,[12] as would be expected from eq. (7). Polytetrafluoroethylene shows two transitions (at 20°C. and at 30°C.) in the crystalline phase.[13] A break was found[1,2] in the thermal conductivity. The breaks in the density-temperature curve at the transition points cause the break in the thermal conductivity according to eq. (7). The relative change of the density of our sample is (in connection with values of Kirby[14]) about 0.72% at the transition point of 20°C.; it is about five times smaller at the transition point of 30°C. According to eq. (7) the break in the thermal conductivity at 20°C. should be 4.2%; in satisfactory agreement with the experimental value of 5% (see Fig. 7). The break in the thermal conductivity at 30°C. is, by eq. (7), smaller than 1%, and can therefore not be observed because of the experimental error.

I wish to thank Professor Dr. K.-H. Hellwege and Dr. W. Knappe for support and helpful discussions.

References

1. Eiermann, K., K.-H. Hellwege, and W. Knappe, *Kolloid-Z.*, **174**, 134 (1961).
2. Eiermann, K., *Kunststoffe-Plastics*, **51**, 512 (1961).
3. Eiermann, K., and K.-H. Hellwege, *J. Polymer Sci.*, **57**, 99 (1962).
4. Eiermann, K., *Kolloid-Z.*, **180**, 163 (1962).
5. Eiermann, K., Dissertation, Darmstadt (February 1963); *Kolloid-Z.*, to be published.
6. Shoulberg, R. H., and J. A. Shetter, *J. Appl. Polymer Sci.*, **6**, S32 (1962).
7. Hellwege, K.-H., J. Hennig, and W. Knappe, *Kolloid-Z.*, **188**, 121 (1963).
8. Maxwell, J. C., *Treatise on Electricity and Magnetism*, Vol. 1, Oxford, New York, 1873, p. 365.
9. Eucken, A., Forsch. *Gebiete Ingenieunw.*, VDJ-*Forschungsh.*, **353**, 3 (1932).
10. Tanaka, K., *Bull. Chem. Soc. Japan*, **33**, 1060 (1960).
11. Eucken, A., *Ann. Physik*, **34**, 185 (1911).
12. Ohlberg, S. M., L. E. Alexander, and E. L. Warrick, *J. Polymer Sci.*, **27**, 1 (1958).
13. Kilian, H. G., Dissertation, Aachen (1958).
14. Kirby, R. K., *J. Res. Natl. Bur. Std.*, **57**, 91 (1956).

Résumé

La conductivité thermique de plusieurs hauts polymères a été mesurée avec un appareil automatique dans la région de température de −190°C à +90°C. La conductivitè thermique des polymères amorphes présente une discontinuité à la température de transition vitreuse. Cette discontinuité peut être expliquèe par une conception modèle qui coordonne une résistance thermique "élémentaire" à chaque liaison et qui est également capable d'interprèter l'anisotropie de la conductivitè thermique des polymères amorphes étirés. Même une relation générale entre les anisotropies de l'expansion thermique et la conductivitè thermique peut être dèrivèe. Dans les polymères partiellement cristallins la conductivité thermique des phases amorphes et cristallines peut être calculèe d'après les valeurs mesurées avec des échantillons de cristallinités différentes. La conductivité thermique de la phase cristalline du polyéthylène suit la loi T^{-1} valable pour les cristaux de faible poids moléculaire. Dans d'autres polymères on trouve des résultats différents: la conductivité thermique de la phase cristalline est sembalble à celle de la phase amorphe; nous trouvons qu'elle peut être décrite et calculée au moyen du modèle dèrivè des polymères amorphes. Ce modèle permet ègalement d'interprèter l'volution de la conductivitè thermique aux points de transition de premier ordre.

Zusammenfassung

Die Wärmeleitfähigkeit einiger Hochpolymerer wurde mit einer automatischen Apparatur im Temperaturbereich von −190°C bis +90°C gemessen. Bei amorphen Polymeren trat bei der Glasumwandlungstemperatur ein Knick in der Wärmeleitfähigkeit auf. Dieser Knick kann durch ein Modell erklärt werden, das für jede Bindung einen "elementaren" Wärmewiderstand annimmt und auch eine Interpretation der Anisotropie der Wärmeleitfähigkeit gedehnter amorpher Polymerer liefert. Ausserdem kann eine universelle Beziehung zwischen der Anisotropie der Wärmeausdehnung und derjenigen der Wärmeleitfähigkeit abgeleitet werden. Bei partiell kristallinem Polymeren kann die Wärmeleitfähigkeit der amorphen und der kristallinen Phase aus den an Proben mit verschiedener Kristallinität gemessenen Werten berechnet werden. Die Wärmeleitfähigkeit der kristallinen Phase von Polyäthylen gehorcht dem für niedermolekulare Kristalle gültigen T^{-1}-Gesetz. Bei anderen Polymeren zeigt sich ein andersartiges Verhalten: die Wärmeleitfähigkeit der kristallinen Phase ist derjenigen der amorphen Phase ähnlich; sie kann mittels des an amorphen Polymeren abgeleiteten Modells beschrieben und berechnet werden. Dieses Modell gestattet auch eine Interpretation des Verlaufes der Wärmeleitfähigkeit an Umwandlungspunkten erster Ordnung.

JOURNAL OF POLYMER SCIENCE: PART C NO. 6, PP. 167–174

Anisotropy of Thermal Conductivity in Stretched Amorphous Linear Polymers and in Strained Elastomers

J. HENNIG and W. KNAPPE, *Deutsches Kunststoff-Institut, Darmstadt, Germany*

Synopsis

Linear amorphous high polymers may be made anisotropic by drawing them at temperatures above the glass-transition temperature and thereafter cooling down in the stretched state. With measurements on polystyrene, polymethylmethacrylate, polyvinylchloride, and polycarbonate it can be shown that thermal conductivity in the direction of stretch is greater and perpendicular to this direction lower than in the unstretched isotropic state. The degree of anisotropy depends on the degree of stretch and on the molecular structure of the polymeric chain. By measuring the anisotropy of thermal expansion it can be demonstrated that thermal expansivity in the direction of stretch will become lower and perpendicular to this direction greater than in the isotropic polymer. There exists a close relation between the anisotropy of thermal conductivity and thermal expansivity. From measurements on polyvinylchloride it follows that anisotropy of thermal conductivity remains rather unchanged when heating the polymer to temperatures above the glass-transition range in the stretched state. Therefore it may be expected that also strained elastomers will have anisotropy in thermal conductivity. Measurements on several strained elastomers in the direction perpendicular to strain had been done which show that strained elastomers with strong polar side-groups have a considerable amount of anisotropy, while aliphatic polymers like natural rubber and polyisobutylene have no remarkable effects.

Amorphous linear high polymers can be brought into an anisotropic state by straining them at temperatures above the glass-transition temperature ϑ_g. After being cooled below the glass-transition temperature, the polymer, when unloaded, will remain in the stretched state. Analogous to elastic strain ϵ, the degree of stretch is defined by

$$\eta = (l - l_0)/l_0 \tag{1}$$

where l is the length of the stretched sample and l_0 the length before stretching. η may be controlled by heating the sample and allowing it to contract. In the case of polymers of medium and high molecular weight, l will mostly return to l_0. In some cases amorphous linear polymers may be stretched at temperatures below the glass-transition temperature (cold-drawing, cold-stretching), and η or l_0 may also be controlled by contraction after heating.

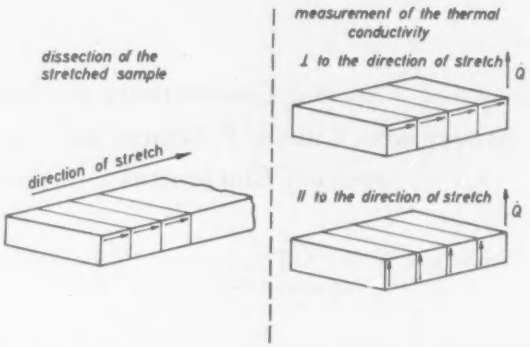

Fig. 1. Measurement of the thermal conductivity of stretched samples.

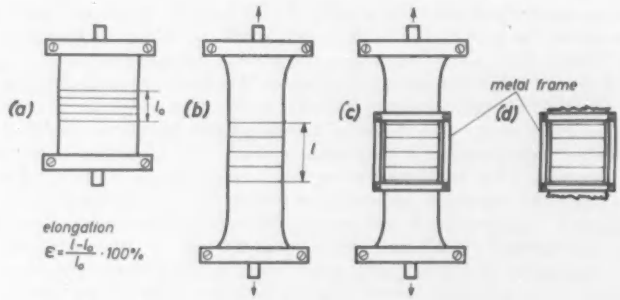

Fig. 2. Preparation of strained specimens.

Anisotropy is caused by orienting the links of the polymeric chain in the direction of stretch. Then the anisotropy of the molecular structure in the monomer will cause some macroscopic anisotropy, depending on the monomer structure and the degree of orientation as well as the degree of stretch.

Since stretched amorphous polymers may exist only below the glass-transition temperature, there is no segmental motion in the stretched state (frozen-in orientation). According to the theory of rubber elasticity, there must be the same kind of orientation, but it is combined with segmental motion in strained elastomers with a low degree of crosslinking. Therefore, it may be supposed that in some cases the observed macroscopic anisotropy would be the same below and above the glass-transition temperature, as in the case of birefringence caused by orientation. We have done some experiments in this field, since there is little information about the anisotropy of thermal conductivity.

Measuring the thermal conductivity of stretched polymers is not difficult, if they are kept below the glass-transition temperature, where there is no contraction of the specimen. We used specimens of the dimension of 80

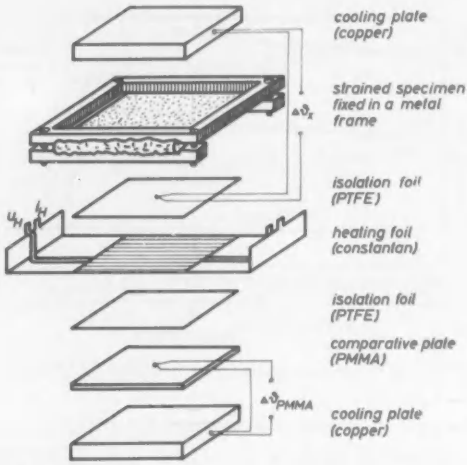

Fig. 3. Experimental arrangement for measurement of thermal conductivity.

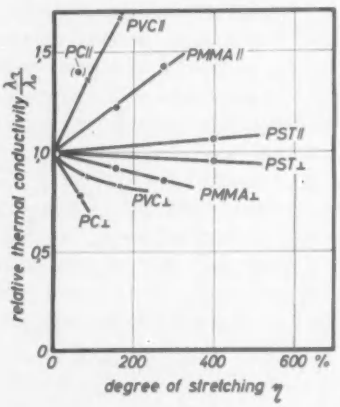

Fig. 4. Relative thermal conductivity of stretched polymers.

× 80 × 3–5 mm. in the form of rectangular bars, machined from the stretched material.[1] These bars were held together with a small metallic frame. By turning the bars in a right angle, the thermal conductivity can be measured first in the direction of stretch ($\lambda_\parallel$) and then perpendicular to this direction ($\lambda_\perp$), as shown in Figure 1.

For stationary measurements we used a two-plate apparatus described elsewhere.[2] This apparatus does not need a guard ring. By improving this method it was shown that it is not necessary to have two specimens of equal geometry and thermal conductivity. It is sufficient to have only one test specimen, when the thermal resistivity of the other plate is known.

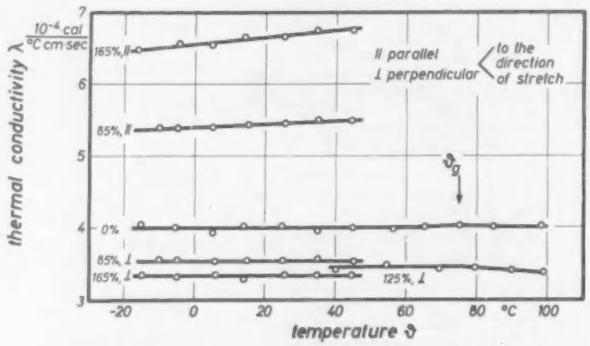

Fig. 5. Thermal conductivity of stretched PVC.

More difficulties arise in measuring thermal conductivity of strained elastomers, since contraction must be prevented. As Figure 2 shows, sheets of elastomeric materials were strained and in this state clamped in a metallic frame. The clamped specimen was put into the two-plate apparatus, as shown in Figure 3. By taking first an unstrained specimen without frame and then a clamped specimen of the same unstrained material, it was shown that the value of the thermal conductivity is not influenced by the greater surface and the metallic frame of the second specimen. Thermal conductivity of strained elastomers in the direction perpendicular to stretch could be measured by this method.

Earlier experiments on stretched polystyrene (PST), polymethylmethacrylate (PMMA), polyvinylchloride (PVC), and polycarbonate (PC) were limited to the temperature range below the glass-transition temperature.[3] They led to the result that thermal conductivity in the direction of stretch is greater than perpendicular to this direction. Irregardless of the degree of stretch the following relation has been found valid:

$$3/\lambda_0 = 1/\lambda_\parallel + 2/\lambda_\perp \tag{2}$$

λ_0 is the thermal conductivity of the isotropic unstretched sample. The results are summarized in Figure 4. It is shown that for the same degree of stretch the anisotropy could have very different values. Thus, the ratio $(\lambda_\parallel/\lambda_\perp)$ for $\eta = 100\%$ will rise from PST (1.03) over PMMA (1.22) and PVC (1.64) to PC (2.8). From our experiments concerning the anisotropy of thermal expansion, it can be seen that there is a close relation between anisotropy of thermal conductivity and thermal expansivity, which in a first approximation could be described by the following relation.[4]

$$\lambda_0/\lambda_{\parallel(\perp)} = 0.8\,\beta_{\parallel(\perp)}/\beta_0 + 0.2 \tag{3}$$

β is the coefficient of linear thermal expansivity. Equation (3) shows that the linear thermal expansion in the direction of stretch is smaller than in the direction perpendicular to it.

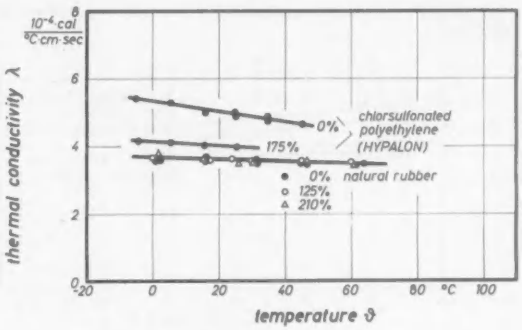

Fig. 6. Thermal conductivity of strained elastomers.

At first it seemed important to prove whether the anisotropy of stretched materials would remain at temperatures above the glass transition. In this temperature range the linear polymer will behave similar to a strained elastomer. Therefore any contraction of the specimen must be prevented. The measurement of the thermal conductivity perpendicular to the direction of the stretch should not be a problem if the contraction of the specimen is retarded by the cooling plates, which are firmly fixed in position, and by the metallic frame around the specimen. The results of some measurements on PVC are summarized in Figure 5. The curve for $\lambda_\perp$ for $\eta = 125\%$ shows only small changes in the glass-transition range. Thus, anisotropy remains nearly unchanged by segmental motion. Therefore one should also find similar effects in strained elastomers.

We chose elastomers without fillers in order to exclude the influence which might arise from the orientation of the filler particles. A good many synthetic rubbers do not have enough strength to withstand a strain $\epsilon > 50\%$ without reinforcing fillers. Therefore, experiments with polybutadiene and copolymers of butadiene and styrene are not yet possible. Natural rubber has a good mechanical strength without reinforcing fillers. Figure 6 shows that natural rubber has no anisotropy of thermal conductivity up to strains of 210%, in accordance with the measurements of Hellmuth and Müller.[5] The same will hold for polyisobutylene, which also, like natural rubber, consists of carbon and hydrogen atoms linked by aliphatic bonds. For polyisobutylene the absolute value of thermal conductivity at 20°C. is about 3.5×10^{-4} cal./°C. cm. sec., which is a little lower than that for natural rubber. On the contrary, we observed a considerable degree of anisotropy with strained chlorosulfonated polyethylene. Furthermore, we find other elastomers showing smaller effects (Fig. 7), for example, polychloroprene and an acrylonitrile-butadiene copolymer. The curve of the strained polyurethane elastomer shows a slight decrease in slope near 40°C. This was probably caused by melting of crystalline regions. On the contrary to crystallization of the isotropic unstrained elastomer,[6] there is

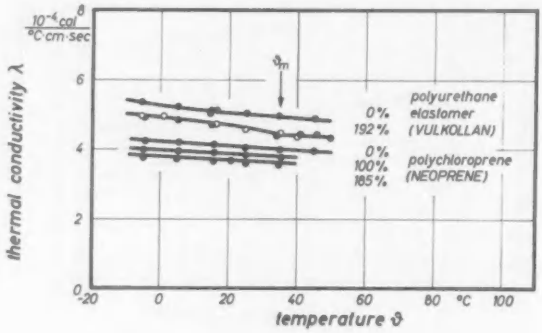

Fig. 7. Thermal conductivity of strained elastomers.

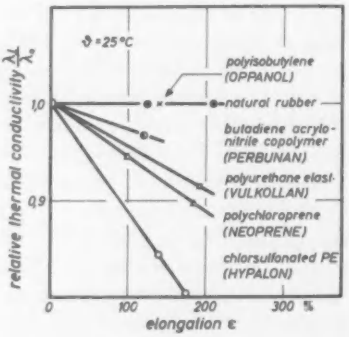

Fig. 8. Relative thermal conductivity as function of elongation.

no observable hysteresis when the strained polymer is cooled. Finally in Figure 8 all our measurements on elastomers are compared.

From Figure 8 it may be seen that, as in stretched linear amorphous polymers, there are different degrees of anisotropy. In completely aliphatic elastomers there is little anisotropy, while strong polar side groups like —Cl and —CN often show these effects. It is surprising that the aromatic side group in polystyrene has only a small effect on anisotropy, while aromatic rings in the chain seem to cause great anisotropy in polycarbonate.

Generally, it may be concluded that there are no differences between the mechanism of heat conduction in stretched amorphous linear polymers and in strained elastomers. Therefore eq. (2) should also be valid for strained elastomers. This assumption seems to be reasonable, because isotropic unstretched linear polymers show only small changes in thermal conductivity when passing through the glass-transition range. These changes seem to be caused by changes in thermal expansivity, which generally arise in the glass-transition range.[4]

Greater effects and more complicated relations will be found with partially crystalline polymers, since the orientation of the crystallites will have the greatest influence on thermal conductivity. Thus, we found the values $\lambda_\perp = 6.7 \times 10^{-4}$ and $\lambda_\parallel = 21 \times 10^{-4}$ cal./°C. cm. sec. for stretched polyethylene ($\eta = 175\%$) of medium density, while λ_0 was 8.0×10^{-4} cal./°C. cm. sec.

A theoretical interpretation of the results on noncrystalline polymers should take into consideration the earlier work of Kuhn and Grün[7] on optical anisotropy in stretched chains. From their work an equation like (2) can also be derived.

References

1. Eiermann, K., and K.-H. Hellwege, *J. Polymer Sci.*, **57**, 99 (1962).
2. Knappe, W., *Z. Angew. Physik*, **12**, 508 (1960).
3. Hellwege, K.-H., J. Hennig, and W. Knappe, *Kolloid-Z.*, **188**, 121 (1963).
4. Eiermann, K., Dissertation, Techn. Hochschule, Darmstadt, February 1963; *Kolloid-Z.*, to be published.
5. Hellmuth, W., and F. H. Müller, *Kolloid-Z.*, **185**, 159 (1962).
6. Flocke, H. A., *Kolloid-Z.*, **188**, 114 (1963).
7. Kuhn, W., and F. Grün, *Kolloid-Z.*, **101**, 248 (1942).

Résumé

Des hauts polymères linéaires amorphes deviennent anisotropes en les étirant à une température plus élevée que la température de transition vitreuse, après quoi on les fait refroidir à l'état étiré. Avec des mesures effectuées sur du polystyrène et du polycarbonate, on a pu montrer que la conductivité thermique est plus grande dans la direction de l'étirement et moins grande dans la direction perpendiculaire qu'à l'état isotrope non-étiré. Le degré d'anisotropie dépend du degré de tension et de la structure molèculaire de la chaîne. En mesurant l'anisotropie de l'expansion thermique, on a trouvé que l'expansivité thermique dans la direction de l'ètirement devient plus faible et qu'elle devient plus élevée que le polymère isotrope dans la direction perpendiculaire. Il y a une relation étroite entre l'anisotropie de la conductivité thermique et l'expansivité thermique. Aux dépens de mesures sur le chlorure de polyvinyle, on trouve que l'anisotropie de la conductivitè thermique reste, même en chauffant le polymère étiré à une température plus élevée que sa température de transition vitreuse. Â cause de cela, on peut s'attendre à ce que les élastomères étirés eux-aussi auront une anisotropie de conductivité thermique. Des mesures, sur différents élastomères étirés, dans la direction perpendiculaire à la direction de l'étirement, ont été effectuées et montrent que les élastomères étirés possédant des groupes fortement polaires ont une anisotropie considérable, tandis que des polymères aliphatiques, comme le caoutchouc naturel et le polyisobutylène, ne montrent pas d'effets mesurables.

Zusammenfassung

Lineare amorphe Hochpolymere können durch Reckung bei Temperaturen oberhalb der Glasumwandlungstemperatur und darauffolgende Abkühlung im gedehnten Zustand anisotrop gemacht werden. Messungen an Polystyrol, Polymethylmethacrylat, Polyvinylchlorid und Polykarbonat zeigen, dass die Wärmeleitfähigkeit in der Dehnungsrichtung grösser und senkrecht dazu kleiner ist als im ungedehnten isotropen Zustand. Der Grad der Anisotropie hängt vom Dehnungsgrad und von der Molekularstruktur der Polymerkette ab. Durch Messung der Anisotropie der Wärmeausdehnung kann gezeigt werden, dass die Wärmeausdehnung in der Dehnungsrichtung kleiner und senkrecht

dazu grösser wird als im isotropen Polymeren. Es besteht eine enge Beziehung zwischen der Anisotropie der Wärmeleitfähigkeit und derjenigen der Wärmeausdehnung. Aus Messungen an Polyvinylchlorid folgt, dass die Anisotropie der Wärmeleitung beim Erhitzen des Polymeren im gedehnten Zustande auf Temperaturen oberhalb des Glasumwandlungsbereiches fast ungeänderet bleibt. Man kann daher erwarten, dass auch gedehnte Elastomere eine Anisotropie der Wärmeleitfähigkeit besitzen werden. Messungen an einigen gedehnten Elastomeren senkrecht zur Dehnungsrichtung zeigten, dass gedehnte Elastomere mit stark polaren Seitengruppen einen beträchtlichen Betrag an Anisotropie besitzen, während aliphatische Polymere wie Naturkautschuk und Polyisobutylen keine bemerkenswerten Effekte aufweisen.

JOURNAL OF POLYMER SCIENCE: PART C NO. 6, PP. 175–182

Thermogravimetry of Polymer Pyrolysis Kinetics

HUGH C. ANDERSON, *Chemistry Research Department, U. S. Naval Ordnance Laboratory, Silver Spring, Maryland*

Synopsis

Two thermogravimetric methods were developed to show whether rate of weight loss varies with extent of pyrolysis of a polymer. The first of these, a kinetic technique, involves obtaining (at various degrees of degradation) the activation energy, the order of decomposition, and the Arrhenius preexponential factor by solving three simultaneous equations. The data for these equations are obtained by performing three thermogravimetric experiments at three constant heating rates. The second method, which involves cycling the polymer between 25°C. and a fixed higher temperature, is based on the compound interest law. If the rate of weight loss changes with extent of decomposition, the experimental points deviate from the theoretical curve; if the rate does not vary, the experimental points coincide with the curve. Both techniques show that the rate of weight loss does not change appreciably with degree of pyrolysis of Teflon. For a copolymer of tetrafluoroethylene and hexafluoropropylene, these methods show that rate of weight loss does vary with degree of pyrolysis.

If a polymer is decomposed to an extent of 10% (as determined by weight loss), the structure of the residue may be different from that of the original material. Then, if the residue is decomposed another 10%, the structure of this second residue could be different from those of the original polymer and of the first residue. This is shown more clearly in Figure 1. These changes in structure can alter the mechanism and rate of decomposition as the material is further pyrolyzed. Since the usual thermogravimetric method[1,2] yields rates averaged over wide degradation ranges, it may fail to reveal rate changes due to modifications in the structure of the residue.

The purpose of the work described herein was to develop methods to indicate whether the rate of decomposition changes as the polymer is pyrolyzed. The first of these, a kinetic method, was possible because of our ability to perform thermogravimetric experiments at various constant heating rates. Based upon the use of three heating rates, an equation was derived for calculating the activation energy, the order of decomposition, and the Arrhenius pre-exponential factor. For the second approach, an equation based on a modification of the compound interest law[3] was derived. It was then possible to use a thermogravimetric cycling procedure to show if rate of decomposition changes with extent of pyrolysis. These two techniques were applied to polytetrafluoroethylene (DuPont's Teflon 5) and a FEP copolymer (DuPont's Teflon 100) of tetrafluoroethylene and hexafluoropropylene.

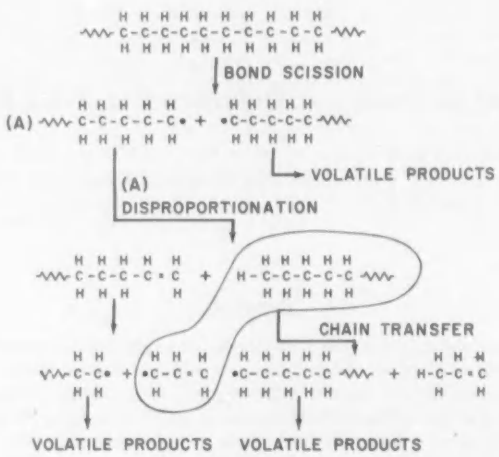

Fig. 1. Possible changes in structure as a polymer pyrolyzes.

Theoretical

For the kinetic method, eq. (4) was derived by combining eqs. (1)–(3) and multiplying the left side of the resulting equation by dT/dT and taking the logarithm:

$$\frac{dx}{dt} = k\,(a - x)^n \tag{1}$$

$$\frac{dx}{(a-x)^n} = \frac{dw}{(w_i - w)^n} \tag{2}$$

$$k = A \exp\left\{-\frac{E}{RT}\right\} \tag{3}$$

$$\log\left(\left(\frac{dT}{dt}\right)\left(\frac{dw}{dT}\right)\right) = \log A + n \log (w_i - w) - \frac{E}{2.3RT} \tag{4}$$

where a = initial number of moles of sample; x = number of moles lost at temperature T (°K.); w_i = initial weight of sample; w = weight lost at temperature T; E = activation energy; n = order of decomposition; and A = Arrhenius pre-exponential factor. In order to solve for the three kinetic parameters (E, n, and A), data are required for three simultaneous equations. Since rate of weight loss and heating rate are dynamic processes, weight-loss curves will shift along the temperature axis (Fig. 2) when obtained at different constant heating rates. With three such curves, all the necessary data become available for the required solution.

The thermogravimetric cycling experiments for the second method were performed on the following assumption. When a polymer is decomposed

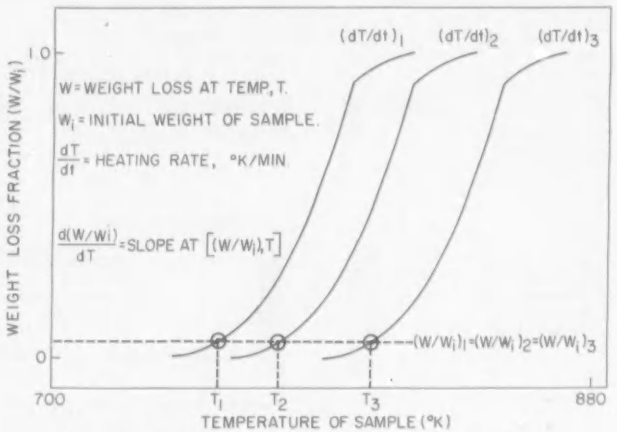

Fig. 2. Hypothetical thermogravimetry of a single polymer.

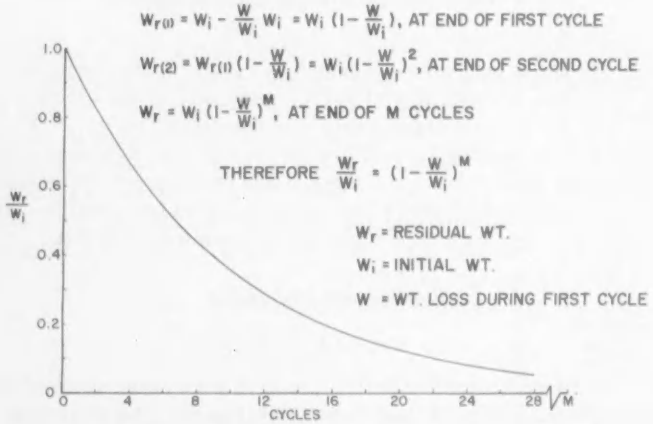

Fig. 3. Hypothetical thermogravimetric cycling curve.

partially by repeated cycling between 25°C. and a fixed higher temperature W_r/W_i for each cycle should follow a curve of $W_r/W_i = (1 - W/W_i)^M$, in which W_r = weight of polymer remaining after cycle M; W_i = initial weight; and W = weight loss during the first cycle (Fig. 3).

Experimental

Figure 4 shows a modification of the weighing chamber for the thermogravimetric apparatus described previously.[4,5] Approximately 9 to 11.5 mg. samples of 100-mesh Teflon 5 and Teflon 100 powder were pyrolyzed at a pressure of 1×10^{-3} mm. Hg. The heating rates were controlled to within ± 10%. Precision of the weight-loss measurements was ±0.02

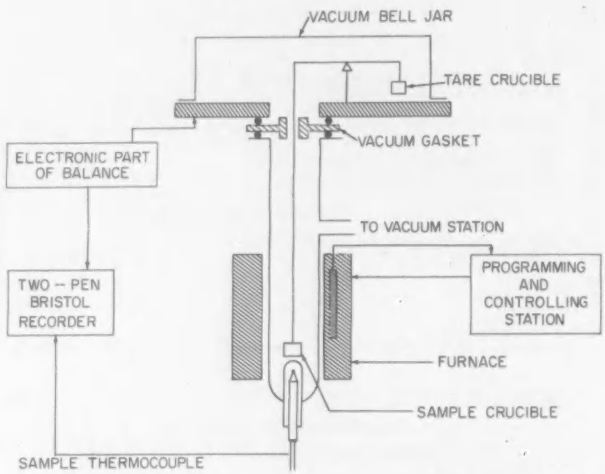

Fig. 4. Thermogravimetric experimental arrangement.

mg., and the temperature was measured to ±0.5°C. Heating rates of 1, 2, and 4°C./min. between 25 and 620°C. were used for the kinetic experiments. For the cycling experiments, the theoretical curves in Figure 7 were obtained by heating the polymer for the first time at a rate of 4°C./min. up to the temperatures indicated. The fractional weight remaining (W_r/W_i) was then calculated by assuming the initial fractional weight-loss to be constant. For these experiments, W/W_i was 0.11 ± 0.01.

Results and Discussion

A. Kinetic Experiments

Data necessary for solving for E, n, and A were obtained from typical curves for Teflon 5 (Fig. 5) and Teflon 100 (Fig. 6). An IBM 7090 computer was used to solve the simultaneous equations, and the Gauss reduction method[6] was used to spot check the results. The calculated kinetic values are given in Table I for Teflon 5 and in Table II for Teflon 100.

That the kinetic values in Table I do not differ appreciably for various fractions of weight loss indicates that the rate of degradation of Teflon 5 does not change with degree of pyrolysis. These results agree with the following generally proposed mechanism[12] of Teflon pyrolysis. Initiation occurs by random splitting of a C—C bond into a pair of free radicals. These radicals remain in the vicinity of the site where they are formed and depropagate by stepwise ejection of monomer molecules from the radical ends. Monomer then diffuses rapidly away from the reaction site in vacuum pyrolysis. The results also show that the rate of decomposition is independent of the molecular weight of the polymer.

TABLE I
Kinetic Values for Pyrolysis of Teflon 5 Homopolymer

W/W_i	E (kcal.)[a]	n[a]	A (1/min.) 10^{-20}[a]
0.1	77	1.00	3.7
0.2	78	1.00	4.3
0.3	77	1.00	3.7
0.4	77	0.99	3.7
0.5	76	1.02	4.8
0.6	78	1.00	3.8
0.7	78	1.01	3.7
0.8	76	1.01	3.8
0.9	77	1.07	4.8
Average	77.0	1.01	4.0
Madorsky[7]	80.5	1.0	2.8
Siegle[8]	83.0	1.0	27.0
Anderson[9]	75.0 ± 4	1.02 ± 0.07	—
Doyle[10]	67.0	—	—

[a] Each group of values for E, n, and A is the average of three determinations. Maximum average deviations were: E, ±7%; n, ±10%; and A, ±20%.

Curves in Figure 6 and kinetic values in Table II indicate that there are at least two stages in the decomposition of Teflon 100 copolymer. The initial stage of decomposition suggests a lower stability of chain segments containing hexafluoropropylene units. Wall[11] reported that a similar copolymer produced less light volatiles than pure Teflon; 75 to 84% as compared to about 95% for the latter. The main components of these volatiles were C_3F_6 and C_2F_4, C_3F_6 being more abundant in the early stages of pyrolysis. At 10% degradation, the light volatiles contained 85%

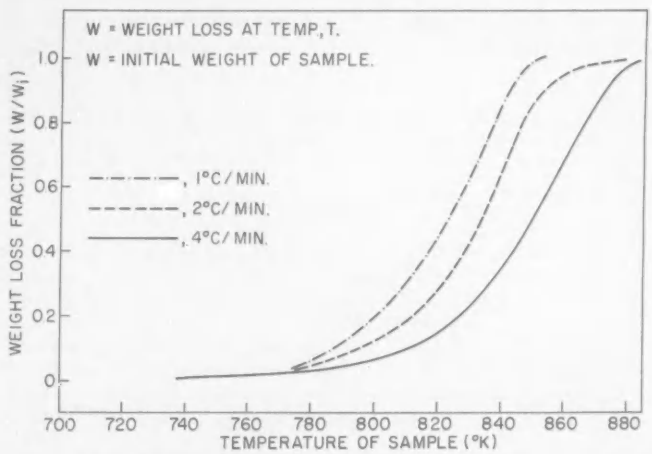

Fig. 5. Thermogravimetry of polytetrafluoroethylene

TABLE II
Kinetic Values for Pyrolysis of Teflon 100 Copolymer

W/W_i	E (kcal)[a]	n[a]	$A(1/\text{min.})\ 10^{-13a}$
0.1	34.8	0.93	0.0004
0.2	44.4	0.88	0.1
0.3	60.2	0.91	222.0
0.4	55.6	0.90	48.0
0.5	48.2	1.00	4.0
0.6	42.3	1.09	1.0
Average	48.0	0.95	46.0
Wall[11]	55.0	1.0	6.0

[a] Each group of values for E, n, and A is the average of three determinations. Maximum average deviations were: E, ±5%; n, ±10%; and A, ±15%.

C_3F_6 and 9% C_2F_4, whereas at 92% decomposition, the volatiles contained 19% C_3F_6 and 68% C_2F_4.

B. Cycling Experiments

The average results of the cycling experiments are shown in Figure 7. The close agreement between the experimental point and the theoretical curve for Teflon indicates further that the rate of weight loss does not change appreciably with degree of decomposition. For the early stages of degradation of the copolymer, the large deviations of the experimental points from the theoretical curve show a definite change in rate of weight loss with increasing decomposition. In fact, after the third cycle, W_r/W_i remained constant through two additional 500°C. cycles. For the second stage of degradation, the deviations of the experimental values of W_r/W_i

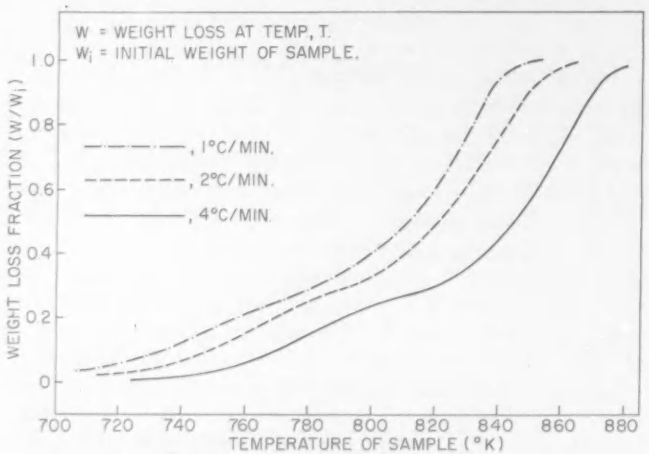

Fig. 6. Thermogravimetry of a copolymer of tetrafluoroethylene and hexafluoropropylene.

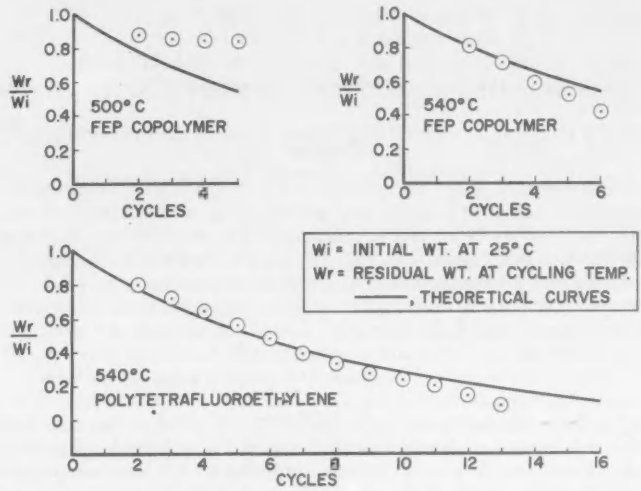

Fig. 7. Thermogravimetric cycling curves.

from the hypothetical curve are not as great as they were for the first step. The hypothetical curve for the second stage of decomposition was obtained by taking the amount of polymer remaining after the fifth cycle in the first stage as the initial weight (W_i).

Conclusions

Either the kinetic or cycling experiment can be used to tell whether the rate of weight loss varies with extent of pyrolysis. The latter method is preferred for this purpose because it is much simpler. The kinetic method can then be used to obtain precise kinetic data at selected extents of pyrolysis.

The author wishes to thank Drs. F. Daniels (University of Wisconsin), E. S. Freeman (Picatinny Arsenal), and W. J. Bailey (University of Maryland) for their advice concerning this work.

References

1. Freeman, E. S., and B. Carroll, *J. Phys. Chem.*, **62**, 394 (1958).
2. Anderson, D. A., and E. S. Freeman, *J. Appl. Polymer Sci.*, **1**, 192 (1959).
3. Mellor, J. W., *Higher Mathematics*, Dover, New York, 1955, p. 56.
4. Anderson, H. C., *J. Appl. Polymer Sci.*, **6**, 484 (1962).
5. Anderson, H. C., *Kolloid-Z.*, **184**, 26 (1962).
6. Hildebrand, F. B., *Introduction to Numerical Analysis*, McGraw-Hill, New York, 1956, p. 428.
7. Madorsky, S. L., V. E. Hart, S. Straus, and V. A. Sedlak, *J. Res. Natl. Bur. Std.*, **51**, 327 (1953).
8. Siegle, J. C., and L. T. Muus, paper presented at 130th American Chemical Society Meeting, Sept. 1956.

9. Anderson, H. C., *Makromol. Chem.*, **51**, 233 (1962).
10. Doyle, C. D., *J. Appl. Polymer Sci.*, **5**, 285 (1961).
11. Wall, L. A., and S. Straus, *J. Res. Natl. Bur. Std.*, **65A**, 227 (1961).
12. Friedman, H. L., paper presented at 136th American Chemical Society Meeting, Sept. 1959.

Résumé

Deux méthodes thermogravimétriques ont été développées pour vérifier si la vitesse de perte de poids variait en fonction du degré d'avancement de la pyrolyse d'un polymère. La première de celle-ci, une technique cinétique, demande qu l'on détermine (à différents degrés de dégradation) l'énergie d'activation, l'ordre de la décomposition et le facteur d'Arrhénius pré-exponentiel en résolvant trois équations combinées. Les données pour ces équations sont obtenues en exécutant trois expériences thermogravimétriques à des vitesses de chauffage constantes. La seconde méthode, qui inclut la cyclisation du polymère entre 25°C et une température plus haute fixèe d'avance, est basèe sur la loi de l'intèrét composé. Si la vitesse de la perte de poids change suivant le degrè de décomposition, les points expérimentaux, dévient de la courbe théorique; si la vitesse ne varie pas, les points expérimentaux coincident avec la courbe. Les deux techniques montrent que la vitesse de la perte de poids ne change pas fort avec le degrè de pyrolyse du Téflon. Pour un copolymère du tètrafluoroéthylène et de l'hexafluoropropylène, les deux méthodes montrent que la vitesse de la perte de poids varie avec le degrè de pyrolyse.

Zusammenfassung

Zwei thermogravimetrische Methoden wurden entwickelt, um zu klären, ob die Geschwindigkeit des Gewichtsverlustes vom Ausmass der Pyrolyse eines Polymeren abhängt. Beim ersten Verfahren, einer kinetischen Methode, wird durch Lösung drier Simultangleichungen die Aktivierungsenergie, die Ordnung der Zersetzung und der preexponentielle Arrheniusfaktor (bei verschiedenen Abbaugraden) erhalten. Die Daten für diese Gleichungen wurden aus drei thermogravimetrischen Versuchen bei drei konstanten Erhitzungsgeschwindigkeiten erhalten. Die zweite Methode beruht auf der Durchführung eines Temperaturzyklus mit dem Polymeren zwischen 25°C und einer festgelegten höhen Temperatur und dem "compound interest"-Gesetz. Bei Anderung der Geschwindigkeit des Gewichtsverlustes mit dem Ausmass der Zersetzung weichen die experimentellen Punkte von der theoretischen Kurve ab; bei Unabhängigkeit der Geschwindigkeit fallen die experimentellen Punkte mit der Kurve zusammen. Beide Methoden zeigen, dass die Geschwindigkeit des Gewichtsverlustes nicht wesentlich vom Pyrolysegrad von Teflon abhängt. Hingegen zeigen die Methoden bei einem Copolymeren von Tetrafluoräthylen und Hexafluoropropylen eine Abhängigkeit der Geschwindigkeit des Gewichtsverlustes von Pyrolysegrad.

JOURNAL OF POLYMER SCIENCE: PART C NO. 6, PP. 183–195

Kinetics of Thermal Degradation of Char-Forming Plastics from Thermogravimetry. Application to a Phenolic Plastic

HENRY L. FRIEDMAN, *Space Sciences Laboratory, Missile and Space Division, General Electric Company, Valley Forge Space Technology Center, King-of-Prussia, Pennsylvania*

Synopsis

A technique was devised for obtaining rate laws and kinetic parameters which describe the thermal degradation of plastics from TGA data. The method is based on the intercomparison of experiments which were performed at different linear rates of heating. By this method it is possible to determine the activation energy of certain processes without knowing the form of the kinetic equation. This technique was applied to fiberglass-reinforced CTL 91-LD phenolic resin, where the rate law $-(1/w_0)(dw/dt) = 10^{18} e^{-55{,}000/RT}[(w - w_f)/w_0]^5$, nr.$^{-1}$, was found to apply to a major part of the degradation. The equation was successfully tested by several techniques, including a comparison with constant temperature data that were available in the literature. The activation energy was thought to be correct within 10 kcal.

Introduction

Kinetics of thermal degradation of solids have been evaluated from thermogravimetric analysis (TGA) at linear rates of temperature rise in a number of studies. van Krevelen, van Heerden, and Huntjens[1] studied the decomposition of coal. Freeman and Carroll[2] investigated the degradation of calcium oxalate monohydrate. Their technique was applied to the decomposition of a styrenated polyester by Anderson and Freeman,[3] and was modified by the same authors[4] for polystyrene and polyethylene. Doyle[5] studied the degradation of a large number of plastics. Friedman[6] investigated the decomposition of a glass-reinforced phenol-formaldehyde. A more sophisticated approach will be used in the present paper than was employed for the earlier work.

In all of the earlier studies, calculations were based on experiments which were performed at a single rate of temperature rise. In the present paper, kinetic calculations are based on an intercomparison of experiments which were carried out at several different rates of temperature rise.

Experimental

Fiberglass-reinforced CTL 91-LD phenolic resin (a product of Cincinnati Testing and Research Laboratory) was used for this study. The laminate

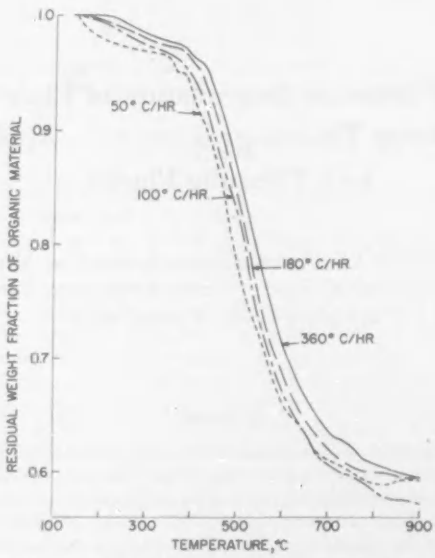

Fig. 1. TGA curves of CTL 91-LD phenolic on glass-free basis.

was prepared from resin-impregnated glass sheets that were supplied by U. S. Polymeric Chemicals, Inc. The sheets, which originally consisted of 42 wt.-% resin, were B-staged in a 200°F. oven for 1 hr. They were then cured in a 225°F. press at 100 psi for 15 min., followed by 265°F. at 100 psi for 3 hr. The cured laminate was allowed to cool to room temperature in the press, and was then post-cured in a 265°F. oven for 16 hr.

In order to prepare TGA samples, the surface layers were split off and discarded. The underlying material was converted to thin flakes by end milling under liquid nitrogen. The flakes were dried in a desiccator overnight, and were further dried by holding the sample in a porcelain crucible in the Chevenard thermobalance for 1 hr. at 100°C. just before TGA was allowed to commence. Samples lost less than 1% of their original weight during the preconditioning period.

Four 200-mg. samples of the flakes were subjected to TGA at linear heating rates of 50, 100, 180, and 360°C./hr. Degradation was carried out in a stream of dry nitrogen to maximum temperature of 900°C. After TGA was completed, the residue from each test was burned in air at 1000°C. until only glass remained. Original resin contents were found to range from 35.0 to 36.1 wt.-%.

Residual weight fractions of organic material were calculated on a glass-free basis, and are shown as a function of temperature in Figure 1. Note that the curves are displaced to higher temperatures with increased heating rate, as would be predicted from kinetic theory. Rates of weight loss are plotted as a function of time and temperature in Figure 2. Rates were

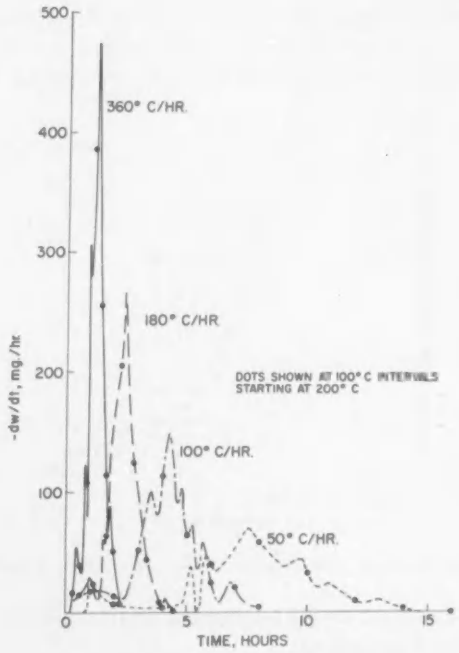

Fig. 2. Derivatives of TGA curves.

measured from enlarged graphs of Figure 1 with a Gerber derivimeter. All of the rate curves had the same general shape. Slow weight loss commenced almost immediately and continued to above 300°C. Between 300 and 400°C., the rate of loss of weight increased as the temperatures were elevated, reached a maximum in the vicinity of 500°C., and then decreased for the remainder of the heating period. Inspection of Figure 2 shows that there are a number of hills and valleys in the rate curves. Since they vary markedly from curve to curve, they are thought to be caused by scatter of the TGA data rather than indications of changes in the degradation process.

The early weight loss accounted for less than 10% of the total loss, and appeared to be associated with a different process. It was, therefore, decided to eliminate this portion from the kinetic analysis. An arbitrary initial weight of plastic was chosen from the TGA data at a temperature between 300 and 400°C. where examination of the rate curves showed that the major weight loss process appeared to begin. Although it was likely that the main degradation process started at somewhat lower temperatures, and that the early degassing process continued to higher temperatures, it was felt that the errors associated with rate measurements would be far more serious than errors caused by reasonable estimate of initial weight.

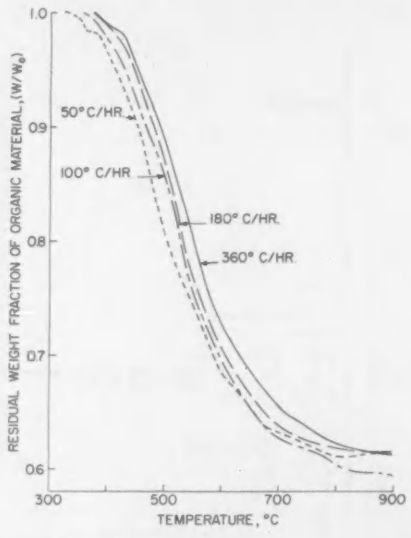

Fig. 3. TGA curves corrected for some early degassing.

Figure 3 shows residual weight fractions of organic material, with the early weight loss process eliminated.

Kinetic Analysis

The following very general kinetic equation was assumed to hold for this material.

$$(-1/w_0)(dw/dt) = Ae^{-\Delta E/RT}f(w/w_0) \tag{1}$$

where w = weight of organic material, w_0 = original weight of plastic, t = time (in hours), A = pre-exponential factor of rate constant (per hour), ΔE = activation energy of rate constant, (in calories/mole), R = gas constant (1.987 cal./°K. mole), T = absolute temperature, and $f(w/w_0)$ = a function of the weight of organic material. Taking logarithms of eq. (1) gives

$$\ln[(-1/w_0)(dw/dt)] = \ln A + \ln f(w/w_0) - \Delta E/RT \tag{2}$$

(fw/w_0) is assumed to be constant for constant values of w/w_0. This is comparable to assuming that the chemistry of the process is independent of temperature, and is dependent only on the instantaneous weight of the organic material. A dozen values of w/w_0 were selected, ranging from 0.675 to 0.950, at equal intervals. Values of $(1/w_0)(dw/dt)$ and T were determined for each w/w_0 for each TGA experiment. Plots of $\ln[(-1/w_0)(dw/dt)]$ versus $1/T$ are shown for each value of w/w_0 in Figure 4. The slope of each line is equal to $-\Delta E/R$, while the intercept is $\ln[Af(w/w_0)]$.

The lines of Figure 4 were obtained from least squares treatments of the data. Values of ΔE and ln $[Af(w/w_0)]$ are plotted as functions of w/w_0 in Figure 5. ΔE varies from 50 to 72 kcal./mole. The range of variation

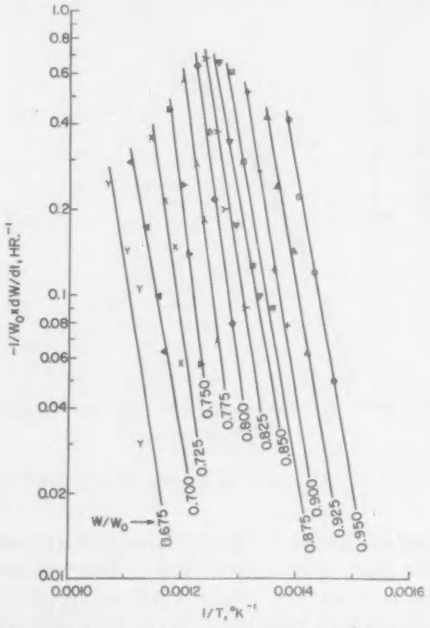

Fig. 4. Arrhenius-type plots for determining kinetic parameters.

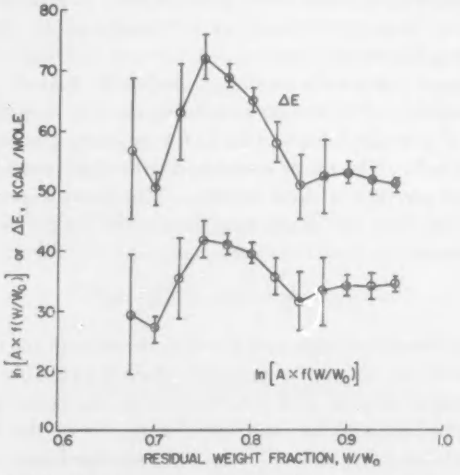

Fig. 5. Kinetic parameters as a function of sample weight.

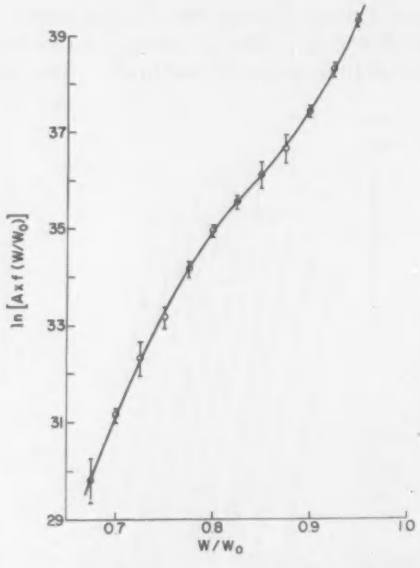

Fig. 6. Plot of ln $[Af(w/w_0)]$ as a function of sample weight.

that is associated with each point represents only the probable error of the points based on the least squares treatment. The real errors are larger. Note, however, that trends in the values of ΔE and ln $[Af(w/w_0)]$ are identical. This indicates that a positive error in A, which would make the reaction appear to go faster, is compensated for by a positive error in ΔE, which would tend to make the reaction appear to go slower. Negative errors would balance in the reverse way. Thus it appears that the kinetics of the overall process are consistent.

The 12 different ΔE's were averaged to give 57.7 kcal. Experimental parameters and the ΔE were substituted in eq. (2) to give 48 values of ln $[Af(w/w_0)]$. Average values of ln $[Af(w/w_0)]$ are plotted as a function of w/w_0 in Figure 6. The range associated with each point is the standard deviation of the average of four values. The smooth curve in Figure 6 tended to confirm that the kinetics of the overall process were consistent. (fw/w_0) was assumed to have the form

$$f(w/w_0) = [(w - w_f)/w_0]^n \tag{3}$$

where w_f = final weight of char and n = kinetic order of the reaction. $w - w_f$ is a measure of the amount of material which is available for decomposition at any instant of time, and is a convenient mathematical form which allows the degradation to be completed when all of the original plastic is converted to char. Equation (3), or very similar forms, can be derived from theory for processes where a solid reactant is converted to a constant

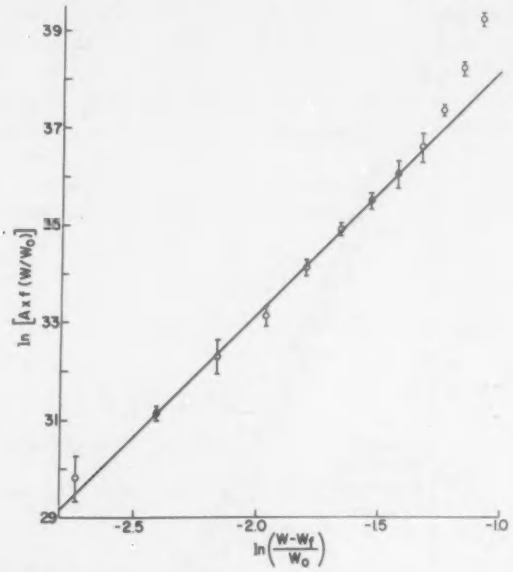

Fig. 7. Plot for the determination of A and kinetic order.

ratio of gaseous and solid products. Multiplying both sides of eq. (3) by A and taking logarithms yields

$$\ln [Af(w/w_0)] = \ln A + n \ln [(w - w_f)/w_0] \tag{4}$$

If the assumed form of $f(w/w_0)$ is correct, then a plot of $\ln [Af(w/w_0)]$ versus $\ln [(w - w_f)/w_0]$ should give a straight line where the slope is n and the intercept is $\ln A$. This type of plot is shown in Figure 7. A straight line resulted for all values of the abscissa below -1.3 (equivalent to w/w_0 below 0.9). The positive deviation at higher weights could be attributed to contributions of the early weight loss process. In calculating values of $(w - w_f)/w_0$, it was necessary to assume a value of w_f. Examination of Figure 3 indicated that decomposition was essentially completed at 900°C., so the convenient average value of $w_f/w_0 = 0.61$ was selected. Calculations based on Figure 7 showed that $n = 5.0$ and $A = 5.98 \times 10^{18}$ hr.$^{-1}$. The form of the overall kinetic equation is

$$(-1/w_0)(dw/dt) = k[(w - w_f)w_0]^5 \tag{5}$$

where $k = Ae^{-\Delta E/RT}$ hr.$^{-1}$.

Tests of the Kinetic Equation

Three different tests were made on the applicability of eq. (5). The first was an examination of Arrhenius plots for the individual runs. k's were calculated from eq. (5) by using the values of the other terms which

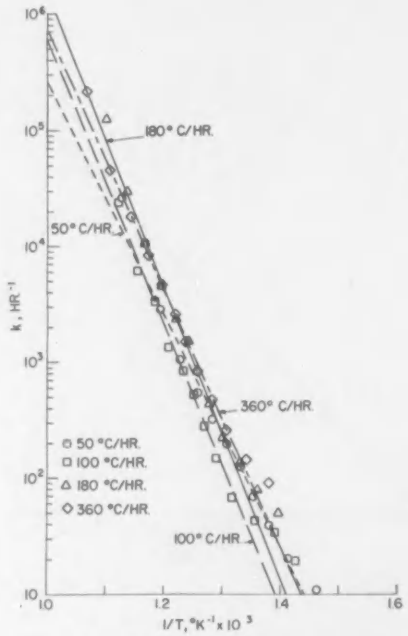

Fig. 8. Arrhenius plots of the TGA data.

were calculated earlier in the paper. w_t/w_0 was assumed to be 0.61 for all but the 100°C./hr. run, where the value of 0.59 was employed. Arrhenius plots of the four runs are shown in Figure 8. The lines are based on visual inspection of the data. The ΔE's and A's which were derived from the lines are listed in Table I. Note that the values of k are higher than

TABLE I
Kinetic Parameters Calculated by Different Methods

	ΔE, kcal.			A, hr.$^{-1}$	
Rate, °C./hr.	Kinetic analysis section	Arrhenius plot method	Second derivative test	Kinetic analysis section	Arrhenius plot method
50	Twelve values ranging	46	47		2.63×10^{15}
100	from 50 to 72 kcal.	55	66		4.79×10^{17}
180		58	70		5.13×10^{18}
360		51	56		9.55×10^{16}
Average	57.7	55[a]	60	5.98×10^{18}	10^{18a}

[a] Arrhenius plot average values were calculated from examination of all data in Figure 8.

the Arrhenius lines at the lowest temperatures. This is thought to be due to the early weight loss process, and is comparable to the deviations from linearity in Figure 6. The method of least squares was applied to all the data of Figure 8, except for the two lowest temperatures of each TGA run. ΔE was found to be 55 kcal., while A is 10^{18} hr.$^{-1}$. These values will be used for all further calculations.

The second test is based on the fact that at the maximum $(-dw/dt)$, the second derivative $(-d^2w/dt^2)$ is equal to zero. Since the heating rate is linear

$$dT/dt = \rho \tag{6}$$

where ρ = heating rate (in °C./hr.). Substituting eq. (6) in eq. (5) and rearranging gives

$$-dw/dT = (A/\rho w_0^4)e^{-\Delta E/RT}(w - w_f)^5 \tag{7}$$

Taking derivatives of eq. (7) yields

$$-d^2w/dT^2 = (A/\rho)[(w - w_f)/w_0]^4 e^{-\Delta E/RT} [5(dw/dT) + (w - w_f)(\Delta E/RT^2)] \tag{8}$$

For $(-\mathrm{d}^2w/dT^2) = 0$ at the maximum rate

$$5(dw/dT)_m + (w_m - w_f)(\Delta E/RT_m^2) = 0 \tag{9}$$

where subscript m refers to maximum rate. Equation (9) may be arranged to

$$\Delta E = 5RT_m^2(-dw/dT)_m/(w_m - w_f) \tag{10}$$

The four values of ΔE which were calculated from eq. (10) are listed in Table I.

The third test was to derive the individual TGA curves from eq. (5). Equation (5) was rearranged for integration to give

$$-\int_{w_0}^{w} \frac{dw}{(w - w_f)^5} = \frac{A}{\rho w_0^4}\int_{T_0}^{T} e^{-\Delta E/RT}\,dT \tag{11}$$

where w_0 = the arbitrary choice of initial weight of plastic and T_0 = absolute temperature at w_0.

Integration and solution for w gives

$$w = w_f + \frac{\rho^{0.25} w_0(w_0 - w_f)}{\left\{\rho w_0^4 + 4A(w_0 - w_f)^4\left[Te^{-\Delta E/RT} - T_0 e^{-\Delta E/RT_0} + \frac{\Delta E}{R}\left(\int_{v_0}^{\infty}\frac{e^{-v}}{v}\,dv - \int_{v}^{\infty}\frac{e^{-v}}{v}\,dv\right)\right]\right\}^{0.25}} \tag{12}$$

where $v = \Delta E/RT$ and $v_0 = \Delta E/RT_0$.

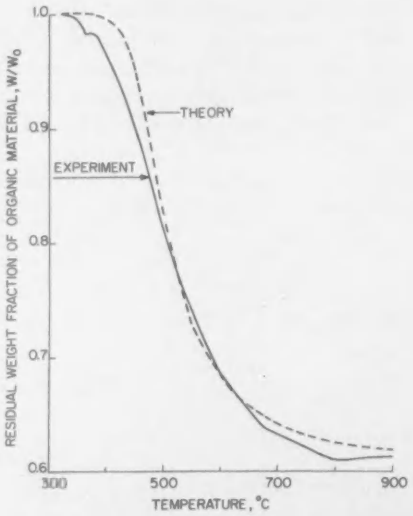

Fig. 9. Experimental and theoretical TGA curves for the 50°.C/hr heating rate.

Solutions for the integrals which appear in eq. (12) are tabulated in several sources.[7,8] The data of Coulson and Duncanson[8] were used for this work. Figure 9 shows a typical thermogram that was derived by this technique. Note that in the lower temperature range the experimental curve shows a higher weight loss than the theoretical curve. This was expected, since the kinetic analysis and Arrhenius plots had both shown that the early weight loss process continues after temperatures which are greater than T_0.

Discussion

The various tests of eq. (5) showed that the kinetic analysis of CTL 91-LD phenolic degradation that was formulated in this paper is reasonable for a large part of the decomposition process. The main deviation between experiment and analysis occurred during early degradation, where the actual weight loss exceeded the calculated loss. The earliest weight loss can probably be attributed to desorption of absorbed gases. The resin was probably not completely cross-linked at the point where TGA started. As heating continued, further cross-linking probably occurred, and further weight loss could be attributed to the evolution of some condensation products. Since degradation probably started before crosslinking was completed, there is probably no simple value for w_0, in the way that it was used. Examination of Figure 9 shows that a slightly lower w_0 would make the theoretical curve fit the experiment better. It is altogether reasonable, when one considers the argument that was presented above, that the effective w_0 be lower than the chosen value. It is also not surprising that the

theoretical weight at 900°C. is slightly higher than the experimental figure. Adjustments could probably be made in the choice of both w_0 and w_f, so that very accurate theoretical TGA curves would result, except for the very earliest weight loss processes.

A fifth-order weight dependence is unusual for polymer degradation. Of course, order does not mean the same thing in this type of process as it does for a gas or a solution. Since this resin is a highly crosslinked material, it is likely that the high order was associated with a rather complex mechanism which occurred in the solid state. Note, however, that a preexponential factor of about 3×10^{14} sec.$^{-1}$ and an activation energy of 55 kcal. are not unusual for some thermoplastics.

Inspection of the low temperature end of the TGA curves showed that very low activation energies could be attributed to that part of the decomposition. In the earlier kinetic analysis,[6] this author studied TGA experiments which were performed only at 180°C./hr. on a sample where the resin content had not been determined. Since that analysis covered temperatures ranging between 404 and 524°C., it is reasonable that an activation energy of 15 kcal. was calculated. Madorsky and Strauss[9] investigated the thermal degradation of the non-reinforced phenolic in vacuum and at constant temperature. Rate measurements at 7% degradation at 355 and 380°C. were used by these authors to estimate the activation energy of degradation as 18 kcal., in agreement with the previous study.[6] Nevertheless, the present author feels that the early degradation should be studied further by methods which would yield reproducible rates.

Madorsky and Strauss carried out a few experiments to comparatively high extents of reaction, and it is possible to compare their data with that of the present work. Total per cent of volatilization was reported as a consequence of heating for a given length of time at 420, 500, and 800°C. To compare data, eq. (5) was integrated to give

$$w = w_f + \frac{w_0(w_0 - w_f)}{[w_0^4 + 4 \times 10^{13} t e^{-55,000/RT} (w_0 - w_f)^4]^{0.25}} \tag{13}$$

These workers determined elemental analyses for several samples which were pyrolyzed to various extents of decomposition at various temperatures. After 5 min. of pyrolysis at 1200°C. a residue was produced with 51.6% of the original sample weight where 99.2% of the residue was carbon. Complete conversion to carbon would be expected at a residue weight of about 51%. Since the present samples had reached rather constant weight after the comparatively lengthy heatings to 900°C., it is likely that they had been converted to pure carbon. Elemental chemical analysis of these chars would have been desirable. Differences in the w_f's could readily be caused by different batches and differences in sample preparation. Although eq. (13) ignored early weight loss and w_0 was defined on a different basis than that by which the equation was derived, it was felt that the calculation would still be meaningful. w_f is probably the most

important parameter for this calculation so long as the extent of reaction is great enough for most or all of the early weight loss gases to be evolved. The three runs that were chosen seemed to qualify reasonably well on this basis. The results of comparison are listed in Table II. The agreement between the results is excellent and lends further support to the present kinetic analysis.

The kinetic analysis technique that was employed in this paper has several advantages. By its use it was possible to calculate an activation energy for the main degradation process without any knowledge of the form of the kinetic equation. It was also useful for the purpose of deriving a semiempirical rate law, which would be difficult to arrive at by other methods. This method could also serve as a check for systems where the rate laws seem to be so simple that TGA experiments would only be carried out at one rate of heating under normal circumstances.

TABLE II
Comparison Between Results of the Present Work with Experiments of Madorsky and Straus

Temperature, °C.	Heating time, min.	w/w_0	
		Observed	Calculated
420	130	0.84	0.87
500	30	0.72	0.71
800	5	0.56	0.54

The author is particularly grateful to C. D. Doyle and Mrs. M. A. Spodnewski of the Advanced Technology Laboratories of the General Electric Company, Schenectady, N. Y., for carrying out all of these experiments. He is also indebted to S. Blecher and Mrs. R. Flitter for their help with the mathematics and computations.

This work was performed under the auspices of the U. S. Air Force Space Systems Division, Contract No. AF 04(647)-269.

References

1. van Krevelen, D. W., C. van Heerden, and F. J. Huntjens, *Fuel.*, **30**, 253 (1951).
2. Freeman, E. S., and B. Carroll, *J. Phys. Chem.*, **62**, 394 (1958).
3. Anderson, D. A., and E. S. Freeman, *J. Appl. Polymer Sci.*, **1**, 192 (1959).
4. Anderson, D. A., and E. S. Freeman, *J. Polymer Sci.*, **54**, 253 (1961).
5. Doyle, C. D., *J. Appl. Polymer Sci.*, **5**, 285 (1961).
6. Friedman, H. L., Proceedings of Wright Air Development Division Conference on Behavior of Plastics in Advanced Flight Vehicle Environments, Wright-Patterson AFB, Ohio, WADD TR 60-101, 295, September 1960.
7. Jahnke, E., and F. Emde, *Tables of Functions with Formulae and Curves*, Dover, New York, 1945.
8. Coulson, C. A., and W. E. Duncanson, *Phil. Mag.*, **33**, 754 (1942).
9. Madorsky, S. L., and S. Strauss, *Mod. Plastics*, **38**, No. 6, 134 (1961).

Résumé

On a mis au point une méthode rélévant les équations de vitesses et les paramètres cinétiques qui décrivent la dégradation thermique de plastiques à partir de données TGA.

La méthode est basée sur la comparison des expériences obtenues à diverses vitesses linéaires d'échauffement Cette méthode permet de déterminer l'énergie d'activation de certains processus, sans en connaître la forme de l'équation cinétique. On applique cette technique à la résine phénolique renforcée avec des fibres de verre CTL 91-LD dont l'équation de vitesse: $-(1/w_0)(dw/dt) = 10^{18}\, e^{-55{,}000/RT}\,[(w - w_f)/w_0)]^5$, hr^{-1}, a été trouvée appliquable à la majorité des dégradations. L'équation a été vérifiée à l'aide de plusieurs techniques, y compris une comparaison avec des données d'expériences à température constante, trouvées dans la littérature. On démontre que l'énergie d'activation est correcte à moins de 10 kcal près.

Zusammenfassung

Ein Verfahren zur Ermittlung der Geschwindigkeitsgesetze und kinetischen Parameter beim thermischen Abbau plastischer Stoffe aus TGA-Daten wird angegeben. Das Verfahren beruht auf dem wechselseitigen Vergleich von Versuchen bei verschiedener linearer Erhitzungsgeschwindigkeit. Mit dieser Methode kann die Aktivierungsenergie gewisser Prozesse ohne Kenntnis der Form der kinetischen Gleichung bestimmt werden. Das Verfahren wurde auf glasfaserverstärktes CTL 91-LD-Phenolharz angewendet, das im Hauptteil des Abbaues dem Geschwindigkeitsgesetz $-(1/w_0)(dw/dt) = 10^{18}\, e^{-55{,}000/RT}[(w - w_f)/w_0]^5$, hr^{-1} gehorcht. Die Gleichung konnte mit Erfolg nach mehreren Methoden überprüft und mit Literaturwerten bei konstanter Temperatur verglichen werden. Die Aktivierungsenergie dürfte mit einer Genauigkeit von 10 kcal korrekt sein.

JOURNAL OF POLYMER SCIENCE: PART C NO. 6, PP. 197–207

Form III to Form II Phase Transition of Polybutene-1

C. GEACINTOV, R. S. SCHOTLAND, and R. B. MILES, *Research and Technical Division, Mobil Chemical Co., Metuchen, New Jersey*

Synopsis

The Form III to Form II transition of crystalline polybutene-1 at elevated temperature has been observed by differential thermal analysis (DTA), dilatometry, x-ray diffraction, and photomicrography. DTA thermograms of polybutene-1 in Form III were found to exhibit endotherms at 94°C., and 110°C., corresponding to the transformation of Form III and melting of Form II, respectively. The origin of an exothermic peak observed at 96°C., is not entirely resolved at the present time. The transition of polybutene-1 in the Form III modification was also studied by x-ray diffraction methods. It was shown that the intensity of the peak at $2\theta = 12.1°$, corresponding to the Form III crystalline phase, begins to decrease in size at 88°C., while simultaneously the peak at $2\theta = 11.7°$, corresponding to the Form II modification, starts to grow. The transformation is complete at 98°C. The nature of the Form III to Form II transition of polybutene-1 is discussed in the paper; two alternative mechanisms are deemed possible: a solid-solid transition or a transition involving a short-lived intermediate molten state.

Introduction

The synthesis of isotactic polybutene-1 was initially reported by Natta[1] in 1955. Subsequent structural studies revealed that polybutene-1 exists in at least three crystalline polymorphic modifications. The characteristic polymorphism of polybutene-1 is of great theoretical and practical interest and it was not surprising therefore, that this polymer has become the object of detailed investigations in a number of laboratories throughout the world.

On crystallization from the melt, polybutene-1 assumes a metastable tetragonal crystal structure (Form II), which upon standing at room temperature and atmospheric pressure, undergoes a crystal-crystal transformation to a stable rhombohedral structure (Form I). The transformation of Form II to Form I may be greatly accelerated by the application of mechanical stress or pressure, a result which is to be expected on the basis of the greater extension[2, 3] of the Form I helix as compared to the Form II helix. A tighter packing of the chains in Form I is therefore possible, and this in turn leads to a higher density and improved stability of polybutene-1 in the Form I modification.

More recently a third stable modification of polybutene-1, known as Form III, has been isolated by precipitating the polymer from solution. The characteristic x-ray diffraction pattern for this modification was

published by Zannetti et al.,[4] while Danusso and Gianotti[5] reported on the dilatometric and thermodynamic fusion properties of all three modifications of isotactic polybutene-1. The method used by the latter authors did not permit observation of an unusual transition of the Form III modification of polybutene-1, recently reported by ourselves[6] and Clampitt and Hughes.[7] The results presented in the present paper deal with the transition of polybutene-1 in Form III to the Form II modification, as observed by differential thermal analysis (DTA), dilatometry, x-ray diffraction, and photomicrography.

Experimental

Sample Preparation

Polybutene-1 used in our research was prepared by the usual Ziegler-type catalysis system and had an intrinsic viscosity $[\eta] = 1.52$ at 60°C., in *n*-heptane; this value corresponds to a viscosity-average molecular weight of 646,000 as calculated by the Mark-Houwink relationship reported by Stivala et al.[8] The sample was 96% insoluble in boiling ether and the ash content did not exceed 160 ppm.

As reported earlier, polybutene-1 in the Form III modification can be obtained by freeze-drying a dilute benzene solution of the polymer on a high vacuum line,[6] or by precipitating the polymer from benzene solution with methanol at room temperature.[5] Since these techniques result in a fluffy or spongy polymer, which does not lend itself well to physical measurements, the preferred method of sample preparation, was to cast films from dilute carbon tetrachloride or toluene solution onto glass plates at room temperature. The polymer solutions (5–20% by weight) were spread out on the surface of the glass plates by means of an adjustable Gardner Ultra Applicator. After the solvent had evaporated, polybutene-1 films in Form III of uniform thickness could be peeled off the glass plates by immersing the latter in cold water.

Yet another sample preparation method was to use a dip-coating technique in which a glass or metal cylinder is slowly withdrawn from a carbon tetrachloride solution of polybutene-1 at room temperature by a $^1/_3$ rpm synchronous motor. This technique allowed us to prepare large sheets of polybutene-1 in Form III, of greater thickness than normally possible by the casting method. The dip-coating technique makes it possible to build up the thickness of the film sample by repeated immersion and withdrawal of the cylinder from the polymer solution. It should be noted at this point that the solution temperature and concentration is a critical factor in the dip-coating method of film preparation. At elevated temperature (e.g., 80°C.) polybutene-1 in Form I is obtained directly from solution.

X-Ray Equipment and Methods

X-ray diffraction measurements were performed using a Philips Wide Range X-Ray Diffractometer with nickel-filtered Cu-Kα radiation and

a 1°/min. scanning speed. The scattered radiation was detected with a proportional counter over a range of $2\theta = 11–13°$. A pulse height analyzer was used to decrease the background scatter. The divergence slit was 1°, with receiving slit of 0.006 in. and a scatter slit of 1°.

The heating block used to heat the samples in the x-ray beam was specially designed and built in our laboratories. It consists essentially of a brass block which was machined to the proper dimensions so that it could be attached to the sample holder stage of the x-ray goniometer by means of the screws provided for the usual x-ray sample holder spring. The hot-stage block was heated by a small heater (Watlow-St. Louis, GIAI3A 115 V., 55 watt) cannibalized from a DuPont Differential Thermal Analyzer unit, which fit snugly into the cavity provided for that purpose. The heating rate and temperature of the hot-stage block was controlled by a Variac transformer. The block temperature was measured by means of a copper-constantan thermocouple inserted into the face of the block just under the centerline. The block was insulated on three sides with reflecting electrical tape and the temperature could be maintained constant with ±0.5°C., over the range of interest, i.e., 80–135°C.

Calibration of the heating block was achieved by determining the melting point of standard compounds at various locations on the surface of the heating block. Kofler Hot Bench calibrating substances by Reichert (Vienna, Austria) were used for that purpose. As evidenced by the simultaneous melting of the test substances at various locations on the surface of the block, the temperature was homogeneous over the area subjected to x-radiation under actual experimental conditions. A plot of emf vs. melting point of four standards (azobenzene: 68°C., benzil: 95°C., acetanilide: 115°C. and phenacetin: 135°C.), resulted in a straight line which was used to determine the temperature of the polymeric material during the transition period. Heat losses from the films under investigation (3–5 mils in thickness) to the surrounding atmosphere could be reduced by covering the films with a 0.005 in. thick beryllium foil (from the Brush Beryllium Corporation).

In all our experiments, the sample was quickly brought to 80–85°C. The heating rate was then reduced to 0.2–0.3°C./min. This heating rate was maintained in small increments of temperature necessitated by the limiting temperature at successive Variac settings. In this manner we were able to approximate equilibrium conditions over the temperature range of interest in which the transformation of Form III to Form II takes place.

DTA: Apparatus Design and Method

The DTA apparatus, as shown schematically in Figure 1, was a modified version of a unit developed by F. L. Finger and H. J. L. Schuurmans at Monsanto Chemical Company. It permits the detection of transition phenomena in polymers, as well as the accurate measurement of the temperatures at which these transitions occur. The equipment consists

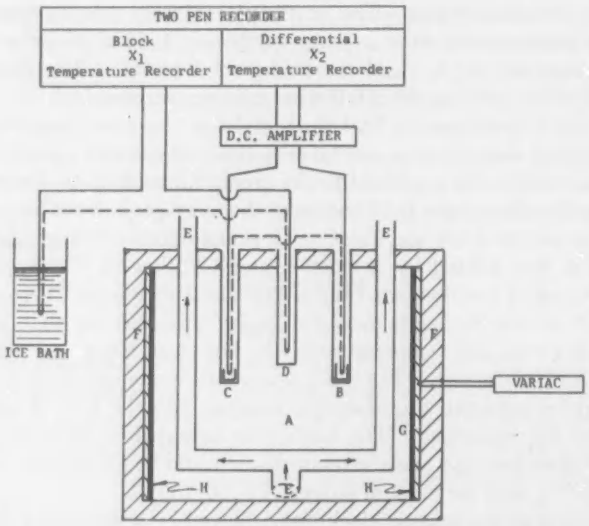

Fig. 1. Schematic view of the DTA apparatus consisting of (*A*) furnace block; (*B*) sample cell and thermocouple; (*C*) reference cell and thermocouple; (*D*) block temperature cell and thermocouple; (*E*) cooling channel; (*F*) asbestos insulation; (*G*) nichrome wire heating element and Variac; amplifier and recorder; and (*H*) asbestos tape.

basically of: (*1*) sample and reference cells contained within a furnace block; (*2*) thermocouples for measuring the temperature difference between the sample and reference material and block temperature; (*3*) a D-C breaker amplifier to amplify the differential signal; (*4*) a recorder to register this signal as a function of time and temperature.

The furnace block was constructed of aluminum with a diameter of 3 in. and a length of 5 in. Two symmetrically located wells, 0.247 in. in diameter and 2 in. in depth, were drilled into the block to hold the Pyrex sample and reference cells. In addition, the block was provided with a third well 0.236 in. in diameter and $1^3/_4$ in. in depth to accommodate a cell used to measure the block temperature. Particular attention was directed toward achieving matched sample and reference cells. The outside diameters were identical as were the wall thicknesses of $^3/_{64}$ in. and both cells fit precisely into the wells of the furnace block. A female ground joint on the upper section of all three cells accommodated a one-holed stopper for centering the inserted thermocouple. Proper centering of the thermocouples was assured by providing the latter with stainless steel sheaths. Calibrated copper-constantan thermocouples of No. 30 B & S gauge were used as the temperature sensing device.

Ribbon-type Nichrome wire was wound around the block over a $^1/_8$ in. layer of asbestos, applied as electrical insulation. A Variac regulator served to adjust the initial current supplied to the heater circuit. This

arrangement precluded linear heating rates over the entire experimental temperature range, but reproducible linear rates were nevertheless possible over an extended region encompassing the phase transitions. As a further precaution, the block was provided with a ground terminal to eliminate the influence of induced currents. Finally, the block was surrounded by a 2 in. layer of asbestos insulation. One other feature of the furnace design was a cooling channel which permitted controlled cooling experiments.

The differential emf generated by the thermal effect was amplified through a Keithley Model 149 milli-microvoltmeter capable of a maximum full-scale sensitivity of 0.1 μv., with an output of 10 v. Utilization of this sensitivity was limited by noise arising in the external input circuit. In practice, it was possible to use 10 μv. full scale sensitivity and with proper magnetic shielding of the input circuit, 3 μv. full scale sensitivity.

The thermocouple signals were registered on a Leeds and Northrup Speedomax G two pen recorder; one pen recorded the block temperature and the other, the temperature difference between the sample and reference cells.

The thermogram presented in this paper was obtained by tightly wrapping a 20 mg. Form III polybutene-1 cast film directly around the thermocouple and placing it in the sample cell. The reference cell was loaded with an equal amount of powdered glass into which the second thermocouple junction was inserted. A linear heating rate of 1.6°C./min. was recorded over the temperature range of interest. The thermal effect was sufficiently large so that a 30 μv. full-scale sensitivity was employed. It was possible to reproduce the above transitions to within ±0.5°C. for samples having identical thermal histories.

Dilatometry

Dilatometric measurements were performed using a modified Kovacs apparatus.[9] A 1-mm. ID capillary was used and the total inner volume of the dilatometer was 17 cm.^{3}. A 2.5 g. cast film sample was placed in the bulb, and the dilatometer was assembled. After attaching the apparatus to a high vacuum system and evacuating it to a pressure of 10^{-3} mm. for about $^1/_2$ hr., it was filled with freshly distilled instrument grade mercury under vacuum. A heating rate of 0.2°C./min. was employed between 25 and 92°C. Between 92 and 130°C. a rate of 0.1°/min. was used. Polymer specific volumes at temperatures corresponding to the melt could be reproduced to within ±0.0005 cm.^{3}/g. Transition temperatures were found to be reproducible for samples having identical thermal histories.

Results and Discussion

A representative thermogram of the Form III to Form II transition of polybutene-1 is shown in Figure 2. The first endotherm at 94°C. can be attributed to the Form III modification of polybutene-1; the second

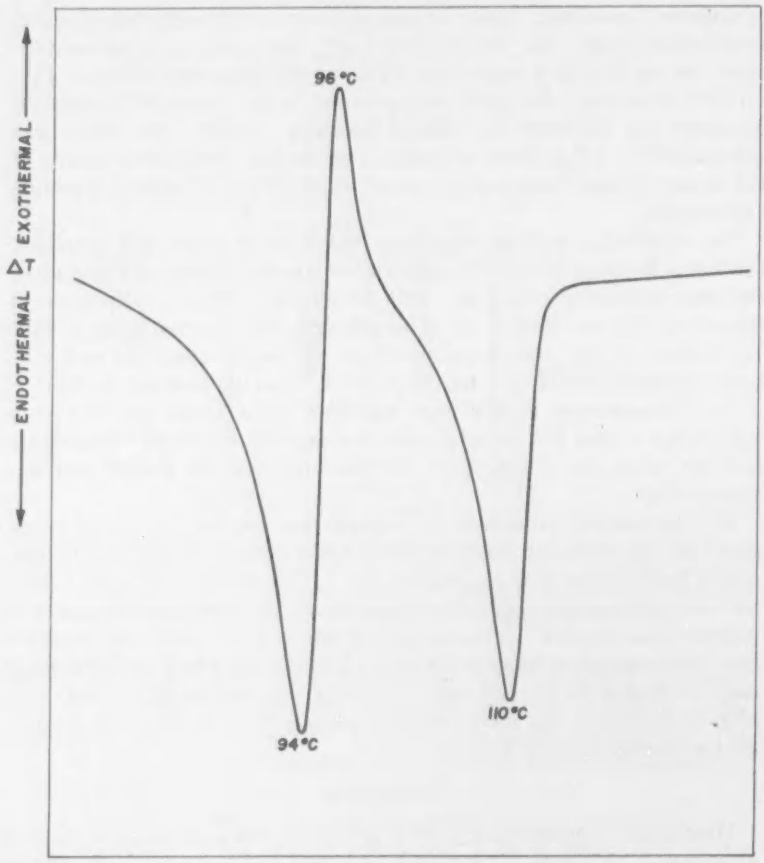

Fig. 2. DTA thermogram of Form III to Form II phase transition of polybutene-1 (heating rate 1.6°C./min.).

endotherm at 110°C. is undoubtedly due to melting of the form II modification, as shown previously by ourselves[6] and others.[7] The presence of a strong exothermic peak at 96°C., which is invariably recorded under our experimental conditions, points to the occurrence of an exothermic process during the transition of Form III to Form II. The intuitively obvious explanation for this phenomenon would be a process in which melting is followed by recrystallization. The recrystallization of gutta percha[10] at 64°C., is a classic example of a reaction of this type.

On the other hand, the transition of Form III to Form II may be another instance of a first-order crystal-crystal transition in the solid state of the type known to occur in 1,4-*trans*-polybutadiene;[10–12] a DTA thermogram of the latter has been published by Dannis.[13] Careful examination of

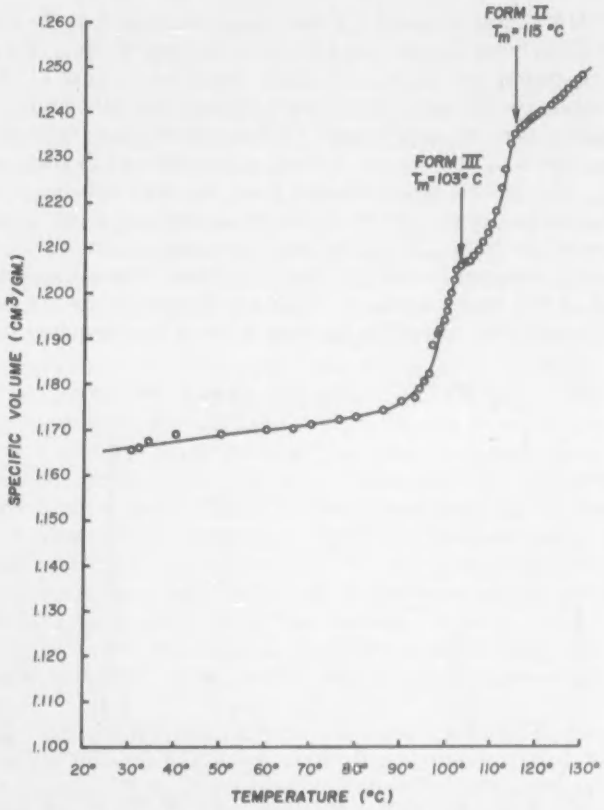

Fig. 3. Dilatometric melting curve of polybutene-1 in Form III.

the thermal record trace presented by this author revealed that there was no evidence of an exothermic peak accompanying the first-order transition known to occur in 1,4,-*trans*-polybutadiene. We were able to confirm the above results on our own apparatus by subjecting a sample of 1,4-*trans*-polybutadiene (prepared by the Phillips Petroleum Company), to the exact treatment our polybutene-1 samples were normally subjected. This procedure eliminated the possibility of instrumental error on our part. On the basis of differential thermal analysis results only, it was therefore reasonable to assume that the Form III to Form II transition of polybutene-1 differs from the transition known to occur in 1,4-*trans*-polybutadiene.

We sought to verify our observation by a number of different methods. For example, further confirmation of the Form III to Form II transition was provided by the specific volume versus temperature curves measured dilatometrically. A melting curve (Fig. 3) with two distinct breaks at

103 and 115°C. was obtained. These breaks correspond to the transition of Form III to Form II, and Form II to the melt, respectively. The melting transition corresponding to 115°C. was identified as that of Form II. Confirmation of this fact was obtained from additional specific volume-temperature data of polybutene-1 freshly crystallized from the melt (cooling rate 0.1°/min. with a heating cycle identical to that described above). The melting points derived from the peak maxima of the differential thermal method were necessarily lower than those obtained by dilatometric methods. While the latter technique measures the highest temperature required to melt the largest crystals of the sample, the temperature of the peak maxima by DTA are determined by the heat flow into the sample cell as well as the absorption of heat required for fusion

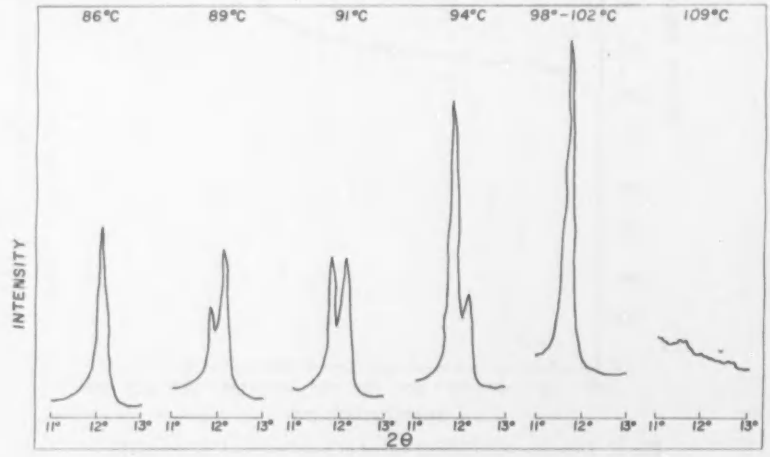

Fig. 4. X-ray diffraction pattern of polybutene-1 Form III to Form II phase transition.

of the crystalline material. To determine melting temperatures which are of thermodynamic significance, it is necessary to employ slow heating rates, so that sufficient time is allowed for the formation of the more perfect crystallites. The dilatometric heating rate of 0.2°C./min. was deemed sufficient for that purpose, thereby leading to higher melting points than those observed by DTA methods. Similar behavior has been noted with many other polymers studied in the past.

If melting followed by recrystallization is inherent to the Form III to Form II transition process, then it would be expected that the dilatometric (specific volume-temperature) curve would exhibit a minimum, corresponding to the recrystallization process, as shown by Mandelkern et al.[10] for the case of gutta percha. However, the dilatometric curve which we have obtained for the Form III to Form II transition of polybutene-1 (Fig. 3) failed to exhibit a minimum. In fact, our curve is

somewhat similar to the specific volume-temperature curve for *trans*-tactic polybutadiene published by Natta and Moraglio.[14]

Additional information on the Form III to Form II transition of polybutene-1, was obtained by heating a film sample in the Form III modification on the specially designed hot-stage, described in the experimental section, which was mounted on an x-ray diffraction unit. The hot-stage temperature could be controlled with great accuracy. We were therefore able to scan the region between $2\theta = 11°$–$13°$ at any desired temperature, thereby enabling us to follow the increase and decrease of the peaks characteristic of Form III and Form II at $2\theta = 12.1°$ and 11.7°, respectively. Some characteristic patterns are reproduced in Figure 4. From room temperature to 86°C., the peak of Form III at $2\theta = 12.1°$ decreased slightly in intensity. The first noticeable change occurs at 88°C., where a slight shoulder on the low angle side of the Form III peak was recorded. At 89°C., the peak at $2\theta = 11.7°$ has grown to the size shown in the second pattern of Figure 4. Simultaneously, the peak corresponding to Form III decreases in magnitude. At 91°C., both peaks are approximately equivalent in size and at 94°C., the peak corresponding to Form III has almost disappeared, as shown in Figure 4. The last vestige of this peak is lost at 110.8°C. From 98 to 102°C., the peak corresponding to Form II grows in size, apparently due to the slow heating process to which the polymer is subjected on the hot-stage. Finally, Form II starts to melt at 102°C. and all traces of crystallinity have disappeared at a temperature of 109°C., when only a completely amorphous pattern is recorded.

As shown by the diffraction patterns of Figure 4, we failed to record any increase of the amorphous background during the Form III to Form II transition process. This would seem to indicate that there is no intermediate long-lived molten state of polybutene-1 during the transition. This assumption was further confirmed by a photomicrographic investigation of the Form III to Form II transition of polybutene-1.* Examination of the transition with a polarizing hot-stage microscope showed that birefringence, and therefore crystallinity disappears only above 115°C. This finding is in line with our dilatometric and x-ray results. So far, we have been unable to grow polybutene-1 spherulites in Form III and are therefore unable to observe the change, if any, of the birefringence orientation upon transition of Form III to Form II. The exact nature of the transition may become apparent by further study of the x-ray diffraction patterns. Extending the scanning range may provide an answer to the exothermic peak measured by DTA.

As far as it is known, the structure of the Form III modification of polybutene-1 has not yet been determined and this makes it quite difficult of course to offer an explanation for the transition on the basis of a physical model. It seems probable that the chains in Form III, whatever

* This examination was kindly carried out by Dr. M. Nahmmacher of E. Leitz, Inc., New York, New York.

their conformation may be, acquire sufficient energy at the transition temperature to break interchain cohesive forces over a sufficient length of the chain to allow a sudden convolution of a chain segment into the 11_3 helix of Form II. Inception of the transition should be facilitated by the presence of "defects" in the polymer such as: molecular holes, chain ends, trace impurities and the border between crystalline and amorphous areas.

Experimental evidence gathered to date proves beyond doubt that polybutene-1 in the Form III modification undergoes a transition to the Form II modification at elevated temperatures (94 – 103°C., depending upon the thermal treatment and experimental method). Although there is considerable evidence in favor of a solid-solid transition, the presence of an exothermal peak in the DTA thermogram may indicate that the transition mechanism involves a short-lived molten state. An exothermal peak, however, could also be caused by crystallization of previously amorphous regions.

It is evident from the above, that polybutene-1 has proved to be an extremely fascinating subject of scientific investigation and there is little doubt that some of the problems remaining at the present time will be solved in due course.

The authors wish to thank the Messrs. D. J. Di Biasi, F. A. Nagy, and R. D. Vibronek for their competent technical assistance, and Mr. A. Di Frenza for skillful machining of the x-ray hot-stage block.

The authors are also grateful to their colleagues at Mobil Chemical Company, and in particular to Dr. H. J. L. Schuurmans, for many helpful discussions.

References

1. Natta, G., *Atti Accad. Naz. Lincei*, **4**, 61 (1955).
2. Natta, G., P. Corradini, I. W. Bassi, *Nuovo Cimento Suppl.*, **1**, 52 (1960).
3. Jones, A. T., *J. Polymer Sci.*, **B1**, 455 (1963).
4. Zannetti, R., P. Manaresi, and G. C. Buzzoni, *Chim. Ind.*, **43**, 735 (1961).
5. Danusso, F., and G. Gianotti, *Makromol. Chem.*, **61**, 139 (1963).
6. Geacintov, C., R. S. Schotland, and R. B. Miles, *J. Polymer Sci.*, **B1**, 587 (1963).
7. Clampitt, B. H., and R. H. Hughes, paper presented at 145th ACS meeting, New York, September 1963.
8. Stivala, S. S., R. J. Valles, and D. W. Levi, *J. Appl. Polymer Sci.*, **7**, 97 (1963).
9. Kovacs, A. J., paper presented at the Simposio Internazionale di Chimica Macromolecolare; *Ric. Sci. Suppl.*, **25**, 3 (1955).
10. Mandelkern, L., F. A. Quinn, and D. E. Roberts, *J. Am. Chem. Soc.*, **78**, 926 (1956).
11. Natta, G., and P. Corradini, *J. Polymer Sci.*, **38**, 29 (1959).
12. Nikitin, V. A., V. A. Volkova, N. V. Mikhailova, and Iu. G. Baklagina, *Vysokomolekul Soedin.*, **1**, 1094 (1959).
13. Dannis, M. L., *J. Appl. Polymer Sci.*, **7**, 231 (1963).
14. Natta, G., and G. Moraglio, *Rubber Plastics Age*, **44**, 42 (1963).

Résumé

La transition de la forme III en forme II du polybutène-1 cristallin à tempèrature èlevèe a ètè observèe par analyse thermique diffèrentielle (DTA), par dilatomètrie, par

diffraction aux rayons-X et par microphotographie. On a trouvè que les thermogrammes DTA du polybutène-1 dans la forme III prèsentent des endothermes à 94°C et 110°C, ce qui correspond respectivement à la transformation de la forme II et à la fusion de la-forme II. L'origine d'un pic exothermique observè à 96°C n'a pas encore ètè entièrement rèsolue à l'heure actuelle. La transition du polybutène-1 dans la forme III a ègalement ètè ètudiée par les mèthodes de diffraction aux rayons-X. On a montrè que l'intensitè du pic à $2\theta = 12.1°$, correspondant à la phase cristalline de la forme III, commence à diminuer à 88°C, alors que simultanèment le pic à $2\theta = 11.7°$, qui correspond à la modification de la forme II commence à augmenter. La transformation est complète à 48°C. La nature de la transition du polybutène-1 de la forme III dans la forme II est discutée dans cet article; deux mècanismes diffèrentes semblent être possibles: une transition solide-solide ou bien une transition impliquant un intermèdiaire de courte durèe de vie à l'ètat fondu.

Zusammenfassung

Die Umwandlung des kristallinen Polybuten-1 bei erhöhter Temperatur von Form III zu Form II wurde mittels Differentialthermoanalyse (DTA), Dilatometrie, Röntgenbeugung und Mikrophotographie beobachtet. DTA-thermogramme von Polybuten-1 in Form III zeigten Endothermitäten bei 94°C und 110°C, die der Umwandlung von Form III bzw. dem Schmelzen von Form II entsprechen. Der Ursprung eines bei 96°C beobachteten exothermen Maximums ist zur Zeit noch nicht ganz klar. Die Umwandlung von Polybuten-1 in die Form-III-Modifikation wurde auch mit Röntgenbeugungsmethoden untersucht. Die Intensität der Spitze bei $2\theta = 12.1°$, die der kristallinen Phase der Form II entspricht, beginnt bei 88°C an Grösse abzunehmen, während gleichzeitig die der Form-II-Modifikation entsprechende Spitze bei $2\theta = 11.7°$ zu wachsen beginnt. Die Umwandlung ist bei 98°C vollständig. Die Natur der Umwandlung des Polybuten-1 von Form III zu Form II wird in der Arbeit diskutiert; zwei alternative Mechanismen werden für möglich gehalten: eine Fest-Fest-Umwandlung oder eine Umwandlung über einen kurzlebigen geschmolzenen Zwischenzustand.

JOURNAL OF POLYMER SCIENCE: PART C NO. 6, PP. 209–211

The Low-Melting Crystalline Modifications of Isotactic Polybutene-1

H. W. HOLDEN, *Central Research Laboratory, Canadian Industries Limited, McMasterville, Quebec, Canada*

Synopsis

The effect of annealing on the low-melting crystalline modification (III) of isotactic polybutene-1 has been studied by differential thermal analysis. The extrapolated equilibrium melting point of modification III is estimated to be 109.1°C. with 50% confidence limits at 108.0° and 110.6°C. In the temperature range where annealing effects are observed, conditions are suitable for the simultaneous formation, in the partially melted sample, of modification II and more highly ordered modification III.

Isotactic polybutene-1 has been studied in its various crystalline modifications by differential thermal analysis (DTA), using the same apparatus and techniques described elsewhere[1] in this symposium. It has been found that the modification III (obtained as a precipitate from solution) can be annealed to produce much more highly ordered crystals of the same modification. The well-defined relation between annealing temperature and melting-peak temperature yields an extrapolated value for the equilibrium melting point of 109.1°C. The result is an illustration of a successful use of DTA, where dilatometric measurements on the pure polymer break down because of concurrent formation of modification II. Figure 1 is a graphical summary of results obtained for modification III and partial results for modification II. The graph is constructed as described in detail in reference 1.

The theory of Hoffman and Weeks[2] predicts the linear relationship between crystallization temperature T_x and melting temperature T_m, from which the equilibrium melting temperature $T_m°$ is determined by the condition $T_x° = T_m°$. On the assumption that the straight line relation is valid, the least-squares fit of the nine points gives the equation: $T_m = 24.8_7 - 0.772\ T_x$. Because of the difficult extrapolation, it is necessary to evaluate the experimental reliability of the result. Values of T_m, and confidence limits for the average value of T_m were computed for a series of values of T_x near $T_x°$ ($= T_m°$); lines for these upper and lower confidence limits were plotted to obtain graphical solutions with the line $T_x = T_m$. For 50% confidence limits, the values obtained were 108.0 and 110.6°C.; for 95% limits they were 106.0 and 115.5°C.

Danusso and Gianotti[3] have estimated $T_m°$ to be 106.5°C., using the

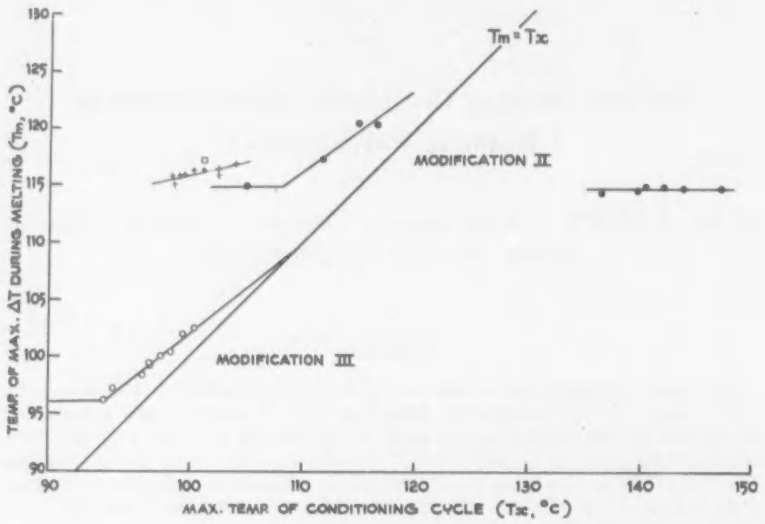

Fig. 1. Isotactic polybutene-1: Relation between conditioning temperature and melting temperature for two crystalline modifications. *Modification II:* (●) crystallites obtained by uniform (3°C./min.) cooling of melt; exothermic process, first detectable at 95°C., reaches maximum at 90°C.; examples are included where solid has subsequently been annealed near melting temperature. (□) Crystallites obtained by isothermal crystallization at 101.2°C.; (+) crystallites obtained by conversion of modification III at temperatures determined by melting of modification III. *Modification III:* horizontal line is drawn at melting peak temperature of sample as prepared by solution precipitation; (○) crystallites obtained by annealing of starting material at temperatures indicated.

Flory equation for the melting points of polymer solvent mixtures.[4] The discrepancy of 2.6° between the two determinations, could fully be accounted for by overlap in error limits or by differences in tacticity. Difficulty in attaining equilibrium conditions at the final melting point of polymer solvent mixtures could give a low bias to the estimate of $T_m°$.

An exothermic extremum observed immediately after the melting endotherm of modification III is quite reasonably attributed to crystallization of modification II from the melt.[5] An interesting feature is that the process is correspondingly delayed in the annealed samples until the modification III has melted, at considerably higher temperatures. A systematic variation in melting-peak temperature of modification II is observed with the variation in the temperature of the crystallization extremum. Isothermal crystallization of a melt previously conditioned at high temperature was observed to proceed at a much slower rate at 101.2°C. than the corresponding process after melting of modification III. The weight of evidence favors the following explanation. Since during annealing of modification III small melt domains form at a temperature where primary nucleation of modification II is fast, there will be a competition for formation

of the two crystalline forms from the melt. When the sample is maintained at the annealing temperature for less than four minutes and then quenched, low melting crystallites of modification III can be obtained; during a longer annealing cycle it appears that all melt formed is converted to either type II or high-melting type III crystallites. This is confirmed by leaving the conditioned sample for several days to permit spontaneous transformation of some of the type II form to type I.[5,6] The resulting thermogram has melting peaks for each of the three known modifications, as well as the exothermic signal for crystallization of some modification II.

A similar study of the temperature range near the melting point of modification II is unlikely to lead to reliable estimates of the equilibrium melting point. Spontaneous nucleation and persistence of modification I during various stages of the conditioning cycle are thought to be the main sources of scatter of results. There is, however, a general indication that T_m° would exceed the estimate of 124°C. reported by Danusso and Gianotti.[3]

We wish to thank Dr. A. W. Birley, Plastics Division of Imperial Chemical Industries Limited, for supplying the polybutene sample to this laboratory.

References

1. Holden, H. W., *J. Polymer Sci.*, **C6**, 53 (1964).
2. Hoffman, J. D., and J. J. Weeks, *J. Res. Natl. Bur. Std.*, **64A**, 73 (1960).
3. Danusso, F., and G. Gianotti, *Makromol. Chem.*, **61**, 139 (1963).
4. Flory, P. J., *J. Chem. Phys.*, **17**, 223 (1949).
5. Clampitt, B. H., and R. H. Hughes, *J. Polymer Sci.*, **C6**, 43 (1964).
6. Boor, J., and J. C. Mitchell, *J. Polymer Sci.*, **A1**, 59 (1963).

Résumé

On a étudié par analyse différentielle thermique, l'effet de recuit sur les modifications (III) cristalline de polybutène-1 de faible point de fusion. On estime que le point d'équilibre de la modification (III) obtenu par extrapolation est de 109.1°C avec des limites de validite de 50% entre 108.0 et 110.6°C. Dans le domaine de tempèrature où les effets de recuit sont observés, les conditions sont favorables pour la formation simultanée dans un échantillon partiellement fondu de la modification II, et de la modification III plus fortement ordonnées.

Zusammenfassung

Der Einfluss des Temperns auf die niedrigschmelzende kristalline Modifikation (III) von isotaktischem Polybuten-1 wurde mittels Differentialthermoanalyse untersucht. Der extrapolierte Gleichgewichtsschmelzpunkt von Modifikation III wird zu 109,1°C mit 50% Konfidenzlimit bei 108,0 und 110,6°C bestimmt. Im Temperaturbereich, in welchem Temperungseffekte beobachtet werden, bestehen geeignete Bedingungen für die gleichzeitige Bildung von Modifikation II und der höher geordneten Modifikation III in der teilweise geschmolzenen Probe.

AUTHOR INDEX

Abu-Isa, I.: 149
Anderson, H. C.: 175
Bair, H. E.: 109
Bodily, D. M.: 137
Boy, R. E., Jr.: 17
Clampitt, B. H.: 43
Cox, R. H.: 17
Crawford, V. A.: 149
Dole, M.: 149
Donald, H. J.: 93
Eiermann, K.: 157
Friedman, H. L.: 183
Geacintov, C.: 197
Gillham, J. K.: 125
Grewer, T.: 33
Haly, A. R.: 149
Hellmuth, E.: 101
Hennig, J.: 167
Holden, H. W.: 53, 209
Hughes, R. H.: 43
Humes, E. S.: 93
Jenkins, L. T.: 27
Karasz, F. E.: 109
Kilian, H. G., 101
Knappe, W.: 167
Lewis, A. F.: 125
Martin, H.: 83
Miles, R. B.: 197
Müller, F. H.: 83, 101, 117
Neill, W. K.: 65
O'Reilly, J. M.: 109
Schotland, R. S.: 197
Schulken, R. M., Jr.: 17
Schwenker, R. F., Jr.: 1
Slade, P. E., Jr.: 27
Tang, W. K.: 65
Weimann, N.: 117
White, L. W.: 93
Wilski, H.: 33
Wunderlich, B.: 137
Zuccarello, R. K.: 1

SUBJECT INDEX

Anisotropy, of thermal conductivity, 167
Calorimetric measurements, during stretching of polycarbonate, 117
α-Cellulose, pyrolysis and combustion, 65
Combustion, of α-cellulose, 65
Crystalline modifications, low-melting, of isotactic polybutene-1, 209
Crystallization, of polymers, 93
of polypropylene, 93
Differential thermal analysis, branched and chlorinated polyethylenes, 101
crystallization of polypropylene, 93
dynamic, glass transition interval, 137
linear polyesters, 17
polybutene-1, 43
studies of melting and crystallization of polymers, 83
study of effects of thermal history, 53
synthetic fibers, 1
Elastomers, strained, thermal conductivity, 67
Flame retardants, effect on pyrolysis and combustion of α-cellulose, 65
Glass transition, in isotactic polypropylene, 149
Glass transition interval, dynamic differential thermal analysis, 137
Kinetics, of thermal degradation of char-forming plastics, 183
Lexan polycarbonate, thermodynamic properties from 110–560°K., 109
Melting, of polymers, 83
Phase transition, form III to form II, of polybutene-1, 197
Plastics, char-forming, thermal degradation, 183
phenolic, application of kinetics, 183
Polybutene-1, differential thermal analysis, 43
form III to form II phase transition, 197
isotactic, low-melting crystalline modifications, 209
specific heat, 33
Polycarbonate, calorimetric measurements during stretching, 117
Polyesters, linear, differential thermal analysis, 17
Polyethylene, branched and chlorinated, differential thermal analysis and x-ray analysis, 101
effects of thermal history, 53
Polymers, high, thermal conductivity, 157
melting and crystallization, 83
pyrolysis kinetics, thermogravimetry, 175
stretched amorphous linear, thermal conductivity, 167
synthetic high, specific heat, 149
thermal behavior by torsional braid analysis, 125
Polypropylene, crystallization measured by differential thermal analysis, 93
isotactic, glass transition, 149
Polyurethane elastomers, thermal analysis, 27
Pyrolysis, of α-cellulose, 65
Specific heat, polybutene-1, 33
synthetic high polymers, 149
Stretching, heat effects by, 117
Synthetic fibers, differential thermal analysis, 1
Thermal analysis, polyurethane elastomers, 27
Thermal behavior, of polymers, 125
Thermal conductivity, high polymers, 157
stretched amorphous linear polymers and in strained elastomers, 167
Thermal degradation, of char-forming plastics, 183
Thermal history, effects on polyethylene, 53
Thermodynamic properties, of Lexan polycarbonate, 109
Thermogravimetry, polymer pyrolysis kinetics, 175
thermal degradation of char-forming plastics, 183
Torsional braid analysis, studies of thermal behavior, 125
X-ray analysis, some branched and chlorinated polyethylenes, 101
X-ray measurement, union with differential calorimetric measurements, 101

Announcing the latest volumes in POLYMER REVIEWS

NEWER METHODS OF POLYMER CHARACTERIZATION

Volume 6 of Polymer Reviews

Edited by BACON KE, *C. F. Kettering Research Laboratory, Yellow Springs, Ohio.* A collection of new and recently developed methods for characterizing synthetic and natural macromolecules, with a detailed discussion of how these new techniques can be applied to both new and conventional problems. The author presents a wide variety of physical and physico-chemical methods, including x-ray and electron diffraction, magnetic resonance, thermal methods, solution properties, and monolayers.

SECTION HEADINGS: Infrared Spectra. Low-Angle X-Ray Studies of Polymers. Electron Diffraction. High Resolution Nuclear Magnetic Resonance. Optical Rotary Dispersion. Optical Characterization of Polymer Films. Density-Gradient Ultracentrifugation. Flow Birefringence. Differential Calorimetry. Monomolecular Film Studies of Polymers. Column Fractionation. Characterization of High Polymers in Solution at Elevated Temperatures. Elasto-Osmometry. Study of Microtacticity.

1964. 722 pages. $24.50.

POLYMER SINGLE CRYSTALS: Volume 5 of Polymer Reviews

By P. H. GEIL, *Camille Dreyfus Laboratory, Research Triangle Institute, Durham, North Carolina.* This review covers in detail the morphology of crystalline polymers. The author has based his book on data from both solution and melt. In addition, Mr. Geil discusses the initial steps that have been taken toward the description of polymers on a molecular scale through the joint application of microscopy and a number of other techniques.

"My evaluation of this book can be summarized in a prediction: In a relatively short time, well-worn copies of Geil's book will be found in the laboratories of practically every worker interested in the physical properties of crystalline polymers, regardless of whether his main interest is in fundamental research or technological application." — JOHN D. HOFFMAN, *Polymers Division, National Bureau of Standards.*

CONTENTS: Introduction. Single Crystals From Solution. Hedrites. Spherulites. Annealing. Theoretical Calculations of Folding. Orientation. AS-Polymerized and Amorphous Polymers. Properties and Morphology. *1963. 560 pages. $16.00.*

Order your on-approval copies from:

INTERSCIENCE PUBLISHERS

a division of

JOHN WILEY & SONS, Inc., 605 Third Avenue, New York, N.Y. 10016